



April 4, 2008

ATTN: Document Control Desk  
Director, Spent Fuel Project Office  
Office of Nuclear Material Safety and Safeguards  
**U.S. Nuclear Regulatory Commission**  
Washington, DC 20555-0001

**SUBJECT: RAI Responses for Mixed Oxide Fresh Fuel Package License Amendment, Docket No. 71-9295 (TAC No. L24054)**

This transmittal contains the responses to the NRC Request for Additional Information (RAI) provided to Packaging Technology (currently AREVA Federal Services LLC) in the letter dated November 2, 2007. These RAIs are a result of a requested license amendment to the MOX Fresh Fuel Package (USA/9295/B(U)F-96).

The RAI responses are included in Attachment A. Because the RAIs included questions relating to the AA433, including structural analysis (B6-1), engineering controls (B6-2), and engineering drawings (C6-2), it was decided that the most straightforward approach was to design two separate rod boxes to simplify resolution of NRC concerns. These rod boxes, replacing the AA433, are identified as AFS-B and AFS-C.

Because of the numerous nomenclature changes, Appendix B and Appendix C are replaced in their entirety. Minor changes are also made to the main Safety Analysis Report (SAR) as follows:

- Table of Contents has been updated
- Chapter 1 has been revised to remove reference to the AA433.
- Editorial errors in Chapter 3 have been corrected. The HAC temperature limits had been listed incorrectly in Table 3.3-3, although the correct values were listed in Table 3.5-1. Also, a number of the figure callouts in Section 3.5.3.1 were incorrect and have been corrected.
- A minor change has been made to Chapter 7 to clarify that the swivel clamps must be locked with a hex nut subsequent to fuel assembly loading.

The SAR changes related to the RAI responses are incorporated into Revision 6 of the SAR. One copy of replacement pages for Revision 6 of the SAR is provided. The page delete/insert instructions are included in Attachment B. Revision 6 of the SAR is also included electronically as a PDF file, as noted in Attachment C.

If you have any questions or comments regarding this submittal, please contact me at (253) 552-1326, or at [fred.yapuncich@areva.com](mailto:fred.yapuncich@areva.com).

Sincerely,

Fred Yapuncich, Project Manager  
**AREVA Federal Services LLC**

Enclosures: As Noted

cc: M. Rahimi, NRC/NMSS-DSFST  
R. Clark, Shaw AREVA MOX Services  
P. Mann, DOE  
R. Migliore

Project File 99008

AREVA Federal Services LLC

MMSS01

-Page 2-

**Attachment A  
RAI Responses**

Note: The RAIs have not been restated in their entirety.

- B6-1** Justify the most reactive configuration if no structural credit is taken for the AA433 or fuel rods explicitly or explicitly.

*Response:* The AA433 in Appendix B has been replaced with a different box, named the AFS-B. The AFS-B may contain up to 175 standard MOX fuel rods. SAR drawings of the AFS-B are included in the application. It is demonstrated in Chapter B2, *Structural Evaluation*, that the AFS-B provides support to the MOX rods superior to fuel rods within a fuel assembly, which were shown to survive an HAC event without gross rod damage (such as broken fuel rods). The criticality analysis has not been revised, and is highly conservative because the AFS-B is not credited.

- B6-2** Provide engineering-based instead of administrative-based controls for implementing the load limit of one AA433 with 175 standard MOX rods per MFFP.

*Response:* Note that the AA433 in Appendix B has been replaced with the AFS-B, and the AA433 in Appendix C has been replaced with the AFS-C. Although the AFS-B and AFS-C have the same outer dimensions and general design, each is clearly labeled so that mixing of the AFS-B and AFS-C in the same MFFP may be acceptably controlled.

- C6-1** Provide the bases for the bounding values used to analyze PNL [and Exxon] fuel rods. A phone call between AFS and NRC on November 28, 2007 further established that the primary concern is that U-235 values for the “bounding” compositions provided in Table C6.2-3 are not the maximum values listed in the table.

*Response:* Both the Exxon and PNL rods utilize natural uranium. In all models, the U-235 weight percent (i.e., U-235/U= 0.71%) is fixed and does not change. Also, the plutonium isotopics (e.g., Pu-239/Pu) are fixed in all models and do not change; these values are provided in Table C6.2-2.

In MOX fuel, because the uranium is natural, the reactivity is controlled by the mass of plutonium. Therefore, the mass of plutonium per rod is treated as a fundamental input quantity in Appendix C. For simplicity, the effective pellet density is fixed at the maximum value of 10.85 g/cm<sup>3</sup> in all models, consistent with the original MOX application. In the MCNP models, the mass of PuO<sub>2</sub> is treated as an independent variable, while the mass of UO<sub>2</sub> treated as a dependent variable selected to result in an effective pellet density of 10.85 g/cm<sup>3</sup>.

For example, if the mass of plutonium is increased, to maintain a constant pellet density, the mass of uranium must decrease. Conceptually, the lower reactivity UO<sub>2</sub> is being replaced with the higher reactivity PuO<sub>2</sub> as the plutonium mass is increased. Therefore, the Pu/(Pu+U) fraction, and hence the mass of UO<sub>2</sub> in the model, is allowed to “float” for the various configurations. If both the plutonium and uranium were maximized simultaneously, the resulting pellet density would be non-physical. The intent of the parametric study is to determine bounding rods that are capable of being fabricated.

-Page 3-

This is a different approach than was used for the "standard" MOX rod in the original SAR. For the standard MOX rod, the Pu/(Pu+U) was treated as fixed at 6.0%, and the mass of plutonium not treated as input. This is the reason for the note at the bottom of Table C6.2-3, "The Pu/(Pu+U) values are not limiting values." It is not desired that Pu/(Pu+U) be included in the Certificate of Compliance as a limit for Appendix C contents. In Appendix C, the limiting quantity is the mass of plutonium per rod.

To help clarify the fundamental differences between the various rod types, Table C6.2-3 is reproduced in Table 1, adding the volume of the pellet stack and the total grams of each isotope. Note that in this table, the weight percent is the fraction of the total pellet mass, including oxygen. The total fissile mass per rod is provided in the last row, and is the sum the U-235, Pu-239, and Pu-241 masses.

As shown in Table 1, two different Exxon rods were modeled, Exxon1 and Exxon2. Exxon1 rods contain 60 g of plutonium, and Exxon2 rods contain 65 g of plutonium, while the geometry is identical for both. As noted by the NRC reviewers, the U-235 weight percent within the rod decreases from 0.594% to 0.592% when the mass of plutonium increases by 5 g. As explained above, this is expected, because the mass of PuO<sub>2</sub> is increased by displacing UO<sub>2</sub>. However, the U-235 mass is essentially the same for both (8.0 g), and the overall fissile mass increases from 59.6 g to 63.9 g. Therefore, Exxon2 bounds Exxon1.

For the PNL rods, four different rod models are considered, and geometry is varied as well as mass. Both PNL1 and PNL2 have 40 g of plutonium, although PNL1 has an active fuel length of 36-in, while PNL2 has an active fuel length of 28-in. Because the density is fixed in all models, as the active fuel length is reduced, the Pu/(Pu+U) must increase because the plutonium mass is fixed. As shown in Table 1, the U-235 mass of PNL2 is less than PNL1. The reason is that the pellet stack is simply shorter, and the mass of uranium is not conserved. However, PNL2 is more reactive than PNL1, because reducing the active fuel length reduces neutron leakage (compare Cases D1 and D2 in Table C6.4-4). It is not desired to conserve uranium mass between PNL1 and PNL2 because the density of such a rod would be non-physical.

PNL2 and PNL3 have the same plutonium mass of 40 g, and the same active fuel height of 28-in. However, PNL3 has a larger pellet diameter than PNL2. Therefore, Pu/(Pu+U) must decrease to maintain the same plutonium mass, while the U-235 mass will increase. Therefore, PNL3 has a slightly higher fissile mass than PNL2. This may be the reason the reactivity of PNL3 is slightly higher than PNL2 (compare Cases D3 and D4 in Table C6.4-4.)

PNL3 and PNL4 are geometrically identical, although PNL3 has 40 g of plutonium, and PNL4 has 42 g of plutonium. Therefore, Pu/(Pu+U) must increase to maintain the same plutonium mass, while the U-235 mass will decrease. However, the fluctuation in U-235 mass is essentially zero, as indicated in Table 1. The overall fissile mass of PNL4 bounds all four PNL rod models, and has a small axial height to minimize neutron leakage. Therefore, PNL4 is the bounding PNL rod model.

-Page 4-

In addition to the most reactive parameters determined in this parametric study, conservative assumptions are made in regard to the plutonium isotopics, in particular the Pu-241 weight fraction, as no credit is taken for Pu-241 decay. Approximately 75% of the Pu-241 mass shown in Table 1 will have decayed away before the time of shipment, although this decay has not been credited.

It should be noted that the PNL rods contribute little to the reactivity, as the Exxon rods dominate when both types of rods are inside the AFS-C. The PNL rods contribute  $\sim 0.002$  to  $k_s$ , which is within statistical fluctuation.

Table 1

Parameter	Exxon1	Exxon2 bounding	PNL1	PNL2	PNL3	PNL4 bounding
Pellet Density (g/cm <sup>3</sup> )	10.85	10.85	10.85	10.85	10.85	10.85
Pellet Stack Volume (cm <sup>3</sup> )	124.406	124.406	109.257	84.978	95.023	95.023
Active Fuel Height (in)	70	70	36	28	28	28
Pellet OD (in)	0.3716	0.3716	0.4856	0.4856	0.5135	0.5135
Pu mass (g)	60	65	40	40	40	42
Pu/(Pu+U)	5.041%	5.462%	3.829%	4.920%	4.400%	4.620%
U-235	0.594%	0.592%	0.602%	0.595%	0.598%	0.597%
U-238	83.115%	82.746%	84.175%	83.220%	83.675%	83.483%
Pu-239	3.533%	3.828%	2.683%	3.448%	3.084%	3.238%
Pu-240	0.622%	0.674%	0.473%	0.607%	0.543%	0.570%
Pu-241	0.289%	0.313%	0.219%	0.282%	0.252%	0.265%
O	11.847%	11.847%	11.848%	11.847%	11.848%	11.848%
Total	100%	100%	100%	100%	100%	100%
U-235 (g)	8.0	8.0	7.1	5.5	6.2	6.2
U-238 (g)	1121.9	1116.9	997.8	767.3	862.7	860.7
Pu-239 (g)	47.7	51.7	31.8	31.8	31.8	33.4
Pu-240 (g)	8.4	9.1	5.6	5.6	5.6	5.9
Pu-241 (g)	3.9	4.2	2.6	2.6	2.6	2.7
O (g)	159.9	159.9	140.5	109.2	122.2	122.1
Fissile (U235+Pu239+ Pu241) (g)	59.6	63.9	41.5	39.9	40.6	42.3

**C6-2** Provide engineering drawings to show structural arrangement of the contents including PNL pins, Exxon pins, and other structural components (e.g., basket, spacers, dunnage rods) within each AA433 rod container.

*Response:* Note that there is no requirement, from a criticality perspective, for the Exxon and PNL rods to be separated. Figures 6.4-11 and 6.4-12 show cases in which the Exxon and PNL rods are allowed to mix (see also Cases G2 through G8 in Table C6.4-7). When the Exxon and PNL rods are mixed, moderation is reduced and the reactivity decreases.

-Page 5-

To better illustrate the intended shipping hardware, SAR drawings have been provided with this application for the AFS-C, which has replaced the AA433. In the AFS-C, the Exxon and PNL rods are placed in separate compartments. It is demonstrated in Chapter C2, *Structural Evaluation*, that the rods remain in their separate compartments under HAC.

Because the AFS-C has different dimensions than an AA433, the AFS-C may fit an additional 2 Exxon rods and 1 PNL rod compared to the AA433, for a maximum of 116 Exxon and 69 PNL rods. As the criticality analysis is performed for 121 Exxon rods and 81 PNL rods in the limiting case, the criticality analysis has not been revised.

-Page 6-

**Attachment B**  
**Delete/Insert Instructions**  
**Revision 6 of MFFP Safety Analysis Report**

<b>SAR Section</b>	<b>Delete Pages from Rev. 5</b>	<b>Insert Pages to Rev. 6</b>
Cover and Spine, Vol. 1	Cover and spine, Vol. 1	Cover and spine, Vol. 1
Title page, Vol. 1	Title page, Vol. 1	Title page, Vol. 1
Table of Contents	xiii through xxii	xiii through xxii
Chapter 1	1.1-1 and 1.1-2	1.1-1 and 1.1-2
Chapter 3	3.3-7 and 3.3-8	3.3-7 and 3.3-8
	3.5-5 through 3.5-8	3.5-5 through 3.5-8
Chapter 7	7.1-5 and 7.1-6	7.1-5 and 7.1-6
Cover and Spine, Vol. 2	Cover and spine, Vol. 2	Cover and spine, Vol. 2
Title page, Vol. 2	Title page, Vol. 2	Title page, Vol. 2
Appendix B	All Appendix B pages	New Appendix B
Appendix C	All Appendix C pages	New Appendix C

-Page 7-

**Attachment C**  
**Contents of Electronic Media**

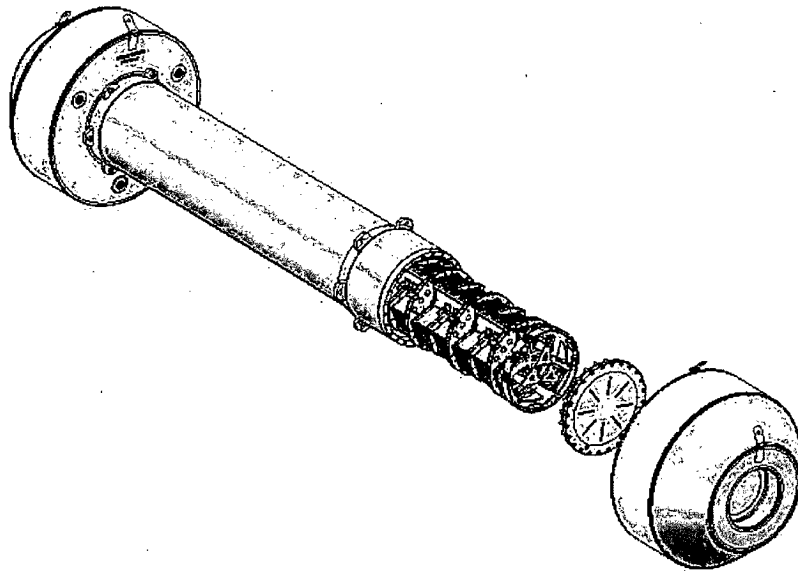
This submission is composed of both paper copies and electronic copies. The electronic copies are contained within an envelope labeled, "MFFP Docket 71-9295 Electronic Copy of Document." The envelope contains one compact disc of the following:

<b>Title</b>	<b>Media Type</b>	<b>Contents</b>
MOX Fresh Fuel Package Safety Analysis Report	CD-ROM	One file of the complete text of the submittal, including replacement pages:  <b>001 MFFP SAR, Rev 6.PDF</b> <b>(872 pages, 29.758 MB)</b>

DOCKET 71-9295



# Mixed Oxide Fresh Fuel Package



## *Safety Analysis Report*

Volume 1  
Revision 6  
April 2008



A6.3.4 Demonstration of Maximum Reactivity ..... A6.3-1

**A6.4 Single Package Evaluation ..... A6.4-1**

A6.4.1 Single Package Configuration ..... A6.4-1

    A6.4.1.1 NCT Configuration ..... A6.4-1

    A6.4.1.2 HAC Configuration ..... A6.4-1

A6.4.2 Single Package Results ..... A6.4-2

**A6.5 Evaluation of Package Arrays Under Normal Conditions of Transport..... A6.5-1**

**A6.6 Package Arrays Under Hypothetical Accident Conditions..... A6.6-1**

A6.6.1 HAC Array Configuration ..... A6.6-1

A6.6.2 HAC Array Results ..... A6.6-1

**A6.7 Fissile Material Packages for Air Transport..... A6.7-1**

**A6.8 Benchmark Evaluations ..... A6.8-1**

**A6.9 Appendices..... A6.9-1**

A6.9.1 Single Package Model ..... A6.9.1-1

A6.9.2 Infinite Array Model ..... A6.9.2-1

**A7.0 PACKAGE OPERATIONS ..... A7-1**

A7.1 Package Loading ..... A7-1

A7.2 Package Unloading ..... A7-1

A7.3 Preparation of an Empty Package for Transport..... A7-1

A7.4 Preshipment Leakage Rate Test ..... A7-1

**A8.0 ACCEPTANCE TESTS AND MAINTENANCE PROGRAM ..... A8-1**

## **APPENDIX B: EXCESS MATERIAL ASSEMBLY AND AFS-B WITH MOX RODS**

<b>B1.0 GENERAL INFORMATION</b> .....	<b>B1.1-1</b>
<b>B1.1 Introduction</b> .....	<b>B1.1-1</b>
<b>B1.2 Package Description</b> .....	<b>B1.2-1</b>
B1.2.1 Packaging .....	B1.2-1
B1.2.2 Containment System.....	B1.2-1
B1.2.3 Contents of Packaging.....	B1.2-2
B1.2.3.1 Radionuclide Inventory.....	B1.2-2
B1.2.3.2 Maximum Payload Weight .....	B1.2-2
B1.2.3.3 Maximum Decay Heat .....	B1.2-3
B1.2.3.4 Maximum Pressure Buildup .....	B1.2-3
B1.2.4 Operational Features.....	B1.2-3
<b>B1.3 General Requirements for All Packages</b> .....	<b>B1.3-1</b>
<b>B1.4 Appendices</b> .....	<b>B1.4-1</b>
B1.4.1 Nomenclature .....	B1.4-1
B1.4.2 Packaging General Arrangement Drawings .....	B1.4-1
<b>B2.0 STRUCTURAL EVALUATION</b> .....	<b>B2-1</b>
<b>B2.1 Structural Design</b> .....	<b>B2-1</b>
B2.1.1 Discussion .....	B2-1
B2.1.2 Design Criteria .....	B2-1
B2.1.3 Weights and Center of Gravity.....	B2-2
<b>B2.2 Materials</b> .....	<b>B2-2</b>
<b>B2.3 Fabrication and Examination</b> .....	<b>B2-3</b>
<b>B2.4 Lifting and Tie-down Standards for All Packages</b> .....	<b>B2-3</b>
<b>B2.5 General Considerations</b> .....	<b>B2-3</b>
<b>B2.6 Normal Conditions of Transport</b> .....	<b>B2-3</b>
B2.6.1 Heat .....	B2-3
B2.6.2 Cold .....	B2-4
B2.6.3 Reduced External Pressure.....	B2-4
B2.6.4 Increased External Pressure .....	B2-4
B2.6.5 Vibration and Shock.....	B2-4
B2.6.6 Water Spray .....	B2-4

B2.6.7	Free Drop.....	B2-4
B2.6.8	Corner Drop.....	B2-5
B2.6.9	Compression.....	B2-5
B2.6.10	Penetration.....	B2-5
<b>B2.7</b>	<b>Hypothetical Accident Conditions.....</b>	<b>B2-5</b>
B2.7.1	Free Drop.....	B2-5
B2.7.2	Crush .....	B2-8
B2.7.3	Puncture.....	B2-8
B2.7.4	Thermal .....	B2-8
B2.7.4.1	Summary of Pressures and Temperatures.....	B2-8
B2.7.4.2	Differential Thermal Expansion .....	B2-9
B2.7.4.3	Stress Calculations.....	B2-9
B2.7.5	Immersion – Fissile Material.....	B2-9
B2.7.6	Immersion – All Packages.....	B2-9
B2.7.7	Deep Water Immersion Test (for Type B Packages Containing More than $10^5$ A <sub>2</sub> ).....	B2-9
B2.7.8	Summary of Damage.....	B2-9
<b>B2.8</b>	<b>Accident Conditions for Air Transport of Plutonium.....</b>	<b>B2-9</b>
<b>B2.9</b>	<b>Accident Conditions for Fissile Material Packages for Air Transport.....</b>	<b>B2-9</b>
<b>B2.10</b>	<b>Special Form.....</b>	<b>B2-10</b>
<b>B2.11</b>	<b>Fuel Rods .....</b>	<b>B2-10</b>
<b>B2.12</b>	<b>Appendices.....</b>	<b>B2-10</b>
<b>B3.0</b>	<b>THERMAL EVALUATION.....</b>	<b>B3.1-1</b>
<b>B3.1</b>	<b>Description of Thermal Design.....</b>	<b>B3.1-1</b>
B3.1.1	Design Features .....	B3.1-1
B3.1.2	Content’s Decay Heat.....	B3.1-1
B3.1.3	Summary of Temperatures .....	B3.1-1
B3.1.4	Summary of Maximum Pressures .....	B3.1-2
<b>B3.2</b>	<b>Material Properties and Component Specifications.....</b>	<b>B3.2-1</b>
B3.2.1	Material Properties .....	B3.2-1
B3.2.2	Component Specifications.....	B3.2-1
<b>B3.3</b>	<b>General Considerations.....</b>	<b>B3.3-1</b>
B3.3.1	Evaluations by Analysis .....	B3.3-1
B3.3.1.1	NCT Analytical Model .....	B3.3-1
B3.3.1.2	HAC Analytical Model.....	B3.3-5

B3.3.2	Evaluation by Test .....	B3.3-5
B3.3.3	Margins of Safety .....	B3.3-6
<b>B3.4</b>	<b>Thermal Evaluation for Normal Conditions of Transport .....</b>	<b>B3.4-1</b>
B3.4.1	Heat and Cold .....	B3.4-1
B3.4.1.1	Heat .....	B3.4-1
B3.4.1.2	Cold .....	B3.4-1
B3.4.2	Maximum Normal Operating Pressure .....	B3.4-2
B3.4.3	Maximum Thermal Stresses .....	B3.4-3
B3.4.4	Evaluation of Package Performance for Normal Conditions of Transport .....	B3.4-3
<b>B3.5</b>	<b>Thermal Evaluation under Hypothetical Accident Conditions .....</b>	<b>B3.5-1</b>
B3.5.1	Initial Conditions .....	B3.5-1
B3.5.2	Fire Test Conditions .....	B3.5-1
B3.5.2.1	Analytical Model .....	B3.5-1
B3.5.3	Maximum Temperatures and Pressures .....	B3.5-1
B3.5.3.1	Maximum Temperatures .....	B3.5-1
B3.5.3.2	Maximum Pressures .....	B3.5-2
B3.5.4	Accident Conditions for Fissile Material Packages for Air Transport .....	B3.5-2
B3.5.5	Evaluation of Package Performance for Accident Conditions of Transport .....	B3.5-3
<b>B3.6</b>	<b>Appendices .....</b>	<b>B3.6.1-1</b>
B3.6.1	Computer Analysis Results .....	B3.6.1-1
<b>B4.0</b>	<b>CONTAINMENT .....</b>	<b>B4-1</b>
<b>B5.0</b>	<b>SHIELDING .....</b>	<b>B5-1</b>
<b>B6.0</b>	<b>CRITICALITY EVALUATION .....</b>	<b>B6.1-1</b>
<b>B6.1</b>	<b>Description of Criticality Design .....</b>	<b>B6.1-1</b>
B6.1.1	Design Features Important for Criticality .....	B6.1-1
B6.1.2	Summary Table of Criticality Evaluation .....	B6.1-1
B6.1.3	Criticality Safety Index .....	B6.1-2
<b>B6.2</b>	<b>Fissile Material Contents .....</b>	<b>B6.2-1</b>
<b>B6.3</b>	<b>General Considerations .....</b>	<b>B6.3-1</b>
B6.3.1	Model Configuration .....	B6.3-1
B6.3.1.1	Contents Model .....	B6.3-1
B6.3.1.2	Packaging Model .....	B6.3-1

B6.3.2	Material Properties .....	B6.3-1
B6.3.3	Computer Codes and Cross-Section Libraries .....	B6.3-1
B6.3.4	Demonstration of Maximum Reactivity .....	B6.3-1
<b>B6.4</b>	<b>Single Package Evaluation .....</b>	<b>B6.4-1</b>
B6.4.1	Single Package Configuration .....	B6.4-1
B6.4.1.1	NCT Configuration .....	B6.4-1
B6.4.1.2	HAC Configuration .....	B6.4-1
B6.4.2	Single Package Results .....	B6.4-3
<b>B6.5</b>	<b>Evaluation of Package Arrays Under Normal Conditions of Transport.....</b>	<b>B6.5-1</b>
<b>B6.6</b>	<b>Package Arrays Under Hypothetical Accident Conditions.....</b>	<b>B6.6-1</b>
B6.6.1	HAC Array Configuration .....	B6.6-1
B6.6.2	HAC Array Results .....	B6.6-1
<b>B6.7</b>	<b>Fissile Material Packages for Air Transport.....</b>	<b>B6.7-1</b>
<b>B6.8</b>	<b>Benchmark Evaluations .....</b>	<b>B6.8-1</b>
<b>B6.9</b>	<b>Appendices.....</b>	<b>B6.9-1</b>
B6.9.1	Single Package Model .....	B6.9.1-1
B6.9.2	Infinite Array Model .....	B6.9.2-1
<b>B7.0</b>	<b>PACKAGE OPERATIONS .....</b>	<b>B7-1</b>
B7.1	Package Loading .....	B7-1
B7.2	Package Unloading .....	B7-1
B7.3	Preparation of an Empty Package for Transport.....	B7-1
B7.4	Preshipment Leakage Rate Test .....	B7-2
<b>B8.0</b>	<b>ACCEPTANCE TESTS AND MAINTENANCE PROGRAM .....</b>	<b>B8-1</b>
<b>B8.1</b>	<b>Acceptance Tests .....</b>	<b>B8-1</b>
B8.1.1	Visual Inspections and Measurements .....	B8-1
B8.1.2	Weld Inspections .....	B8-1
B8.1.3	Structural and Pressure Tests .....	B8-1
B8.1.4	Fabrication Leakage Rate Tests .....	B8-1
B8.1.5	Component and Material Tests.....	B8-1
B8.1.6	Shielding Tests .....	B8-1
B8.1.7	Thermal Tests .....	B8-1
<b>B8.2</b>	<b>Maintenance Program .....</b>	<b>B8-2</b>

## APPENDIX C: AFS-C WITH TA-18 MOX RODS

<b>C1.0 GENERAL INFORMATION.....</b>	<b>C1.1-1</b>
<b>C1.1 Introduction.....</b>	<b>C1.1-1</b>
<b>C1.2 Package Description .....</b>	<b>C1.2-1</b>
C1.2.1 Packaging .....	C1.2-1
C1.2.2 Containment System.....	C1.2-2
C1.2.3 Contents of Packaging.....	C1.2-2
C1.2.3.1 Radionuclide Inventory.....	C1.2-2
C1.2.3.2 Maximum Payload Weight .....	C1.2-2
C1.2.3.3 Maximum Decay Heat .....	C1.2-3
C1.2.3.4 Maximum Pressure Buildup .....	C1.2-3
C1.2.4 Operational Features.....	C1.2-3
<b>C1.3 General Requirements for All Packages.....</b>	<b>C1.3-1</b>
<b>C1.4 Appendices.....</b>	<b>C1.4-1</b>
C1.4.1 Nomenclature .....	C1.4-1
C1.4.2 Packaging General Arrangement Drawings .....	C1.4-1
<b>C2.0 STRUCTURAL EVALUATION.....</b>	<b>C2-1</b>
<b>C2.1 Structural Design .....</b>	<b>C2-1</b>
C2.1.1 Discussion .....	C2-1
C2.1.2 Design Criteria .....	C2-1
C2.1.3 Weights and Center of Gravity.....	C2-2
<b>C2.2 Materials.....</b>	<b>C2-2</b>
<b>C2.3 Fabrication and Examination .....</b>	<b>C2-3</b>
<b>C2.4 Lifting and Tie-down Standards for All Packages .....</b>	<b>C2-3</b>
<b>C2.5 General Considerations.....</b>	<b>C2-3</b>
<b>C2.6 Normal Conditions of Transport.....</b>	<b>C2-3</b>
C2.6.1 Heat .....	C2-3
C2.6.2 Cold .....	C2-4
C2.6.3 Reduced External Pressure.....	C2-4
C2.6.4 Increased External Pressure .....	C2-4
C2.6.5 Vibration and Shock.....	C2-4
C2.6.6 Water Spray .....	C2-4
C2.6.7 Free Drop.....	C2-5

C2.6.8	Corner Drop.....	C2-5
C2.6.9	Compression.....	C2-5
C2.6.10	Penetration.....	C2-5
<b>C2.7</b>	<b>Hypothetical Accident Conditions.....</b>	<b>C2-5</b>
C2.7.1	Free Drop.....	C2-5
C2.7.2	Crush .....	C2-10
C2.7.3	Puncture.....	C2-10
C2.7.4	Thermal .....	C2-11
C2.7.4.1	Summary of Pressures and Temperatures.....	C2-11
C2.7.4.2	Differential Thermal Expansion .....	C2-11
C2.7.4.3	Stress Calculations.....	C2-11
C2.7.5	Immersion – Fissile Material.....	C2-11
C2.7.6	Immersion – All Packages.....	C2-11
C2.7.7	Deep Water Immersion Test (for Type B Packages Containing More than $10^5$ A <sub>2</sub> ).....	C2-11
C2.7.8	Summary of Damage.....	C2-11
<b>C2.8</b>	<b>Accident Conditions for Air Transport of Plutonium.....</b>	<b>C2-12</b>
<b>C2.9</b>	<b>Accident Conditions for Fissile Material Packages for Air Transport.....</b>	<b>C2-12</b>
<b>C2.10</b>	<b>Special Form.....</b>	<b>C2-12</b>
<b>C2.11</b>	<b>Fuel Rods .....</b>	<b>C2-12</b>
<b>C2.12</b>	<b>Appendices.....</b>	<b>C2-12</b>
<b>C3.0</b>	<b>THERMAL EVALUATION.....</b>	<b>C3.1-1</b>
<b>C3.1</b>	<b>Description of Thermal Design.....</b>	<b>C3.1-1</b>
C3.1.1	Design Features .....	C3.1-1
C3.1.2	Content’s Decay Heat.....	C3.1-1
C3.1.3	Summary of Temperatures .....	C3.1-2
C3.1.4	Summary of Maximum Pressures .....	C3.1-2
<b>C3.2</b>	<b>Material Properties and Component Specifications.....</b>	<b>C3.2-1</b>
C3.2.1	Material Properties .....	C3.2-1
C3.2.2	Component Specifications.....	C3.2-1
<b>C3.3</b>	<b>General Considerations.....</b>	<b>C3.3-1</b>
C3.3.1	Evaluations by Analysis .....	C3.3-1
C3.3.1.1	NCT Analytical Model .....	C3.3-1
C3.3.1.2	HAC Analytical Model.....	C3.3-5
C3.3.2	Evaluation by Test.....	C3.3-6

C3.3.3	Margins of Safety .....	C3.3-6
<b>C3.4</b>	<b>Thermal Evaluation for Normal Conditions of Transport .....</b>	<b>C3.4-1</b>
C3.4.1	Heat and Cold .....	C3.4-1
C3.4.1.1	Heat .....	C3.4-1
C3.4.1.2	Cold .....	C3.4-2
C3.4.2	Maximum Normal Operating Pressure .....	C3.4-2
C3.4.3	Maximum Thermal Stresses .....	C3.4-4
C3.4.4	Evaluation of Package Performance for Normal Conditions of Transport .....	C3.4-4
<b>C3.5</b>	<b>Thermal Evaluation under Hypothetical Accident Conditions .....</b>	<b>C3.5-1</b>
C3.5.1	Initial Conditions .....	C3.5-1
C3.5.2	Fire Test Conditions .....	C3.5-1
C3.5.2.1	Analytical Model .....	C3.5-1
C3.5.3	Maximum Temperatures and Pressures .....	C3.5-1
C3.5.3.1	Maximum Temperatures .....	C3.5-1
C3.5.3.2	Maximum Pressures .....	C3.5-2
C3.5.4	Accident Conditions for Fissile Material Packages for Air Transport....	C3.5-2
C3.5.5	Evaluation of Package Performance for Accident Conditions of Transport .....	C3.5-3
<b>C3.6</b>	<b>Appendices .....</b>	<b>C3.6.1-1</b>
C3.6.1	Computer Analysis Results .....	C3.6.1-1
<b>C4.0</b>	<b>CONTAINMENT .....</b>	<b>C4-1</b>
<b>C5.0</b>	<b>SHIELDING .....</b>	<b>C5-1</b>
<b>C6.0</b>	<b>CRITICALITY EVALUATION .....</b>	<b>C6.1-1</b>
<b>C6.1</b>	<b>Description of Criticality Design .....</b>	<b>C6.1-1</b>
C6.1.1	Design Features Important for Criticality .....	C6.1-1
C6.1.2	Summary Table of Criticality Evaluation .....	C6.1-1
C6.1.3	Criticality Safety Index .....	C6.1-2
<b>C6.2</b>	<b>Fissile Material Contents .....</b>	<b>C6.2-1</b>
<b>C6.3</b>	<b>General Considerations .....</b>	<b>C6.3-1</b>
C6.3.1	Model Configuration .....	C6.3-1
C6.3.1.1	Contents Model .....	C6.3-1
C6.3.1.2	Packaging Model .....	C6.3-1
C6.3.2	Material Properties .....	C6.3-1
C6.3.3	Computer Codes and Cross-Section Libraries .....	C6.3-1



C6.3.4	Demonstration of Maximum Reactivity .....	C6.3-2
<b>C6.4</b>	<b>Single Package Evaluation .....</b>	<b>C6.4-1</b>
C6.4.1	Single Package Configuration .....	C6.4-1
C6.4.1.1	NCT Configuration .....	C6.4-1
C6.4.1.2	HAC Configuration.....	C6.4-1
C6.4.2	Single Package Results.....	C6.4-6
<b>C6.5</b>	<b>Evaluation of Package Arrays Under Normal Conditions of Transport.....</b>	<b>C6.5-1</b>
C6.5.1	NCT Array Configuration .....	C6.5-1
C6.5.2	NCT Array Results.....	C6.5-1
<b>C6.6</b>	<b>Package Arrays Under Hypothetical Accident Conditions.....</b>	<b>C6.6-1</b>
C6.6.1	HAC Array Configuration.....	C6.6-1
C6.6.2	HAC Array Results .....	C6.6-2
<b>C6.7</b>	<b>Fissile Material Packages for Air Transport.....</b>	<b>C6.7-1</b>
<b>C6.8</b>	<b>Benchmark Evaluations .....</b>	<b>C6.8-1</b>
<b>C6.9</b>	<b>Appendices.....</b>	<b>C6.9-1</b>
C6.9.1	Single Package Model .....	C6.9.1-1
C6.9.2	Infinite Array Model .....	C6.9.2-1
<b>C7.0</b>	<b>PACKAGE OPERATIONS .....</b>	<b>C7-1</b>
C7.1	Package Loading.....	C7-1
C7.2	Package Unloading .....	C7-1
C7.3	Preparation of an Empty Package for Transport.....	C7-2
C7.4	Preshipment Leakage Rate Test.....	C7-2
<b>C8.0</b>	<b>ACCEPTANCE TESTS AND MAINTENANCE PROGRAM.....</b>	<b>C8-1</b>
<b>C8.1</b>	<b>Acceptance Tests .....</b>	<b>C8-1</b>
C8.1.1	Visual Inspections and Measurements .....	C8-1
C8.1.2	Weld Inspections .....	C8-1
C8.1.3	Structural and Pressure Tests .....	C8-1
C8.1.4	Fabrication Leakage Rate Tests .....	C8-1
C8.1.5	Component and Material Tests.....	C8-1
C8.1.6	Shielding Tests .....	C8-1
C8.1.7	Thermal Tests.....	C8-1
<b>C8.2</b>	<b>Maintenance Program.....</b>	<b>C8-2</b>



This page left intentionally blank.

## 1.0 GENERAL INFORMATION

This chapter of the Mixed Oxide Fresh Fuel Package (MFFP) Safety Analysis Report (SAR) presents a general introduction and description of the package. The MFFP is utilized for transport of mixed oxide (MOX) fresh fuel assemblies in accordance with the requirements of 10 CFR 71<sup>1</sup> and 49 CFR 173<sup>2</sup>. The major components of the packaging system are shown in Figure 1.1-1. The containment boundary is identified in Figure 1.1-2. Additional figures and schematics are presented in support of the discussion within this chapter. Terminology used throughout this SAR is presented in Section 1.4.1, *Nomenclature*. General arrangement drawings of the packaging are provided in Appendix 1.4.2, *Packaging General Arrangement Drawings*.

The main body of the SAR provides the analysis for the contents of three (3) intact fuel assemblies. Three Appendices have been added to the main SAR to address three additional contents:

**Appendix A:** Replacing up to three (3) standard fuel assemblies with Areva Rod Box 17 (ARB-17) containers. Each ARB-17 may contain up to 17 standard MOX fuel rods. The fuel rods may be undamaged or slightly damaged.

**Appendix B:** Contents of up to one (1) AFS-B rod container, and one (1) Excess Material Assembly (EMA). The AFS-B may contain up to 175 standard MOX fuel rods. For transportation purposes, the EMA is equivalent to a MOX fuel assembly.

**Appendix C:** Contents of up to three (3) AFS-C rod containers containing two types of rods currently stored at Los Alamos Technical Area 18 (TA-18), Exxon rods and Pacific Northwest Laboratory (PNL) rods. TA-18 rods are MOX rods but are not the same as standard MOX rods. Each AFS-C may contain up to 116 Exxon rods and 69 PNL rods.

Each Appendix has eight chapters and follows the same format as the main body of the SAR, referring to the main body of the SAR for information common to both.

### 1.1 Introduction

The Mixed Oxide Fresh Fuel Package, Model: **MFFP**, is designed to transport fresh MOX pressurized water reactor (PWR) reactor fuel assemblies. The packaging is designed to provide a safe means of transporting up to three fresh MOX PWR fuel assemblies, with or without burnable poison rod assemblies (BPRAs) installed.

This SAR contains the information required to conclusively demonstrate that when the MFFP is subjected to the applicable tests described in Subpart F of 10 CFR 71, the applicable requirements of Subpart E of 10 CFR 71 have been met. A combination of analytical and full-scale prototypic testing is used to demonstrate that the MFFP satisfies these requirements. A full-scale, prototypic certification test unit (CTU) was subjected to a series of hypothetical accident condition (HAC) free and puncture drop tests. A detailed discussion of the CTU and certification tests is provided in Appendix 2.12.3, *Certification Test Results*. These tests,

---

<sup>1</sup> Title 10, Code of Federal Regulations, Part 71 (10 CFR 71), *Packaging and Transportation of Radioactive Materials*, Final Rule, 01-26-04.

<sup>2</sup> Title 49, Code of Federal Regulations, Part 173 (49 CFR 173), *Shippers-General Requirements for Shipments and Packagings*, Final Rule, 01-26-04.



coupled with supplementary analytical evaluations, conclusively demonstrated the leaktight<sup>3</sup> containment boundary integrity and criticality control performance of the MFFP.

Based on the shielding and criticality assessments provided in Chapter 5.0, *Shielding Evaluation*, and Chapter 6.0, *Criticality Evaluation*, the Criticality Safety Index (CSI) for the MFFP is zero (0.0), and the Transport Index (TI) is determined at the time of shipment.

Authorization is sought for shipment of the MFFP by all modes of conveyance, except for aircraft, as a Type B(U)F package per the definitions delineated in 10 CFR §71.4.

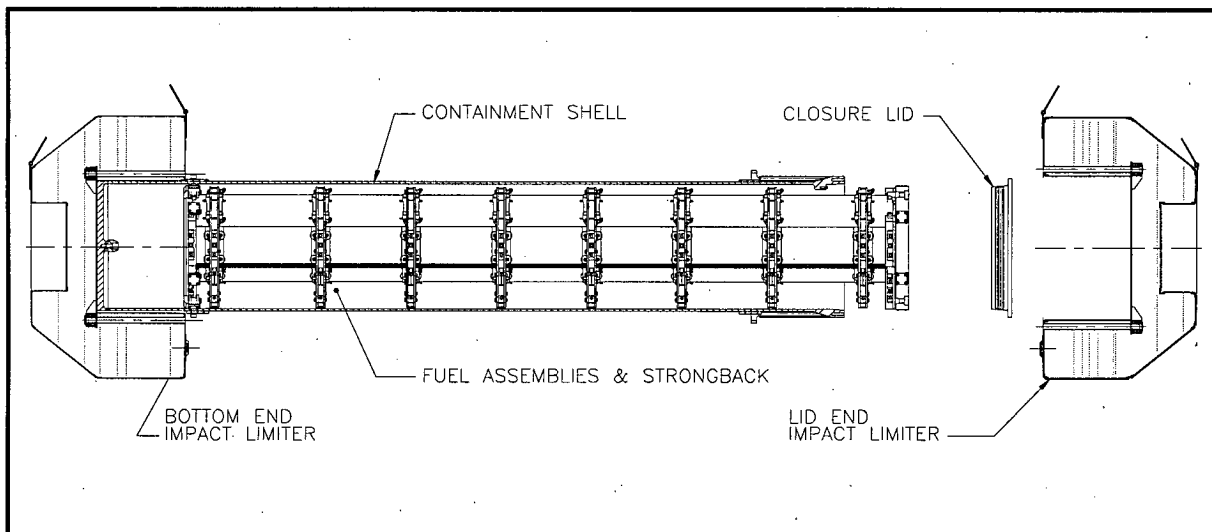


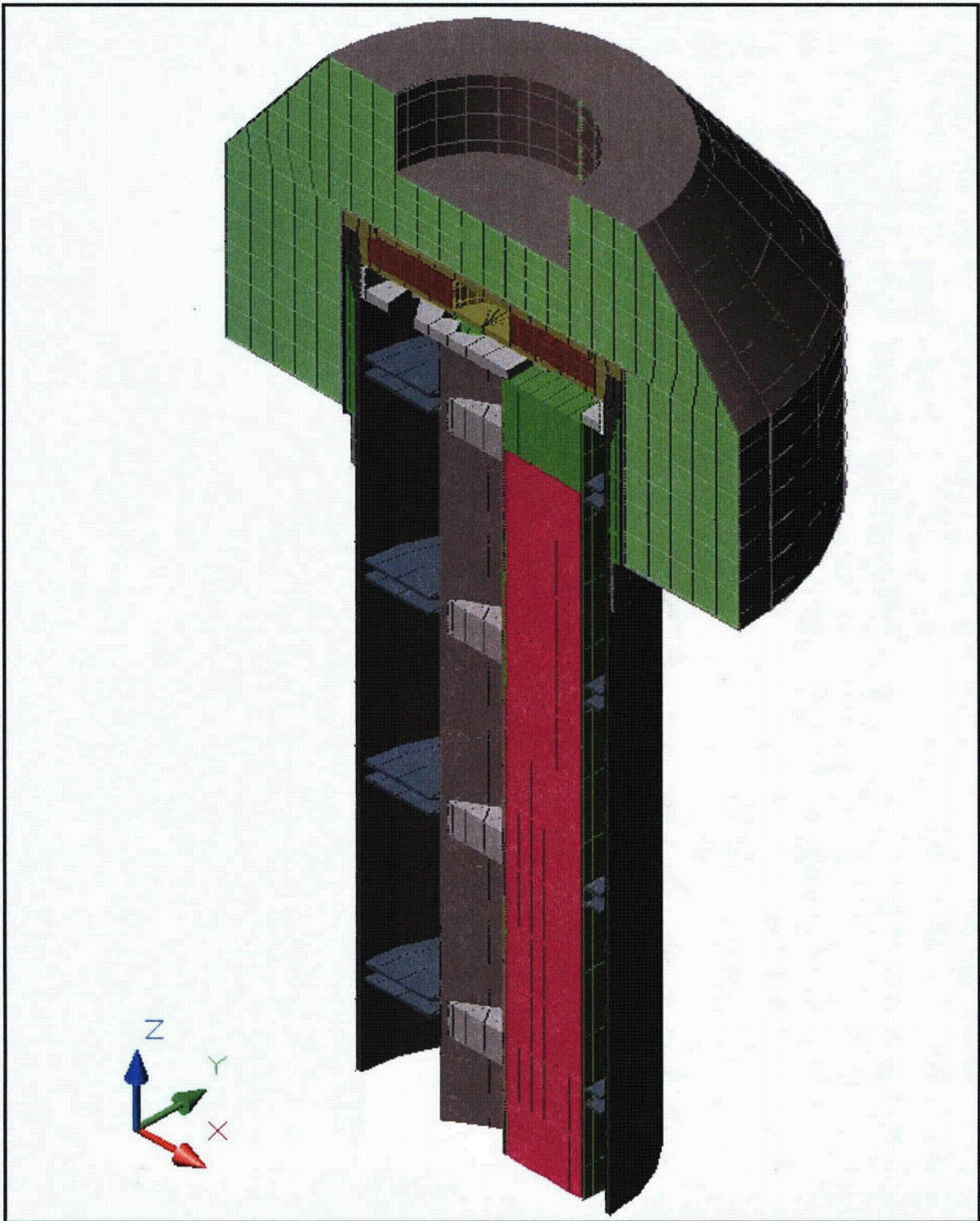
Figure 1.1-1 – Major MFFP Components

<sup>3</sup> Leaktight is defined as  $1 \times 10^{-7}$  standard cubic centimeters per second (scc/s), or less, air leakage per ANSI N14.5-1997, *American National Standard for Radioactive Materials – Leakage Tests on Packages for Shipment*, American National Standards Institute, (ANSI), Inc

**Table 3.3-3 –Summary of Thermal Margins for NCT and HAC Thermal Analyses (°F)**

Item	Hot NCT	Peak HAC	Maximum Allowable		Minimum Temperature Margin <sup>(1)</sup>
			NCT	HAC	
Peak MOX FA	221	518	392	1,337	171
Avg. MOX FA	190	310	392	1,337	202
Poison On Strongback	178	494	850	1,000	506
Poison On FCS	177	652	850	1,000	348
Strongback Structure	178	599	800	800	201
Body Shell	159	1,361	800	2,500	641
Body Collar	149	414	800	1,000	586
Closure Lid	147	301	800	1,000	653
Impact Limiter Lugs	154	1,282	800	2,500	646
<b>Impact Limiter</b>					
• Max. Foam	149	N/A	300	N/A	151
• Bulk Avg. Foam	145	N/A	300	N/A	155
• Skin	149	1,429	800	2,500	651
<b>Impact Limiter Bolts</b>					
• Bolt Head	154	1,283	800	2,500	646
• Bolt Shaft	144	1,006	800	2,500	656
• Bolt Threads	144	295	800	2,500	656
<b>O-ring Seals</b>					
• Closure Lid	159	339	225	400	61 °F
• Vent/Sampling Port	146	295	225	400	79 °F

**Note:** (1) Minimum temperature margin based on **bold** temperatures.



(Note: the positive z-axis is oriented the length of the package and the positive x-axis towards the bottom of the normally horizontal package)

**Figure 3.3-1 – Solid View of NCT Thermal Model**

- The weight loss due to out-gassing not only has direct affect on the heat flux into the remaining virgin foam, but changes the composition of the resulting foam char since the foam constituents are lost at different rates. This change in composition affects both the specific heat and the thermal conductivity of the foam char layer.
- As temperature continues to rise, the developing char layer begins to take on the characteristics of a gas-filled cellular structure where radiative interchange from one cell surface to another becomes a significant portion of the overall heat transfer mechanism. This change in the dominant heat transfer mechanism causes the apparent heat conductivity to take on a highly non-linear relationship with temperature.
- Finally, at temperatures above 1,250 °F, the thermal breakdown of the foam is essentially completed and only about 5 to 10% of the original mass is left. In the absence of direct exposure to a flame or erosion by the channeling of the outgas products through the foam, the char layer will be the same or slightly thicker than the original foam depth. This char layer will continue to provide radiative shielding to the underlying foam material.

Given the observed non-linear variations in the thermal properties and behavior of the FR-3700 foam at elevated temperatures, a thermal modeling method was devised to conservatively simulate the decomposition behavior of the foam during the HAC fire event. As discussed above, the foam begins an irreversible decomposition process at approximately 500 °F, and reaches a stable char at temperatures in excess of 1,250 °F. The decomposition wave front begins at the outer layer and progresses inward with time. The final depth of the char is a function of the foam density and the fire temperature and duration. This decomposition process is conservatively modeled by transforming a thickness of foam equal to the expected final char depth into still air at the beginning of the fire and simulating conduction and radiation across this air-filled 'void' from the hot impact limiter shell to the remaining foam surface. Since the char material would normally completely fill this void and severely restrict the radiative heat transfer mode (the dominant mode at fire temperatures), this approach is conservative.

The depth of the final char thickness which can be expected for the 10 lb<sub>m</sub>/ft<sup>3</sup> density foam used in the top end impact limiter is estimated from a table provided in the FR-3700 product literature<sup>4</sup>, under the section entitled *Fire Protection*, which lists the temperatures obtained from laboratory fire tests. The test specimen was a 5-gallon metal pail filled with the foam material at various densities, and instrumented with thermocouples at specified depths from the top surface. The pail was completely filled with foam and fitted with a metal lid and a burner flame was applied to the lid end of the pail (i.e., the *hot face* or H.F.). The top three rows of the table lists the temperatures achieved at various depths in the foam for 8, 16, and 24 lb<sub>m</sub>/ft<sup>3</sup> density after an elapsed time of 30 minutes<sup>5</sup>, and the maximum temperature reached at each depth. As can be noted from the temperatures achieved at the hot face, the flame temperatures in the tests are considerably hotter than the regulatory fire temperature of 1,475 °F. Therefore, in order to render the data in the table consistent with a regulatory flame temperature of 1,475 °F, the test results were proportionately reduced as a function of depth and an assumed hot face temperature of 1,475 °F. For example, for 8 lb<sub>m</sub>/ft<sup>3</sup> foam at zero depth (i.e., the hot face), the temperature was reduced to 1,475 °F, while at the 1-inch depth the temperature after 30 minutes was reduced to

---

<sup>5</sup> The lower three rows present data for foam with a cover layer of ceramic fiber insulation which is not used in this application and, therefore, not included this discussion.

960 °F. Repeating this process at increasing depths, the temperature was reduced by lesser amounts, until at a depth of 6 inches (where there was no temperature response after 30 minutes) the correction is zero.

The resulting predicted thermal response of the foam for regulatory fire conditions is illustrated in Figure 3.5-5. The figure illustrates the estimated corrected curves for the regulatory flame temperature of 1,475 °F for 8 and 16 lb<sub>m</sub>/ft<sup>3</sup> density foam. Curves for 10, 12, and 14 lb<sub>m</sub>/ft<sup>3</sup> density foams are found by linear interpolation. It should also be noted that this procedure conservatively ignores the non-linear effect of radiation heat transfer wherein the rate of heat transfer to the hot face from the flame would not scale linearly as assumed here, but would scale with the absolute temperature to the fourth power. As such, had this effect been properly accounted for, the actual foam temperatures would be even lower since the heat available to decompose the foam would be significantly lower than assumed by this approach.

Based on the results presented in Figure 3.5-5, the 10 lb<sub>m</sub>/ft<sup>3</sup> foam is predicted to reach approximately 500 °F at a depth of 3 inches after 30 minutes and that the foam temperature at a depth of approximately 4.5 inches would not have responded at all. Given that a temperature of 500 °F represents the point where irreversible foam decomposition occurs, the result indicates that the char depth for 10 lb<sub>m</sub>/ft<sup>3</sup> foam would be 3 inches after 30 minutes of exposure to a 1,475 °F regulatory fire.

Therefore, the performance of the LAST-A-FOAM® FR-3700 during the HAC event is analytically simulated for this application by reducing the depth of foam at each location to conservatively bound the potential loss of the foam from any of the various mechanisms described above. The heat transfer across the resultant void space is then computed based on conduction and radiation across an equivalent air space, despite the fact that the affected foam will typically be simply decomposed to a char layer as opposed to being lost altogether. By removing the foam at the start of the HAC fire transient and by treating the affected foam as a void space for the purposes of computing the radiation heat transfer across the char layer, the modeling conservatively bounds the temperature response of the package to the transient loss of the foam over the time period of the HAC event and the potential loss of a portion of the char layer due to ablation. Specifically, the modeling assumes that the outer 4-inch layer of foam at the circumference of the impact limiter and a 3-inch layer of foam at the flat faces of the impact limiter are lost at the beginning of the HAC event.

### **3.5.3 Maximum Temperatures and Pressures**

#### **3.5.3.1 Maximum Temperatures**

Table 3.5-1 provides a summary of pre-fire, steady-state temperatures, the temperatures at the end of the 30-minute fire event, and the peak temperatures achieved during the subsequent package cooldown. Figure 3.5-6 illustrates the associated temperature distribution within the MFFP at the end of the 30-minute fire. As noted from Table 3.5-1, the peak temperatures for the critical components (e.g., closure and vent port O-ring seals, peak MOX FAs, boral, etc.) are all within their respective allowable limits.

The peak MOX FA temperature achieved during the HAC event is over 800 °F below the allowable short-term limit of 1,337 °F. The strongback and the FCSs effectively shield the FAs from direct exposure to the hot surfaces of the body shell. The peak temperature of 652 °F noted for the boral neutron absorbing material is well below the allowable short-term limit of 1,000 °F.



Although the body shell temperature reaches a peak temperature of approximately 1,360 °F during the HAC event, the time at temperature levels over 1,000 °F is less than 30 minutes (see Figure 3.5-9). As such, no significant permanent loss in material structural properties is expected. In contrast, the body collar and closure lid, which are shielded by the impact limiter structure despite the assumed damage conditions, remain below 500 °F throughout the HAC transient. Figure 3.5-7 illustrates the temperature distribution in the body shell at the end of the 30-minute fire when the peak shell temperature is achieved, while Figure 3.5-8 illustrates the temperature distribution in the shell approximately 2 hours after the end of the 30-minute fire when the peak temperatures at the closure lid bolts is reached.

The peak butyl O-ring seal temperature of 339 °F seen for the closure seal is below the conservatively established short-term limit of 400 °F for exposures of 8 hours or less. The peak vent/sampling port O-ring temperatures are predicted to be approximately 295 °F. As the temperature trends presented in Figure 3.5-10 illustrates, not only are the peak O-ring seal temperatures below the allowable short-term limit of 400 °F, but the transient O-ring seal temperatures demonstrate that the temperature trend for the material complies with the time at temperature limitations defined in Section 3.2, *Material Properties and Component Specifications*.

Figure 3.5-9 and Figure 3.5-10 illustrate the transient temperature response during the simulated HAC event for selected package components.

### 3.5.3.2 Maximum Pressures

With the exception of the consideration for potential out-gassing from components within the body cavity and an assumed 100% failure rate<sup>6</sup> for the MOX fuel rods, the maximum pressure attained for HAC conditions is determined in the same manner as described in Section 3.4.2, *Maximum Normal Operating Pressure*. While the MFFP is designed to protect the MOX FA from catastrophic failure during the pre-fire free and puncture drops and the subsequent 30-minute fire event, this analysis conservatively assumes that the cladding boundary on all fuel rods and poison rods within the MOX FA have been breached. As determined in Section 3.4.2, *Maximum Normal Operating Pressure*, a total of 22.64 g-moles of helium gas exists within the fuel rods of the three (3) MOX FAs within the package.

Further, it is conservatively assumed that the entire mass of the neoprene rubber and the Delrin<sup>®</sup> plastic pads have been volatilized under the elevated temperatures reached within the body cavity during the HAC event. There are approximately 7 pounds of neoprene rubber and 2.3 pounds of Delrin<sup>®</sup> plastic in the body cavity. Volatizing this entire mass would create approximately 143.1 g-moles of gas within the cavity.

Table 3.5-2 presents the predicted pressure within the body cavity prior to the HAC fire, at the end of the 30-minute fire, and 9.5 hours after the end of the fire. As seen, the peak pressure generated within the package cavity is estimated to be 138.2 psia at the end of the fire when the peak cavity gas temperature is reached. The pressure will then decrease as the package cools, reaching 76.5 psia 9.5 hours after the end of the fire.

---

<sup>6</sup> U. S. Nuclear Regulatory Commission, NUREG-1617, Table 4-1, *Standard Review Plan for Transportation Packages for Spent Fuel*, March 2000.



### **3.5.4 Accident Conditions for Fissile Material Packages for Air Transport**

This section does not apply for the MFFP, since air transport is not claimed.

### **3.5.5 Evaluation of Package Performance for Accident Conditions of Transport**

The evaluation of the package performance under HAC conditions demonstrates that the packaging will have sufficient thermal protection remaining after the hypothetical drop and puncture bar damage to protect the thermally sensitive areas of the packaging. All package components are seen as remaining within their associated maximum temperature limits.

6. Unlatch the eight (8) strongback clamp arms and the seven (7) fuel control structures (FCSs) for one of the strongback FA carrier sections by removing the appropriate quick-release pins and rotate each into the full-open position.
7. Ensure that the two fixed clamp pads on the bottom end plate are in their full open positions.
8. Utilizing appropriate lifting equipment, carefully place the FA, still vertically oriented, into the open section of the strongback.
9. Close each of the eight (8) clamp arms and the seven (7) FCSs. Secure each clamp arm and FCS in their closed position with the respective quick-release pin.
10. Using a manual or powered socket wrench, rotate the two tensioning SHCS located at each clamp arm and the bottom end plate clockwise to apply the clamping force to the FA grids. Once all control arms and FCSs are secured, disconnect and remove the lifting equipment from the FA.
11. Rotate the strongback approximately 120 degrees so that the next empty FA section in the strongback is accessible for loading.
12. Repeat Steps 6 through 11 for the second and third FAs (or dummy FAs), as necessary.
13. After the strongback is fully loaded with FAs, close and latch the load/unload station side restraints, and remove the load/unload station top restraint. Ensure the clamp pads on the top plate are fully retracted, and install the top end plate assembly.
14. Install the three (3) outer 3/4-inch SHCS that secure the top plate to the strongback. Tighten to 80 – 90 lb<sub>r</sub>-ft torque, lubricated.
15. Install the three (3) inner 1/2-inch SHCS that secure the top plate to the strongback. Tighten to 23 – 27 lb<sub>r</sub>-ft torque, lubricated.
16. Install the three (3) 3/8-inch SHCS that secure the BPRA restraint weldment to the strongback. Tighten to 23 – 27 lb<sub>r</sub>-ft torque, lubricated.
17. Using a manual or powered socket wrench, rotate the two adjustment screws located at each top plate clamp pad clockwise to apply the clamping force to the FA top nozzle.
18. Tighten the four (4) 3/4-inch swivel clamp pads on the top plate until the screw pad contacts the FA top nozzle. Lock each swivel clamp pad in place with a hex nut.
19. Repeat Step 18 for the second and third FAs (or dummy FAs).

### 7.1.2.2 Loading of the Strongback into the MFFP

#### 7.1.2.2.1 Horizontal Operations

1. Install the strongback lift tool into the receptacle in the center of the top plate of the strongback and connect appropriate lifting equipment. Unlatch the load/unload station side restraints and swing into their full-open position.
2. Lift and transport the strongback from the load/unload station to the insertion/extraction station. Place the strongback on the insertion/extraction station.

**CAUTION:** The strongback must be properly oriented for the insertion operation before the strongback is placed on the insertion/extraction station.

3. Close and latch the strongback restraint arms on the insertion/extraction station. Disconnect from the lifting equipment and remove the strongback lift tool.
4. Connect the insertion/extraction attachment bar by engaging the receptacle in the center of the top plate and raise the strongback.
5. Attach appropriate lifting equipment to the upper attachment point on the insertion/extraction station in preparation for returning the strongback to a horizontal orientation.
6. Detach the installed struts. Lower the insertion/extraction station to a horizontal orientation.
7. Ensure that the MFFP interior is free of debris and/or damage that could prevent proper loading of the strongback.
8. If not already in position, install the sealing surface protector on the MFFP seal flange.  
**NOTE:** The sealing surface protector orientation is labeled along the edge. Correct orientation is required for correct interfacing with the insertion/extraction station.
9. Move and align the MFFP with the package connection collar on the insertion/extraction station.  
**NOTE:** Ensure that the azimuth orientation of the strongback and the lugs integral to the MFFP body are correctly aligned so that strongback insertion can be accomplished without interference.
10. Insert the strongback into the MFFP using the insertion/extraction station. Care shall be taken not to damage the MFFP containment seal surfaces.
11. Install the three (3) 1/2-inch SHCS that secure the strongback to the body. Tighten to 70 – 75 lb<sub>f</sub>-ft torque, lubricated.
12. Disconnect the insertion/extraction station from the strongback.
13. Disconnect and move the MFFP body away from the insertion/extraction station.
14. Remove the sealing surface protector from the MFFP seal flange.

#### **7.1.2.2.2 Vertical Operations**

1. Install the strongback lift tool into the receptacle in the center of the top plate of the strongback and connect appropriate lifting equipment. Unlatch the load/unload station side restraints and swing into their full-open position.
2. Ensure that the MFFP interior is free of debris and/or damage that could prevent proper loading of the strongback.
3. Lift and transport the strongback from the load/unload station and lower into the MFFP. Care shall be taken not to damage the MFFP containment seal surfaces.  
**NOTE:** Ensure that the azimuth orientation of the strongback and the lugs integral to the MFFP body are correctly aligned so that strongback insertion can be accomplished without interference and be removed later using the insertion/extraction station, if desired.
4. Install the three (3) 1/2-inch SHCS that secure the strongback to the body. Tighten to 70 – 75 lbf-ft torque, lubricated.

DOCKET 71-9295

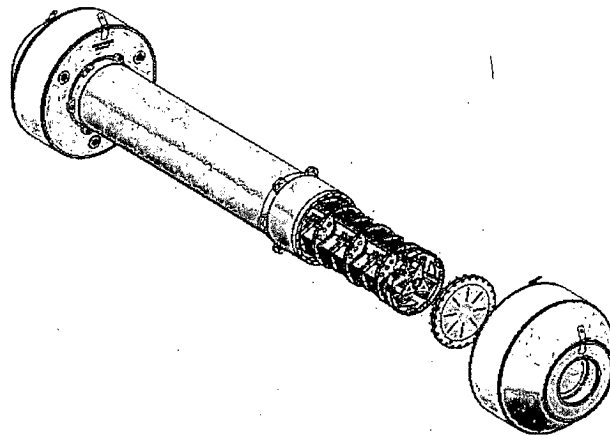


# Mixed Oxide Fresh Fuel Package

**Appendix A: ARB-17**

**Appendix B: AFS-B with 175 MOX rods and  
Excess Material Assembly**

**Appendix C: AFS-C with TA-18 MOX Rods**



***Safety  
Analysis  
Report***

**Volume 2  
Revision 6  
April 2008**

## B1.0 GENERAL INFORMATION

Appendix B of the MOX Fresh Fuel Package (MFFP) Safety Analysis Report (SAR) supports the addition of one (1) AFS-B rod container and one (1) Excess Material Assembly (EMA) as allowable contents of the MFFP. As these items fill only two of the three available strongback locations, the third strongback location is filled with a dummy fuel assembly. Alternately, the AFS-B may be transported separately with two dummy fuel assemblies per strongback, and the EMA may be transported in lieu of a standard fuel assembly.

The AFS-B is a rod container that may transport up to 175 MOX fuel rods. The fuel rod type is identical to the rods comprising the standard MOX fuel assembly described in Chapter 1.0, *General Information*. The EMA is a fuel assembly comprised of MOX fuel rods that do not meet all of the performance requirements of a standard MOX fuel rod, primarily pellet OD and Pu-238 isotopic composition. These out-of-tolerance values have no impact on the licensing analyses.

In this SAR Appendix, reference is made to the main SAR for information that has not changed. Referenced tables, figures, and sections that do not contain the letter "B" (e.g., Table 1.2-1, Figure 3.5-1, Section 6.1.1) refer to items in the main SAR. Referenced tables, figures, and sections that contain the letter "B" (e.g., Table B6.4-1, Figure B1.2-1, Section B6.1.1) refer to items in Appendix B.

### B1.1 Introduction

The Mixed Oxide Fresh Fuel Package, Model: **MFFP**, is designed to transport fresh MOX pressurized water reactor (PWR) reactor fuel assemblies. The AFS-B fuel rod container has outer dimensions consistent with those of a standard fuel assembly and interfaces with the strongback and clamp arms in the same way. The EMA has the same outer dimensions, appearance, and number of fuel rods/guide tubes as a standard MOX fuel assembly.

A full-scale, prototypic certification test unit (CTU) was subjected to a series of hypothetical accident condition (HAC) free and puncture drop tests as part of the original SAR submittal. The results of this testing program are directly applicable to the AFS-B/EMA payload because the loaded AFS-B and EMA weight is bounded by the weight of a fuel assembly (including a BPRA). A detailed discussion of the CTU and certification tests is provided in Appendix 2.12.3, *Certification Test Results*. These tests, coupled with supplementary analytical evaluations, conclusively demonstrated the leaktight<sup>1</sup> containment boundary integrity and criticality control performance of the MFFP.

The thermal analysis for the AFS-B payload is provided in Chapter B3.0, *Thermal Evaluation*. Because an MFFP loaded with an AFS-B and EMA contains significantly less decay heat than three fuel assemblies, MFFP strongback and shell temperatures are bounded by those reported in Chapter 3.0, *Thermal Evaluation*. However, due primarily to the simplistic analytical method employed, for HAC only, the maximum fuel rod temperatures for rods within the AFS-B are computed to be higher than the maximum temperature computed for a fuel assembly. These

---

<sup>1</sup> Leaktight is defined as  $1 \times 10^{-7}$  standard cubic centimeters per second (scc/s), or less, air leakage per ANSI N14.5-1997, *American National Standard for Radioactive Materials – Leakage Tests on Packages for Shipment*, American National Standards Institute, (ANSI), Inc

temperatures are well below the respective temperature limits for a fuel rod. The internal pressure under NCT and HAC with the AFS-B/EMA payload is bounded by the pressure with three fuel assemblies.

Based on the shielding and criticality assessments provided in Chapter B5.0, *Shielding Evaluation*, and Chapter B6.0, *Criticality Evaluation*, the Criticality Safety Index (CSI) for the MFFP is zero (0.0), and the Transport Index (TI) is determined at the time of shipment.

Authorization is sought for shipment of the MFFP containing an AFS-B and/or EMA by all modes of conveyance, except for aircraft, as a Type B(U)F package per the definitions delineated in 10 CFR §71.4.

## B1.2 Package Description

General arrangement drawings of the packaging are provided in Section 1.4.2, *Packaging General Arrangement Drawings*. The addition of the AFS-B and EMA does not alter these packaging drawings. A drawing of the AFS-B rod container is given in Section B1.4.2, *Packaging General Arrangement Drawings*.

### B1.2.1 Packaging

The MFFP packaging description is unchanged from the description provided in Section 1.2.1, *Packaging*. The AFS-B rod container is designed to hold up to 175 MOX fuel rods of the type used in the MOX fuel assemblies. The container has outer cross sectional dimensions of 8.4 inches square, a length from bottom to top of 159.9 inches, and an overall length (to the lift ring bolt head) of 161.2 inches. The primary material of construction of the container is ASTM 6061-T651 aluminum alloy. The two side walls, the bottom plate, and the lid are all 3/4 inches thick. The side plates are attached to the bottom plate with two longitudinal, 3/8-inch groove welds. The lid is attached with twenty-two (22) zinc-plated, 3/8-16 UNC, SAE J429 Grade 8, hex head cap screws. The two square end pieces are made of solid aluminum alloy, and each are attached to the container with eight (8) zinc-plated SAE J429 3/8-16 UNC hex head cap screws made of Grade 8 alloy steel. The lower square end piece is 2.4 inches thick and the upper square end piece is 3.0 inches thick. Each bolt is secured in place using a thin stainless steel lock tab. Two of the eight bolts on each end go horizontally into the lid, in addition to the 22 cap screws on the top of the lid.

Inside the container is a 1/2-inch thick shelf, made of the same aluminum alloy, which fits into 1/4-inch deep grooves in each side wall. The shelf is supported by 1/4-inch thick aluminum gusset plates on 15.3-inch centers. The region between the shelf and the lid is the rod cavity, which is 6.9 inches wide, 3.4 inches deep, and 153.5 inches long. The gussets and the shelf are located with intermittent 1/8-inch fillet welds, none of which are load bearing. Along the inside of the two side plates are two, 2.1-inch wide grooves, 0.4 inches deep. These grooves accommodate the bulkheads used in the AFS-C rod container, but they have no function in the AFS-B container. The components of the AFS-B feature numerous small holes that ensure the AFS-B will not hold pressure.

The lid is lifted by means of two, 1/4-20 UNC threaded holes in the lid. The holes are located such that at least half of the hole is blocked by the top of the sidewall, which prevents an overly-long lifting bolt from possibly damaging any fuel rods. The container is lifted from its top end using a swivel hoist ring. All threaded holes may optionally be fitted with helical-coil thread inserts. The label 'AFS-B' is painted prominently on both sides of the container. The AFS-B is finished with a clear anodize treatment.

An external view of the AFS-B rod container is given in Figure B1.2-1. An internal cross sectional view is given in Figure B2.7-1.

### B1.2.2 Containment System

The containment system description is unchanged from the description provided in Section 1.2.2, *Containment System*.



### B1.2.3 Contents of Packaging

The MFFP may simultaneously transport one (1) AFS-B containing up to 175 standard MOX fuel rods, and one (1) EMA. The 175 fuel rod limit is a geometrical limit based on the size of the cavity, assuming the fuel rods are packed in a hexagonal lattice. If necessary, for a payload of fewer than 175 rods, aluminum or stainless steel dunnage rods are used to take up the remaining space. A non-fuel dummy assembly is utilized in the unoccupied strongback location. The physical size and weight of the non-fuel dummy assemblies are nominally the same as the MK-BW/MOX1 17 × 17 design. Alternately, the AFS-B may be transported separately with two dummy fuel assemblies per strongback, and the EMA may be transported in lieu of a standard fuel assembly.

Because the AFS-B with 175 fuel rods is more reactive than a MOX fuel assembly, it is not acceptable to transport more than one (1) AFS-B per MFFP. Also, the AFS-B cannot be combined in a shipment with more than (1) EMA or standard fuel assembly. For transportation purposes, an EMA and a standard MOX fuel assembly may be considered interchangeable. Examples of acceptable and unacceptable loading configurations are summarized below:

Acceptable Loading Configurations	Unacceptable Loading Configurations
1 AFS-B, 1 EMA/fuel assembly, 1 dummy	1 AFS-B, 2 EMAs/fuel assemblies
1 AFS-B, 2 dummies	2 AFS-Bs, 1 dummy
Any combination of fuel assemblies, EMAs, and dummy fuel assemblies	3 AFS-Bs

The physical parameters for a fuel rod provided in Table 1.2-1 and nuclear design parameters provided in Table 1.2-2 are applicable to rods in the AFS-B. These parameters are also applicable to the EMA, with the exceptions that the OD of the fuel pellets may be out of tolerance (nominal pellet diameter = 0.323 inch), and the weight percent Pu-238 exceeds the 0.05 wt.% limit specified in Table 1.2-2 (EMA fuel rods have Pu-238/Pu as high as 0.19 wt.%). Pu-238 is a neutronic poison and is neglected in the criticality analysis, so there is no safety concern associated with this value being outside of the tolerance. Minor fluctuations of the fuel pellet OD are also negligible.

#### B1.2.3.1 Radionuclide Inventory

The nuclear parameters for the AFS-B rods are unchanged from those provided in Table 1.2-2. As noted above, the rods in the EMA do not meet the performance specifications of a standard fuel rod, although the differences are minor and without safety significance.

#### B1.2.3.2 Maximum Payload Weight

The loaded AFS-B has a payload weight of approximately 1,500 pounds. The EMA, which weighs approximately the same as a standard MOX fuel assembly and will not be loaded with a burnable poison rod assembly (BPRA), weighs less than the 1,580 pound design weight of a fuel assembly loaded with a BPRA. The combined payload weight of the AFS-B, EMA, and dummy fuel assembly is therefore bounded by the value of 4,740 pounds provided in Section 1.2.3.2, *Maximum Payload Weight*.

### B1.2.3.3 Maximum Decay Heat

Assuming that the EMA has a maximum decay heat of 80 watts, and the loaded AFS-B has a maximum decay heat of  $175/264 * 80 = 53$  watts, the maximum decay heat for this payload is 133 watts. This maximum heat load is bounded by the 240 watts provided in Section 1.2.3.3, *Maximum Decay Heat*.

### B1.2.3.4 Maximum Pressure Buildup

The maximum normal operating pressure (MNOP) is bounded by the 10 psig value provided in Section 1.2.3.4, *Maximum Pressure Buildup*. The design pressure of 25 psig is also unchanged.

## B1.2.4 Operational Features

Operating procedures and instructions for loading, unloading, and preparing an empty MFFP for transport with the AFS-B and EMA are provided in Chapter B7.0, *Package Operations*.

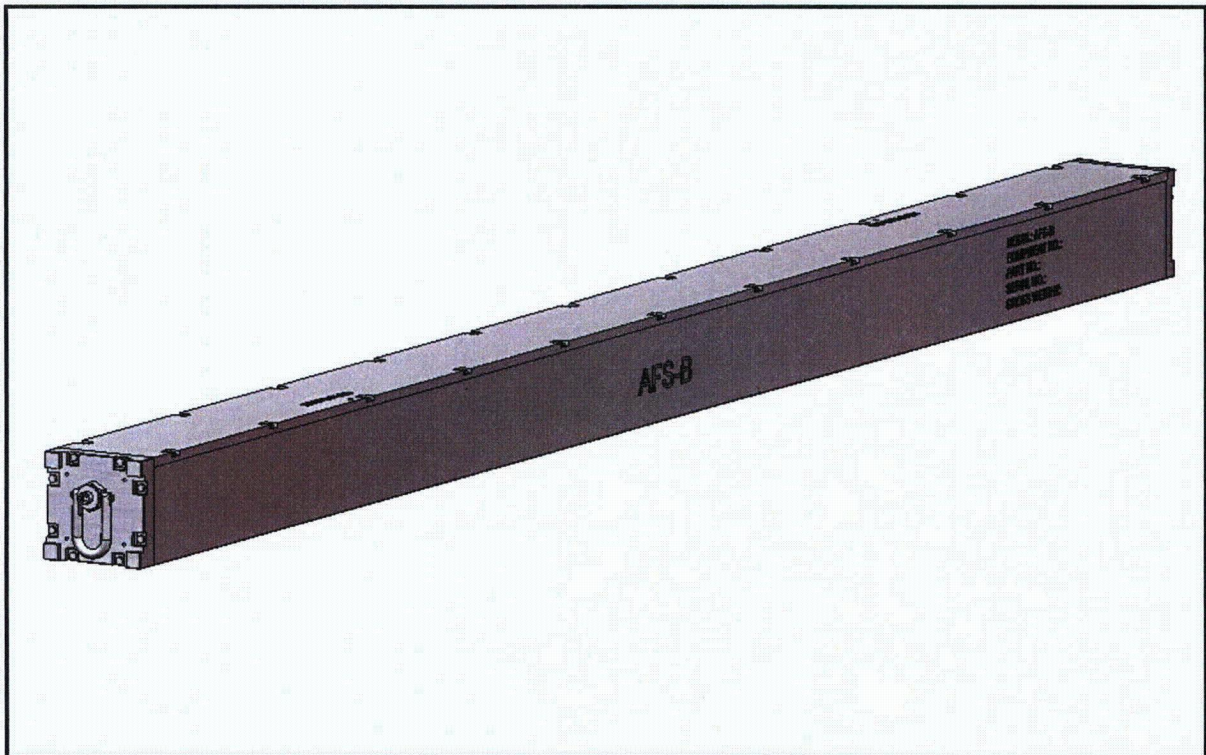


Figure B1.2-1 – AFS-B Rod Container

This page left intentionally blank.

### **B1.3 General Requirements for All Packages**

The AFS-B and EMA have no effect on the way in which the MFFP meets the general requirements for packaging.

This page left intentionally blank.

## B1.4 Appendices

### B1.4.1 Nomenclature

The nomenclature list from Section 1.4.1, *Nomenclature*, is applicable. Additional nomenclature listed below.

**AFS-B** – Container used to transport up to 175 standard MOX fuel rods. The AFS-B interfaces with the strongback in the same manner as a fuel assembly.

**Excess Material Assembly (EMA)** – Fuel assembly comprised of 264 fuel rods that do not necessarily meet the performance requirements of a standard MOX fuel rod. An EMA has the same outer dimensions and visual appearance of a standard fuel assembly.


### B1.4.2 Packaging General Arrangement Drawings

The general arrangement drawings of the body, strongback, and impact limiters are unchanged from those provided in Section 1.4.2, *Packaging General Arrangement Drawings*. The following AFS-B drawing is included in this section:

- 99008-60, Rev. 0, 2 sheets, *AFS-B Assembly*

This page left intentionally blank.

Figure Withheld Under 10 CFR 2.390

		AREVA Federal Services LLC Packaging Projects Tacoma, WA 98402	
AFS-B ASSEMBLY SAR DRAWING			
SCALE: 1:5		WT. ~ LBS	
REV: 0		SHEET 1 OF 2	
DWG SIZE	DWG NO. 99008-60		
CADFILE: 99008600.SLDDRW			



*Figure Withheld Under 10 CFR 2.390*

## B2.0 STRUCTURAL EVALUATION

This chapter of Appendix B provides a structural evaluation of the MFFP when transporting one (1) AFS-B rod container and one (1) Excess Material Assembly (EMA). As these items fill only two of the three available strongback locations, the third strongback location is filled with a dummy fuel assembly. Alternately, the AFS-B may be transported separately with two dummy fuel assemblies per strongback, and the EMA may be transported in lieu of a standard fuel assembly. It is demonstrated that all quantities of interest are bounded by the analyses presented in Chapter 2.0, *Structural Evaluation*.

### B2.1 Structural Design

#### B2.1.1 Discussion

A comprehensive discussion of the MFFP design and standard configuration is provided in Section 1.2, *Package Description*. The MFFP drawings show the detailed geometry of the package, as well as the dimensions, tolerances, materials, and fabrication requirements, and are provided in Appendix 1.4.2, *Packaging General Arrangement Drawings*.

A physical description of the AFS-B rod container is provided in Section B1.2.3, *Contents of Packaging*, and is shown in the drawings in Appendix B1.4.2, *Packaging General Arrangement Drawings*. The AFS-B container is a robust box designed to provide confinement of individual fuel rods under all conditions of transport. The AFS-B container has the same external boundary dimensions as a standard MOX fuel assembly, and thus is loaded, mounted, and unloaded from the strongback in the same manner as a fuel assembly. The structural evaluations and testing performed as part of the original license activities adequately characterize the performance of the MFFP with this payload.

The EMA is structurally identical to a MOX fuel assembly, and its structural response will be the same as a MOX fuel assembly described in Chapter 2.0, *Structural Evaluation*. Therefore, no additional structural evaluations are necessary for this item.

#### B2.1.2 Design Criteria

The MFFP design criteria are unchanged from those provided in Section 2.1.2, *Design Criteria*. The design criteria for the AFS-B rod container are based on the functional requirement that the rod container confine the rods inside the container boundary under all NCT and HAC. Because the AFS-B rod container is transported within the MFFP strongback, it is protected from gross distortion by the fuel control structure (FCS). As shown in Section 2.12.5, *Fuel Control Structure Evaluation*, the FCS provides a limit to any reconfiguration of the fuel assembly which could occur as a result of the worst case HAC event. The MOX fuel assembly consists of a larger number of rods (264) than is contained in the AFS-B rod container (175). In addition, the rods in the MOX fuel assembly are unconfined by any structure other than the FCS, whereas fuel rods in the AFS-B rod container are confined within a container having significant structure. Therefore, gross distortion of the fuel rods or of the AFS-B container, or escape of the fuel rods from the container, will not occur.

To enhance criticality safety by preventing the potential for damage to the fuel rods in the HAC free drop impact event, the AFS-B rod container is designed to minimize the relative motion of the rods under impact conditions. To accomplish this, the AFS-B rod container is designed to limit the “rattle space” of the fuel rods (including any dummy rods as necessary) to less than approximately one half rod diameter.

The only component of the AFS-B container which is not supported externally by the strongback or FCS is the internal shelf. To ensure that the “rattle space” available to the rods cannot increase as a result of the free drop impact event, the internal shelf is designed to have a primary bending stress less than the yield point of the shelf material at NCT maximum temperature.

### B2.1.3 Weights and Center of Gravity

The loaded weight of the AFS-B, conservatively assuming 175 fuel rods, is bounded by 1,500 pounds, which is 5% less than the gross weight of 1,580 pounds for a fuel assembly or dummy fuel assembly. Because the EMA will not contain a burnable poison rod assembly (BPRA), the EMA weight is bounded by the 1,580 pound design weight of the combined fuel assembly and BPRA. Therefore, the weight of the MFFP when transporting one (1) AFS-B, one (1) EMA, and one (1) dummy fuel assembly is bounded by the weights given in Section 2.1.3, *Weights and Center of Gravity*, for transport of MOX fuel assemblies.

The longitudinal center of gravity (CG) of the package is essentially unchanged from that reported in Section 2.1.3, *Weights and Center of Gravity*, or 103.7 inches from the bottom end impact limiter.

## B2.2 Materials

The AFS-B is constructed primarily of ASTM B209, 6061-T651 aluminum plate material. The lid and ends are attached with SAE J429 zinc-plated hex head cap screws made from Grade 8 material. A stainless steel swivel hoist ring is included for lifting. No non-metallic materials are used in the AFS-B. These materials do not result in any chemical or galvanic reactions, and are not significantly affected by radiation. The material properties for the aluminum material at 200 °F needed for calculations are given in Table B2.2-1, and are taken from the ASME B&PV Code,<sup>1</sup> as noted. Note that although there is limited welding of the 6061 material, welding is not used in regions where the material properties of unwelded material are used in stress analysis.

**Table B2.2-1 - Material Properties of ASTM B209 6061-T651 Aluminum Alloy at 200 °F**

Yield Strength, psi	Coefficient of Thermal Expansion, 10 <sup>-6</sup> in/in/°F
33,700	13.0

Notes:

1. Yield strength from ASME B&PV Code, Section II, Part D, Table Y-1.
2. Coefficient of thermal expansion from ASME B&PV Code, Section II, Part D, Table TE-2.

<sup>1</sup> American Society of Mechanical Engineers (ASME) Boiler and Pressure Vessel Code, Section II, Materials, Part D, Properties, 2001 Edition, 2002 and 2003 Addenda.

## B2.3 Fabrication and Examination

The AFS-B rod container is fabricated to the requirements of the drawing shown in Appendix B1.4.2, *Packaging General Arrangement Drawings*. The materials of construction are specified to either ASTM or SAE standards. The rod container is inspected to the dimensional requirements of the drawing. Welds are visually inspected to the AWS D1.2<sup>2</sup> welding code.

## B2.4 Lifting and Tie-down Standards for All Packages

Because the gross weight of the MFFP is lower when transporting the AFS-B rod container and EMA compared to three (3) fuel assemblies, this section is unchanged from Section 2.4, *Lifting and Tie-down Standards for All Packages*.

## B2.5 General Considerations

The AFS-B rod container is evaluated by reasoned argument and by analysis in the following sections. In addition, the results and conclusions of Section 2.5, *General Considerations*, remain unchanged.

## B2.6 Normal Conditions of Transport

### B2.6.1 Heat

It is demonstrated in Section B3.4, *Thermal Evaluation for Normal Conditions of Transport*, that under NCT, all MFFP component temperatures associated with the AFS-B payload are bounded by the standard three (3) fuel assembly payload. Therefore, all associated pressure and thermal stresses are bounded by the values presented in Section 2.6.1, *Heat*. For the AFS-B rod container, the bounding temperature of the sidewalls and the internal shelf is 200 °F. Since the AFS-B is vented, it cannot retain pressure.

#### B2.6.1.1 Differential Thermal Expansion

The evaluation of differential thermal expansion given in Section 2.6.1.2, *Differential Thermal Expansion*, is not affected by use of the AFS-B rod container. An additional evaluation of the differential thermal expansion between the strongback and the AFS-B container will now be made.

From Section 2.6.1.2, *Differential Thermal Expansion*, the design temperature of the strongback is  $T_{SB} = 180$  °F, and the coefficient of thermal expansion for the strongback material is  $\alpha_{SB} = 8.8 \times 10^{-6}$  in/in/°F. As stated above, the bounding temperature for the AFS-B container is  $T_{AFS-B} = 200$  °F, and from Table B2.2-1, the coefficient of thermal expansion is  $\alpha_{AFS-B} = 13.0 \times 10^{-6}$  in/in/°F. The overall length of the container is  $L = 159.9$  inches. The reference temperature is 70 °F. The differential thermal growth of the rod container and the strongback is:

---

<sup>2</sup> ANSI/AWS D1.2, *Structural Welding Code – Aluminum*, American Welding Society (AWS).

$$\delta = \alpha_{\text{AFS-B}}(L)(T_{\text{AFS-B}} - 70) - \alpha_{\text{SB}}(L)(T_{\text{SB}} - 70) = 0.115 \text{ inches}$$

This calculation conservatively assumes that the entire length of the two components is at the respective peak temperatures, and thus overestimates the relative thermal expansion. To prevent axial interference of the AFS-B container with the strongback, the clamp pads will be set with a clearance to the end of the AFS-B container. As stated in Section B7.1, *Package Loading*, the 3/4-10 clamp pad screw will be backed out a minimum of one turn from the position of contact, ensuring a minimum axial clearance between the AFS-B container and the strongback of 0.1 inches at the reference temperature. This is adequate to ensure that the thermal expansion force is negligible or non-existent considering the conservatism of the evaluation above.

### **B2.6.2 Cold**

This section is unchanged from Section 2.6.2, *Cold*.

### **B2.6.3 Reduced External Pressure**

This section is unchanged from Section 2.6.3, *Reduced External Pressure*.

### **B2.6.4 Increased External Pressure**

This section is unchanged from Section 2.6.4, *Increased External Pressure*.

### **B2.6.5 Vibration and Shock**

The vibration normally incident to transportation will have no effect on the AFS-B rod container. The AFS-B container is installed and retained in the same manner as a MOX fuel assembly. The spring loaded clamp arms which hold the container in place will significantly dampen any vibrational loads which could come from the cask body. Furthermore, any fatigue cracks which might occur from vibration, which are too small to be noted during a visual inspection, would have no effect on the ability of the AFS-B to perform its function of confining the rods in a HAC free drop impact. Therefore, vibration and shock are not of concern for the AFS-B rod container.

### **B2.6.6 Water Spray**

This section is unchanged from Section 2.6.6, *Water Spray*.

### **B2.6.7 Free Drop**

Because a loaded AFS-B is slightly lighter than a fuel assembly (including BPRA), the response of the MFFP to a free drop would be essentially the same when compared to the standard payload.

Since the AFS-B rod container is shown to confine the fuel rods in a HAC free drop impact (see Section B2.7.1), its performance will be acceptable for the NCT free drop event.

### **B2.6.8 Corner Drop**

This section is unchanged from Section 2.6.8, *Corner Drop*.

### **B2.6.9 Compression**

This section is unchanged from Section 2.6.9, *Compression*.

### **B2.6.10 Penetration**

This section is unchanged from Section 2.6.10, *Penetration*.

## **B2.7 Hypothetical Accident Conditions**

### **B2.7.1 Free Drop**

The functional criteria of the AFS-B rod container is to confine the fuel rods in the worst-case HAC free drop event. As an additional enhancement to criticality safety, the container should also restrict the relative movement of the rods to minimize the potential for damage to the fuel rods.

The MFFP strongback, including the fuel control structure (FCS), is designed to maintain a complete MOX fuel assembly in a subcritical configuration during the governing free drop event. Using physical test (see Appendix 2.12.3, *Certification Test Results*) and calculations (see Appendix 2.12.5, *Fuel Control Structure Evaluation*), it has been demonstrated that *a*) the fuel rods do not break or fragment, and *b*) the strongback and FCS are capable of confining the rods within a defined geometry. As stated in Section B1.2, *Package Description*, the AFS-B rod container consists of a completely enclosed structure made of 6061-T651 aluminum plates of 3/4-inch nominal thickness. The lid of the container is attached using 22, 3/8-inch diameter bolts. The container has the same boundary dimensions as the MOX fuel assembly, and is mounted in the strongback in the same manner. As such, the AFS-B container represents an added level of confinement for the fuel rods, beyond that provided by the strongback and FCS. For this reason, confinement of the fuel rods by the AFS-B container is ensured. Table B2.7-1 presents added detail which supports this conclusion. As stated in Section B2.1.2, *Design Criteria*, the rod movement in an impact is restricted to a maximum of approximately one-half of a rod diameter.

The rod cavity inside the AFS-B container is formed by the 3/4-inch thick lid plate, the two 3/4-inch thick side plates, thick end plates (minimum thickness of 2.4 inches), and a 1/2-inch thick shelf plate. The shelf plate is located in longitudinal, 1/4-inch deep grooves on the inside face of each 3/4-inch thick side plate, and supported against the bottom plate by gussets at 15.3-inch intervals. Figure B2.7-1 shows a cross section of the AFS-B container. To demonstrate that the rod cavity maintains its internal geometric integrity in the worst-case free drop impact, the following evaluation is performed. The internal geometric integrity assures that the "rattle space" inside the container is minimized to prevent any possible damage to the rods. However, any loss of the rod container contents is precluded by the rod container primary structure, as discussed above. In the following, it is assumed that the impact occurs with the shelf oriented horizontally with the container lid side up. This orientation governs over all others where some component of the rod load is directed toward the thick sidewalls of the container.

In this evaluation, any support from the gusset plates beneath the shelf will be conservatively neglected. The shelf is then a plate, simply supported on its two long sides, and free on its two short sides. A governing impact of 180g is taken from Section 2.12.5.2, *Conditions Analyzed*, for the maximum slapdown impact. From Table 2.12.5-1, the fuel rod weight is 5.33 lb each, and the length is  $L_r = 152.4$  inches. From Figure B2.7-1, the internal width of the cavity is  $b = 6.9$  inches. For 175 rods, the total weight of rods is therefore  $W = 175 \times 5.33 = 933$  lb. Since the rods rest on an area bounded by the rod length and the cavity width, the impact pressure on the shelf is:

$$q = \frac{Wg}{L_r b} = 159.7 \text{ psi}$$

A formula from Roark,<sup>3</sup> Table 26, Case 1a, is used. Even though this formula assumes simple support on the narrow ends as well as the sides, the maximum stress at the center of the plate, which is more than 10 plate-widths distant from the ends, will not be materially affected. The length of the shelf is  $L_s = 153.5$  inches. The ratio  $a/b$  is  $153.5/6.9 = 22.2$ , from which  $\beta = 0.75$ . The maximum stress at the center of the plate is found from:

$$\sigma = \frac{\beta q b^2}{t^2} = 22,810 \text{ psi}$$

where  $t = 0.5$  inches, and the other quantities are as defined above. From Table B2.2-1, the yield strength of the shelf material at the bounding temperature of 200 °F is 33,700 psi. The margin of safety against yield of the shelf is:

$$MS = \frac{33,700}{22,810} - 1 = +0.48$$

Since the shelf does not yield, the "rattle space" available for the rods does not increase as a result of the slapdown free drop event. Other impact orientations would place lower loadings on the shelf. Thus, the AFS-B rod container supports the geometry assumptions made in the criticality analysis of Chapter 6, *Criticality Evaluation*.

---

<sup>3</sup> Young, W. C., *Roark's Formulas for Stress and Strain*, Sixth Edition, McGraw-Hill, 1989.

**Table B2.7-1 – Comparison of the MOX Fuel Assembly and the AFS-B Rod Container in the MFFP Strongback**

<b>MOX Fuel Assembly</b>	<b>AFS-B Rod Container</b>	<b>Conclusion</b>
Strongback clamps on fuel grids	Strongback clamps on container	AFS-B lid is both bolted in place and clamped in place by the strongback
Max weight of 1,580 lb	Max weight of 1,500 lb	AFS-B applies lower inertia loads to the strongback in free drop impact events
264 rods	175 rods	Lighter payload in AFS-B
Rods self-supporting over span between clamp arms	Rods fully supported by thick walls and bolted lid of container	AFS-B eliminates rod bending loads
Rods can move axially a limited amount	Rods are confined by thick, bolted end structures	AFS-B confines rods axially
Rod lateral buckling is controlled by strongback and FCS	Rod lateral buckling is controlled by strongback and FCS, plus: <ol style="list-style-type: none"> <li>1. restricted free space inside container</li> <li>2. rods supported by thick walls of container</li> </ol>	AFS-B adds a significant layer of rod support to that existing in the basic strongback/FCS



*Figure Withheld Under 10 CFR 2.390*

### **Figure B2.7-1 – AFS-B Rod Container Cross Section View**

#### **B2.7.2 Crush**

This section is unchanged from Section 2.7.2, *Crush*.

#### **B2.7.3 Puncture**

The weight of the MFFP containing an AFS-B rod container and EMA is bounded by the weight of the MFFP with a payload of three (3) standard fuel assemblies. Therefore, the system response to a puncture is bounded by the discussion presented in Section 2.7.3, *Puncture*.

#### **B2.7.4 Thermal**

##### **B2.7.4.1 Summary of Pressures and Temperatures**

Package pressures and temperatures due to the HAC thermal event are presented in Section B3.5.3, *Maximum Temperatures and Pressures*. MFFP strongback and shell temperatures under HAC associated with the AFS-B payload are bounded by the standard three (3) fuel assembly payload. From Section B3.5.3.2, *Maximum Pressures*, the maximum internal pressure during the HAC thermal event is 117.1 psig. This pressure is bounded by the 130 psig pressure used in Section 2.7.4, *Thermal*.

### **B2.7.4.2 Differential Thermal Expansion**

This section is unchanged from Section 2.7.4.2, *Differential Thermal Expansion*, as the MFFP strongback and shell temperatures under HAC associated with the AFS-B payload are bounded by the standard three (3) fuel assembly payload.

### **B2.7.4.3 Stress Calculations**

As discussed in Section B2.7.4.1, *Summary of Pressures and Temperatures*, a conservative maximum internal pressure of 117.1 psig is calculated for the HAC thermal event. This pressure is lower than the 130 psig pressure used in Section 2.7.4.3, *Stress Calculations*. Therefore, the stresses calculated in Section 2.7.4.3 conservatively bound the stresses resulting from the payload evaluated in this Appendix.

### **B2.7.5 Immersion – Fissile Material**

This section is unchanged from Section 2.7.5, *Immersion – Fissile Material*. In addition, since each separate cavity of the AFS-B container is vented, full flooding of all cavities by water in the immersion test is assured.

### **B2.7.6 Immersion – All Packages**

This section is unchanged from Section 2.7.6, *Immersion – All Packages*.

### **B2.7.7 Deep Water Immersion Test (for Type B Packages Containing More than $10^5$ A<sub>2</sub>)**

This section is unchanged from Section 2.7.7, *Deep Water Immersion Test*.

### **B2.7.8 Summary of Damage**

The AFS-B rod container maintains its structural integrity and functionality in the worst-case HAC free drop event, which bounds the loadings of all other HAC events on the container. Since the AFS-B rod container is mounted in the same way as a MOX fuel assembly but weighs less, the response of the MFFP to drop and puncture accidents is unchanged when using the AFS-B. Therefore, the AFS-B is acceptable for use as a payload container.

## **B2.8 Accident Conditions for Air Transport of Plutonium**

This section does not apply for the MFFP, since air transport is not claimed.

## **B2.9 Accident Conditions for Fissile Material Packages for Air Transport**

This section does not apply for the MFFP, since air transport is not claimed.

**B2.10 Special Form**

This section does not apply for the MFFP, since special form is not claimed.

**B2.11 Fuel Rods**

This section does not apply for the MFFP, since containment by the fuel rod cladding is not claimed.

**B2.12 Appendices**

There are no appendices to Chapter B2.0. The applicability of the appendices to Chapter 2, *Structural Evaluation*, is given in Table B2.12-1.

**Table B2.12-1** – Applicability of Section 2.12 Appendices to the AFS-B Payload

<b>Appendix</b>	<b>Applicability</b>
2.12.1, Impact Limiter Evaluation	As the weight of the AFS-B is bounded by the weight of a fuel assembly, the impact limiter evaluation from Section 2.12.1 remains bounding.
2.12.2, Certification Test Plan	Unchanged from Section 2.12.2
2.12.3, Certification Test Results	Unchanged from Section 2.12.3
2.12.4, Engineering Test Results	Unchanged from Section 2.12.4
2.12.5, Fuel Control Structural Evaluation	As the weight of the AFS-B is bounded by the weight of a fuel assembly, and because it is more structurally robust than a fuel assembly, the fuel control structural evaluation from Section 2.12.5 remains bounding.
2.12.6, CASKDROP Computer Program	Unchanged from Section 2.12.6
2.12.7, Impact Limiter Weld Joint Test Results	Unchanged from Section 2.12.7
2.12.8, Effect of Bounding Weight on Package Structural Responses	As the weight of the AFS-B is bounded by the weight of a fuel assembly, the package structural responses evaluation from Section 2.12.8 remains bounding.

## B3.0 THERMAL EVALUATION

### B3.1 Description of Thermal Design

This section identifies and describes the principal thermal design aspects of the MOX Fresh Fuel Package (MFFP) for the transportation of the AFS-B rod container and the Excess Material Assembly (EMA) payload. The results presented in this chapter demonstrate the thermal safety of the package and compliance with the thermal requirements of 10 CFR 71<sup>1</sup> and supports the addition of the AFS-B rod container and the EMA as allowable contents of the MFFP.

The analysis demonstrates that the addition of the AFS-B rod container and EMA does not impact the packaging temperatures, and the temperatures for these items reported in Chapter 3.0, *Thermal Evaluation*, remain bounding. However, the peak HAC fuel cladding temperatures estimated for the fuel rods in an AFS-B are higher than the peak temperature computed for a fuel assembly, largely due to the simplified method employed. Nevertheless, the maximum allowable fuel temperature limits are not approached. The internal pressure of the package under HAC is bounded by the pressure resulting from the transportation of three (3) intact MOX fuel assemblies.

#### B3.1.1 Design Features

The principal thermal design features of the MFFP are described in Section 3.1.1, *Design Features*, while the principal features of the AFS-B rod container and the EMA are described in Section B1.2.3, *Contents of Packaging*.

#### B3.1.2 Content's Decay Heat

The payload configuration for the MFFP in this Appendix consists of one (1) AFS-B rod container, one (1) EMA, and one (1) dummy fuel assembly. Alternatively, a single AFS-B container or a single EMA can be loaded with two (2) dummy fuel assemblies. The design maximum decay heat for the AFS-B container is 53 watts, based on a maximum loading of 175 MOX fuel rods and the fact that a standard MOX fuel assembly has 264 fuel rods and a design decay heat loading of 80 watts. However, for conservatism, a decay heat loading of 80 watts is assumed for both the AFS-B rod container and the EMA.

#### B3.1.3 Summary of Temperatures

The maximum temperatures for the MFFP under NCT and HAC are summarized in Table B3.1-1. The packaging temperatures are taken from Table 3.4-1 and Table 3.5-1, respectively. While these packaging temperatures are associated with the transportation of three (3) MOX fuel assemblies, they are bounding for the MFFP temperatures arising from the transportation of a payload consisting of one (1) AFS-B rod container and one (1) EMA. Table B3.1-1 also presents the NCT and HAC temperatures for the AFS-B rod container and its payload of fuel rods. The peak temperature within the AFS-B rod container under NCT conditions is 206 °F (see Section

---

<sup>1</sup> Title 10, Code of Federal Regulations, Part 71 (10 CFR 71), *Packaging and Transportation of Radioactive Material*, 01-01-06 Edition.

B3.4, *Thermal Evaluation for Normal Conditions of Transport*), while the peak temperature achieved under HAC is predicted to be 613 °F (see Section B3.5, *Thermal Evaluation under Hypothetical Accident Conditions*). The peak temperature within the EMA is bounded by the temperatures predicted for the MOX fuel assembly.

#### **B3.1.4 Summary of Maximum Pressures**

The maximum normal operating pressure (MNOP) for the MFFP with the AFS-B rod container and EMA payload resulting from the NCT Hot condition and conservative assumptions is 2.8 psig. This pressure is bounded by the standard package MNOP of 10 psig. Further details of the pressure analysis are presented in Section B3.4.2, *Maximum Normal Operating Pressure*.

The peak pressure generated within the package cavity under HAC is conservatively estimated assuming that the entire inventory of organic material integral to the strongback assembly is totally combusted/pyrolyzed. No organic material is used in the AFS-B rod container.

The maximum pressure under HAC is estimated to be 117.1 psig (131.8 psia) at the end of the fire when the peak cavity gas temperature is reached. The pressure will then decrease as the package cools. Further details of the analysis are presented in Section B3.5.3, *Maximum Temperatures and Pressures*.

Table B3.1-1 –Summary of Temperatures for NCT and HAC (°F)

Item	Hot NCT	Peak HAC	Maximum Allowable		Minimum Temperature Margin <sup>(1)</sup>
			NCT	HAC	
Peak AFS-B Fuel Rod	<b>206</b>	613	<b>392</b>	1,337	186
Peak EMA Fuel Rod	<b>221</b>	518	<b>392</b>	1,337	171
Peak AFS-B Container	183	<b>602</b>	1,100	<b>1,100</b>	498
Avg. AFS-B Container	182	601	-	-	NA
<i>Temperatures for MFFP Package from Table 3.4-1 and Table 3.5-1</i>					
<i>Strongback Structure</i>	<i>178</i>	<i><b>599</b></i>	<i>800</i>	<i><b>800</b></i>	<i>201</i>
<i>Body Shell</i>	<i><b>159</b></i>	<i>1,361</i>	<i><b>800</b></i>	<i>2,500</i>	<i>641</i>
<i>Body Collar</i>	<i>149</i>	<i><b>414</b></i>	<i>800</i>	<i><b>1,000</b></i>	<i>586</i>
<i>Closure Lid</i>	<i><b>147</b></i>	<i>301</i>	<i><b>800</b></i>	<i>1,000</i>	<i>653</i>
<i>Impact Limiter Lugs</i>	<i><b>154</b></i>	<i>1,282</i>	<i><b>800</b></i>	<i>2,500</i>	<i>646</i>
<i>Impact Limiter</i>					
• <i>Max. Foam</i>	<i>149</i>	<i>N/A</i>	<i><b>300</b></i>	<i>N/A</i>	<i>151</i>
• <i>Bulk Avg. Foam</i>	<i>145</i>	<i>N/A</i>	<i><b>300</b></i>	<i>N/A</i>	<i>155</i>
• <i>Skin</i>	<i><b>149</b></i>	<i>1,429</i>	<i><b>800</b></i>	<i>2,500</i>	<i>651</i>
<i>Impact Limiter Bolts</i>					
• <i>Bolt Head</i>	<i><b>154</b></i>	<i>1,283</i>	<i><b>800</b></i>	<i>2,500</i>	<i>646</i>
• <i>Bolt Shaft</i>	<i><b>144</b></i>	<i>1,006</i>	<i><b>800</b></i>	<i>2,500</i>	<i>656</i>
• <i>Bolt Threads</i>	<i><b>144</b></i>	<i>295</i>	<i><b>800</b></i>	<i>2,500</i>	<i>656</i>
<i>O-ring Seals</i>					
• <i>Closure Lid</i>	<i>159</i>	<i><b>339</b></i>	<i>225</i>	<i><b>400</b></i>	<i>61</i>
• <i>Vent/Sampling Port</i>	<i><b>146</b></i>	<i>295</i>	<i>225</i>	<i>400</i>	<i>79</i>

**Note:** (1) Minimum temperature margin based on **bold** temperatures.

This page left intentionally blank.

## B3.2 Material Properties and Component Specifications

### B3.2.1 Material Properties

The material specifications for the MFFP package are defined in Section 3.2.1, *Material Properties*. The AFS-B rod container is fabricated primarily of clear anodized 6061-T6 aluminum. For the purposes of this calculation the material properties of the aluminum is characterized by a single thermal conductivity point of 96 Btu/hr-ft-°F<sup>1</sup> with an emissivity of 0.76<sup>2</sup>. The EMA materials are the same as those for a standard MOX fuel assembly.

### B3.2.2 Component Specifications

For thermal analysis purposes, the components of the EMA have the same specifications as those for the standard MOX fuel assembly. In addition to the materials listed in Section 3.2.2, *Component Specifications*, the only material associated with the AFS-B rod container that is considered temperature sensitive is the aluminum. 6061 aluminum has a melting temperature of approximately 1,100 °F<sup>1</sup>.

No organic material is used in the AFS-B rod container. The characteristics of the organic material within the MFFP package are defined Section 3.2.2, *Component Specifications*.

---

<sup>1</sup> American Society of Mechanical Engineers (ASME) Boiler and Pressure Vessel Code, Section II, *Materials, Part D – Properties*, 2001 Edition, with 2002 and 2003 Addenda, New York.

<sup>2</sup> Gilmore, D. G., Editor, *Satellite Thermal Control Handbook*, The Aerospace Corporation Press, El Segundo, CA, 1994, pp A-8.



This page left intentionally blank.

## B3.3 General Considerations

### B3.3.1 Evaluations by Analysis

The MFFP with the AFS-B rod container and the EMA is analytically evaluated in accordance with 10 CFR 71 and Regulatory Guide 7.8<sup>1</sup> for the bounding NCT and HAC thermal loads. Section 3.3.1, *Evaluation by Analysis*, summarizes the design basis conditions considered in these evaluations.

#### B3.3.1.1 NCT Analytical Model

The NCT analytical thermal model of the MFFP is based on the Thermal Desktop<sup>®2</sup> and SINDA/FLUINT<sup>3</sup> computer programs. Details of these programs, together with a description of the thermal model for the MFFP, are described in Section 3.3.1.1, *NCT Analytical Model*. That analysis demonstrated that a significant thermal margin exists for all package components.

Given that the AFS-B rod container has outer dimensions similar to a standard fuel assembly and interfaces with the strongback and clamp arms of the MFFP in a similar manner, and given that the maximum decay heat of the 175 fuel rods is less than 70% of that for a 264 rod MOX fuel assembly, the methodology used to evaluate the thermal performance of the AFS-B rod container within the MFFP is conservatively based on use of the maximum strongback temperature achieved for the transportation of the three (3) MOX fuel assemblies as a boundary condition for a 1-dimensional heat transfer analysis within the AFS-B rod container. The thermal performance of the EMA is bounded by that predicted for the MOX fuel assembly.

Figure B3.3-1 illustrates a cross-section through a loaded AFS-B rod container. As seen, the 175 fuel rods are expected to be arranged in a consolidated bundle consisting of 10 layers of 17 to 18 rods each. The temperature rise between the strongback and the center fuel rod in the consolidated bundle is computed using the 1-dimensional thermal model of the loaded AFS-B rod container illustrated in Figure B3.3-2.

#### Temperature of AFS-B rod container

The heat transfer between the AFS-B rod container and the strongback (i.e., c-to-h and g-to-h in Figure B3.3-2) is computed as a combination of radiation and conduction across an air gap based on the conservative assumption that the AFS-B container is centered within the fuel control structure (FCS) of the strongback assembly. Given the inside dimension for the FCS of 8.7-in, and an outside dimension of 8.4-in for the AFS-B container, the resulting uniform gap is 0.15-in. The heat transfer between the AFS-B container and the FCS is computed as:

---

<sup>1</sup> Regulatory Guide 7.8, *Load Combinations for the Structural Analysis of Shipping Casks for Radioactive Material*, Revision 1, U. S. Nuclear Regulatory Commission, March 1989.

<sup>2</sup> Thermal Desktop<sup>®</sup>, Version 4.5, Cullimore & Ring Technologies, Inc., Littleton, CO, 2003.

<sup>3</sup> SINDA/FLUINT, *Systems Improved Numerical Differencing Analyzer and Fluid Integrator*, Version 4.5, Cullimore & Ring Technologies, Inc., Littleton, CO, 2001.

$$q' = A \left[ \frac{1}{(\epsilon_c^{-1} - 1) + \frac{1}{F_{c-h}} + (\epsilon_h^{-1} - 1)} \sigma (T_c^4 - T_h^4) + \frac{k}{x} (T_c - T_h) \right] \quad (\text{Eqn. 1})$$

where:

$q'$  = heat transfer rate, Btu/hr

$A$  = heat transfer area, in<sup>2</sup>

$\epsilon_c$  = emissivity of AFS-B rod container = 0.76

$\epsilon_h$  = emissivity of FCS surfaces = 0.20<sup>4</sup>

$F_{c-h}$  = view factor between AFS-B container and FCS surfaces = 1.

$\sigma$  = Stefan-Boltzmann constant =  $1.190278 \times 10^{-11}$  Btu/hr-in<sup>2</sup>-R<sup>4</sup>

$T_c$  = temperature of AFS-B container, °R

$T_h$  = temperature of FCS surfaces, = 178°F or 638°R at the NCT Hot condition<sup>5</sup>

$k$  = thermal conductivity of air, Btu/hr-in<sup>2</sup>-R<sup>6</sup>

$x$  = gap distance between AFS-B and FCS surfaces = 0.15-in

The temperature rise between the center shelf of the AFS-B container and the sidewalls (i.e., e-to-c in Figure B3.3-2) is insignificant due to the combination of the limited heat load and the use of aluminum. Even assuming all 80 watts of decay heat passed between the center shelf and the container sidewalls and that this heat load was limited to the 144-inch active fuel length of the MOX fuel rods, the  $\Delta T$  required to transfer this heat load is estimated via:

$$\Delta T = \frac{\text{Heat Load}}{\text{Area} \frac{\text{conductivity of aluminum}}{\text{average distance for heat to travel}}}$$

$$\Delta T = \frac{80 \text{ watts} \times 3.412 \text{ Btu/watt}}{(0.5 \text{ inches} \times 144 \text{ inches} \times 2 \text{ paths}) \frac{96/12 \text{ Btu/hr} - \text{inch} - \text{F}}{(8.4 \text{ inches}/4)}}$$

$$\Delta T = 0.5^\circ \text{F}$$

The  $\Delta T$  required at the joint between the shelf and the container sidewalls (assuming all heat transfers via the intermittent welds) is estimated via:

$$\Delta T = \frac{80 \text{ watts} \times 3.412 \text{ Btu/watt}}{(0.125 \text{ inches} \times 7 \text{ inches} \times 144 \text{ inches}/15.3 \text{ inches} \times 2 \text{ paths}) \frac{96/12 \text{ Btu/hr} - \text{inch}}{(0.25 \text{ inches})}}$$

$$\Delta T = 0.5^\circ \text{F}$$

<sup>4</sup> Section 3.2.1, *Material Properties*.

<sup>5</sup> Table 3.4-1, *NCT Temperatures*

<sup>6</sup> Table 3.2-6, *Properties of Air*

Finally, the temperature difference to distribute the heat from the joint with the center shelf equally over the sidewalls is estimated via:

$$\Delta T = \frac{80 \text{ watts} \times 3.412 \text{ Btu/watt}}{(0.75 \text{ inches} \times 144 \text{ inches} \times 4 \text{ paths}) \frac{96/12 \text{ Btu/hr - inch}}{(8.4 \text{ inches}/4)}}$$

$$\Delta T = 0.17^\circ \text{ F}$$

Therefore, the center shelf is conservatively predicted to be within 1.2°F of the sidewall temperatures. As such, the estimation of the temperature rise within the consolidated fuel bundle can be computed assuming uniform temperatures on all sides of the AFS-B container.

Temperature of outer edges of fuel bundle

The heat transfer between the AFS-B rod container and the consolidated fuel rod bundle (i.e., b-to-c, d-to-e, and f-to-g in Figure B3.3-2) is computed as a combination of radiation and conduction across an air gap based on the conservative assumption that the consolidated fuel bundle is centered within the AFS-B container. The inside dimension of the AFS-B container is 6.9-in wide and 3.4-in high. The height and average width of the fuel rod stack within the rod container (see Figure B3.3-1) is equal to:

$$\begin{aligned} \text{Height} &= \text{fuel rod diameter}^7 \times (1 \text{ row} + 9 \text{ rows} \times \sin 60^\circ) \\ &= 0.374\text{-in} \times (1 + 7.7942) \\ &= 3.29\text{-in} \end{aligned}$$

$$\begin{aligned} \text{Width} &= \text{fuel rod diameter} \times (18 \text{ rods} + 17 \text{ rods})/2. \\ &= 0.374\text{-in} \times (18 + 17)/2. \\ &= 6.55\text{-in} \end{aligned}$$

Therefore, the average gap between the top and bottom of the consolidated fuel rod bundle and the AFS-B rod container is (3.4-in – 3.29-in)/2 + ¼ of the rod diameter of 0.374-in, or 0.15-in. The gap between the sides of consolidated fuel rod bundle and the AFS-B rod container is (6.9-in – 6.55-in)/2 + ¼ of the rod diameter, or 0.27-in. The average gap is computed as (6.9-in x 0.15-in + 3.4-in x 0.27-in)/(6.9-in + 3.4-in) = 0.19-in.

The heat transfer between the AFS-B container and the outer edges of the consolidated fuel rod bundle is computed as:

$$q' = A \left[ \frac{1}{(\epsilon_b^{-1} - 1) + \frac{1}{F_{b-c}} + (\epsilon_c^{-1} - 1)} \sigma (T_b^4 - T_c^4) + \frac{k}{x} (T_b - T_c) \right] \quad (\text{Eqn. 2})$$

where:

- q' = heat transfer rate, Btu/hr
- A = heat transfer area, in<sup>2</sup>
- ε<sub>c</sub> = emissivity of AFS-B rod container = 0.76

<sup>7</sup> Table 3.6-1, Summary of Design Data for MOX FA

- $\epsilon_b$  = emissivity of fuel rod surfaces = 0.20
- $F_{b-c}$  = view factor between fuel bundle edges and AFS-B container = 1.
- $\sigma$  = Stefan-Boltzmann constant =  $1.190278 \times 10^{-11}$  Btu/hr-in<sup>2</sup>-R<sup>4</sup>
- $T_c$  = temperature of AFS-B container, °R
- $T_b$  = avg. temperature of outer edges of fuel rod surfaces, °R
- $k$  = thermal conductivity of air, Btu/hr-in<sup>2</sup>-R
- $x$  = avg. gap distance between AFS-B and fuel rod surfaces

Temperature of hottest fuel rod

The heat transfer within the consolidated fuel bundle is computed by conservatively assuming the individual rods are separated by a finite distance from each of its neighbors and are not in direct contact. As such, the heat transfer between the rods is computed as radiation and conduction across the air gap separating the individual fuel rods. Since the  $\Delta T$  across the width of the individual fuel rods is insignificant in comparison, it is ignored for the purposes of this calculation. Figure B3.3-3 illustrates the idealized configuration assumed for the fuel bundle for the purposes of estimating the temperature rise within it.

As idealized, the fuel bundle is treated as a series of concentric layers of fuel rods with the temperature in each layer being the same. With the exception of the center rod, the heat transfer via radiation from layer 'n-1' to layer 'n' for  $n \geq 2$  is computed as:

$$q_{rad} = \text{Area} \times \left[ \frac{1}{(\epsilon_{n-1} - 1) + \frac{1}{F_{n-1 \text{ to } n}} + \frac{\text{Area}_{n-1}}{\text{Area}_n} (\epsilon_n - 1)} \sigma (T_{n-1}^4 - T_n^4) \right]$$

$$q_{rad} = 2\pi \times r \times L \times 6(n-1) \times \left[ \frac{1}{(0.2 - 1) + \frac{1}{F_{n-1 \text{ to } n}} + \frac{n-1}{n} (0.2 - 1)} \sigma (T_{n-1}^4 - T_n^4) \right] \quad (\text{Eqn. 3})$$

where:

- $q_{rad}$  = radiation heat transfer rate fuel layer 'n-1' to layer 'n', Btu/hr
- $r$  = radius of fuel rod, = 0.187-in
- $L$  = active length of fuel rod = 144-in
- $n$  = number of the rod layer, with the center rod at  $n = 0$
- $\epsilon_{n-1}$  &  $\epsilon_n$  = emissivity of fuel rod surfaces = 0.20
- $F_{n-1 \text{ to } n}$  = view factor from fuel layer 'n-1' to layer 'n' =  $(2n-1)/(6(n-1))$
- $\sigma$  = Stefan-Boltzmann constant =  $1.190278 \times 10^{-11}$  Btu/hr-in<sup>2</sup>-R<sup>4</sup>
- $T_{n-1}$  = temperature of fuel rods in layer 'n-1', °R
- $T_n$  = temperature of fuel rods in layer 'n', °R

For the radiation heat transfer from the center rod to the next layer (i.e.,  $n=1$ ), the heat transfer is computed as:

$$q_{\text{rad}} = 2\pi \times r \times L \times \left[ \frac{1}{(0.2^{-1} - 1) + \frac{1}{1} + \frac{1}{3}(0.2^{-1} - 1)} \sigma (T_0^4 - T_{n-1}^4) \right] \quad (\text{Eqn. 4})$$

Since no credit is taken for direct contact between the fuel rods, the conduction heat transfer between the rods will be via conduction across the intervening air gap. Each fuel rod will conductively exchange heat with six adjacent rods. Of these conduction points,  $6(2n-1)$  will be between rods in layer 'n-1' to those in rod layer 'n'. The surface area associated with each conduction point is  $2\pi \cdot r \cdot L/6$ , while a conservative separation distance between the surfaces of  $2 \cdot r \cdot (1 - \sin 60^\circ)$  is used. The conduction heat transfer from rod layer 'n-1' to layer 'n' for  $n \geq 1$  is computed as:

$$q_{\text{cond}} = \frac{2\pi \times r \times L/6 \times 6(2n-1) \times k \times (T_{n-1} - T_n)}{2 \times r \times (1 - \sin 60^\circ)}$$

$$q_{\text{cond}} = \frac{\pi \times L \times (2n-1) \times k \times (T_{n-1} - T_n)}{(1 - \sin 60^\circ)} \quad (\text{Eqn. 5})$$

where:

$q_{\text{cond}}$  = conduction heat transfer rate fuel layer 'n-1' to layer 'n', Btu/hr

L = active length of fuel rod = 144-in

n = number of the rod layer, with the center rod at n = 0

k = thermal conductivity of air, Btu/hr-in<sup>2</sup>-R

$T_{n-1}$  = temperature of fuel rods in layer 'n-1', °R

$T_n$  = temperature of fuel rods in layer 'n', °R

### B3.3.1.2 HAC Analytical Model

The analytical thermal model of the MFFP with the AFS-B rod container under HAC uses the same methodology used for the NCT evaluation. Since the NCT methodology is based on steady-state conditions and it ignores the effects of thermal mass and transient heating, the predicted HAC temperatures are conservative. The peak strongback temperature presented in Section 3.5, *Thermal Evaluation under Hypothetical Accident Conditions*, is used as a steady-state boundary temperature for the 1-D thermal model of the AFS-B rod container described above.

### B3.3.2 Evaluation by Test

This section is not applicable since evaluation by test was not performed for the MFFP with the AFS-B rod container and EMA.

### B3.3.3 Margins of Safety

A summary of the maximum temperatures for the MFFP, with their respective temperature margins, for both NCT and HAC are provided in Table 3.3-3.

From Section B3.1.4, *Summary of Maximum Pressures*, the maximum normal operating pressure (MNOP) is 2.8 psig, which is bounded by the calculated MNOP of 2.9 psig for the standard payload of three (3) fuel assemblies. (Note that the reported MNOP for the package is 10 psig, which is obtained by rounding up the 2.9 psig value.) Therefore, the margin of safety (MS) for the 25-psig design pressure is:

$$MS = \frac{25}{2.8} - 1.0 = +7.9$$

From Section B3.1.4, *Summary of Maximum Pressures*, the maximum pressure for HAC is 117.1 psig. This pressure is bounded by the 123.5 psig pressure for the standard three (3) fuel assembly payload. Therefore, the MS of +2.15 reported in Section 3.3.3, *Margins of Safety*, is bounding.

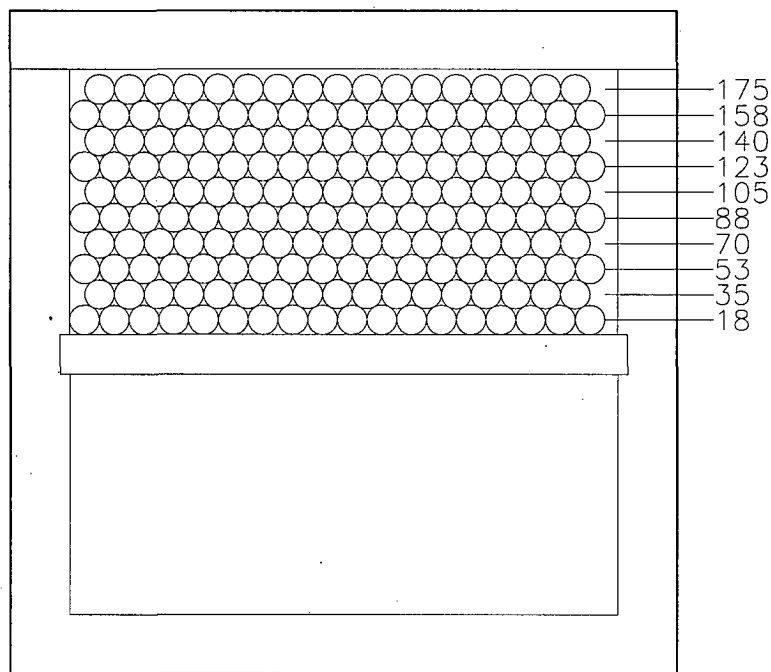
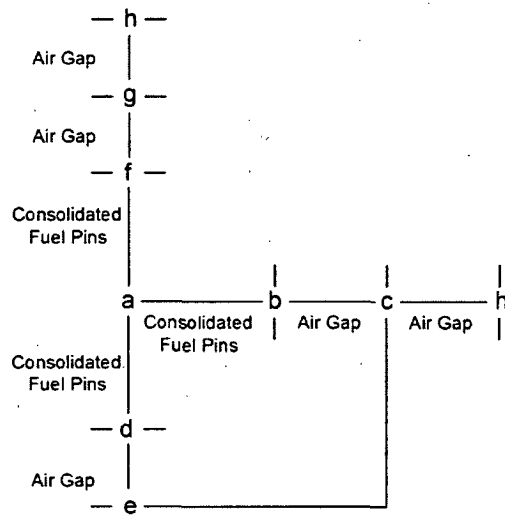


**Figure B3.3-1 - Consolidated Fuel Rod Bundle within AFS-B Rod Container**





- a = center of the consolidated fuel rod bundle
- b = side edge of the consolidated fuel rod bundle
- c = side of AFS-B rod container
- d = bottom side of the consolidate fuel rod bundle
- e = center shelf of AFS-B rod container
- f = top edge of the consolidated fuel rod bundle
- g = top of AFS-B rod container
- h = strongback assembly of MFFP Package

**Figure B3.3-2 - 1-D Thermal Model of AFS-B Rod Box Container**

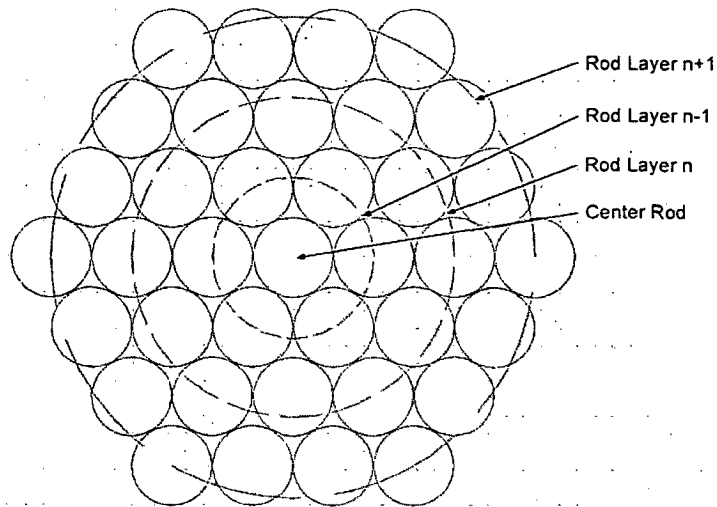


**Figure B3.3-3 - Consolidated Fuel Rod Bundle Modeling**

## B3.4 Thermal Evaluation for Normal Conditions of Transport

### B3.4.1 Heat and Cold

#### B3.4.1.1 Heat

The maximum temperatures for the AFS-B rod container and EMA are determined assuming the peak temperature of 178 °F for the strongback assembly obtained from Section 3.4.1.1, *Heat*, for the NCT Hot condition. Since this temperature is associated with a decay heat loading of 240 watts, it conservatively bounds the strongback temperatures associated with the transport of one (1) AFS-B rod container and one (1) EMA with a combined total decay heat loading of 133 watts. For conservatism, the peak temperatures are determined for a total decay heat loading of 160 watts, divided equally between the AFS-B rod container and the EMA.

Based on the 1-dimensional thermal model described above, a conservative decay heat load of 80 watts for the maximum payload configuration of 175 fuel rods, and an iterative solution of equation #1 from Section B3.3.1.1, *NCT Analytical Model*, the peak temperature for the AFS-B rod container is 183°F for the NCT Hot condition. Adding the 1.2°F  $\Delta T$  determined in Section B3.3.1.1 for the temperature difference between the center shelf and the sidewall, yields a peak AFS-B temperature of 184°F. The average sidewall temperature is 182°F.

The associated peak fuel rod temperature within the AFS-B rod container is computed by iterative solution of equations #3 to #5. Since the fuel bundle is 10 rod layers high and 17 to 18 rod layers wide, the peak temperature of the center fuel rod is conservatively predicted by assuming the fuel bundle extends 8 layers in all directions from the center rod. Based on this assumption, the predicted peak fuel rod temperature within the AFS-B rod container is 206 °F for the NCT Hot condition. This predicted peak temperature is bounding whether the other positions in the strongback are occupied by one EMA and a dummy fuel assembly, or by two dummy fuel assemblies.

The maximum temperature for the EMA is bounded by the predicted maximum temperature for the MOX fuel assembly obtained from Section 3.4.1.1, *Heat*, of 221 °F.

The results presented in Section 3.4.1.1, *Heat*, for the MFFP remain valid and bounding for the MFFP temperatures associated with the transport of the AFS-B rod container and EMA. Specifically, the closure seals and the impact limiter foam temperatures remain below their associated temperature limits. Additionally, the MFFP analysis demonstrated that the accessible package surfaces remain below 122 °F when transported in an ambient temperature of 100 °F and without insolation, as stipulated by 10 CFR §71.43(g).

#### B3.4.1.2 Cold

The minimum temperature distribution for the MFFP with the AFS-B rod container and EMA occurs with a zero decay heat load and an ambient air temperature of -40 °F per 10 CFR §71.71(c)(2). The steady-state analysis of this condition represents a trivial case that requires no thermal calculations be performed. Instead, it is assumed that all package components achieve the -40 °F temperature under steady-state conditions. The -40 °F temperature is within the allowable range of all of the packaging components. The package temperatures for the NCT

Cold condition of -20 °F and no insolation are bounded by those presented in Section 3.4.1.2, *Cold*, for the MFFP.

### B3.4.2 Maximum Normal Operating Pressure

The maximum normal operating pressure (MNOP) for NCT is based on an initial package backfill of air at atmospheric pressure at 70 °F (294 K) and an assumed failure rate of 3% of the MOX fuel rods. For conservatism, the heat up of the gases in the package cavity is assumed to be the same as that determined for the transport of three (3) MOX fuel assemblies for the respective ambient condition. For the purpose of rod pressure determination, the only significant gas contributor is the initial helium backfill as no fission products will exist within the un-irradiated fuel assemblies.

The bulk average gas temperature from Section 3.4.1.1, *Heat*, for the MFFP under the NCT Hot condition is used as the basis for the MNOP calculation with the AFS-B rod container and EMA. Since the decay heat loading assumed for the MFFP bounds the heat dissipation associated with the AFS-B rod container and EMA, the associated bulk average gas temperature will also be bounding. The package cavity has a gross free volume of approximately 105,547 in<sup>3</sup>, based on a package cavity OD of 28.5 inches and a length of 165.45 inches. The displacement volume for the EMA is approximately 4,685 in<sup>3</sup>, while a displacement volume for the strongback assembly is 11,292 in<sup>3</sup> (see Section 3.4.2, *Maximum Normal Operating Pressure*). The displacement volume for an unloaded AFS-B rod container is 4,592 in<sup>3</sup> based on an approximate weight of 450 lbs and a density of 0.098 lbs/in<sup>3</sup>. The volume of the 175 fuel rods is 2,941 in<sup>3</sup> based on a rod diameter of 0.374 in. and a length of 153 in. The solid volume for the dummy fuel assembly is approximately 5,366 in<sup>3</sup>.

The amount of helium fill gas within each MOX fuel assembly fuel rod and poison rod was determined in Section 3.4.2, *Maximum Normal Operating Pressure*, to be 0.0243 and 0.0475 g-moles, respectively. The total helium volume within a MOX fuel assembly is 7.55 g-moles. This helium content bounds that for the EMA. Given that there are a maximum of 175 fuel rods in the AFS-B rod container, the total helium content is 4.25 g-moles.

The initial gas in the package cavity at the time of sealing is calculated as follows:

$$N_{\text{fill}} = \frac{1 \text{ atm} \times V_{\text{free}}}{R \times T_{\text{fill}}}$$

where:

- $T_{\text{fill}}$  = temperature of air within package cavity at time of package closure
- $R$  = Ideal gas constant (0.08206 atm-liter/gmole-K)
- $V_{\text{free}}$  = Package cavity free volume
- = Gross cavity volume minus displacement volumes for the loaded AFS-B rod container, the dummy fuel assembly, the EMA, and the strongback
- = 76,671 in<sup>3</sup> (1,256 liters)

The MNOP is then calculated as follows:

$$\text{MNOP} = \frac{N_{\text{cask}} RT_{\text{NCT}}}{V_{\text{free}}}$$

$$N_{\text{cask}} = N_{\text{fill}} + \text{Rod Failure Rate} \times N_{\text{MOX fill gas}} + N_{\text{outgassing}}$$

where:

$N_{\text{cask}}$  = total moles of gas in package cavity

$N_{\text{fill}}$  = moles air within package cavity at time of package closure

Rod Failure Rate = assumed percentage of failed fuel rods within the AFS-B rod container and the EMA. A 3% failure rate, which matches the regulatory failure rate for normal conditions of transport of spent fuel assemblies, will bound the expected failure rate for fresh fuel.

$N_{\text{MOX fill gas}}$  = moles of rod fill gas within package cavity

$N_{\text{outgassing}}$  = moles gas generated by out-gassing from component material in cask cavity

$T_{\text{NCT}}$  = Bulk average gas temperature within package (K) at the specific condition

= 166°F or 347 K<sup>1</sup>

Based on the above relationships and assumptions, the MNOP for the bounding payload combination of one (1) AFS-B rod container with 175 fuel rods, one (1) EMA, and one (1) dummy fuel assembly is 17.5 psia (2.8 psig). A significant margin exists between this calculated MNOP and the package's NCT design pressure limit of 39.7 psia (25 psig).

No hydrogen or other combustible gases will be generated as result of the thermal or radiation-induced decomposition of the organic material within the package. This conclusion is based on the low peak temperature achieved under NCT transport conditions and the low radioactivity associated with the un-irradiated MOX fuel rods.

### B3.4.3 Maximum Thermal Stresses

The maximum thermal stresses for NCT are bounded by those determined for the MFFP with the MOX fuel assembly payload. See the discussion in Section 2.6.1, *Heat*, and Section 2.6.2, *Cold*.

### B3.4.4 Evaluation of Package Performance for Normal Conditions of Transport

The steady-state thermal analysis presented in Section 3.4, *Thermal Evaluation for Normal Conditions of Transport*, demonstrates that the components of the MFFP with the MOX fuel assembly payload are within their respective allowable temperature limits. That evaluation is valid and bounding for the MFFP with the AFS-B rod container and the EMA.

<sup>1</sup> Table 3.4-1, *NCT Temperatures*

The MNOP resulting from the NCT Hot condition and conservative assumptions is within the package's maximum design pressure limit.

Therefore, the MFFP with the AFS-B rod container and the EMA is found to comply with all of the thermal requirements specified in 10 CFR §71.71.

## B3.5 Thermal Evaluation under Hypothetical Accident Conditions

This section presents the results of the thermal evaluation of the MFFP with the AFS-B rod container and EMA under the hypothetical accident conditions (HAC) specified in 10 CFR §71.73(c)(4)<sup>1</sup>.

### B3.5.1 Initial Conditions

The initial conditions assumed for the MFFP are presented in Section 3.5, *Thermal Evaluation under Hypothetical Accident Conditions*. Due to their robust design, no significant damage is assumed to have occurred to the AFS-B rod container, the EMA, and the dummy fuel assemblies as a result of the drop events that precede the HAC fire event. Even if damaged, the integrity of these components is not important to the thermal safety of the MFFP package.

### B3.5.2 Fire Test Conditions

No fire tests were performed for the MFFP with the AFS-B rod container and EMA.

#### B3.5.2.1 Analytical Model

The analytical model of the MFFP under HAC is described in Section 3.5.2.1, *Analytical Model*, and Section 3.5.2.2, *Performance of Rigid Polyurethane Foam Under HAC Fire Conditions*. The peak temperature for the AFS-B rod container under HAC is estimated using the methodology and 1-dimensional thermal model described in Section B3.3.1.1, *NCT Analytical Model*.

The thermal performance of the EMA under HAC is bounded by the results for the MOX fuel assembly.

### B3.5.3 Maximum Temperatures and Pressures

#### B3.5.3.1 Maximum Temperatures

The maximum temperatures attained in the MFFP components under HAC with the AFS-B rod container and EMA assembly are bounded by those presented in Section 3.5.3.1, *Maximum Temperatures*. The peak strongback assembly temperature predicted from the evaluation of the MFFP is 599 °F and the transient analysis demonstrates that the peak temperature condition lasts for less than 15 minutes.

Based on a decay heat load of 80 watts for the maximum payload configuration of 175 fuel rods and an iterative solution of equation #1 from Section B3.3.1.1, the estimated peak temperature for the AFS-B rod container under HAC conditions is 601°F, while the peak center shelf temperature is estimated to be 602°F. In a similar fashion, based on equation #2 from Section B3.3.1.1, the temperature of the outer surface of the fuel bundle within the AFS-B rod container is predicted to be 606°F. The associated peak fuel rod temperature, computed by iterative solution of equations #3 to #5, is estimated to be 613°F.

---

<sup>1</sup> Title 10, Code of Federal Regulations, Part 71 (10 CFR 71), *Packaging and Transportation of Radioactive Material*, 01-01-06 Edition.

The peak temperature within the EMA is bounded by the temperatures predicted for the intact MOX fuel assembly in Section 3.5.3.1, *Maximum Temperatures*.

Although both the peak temperature and the duration of the elevated temperatures within the package are seen as insufficient to cause significant thermal decomposition of the organic material integral to the strongback assembly, it is conservatively assumed that 100% of the organic material fully decomposes to the extent that the available oxygen permits.

### **B3.5.3.2 Maximum Pressures**

With the exception of the consideration for potential out-gassing from organic components within the package cavity and an assumed 100% failure rate for the fuel rods, the maximum pressure attained under HAC is determined in the same manner as described in Section B3.4.2, *Maximum Normal Operating Pressure*. While the MFFP is designed to protect the enclosed fuel rods from catastrophic failure during the pre-fire free and puncture bar drops and the subsequent 30-minute fire event, this analysis conservatively assumes that the cladding on all fuel rods are breached. As stated in Section B3.4.2, *Maximum Normal Operating Pressure*, the amount of helium fill gas within the EMA is 7.55 g-moles and the total helium content of the AFS-B rod container with 175 fuel rods is 4.25 g-moles. No significant change in the package cavity free volume is expected as a result of the HAC drop event.

Per Section 3.5.3.2, *Maximum Pressures*, approximately 7 pounds of neoprene rubber ( $C_4H_5Cl$ )<sub>n</sub> and 2.3 pounds of Delrin<sup>®</sup> plastic ( $C_6H_{14}O_2$ )<sub>n</sub> are used in the strongback assembly. The breakdown of these organic materials under HAC is limited by the facts that a limited amount of oxygen exists in the cask cavity and the peak cavity temperature and its duration under HAC are too low to permit complete pyrolysis (i.e., the process of breaking up a substance into other molecules as a result of heating in an inert atmosphere). For this evaluation, it is assumed that 75% of the oxygen is consumed generating carbon monoxide and only 25% is used in the generation of carbon dioxide gas. A larger ratio of carbon dioxide generation will result in a lower cask pressure. Under this conservative assumption, volatilizing the entire mass of neoprene rubber and Delrin<sup>®</sup> plastic would generate approximately 137.3 g-moles of additional gas within the cavity.

The peak pressure generated within the package cavity is estimated to be 131.8 psia (117.1 psig) at the end of the 30 minute fire event when the peak cavity gas temperature is reached. This pressure is bounded by the pressure from a payload of three fuel assemblies (138.2 psia). The pressure will then decrease as the package cools. The predicted peak pressure is considered to have a high degree of conservatism since there is insufficient oxygen within the package cavity to permit the full decomposition of the organic material and because both the relatively low peak temperature and the relatively short duration of the elevated temperatures will prevent any significant decomposition from occurring in the absence of active combustion of the material. It is expected that a majority of the organic material will remain in its original, solid form.

### **B3.5.4 Accident Conditions for Fissile Material Packages for Air Transport**

This section does not apply for the MFFP since air transport will not be utilized.

### **B3.5.5 Evaluation of Package Performance for Accident Conditions of Transport**

The evaluation of the MFFP with the AFS-B rod container and EMA under HAC demonstrates that the packaging has sufficient thermal protection remaining after the hypothetical drop and puncture bar damage to protect the thermally sensitive areas of the packaging. All package components are seen as remaining within their associated maximum temperature limits.



This page left intentionally blank.

B3.6 Appendices

B3.6.1 Computer Analysis Results

The safety evaluations are based on hand calculations. The following are reproduction of the spreadsheet pages used to compute the temperatures within the AFS-B rod container.

NCT Conditions - 175 MOX Rods

AFS-B box to FCS surfaces		Inches	Btu/hr-in-F	Watts			Watts	Watts	Watts	Average sidewall temperature
Box Width	Rod Length	Avg. Gap	Air k @ 180F	Box emiss	FCS emiss	Decay Heat	Box Temp. F	FCS Temp. F		
8.4	144	0.150	0.00144	0.76	0.2	80	182.8	179		
8.4	159.9	0.150	0.00144	0.76	0.2	80	182.3	178		

AFS-B box to fuel rod surfaces		Inches	Inches	Btu/hr-in-F	Watts			Watts	Watts	Watts
Box Width	Box Height	Rod Length	Avg. Gap	Air k @ 180F	Rod emiss	Box emiss	Decay Heat	Rod Temp. F	Box Temp. F	Qtotal
6.9	3.4	144	0.19	0.00144	0.2	0.76	80	192	182.8	80.10

HAC Conditions - 175 MOX Rods

AFS-B box to FCS surfaces		Inches	Btu/hr-in-F	Watts			Watts	Watts	Watts	Average sidewall temperature
Box Width	Rod Length	Avg. Gap	Air k @ 600F	Box emiss	FCS emiss	Decay Heat	Box Temp. F	FCS Temp. F		
8.4	144	0.150	0.00216	0.76	0.2	80	601.3	599		
8.4	159.9	0.150	0.00216	0.76	0.2	80	601.04	599		

AFS-B box to fuel rod surfaces		Inches	Inches	Btu/hr-in-F	Watts			Watts	Watts	Watts
Box Width	Box Height	Rod Length	Avg. Gap	Air k @ 600F	Rod emiss	Box emiss	Decay Heat	Rod Temp. F	Box Temp. F	Qtotal
6.9	3.4	144	0.19	0.00216	0.2	0.76	80	605.5	601.3	80.77

**Temperature Legend**  
 - user input temperature  
 - temperature linked to other cells on spreadsheet  
 - temperature obtained from [4] calculation

PEAK MOX ROD TEMPERATURES

NCT Conditions - 175 MOX Rods

From Rod Layer	To Rod Layer	Inch Rod Dia.	Inch Rod Length	Btu/hr-in-F Air k @ 200F	Rod emiss	Watt Rod Power	Watt Total Power	F Inner Rod T	F Outer Rod T	Watt Qrad	Watt Qcond	Watt Qtotal
7	8	0.374	144	0.00148	0.2	0.457	77.257	195.2	192	8.589	70.463	79.052
6	7	0.374	144	0.00148	0.2	0.457	58.057	198	195.2	6.596	53.434	60.031
5	6	0.374	144	0.00148	0.2	0.457	41.600	200.3	198	4.630	37.140	41.770
4	5	0.374	144	0.00148	0.2	0.457	27.886	202.2	200.3	3.150	25.102	28.253
3	4	0.374	144	0.00148	0.2	0.457	16.914	203.4	202.2	1.549	12.331	13.880
2	3	0.374	144	0.00148	0.2	0.457	8.686	204.5	203.4	1.005	8.074	9.078
1	2	0.374	144	0.00148	0.2	0.457	3.200	205.2	204.5	0.364	3.083	3.446
0	1	0.374	144	0.00148	0.2	0.457	0.457	205.5	205.2	0.031	0.440	0.472

HAC Conditions - 175 MOX Rods

From Rod Layer	To Rod Layer	Inch Rod Dia.	Inch Rod Length	Btu/hr-in-F Air k @ 600F	Rod emiss	Watt Rod Power	Watt Total Power	F Inner Rod T	F Outer Rod T	Watt Qrad	Watt Qcond	Watt Qtotal
7	8	0.374	144	0.00216	0.2	0.457	77.233	607.3	605.5	20.995	57.672	78.667
6	7	0.374	144	0.00216	0.2	0.457	58.039	608.9	607.3	16.234	44.429	60.663
5	6	0.374	144	0.00216	0.2	0.457	41.587	610.2	608.9	11.187	30.545	41.732
4	5	0.374	144	0.00216	0.2	0.457	27.877	611.3	610.2	7.748	21.146	28.894
3	4	0.374	144	0.00216	0.2	0.457	16.909	612.2	611.3	4.915	13.457	18.371
2	3	0.374	144	0.00216	0.2	0.457	8.683	612.8	612.2	2.311	6.408	8.719
1	2	0.374	144	0.00216	0.2	0.457	3.199	613.2	612.8	0.874	2.563	3.437
0	1	0.374	144	0.00216	0.2	0.457	0.457	613.4	613.2	0.087	0.427	0.515

**Temperature Legend**  
 - user input temperature  
 - temperature linked to other cells on spreadsheet  
 - temperature obtained from AFS-to-FCS worksheet

This page left intentionally blank.

## B4.0 CONTAINMENT

The AFS-B does not provide containment. Therefore, package containment is unchanged from the description provided in Chapter 4.0, *Containment*.

This page left intentionally blank.

## B5.0 SHIELDING EVALUATION

The compliance of the MFFP packaging with respect to the dose rate limits established by 10 CFR §71.47<sup>1</sup> for normal conditions of transport (NCT) or 10 CFR §71.51(a)(2) for hypothetical accident conditions (HAC) are satisfied when limiting the MFFP package to three (3) Mixed Oxide (MOX) fresh fuel assemblies (FAs) having a radioisotope content listed in Table 1.2-2. Replacing 3 FAs with one (1) EMA and one (1) AFS-B containing up to 175 fuel rods would reduce the dose rates, because in this configuration the MFFP would contain no more than 439 fuel rods, compared to the 792 fuel rods for three standard FAs.

Under these conditions, the maximum surface dose rate will be less than the limit of 200 mrem/hr for NCT and verified by measurement. This dose rate limit is for payload packages prior to addition of any lead, steel or other shielding material for *as-low-as-reasonably-achievable* (ALARA) dose reduction purposes during non-transport handling operations.

Prior to transport, the MFFP package shall be monitored for both gamma and neutron radiation to demonstrate compliance with 10 CFR §71.47. As noted in Section 2.6.7, *Free Drop*, the MFFP package is not significantly deformed under NCT free drop conditions. Therefore, the package will meet the dose rate limits for NCT if the measurements demonstrate compliance with the allowable dose rate levels in 10 CFR §71.47 (200 mrem/hr). The transport index, as defined in 10 CFR §71.4, will be determined by measuring the dose rate a distance of one meter from the package surface per the requirements of 49 CFR §173.403<sup>2</sup>.

Shielding materials are not specifically provided by the MFFP package, and none are permitted within the package to meet the dose rate limits of 10 CFR §71.47 for NCT. Because significant fuel deformation or package deformation does not occur under HAC, the HAC surface dose rates and 1-meter dose rates will not be significantly different from the NCT dose rates. This result ensures that the post-HAC, allowable dose rate of 1 rem/hr a distance of one meter from the package surface per 10 CFR §71.51(a)(2) will be met because the surface dose rate will remain below the 200 mrem/hr limit.

---

<sup>1</sup> Title 10, Code of Federal Regulations, Part 71 (10 CFR 71), *Packaging and Transportation of Radioactive Material*, 01-01-06 Edition.

<sup>2</sup> Title 49, Code of Federal Regulations, Part 173 (49 CFR 173), *Shippers - General Requirements for Shipments and Packagings*, 10-01-06 Edition.

This page left intentionally blank.

## B6.0 CRITICALITY EVALUATION

The following analyses demonstrate that the MFFP complies with the requirements of 10 CFR §71.55<sup>1</sup> and §71.59. The analyses presented herein show that the criticality requirements are satisfied when one (1) excess material assembly (EMA), one (1) AFS-B rod container holding up to 175 MOX fuel rods, and one (1) dummy fuel assembly are transported in an MFFP.

### B6.1 Description of Criticality Design

#### B6.1.1 Design Features Important for Criticality

The AFS-B is conservatively ignored in this criticality analysis. However, as noted in Section B2.0, *Structural Evaluation*, the AFS-B sufficiently protects the fuel rods so that damage to the fuel rods will not occur. Therefore, there are no specific design features of the AFS-B important for criticality. The design features of the MFFP important to criticality are discussed in Section 6.1.1, *Design Features Important for Criticality*.

#### B6.1.2 Summary Table of Criticality Evaluation

The results of the criticality calculations are summarized in Table B6.1-1. The NCT results are bounded by the three fuel assembly results reported in Table 6.1-1, and those results are simply reproduced in the table below. The HAC analysis results are more reactive than the standard three fuel assembly analysis because the 175 AFS-B rods are conservatively allowed to expand to fill the cavity formed between the strongback and FCS. The maximum calculated  $k_s$  is 0.9240, which occurs for the HAC infinite array case with fully moderated internal region and void external region. The maximum  $k_s$  is below the USL of 0.9288.

Note that the results in Table B6.1-1 are artificially high because no credit is taken for the AFS-B, allowing the fuel rods to arrange in the most reactive pitch. In actuality, if the analysis were repeated taking credit for the AFS-B, the reactivity would drop considerably because there is very little space available inside the AFS-B for moderation, as all available void space is filled with dunnage rods.

---

<sup>1</sup> Title 10, Code of Federal Regulations, Part 71 (10 CFR 71), *Packaging and Transportation of Radioactive Material*, 01-01-06 Edition.



**Table B6.1-1 – Summary of Criticality Analysis Results**

<b>Normal Conditions of Transport (NCT)</b>			
<b>Case</b>	<b><math>k_{eff}</math></b>	<b><math>\sigma</math></b>	<b><math>k_s</math></b>
Single Unit Maximum $k_s$	0.2858	0.0008	0.2874
Infinite Array Maximum $k_s$	0.6027	0.0006	0.6039
<b>Hypothetical Accident Conditions (HAC)</b>			
<b>Case</b>	<b><math>k_{eff}</math></b>	<b><math>\sigma</math></b>	<b><math>k_s</math></b>
Single Unit Maximum $k_s$	0.9186	0.0010	0.9207
Infinite Array Maximum $k_s$	0.9219	0.0010	0.9240
USL		0.9288	

**B6.1.3 Criticality Safety Index**

An infinite number of MFFPs are evaluated in a close-packed hexagonal array. Therefore, "N" is infinite, and in accordance with 10 CFR §71.59 the criticality safety index (CSI) is  $50/N = 0$ .

## B6.2 Fissile Material Contents

The contents are one (1) EMA and one (1) AFS-B containing up to 175 standard MOX fuel rods. The third strongback location is loaded with a dummy fuel assembly, as defined in Section B1.2.3, *Contents of Packaging*. The fuel rod parameters for the rods in the AFS-B are unchanged from the standard MOX fuel rod and are provided in Section 6.2, *Fissile Material Contents*.

The EMA is a one-of-a-kind MOX fuel assembly composed of fuel rods that do not meet all of the performance requirements of a standard fuel rod. The EMA is composed of 264 MOX fuel rods in the same arrangement as a standard MOX fuel assembly. Some EMA fuel pellets do not meet the dimensional tolerances of a standard fuel pellet. In addition, the Pu-238 weight percent is out of tolerance for some of the rods. However, the total EMA fissile Pu mass is significantly less than the Pu mass analyzed for the standard bounding assembly in Chapter 6.0, *Criticality Evaluation*.

The maximum Pu/(U+Pu) for any rod in the EMA is 5.01%, while the average Pu/(U+Pu) for the EMA is only 3.41%. For the standard assembly, each rod is modeled at the maximum value of 6.0% Pu/(U+Pu). Therefore, the EMA has significantly less plutonium than a standard assembly and will be less reactive.

The maximum rod Pu-238 wt.% in the EMA is 0.19%, and the average Pu-238 wt.% is 0.086%. Both of these values exceed the current SAR limit of 0.05% for Pu-238 listed in Table 6.2-3. However, Pu-238 acts as a poison for criticality and is not modeled in the standard assembly. Therefore, the higher Pu-238 content will further lower the EMA reactivity when compared to a standard assembly. The remaining isotopic values are within the ranges provided in Table 6.2-3.

This page left intentionally blank.

## B6.3 General Considerations

Criticality calculations for the MFFP are performed using the three-dimensional Monte Carlo computer code MCNP5<sup>1</sup>.

### B6.3.1 Model Configuration

#### B6.3.1.1 Contents Model

The AFS-B is not modeled in the criticality evaluation. Because the AFS-B is not modeled, the fuel rods are assumed to arrange themselves in the most reactive configuration within the cavity formed between the strongback and FCS. To maintain model symmetry, a variety of regular square arrangements are modeled, including 14x14, 13x13, 12x13, 12x12, 11x11, and 10x10. (Note that the 14x14 arrangement (196 rods) is not physically possible due to the 175 rod limit of the AFS-B cavity.) A limited number of non-regular pitch cases are also developed.

Stainless steel or aluminum dunnage rods are used in the AFS-B to prevent lateral movement of the fuel rods. These dunnage rods are ignored in the criticality models.

The rod arrangements of the contents represents an extremely conservative and incredible arrangement, as the AFS-B, even if damaged in an accident, would displace a large volume and would not allow the rod arrangements assumed in this analysis.

#### B6.3.1.2 Packaging Model

The packaging model is unchanged from the description provided in Section 6.3.1.2, *Packaging Model*.

### B6.3.2 Material Properties

The material properties are unchanged from the descriptions provided in Section 6.3.2, *Material Properties*.

### B6.3.3 Computer Codes and Cross-Section Libraries

The computer codes and cross section libraries are unchanged from the descriptions provided in Section 6.3.3, *Computer Codes and Cross-Section Libraries*.

### B6.3.4 Demonstration of Maximum Reactivity

The most reactive single package model is for the HAC case hs\_11x11\_ema\_161. The parameters of the most reactive case are:

---

<sup>1</sup> MCNP5, "MCNP – A General Monte Carlo N-Particle Transport Code, Version 5; Volume II: User's Guide," LA-CP-03-0245, Los Alamos National Laboratory, April, 2003.

- 161 fuel rods in an 11x11 lattice to represent the rods in an AFS-B, with two rods in each of the outer lattice locations.
- The EMA modeled as a standard fuel assembly with 6.0% Pu/(Pu+U) and fully expanded fuel rods to maximize reactivity.
- Fully moderated with water, including the pellet to cladding gap.
- Steel reflection, which bounds reflection by water.
- 100% theoretically dense pellets to maximize the plutonium mass.
- Miscellaneous minor steel components in the package are homogenized into the water region inside the package.

The most reactive HAC array model uses the most reactive HAC single package model as a base case. Properties of the most reactive HAC array model are:

- Infinite hexagonal reflection.
- Void between packages.
- Dummy fuel assembly modeled as steel to increase neutron transmission between packages.

## B6.4 Single Package Evaluation

Compliance with the requirements of 10 CFR §71.55 is demonstrated by analyzing an optimally moderated single-unit MFFP. The figures and descriptions provided in Section 6.3.1, *Model Configuration*, describe the basic geometry of the single-unit models, although the contents are different.

### B6.4.1 Single Package Configuration

#### B6.4.1.1 NCT Configuration

No MCNP models are developed for the NCT configuration with a payload of 1 EMA and 1 AFS-B containing 175 rods. Under NCT, in the absence of moderation the reactivity will be bounded by the standard three fuel assembly analysis of Section 6.4.1.1, *NCT Configuration*, because the reactivity for the dry condition is governed by the fissile mass in the package. Under the assumed configuration with 1 AFS-B and 1 EMA, the MFFP would contain no more than  $175 + 264 = 439$  fuel rods. The standard three fuel assembly models contain  $264 * 3 = 792$  fuel rods. Therefore, the NCT results for three fuel assemblies bound the AFS-B/EMA configuration. Therefore, no NCT models for the AFS-B/EMA configuration are required.

#### B6.4.1.2 HAC Configuration

Under HAC, explicit models are required because it is assumed the rods in the AFS-B reach optimum moderation, while expansion of a standard fuel assembly is limited by the FCS and strongback. The approach is to conservatively model the contents of an AFS-B within the MFFP.

The package is assumed to be flooded. Because the AFS-B is not modeled, it is assumed that the rods are free to arrange themselves into the most reactive configuration. As a point of interest, the most reactive rod pitch is first determined by simply modeling an arbitrary number of rods (13x13) in a square array reflected by water, see Figure B6.4-2. Note that the packaging, including the poison plates, are ignored. The pitch is varied until the maximum reactivity is obtained. The results in Table B6.4-1 indicate that the most reactive rod pitch is 2.4 cm. As the inner dimensions of the cavity is 8.8", the number of rods that will fit at the optimum pitch is only  $[(8.8)(2.54)/2.4]^2 \sim 87$ . A pitch of 2.2 cm is nearly as reactive, with a corresponding  $\sim 103$  rods. 103 rods may be approximately modeled as a 10x10 array.

Because the optimum pitch results in a reduced number of rods that may fit in the cavity, there is a reactivity tradeoff between the pitch and the fissile mass, because these quantities cannot be optimized simultaneously. If a regular pitch is assumed, the optimum pitch will have a greatly reduced number of rods. Conversely, if the maximum 175 rods are modeled, the pitch will not be optimized for all rods.

Through non-regular modeling of the rod arrangements, it is possible to create scenarios in which the pitch is nearly optimized throughout most of the cavity, but clusters of rods are added to other regions of the cavity to bring the total number of rods to a larger value, up to 175. In

this manner, a larger number rods may be modeled, although the pitch is not optimized in all regions of the model.

The worst-case single package model for three fuel assemblies from Section 6.4, *Single Package Evaluation* (case max\_hac\_single\_srnddn20), is used as the base packaging model for these cases, although all rods are initially positioned at the axial height of a rod in the standard MOX fuel assembly. The AFS-B/EMA model geometry is shown in Figure B6.4-3. Note that all cases use steel as the external reflector rather than water because a steel reflector is shown in Section 6.4 to be slightly more reactive than water. The EMA is conservatively modeled as a standard fuel assembly with the pitch expanded to the maximum extent, consistent with the most reactive assembly configuration from Section 6.4.1.2, *HAC Configuration*. The dummy fuel assembly is simply modeled as water. Results are provided in Table B6.4-2 and are discussed in the following paragraphs.

In the following cases, the number of rods does not sum to the limit of 175 and are evenly distributed throughout the cavity: 14x14, 13x13, 12x13, 12x12, 11x11, and 10x10. (Note that the 14x14 arrangement (196 rods) is not physically possible due to the 175 rod limit of the AFS-B cavity.) These cases are termed "standard pitch" cases, and the outer rows of rods do not touch the poison plates. In the "expanded pitch" cases, the rods are further expanded to the poison plates, see Figure B6.4-4. Comparing these "regular pitch" cases, the 12x13 expanded pitch case (156 rods) is the most reactive, although the 10x10 case (100 rods) is much closer to the optimum pitch. Clearly, the fissile mass is so greatly reduced when the optimum pitch is modeled that the most reactive case is for a non-optimum pitch with a higher fissile mass.

A limited number of cases are developed that model non-regular rod pitches. The 12x13 standard pitch, 12x13 expanded pitch, 12x12, 11x11, and 10x10 standard pitch cases are modified to add additional rods to the lattice to increase the number of rods up to the limit of 175. These various configurations are shown in Figure B6.4-5 through Figure B6.4-7. The most reactive case is hs\_11x11\_ema\_161, which has two rods in each of the outer array locations, for a total of 161 rods. Note that the reactivity of this case is statistically equivalent to the reactivity of the 12x13 expanded pitch case with a regular pitch.

It must be stressed that none of the proposed rod scenarios (either regular or non-regular) are credible because the AFS-B, even if severely damaged, would displace most of the volume available for rod expansion and would preclude such rod arrangements from forming (see Figure B6.4-1 for a cross sectional sketch of the AFS-B with 175 rods). Ignoring the AFS-B is conservative for modeling purposes, but should not be viewed as a credible or likely scenario. It is also demonstrated in Chapter B2.0, *Structural Evaluation*, that the AFS-B will maintain its design function of protecting the fuel rods in an accident.

For the previous cases, no axial shifting is assumed. Consistent with the three fuel assembly models, the most reactive case determined above (hs\_11x11\_ema\_161) is further analyzed for axial shifting of the both the AFS-B and EMA rods.

In case hs\_11x11\_ema\_161, the EMA rods are allowed to shift downward in the same pattern that resulted in the most reactive condition for the three fuel assembly model (max\_hac\_single\_srnddn20). The multiplication factor actually dropped slightly, indicating that this change is within the statistical uncertainty of the Monte Carlo method. Therefore, the remaining models use the EMA in the standard configuration.

Four rod shifting scenarios are considered for the AFS-B rods: (1) all rods shifted down (maxdn), (2) all rods shifted up (maxup), (3) rods alternately shifted up or down (mix), and (4) rods shifted up or down in a checkerboard pattern (mix2). No AFS-B rod shifting scenario results in a reactivity increase, and the observed differences are likely the result of statistical fluctuation.

The most reactive condition is case `hs_11x11_ema_161`, with a  $k_s = 0.92067$ , which is below the USL of 0.9288. Note that this reactivity is artificially high because the geometry control provided by the AFS-B was conservatively neglected.

### **B6.4.2 Single Package Results**

The optimum pitch search results are provided in Table B6.4-1. The multiplication factors are high because no poison plates are modeled. Results for the HAC single package are provided in Table B6.4-2. The most reactive case in each table is listed in boldface.



Table B6.4-1 – Most Reactive Rod Pitch

Case	Pitch (cm)	$k_{eff}$	$\sigma$	$k_s$ ( $k+2\sigma$ )
13x13_p09	1.8	1.03880	0.00099	1.04078
13x13_p1	2	1.07919	0.00099	1.08117
13x13_p11	2.2	1.09440	0.00106	1.09652
<b>13x13_p12</b>	<b>2.4</b>	<b>1.10038</b>	<b>0.00098</b>	<b>1.10234</b>
13x13_p13	2.6	1.09115	0.00093	1.09301
13x13_p14	2.8	1.07248	0.00099	1.07446

Table B6.4-2 – Criticality Results for HAC Single Package

Case	AFS-B X-pitch (cm)	AFS-B Y-pitch (cm)	Number of Rods in AFS-B	$k_{eff}$	$\sigma$	$k_s$ ( $k+2\sigma$ )
No axial shifting						
hs_14x14_ema	1.5966	1.5966	196	0.90106	0.00104	0.90314
hs_13x13_ema	1.7194	1.7194	169	0.91139	0.00102	0.91343
hs_12x13_ema	1.8628	1.7194	156	0.91179	0.00099	0.91377
hs_12x13_ema_175	1.8628	1.7194	175	0.91679	0.00101	0.91881
hs_12x13max_ema	1.9458	1.7836	156	0.91716	0.00099	0.91914
hs_12x13max_ema_175	1.9458	1.7836	175	0.89781	0.00095	0.89971
hs_12x13max_ema_175r	1.9458	1.7836	175	0.91022	0.00102	0.91226
hs_12x12_ema	1.8628	1.8628	144	0.91102	0.00101	0.91304
hs_12x12_ema_175	1.8628	1.8628	175	0.91640	0.00099	0.91838
hs_11x11_ema	2.0360	2.0360	121	0.90243	0.00098	0.90439
<b>hs_11x11_ema_161</b>	<b>2.0360</b>	<b>2.0360</b>	<b>161</b>	<b>0.91859</b>	<b>0.00104</b>	<b>0.92067</b>
hs_11x11_ema_175	2.0360	2.0360	175	0.91742	0.00097	0.91936
hs_10x10_ema	2.2354	2.2354	100	0.88423	0.00098	0.88619
hs_10x10_ema_136	2.2354	2.2354	136	0.90474	0.00097	0.90668
hs_10x10_ema_164	2.2354	2.2354	164	0.90752	0.00102	0.90956
hs_10x10_ema_175	2.2354	2.2354	175	0.90513	0.00098	0.90709
With axial shifting						
hs_11x11_emadn_161	2.0360	2.0360	161	0.91614	0.00102	0.91818
hs_11x11dn_ema_161	2.0360	2.0360	161	0.91660	0.00096	0.91852
hs_11x11up_ema_161	2.0360	2.0360	161	0.91707	0.00096	0.91899
hs_11x11mix_ema_161	2.0360	2.0360	161	0.91768	0.00098	0.91964
hs_11x11mix2_ema_161	2.0360	2.0360	161	0.91363	0.00102	0.91567

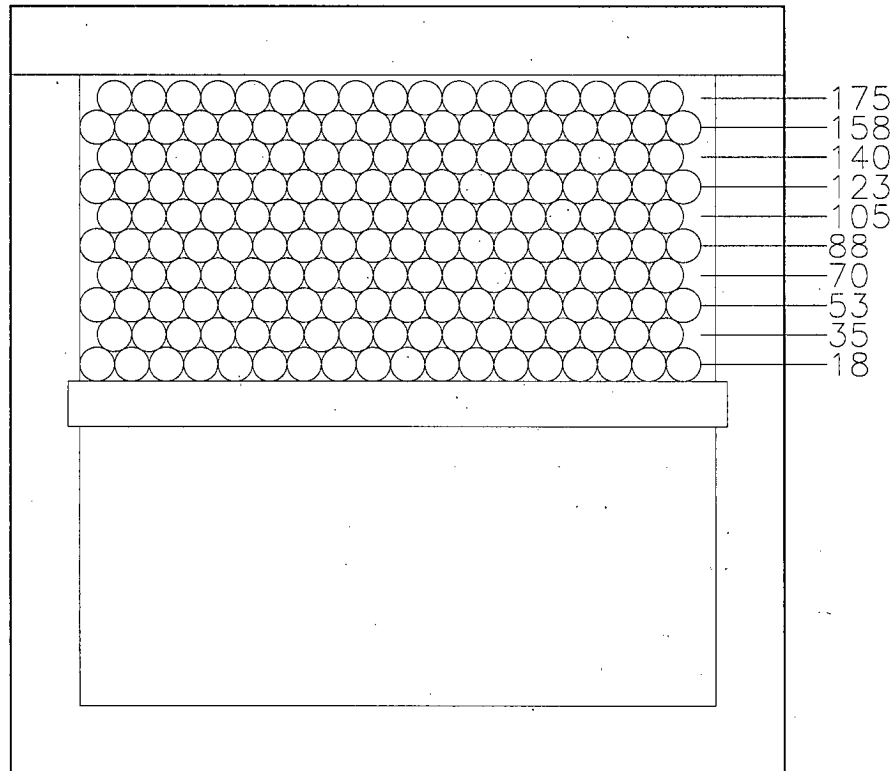
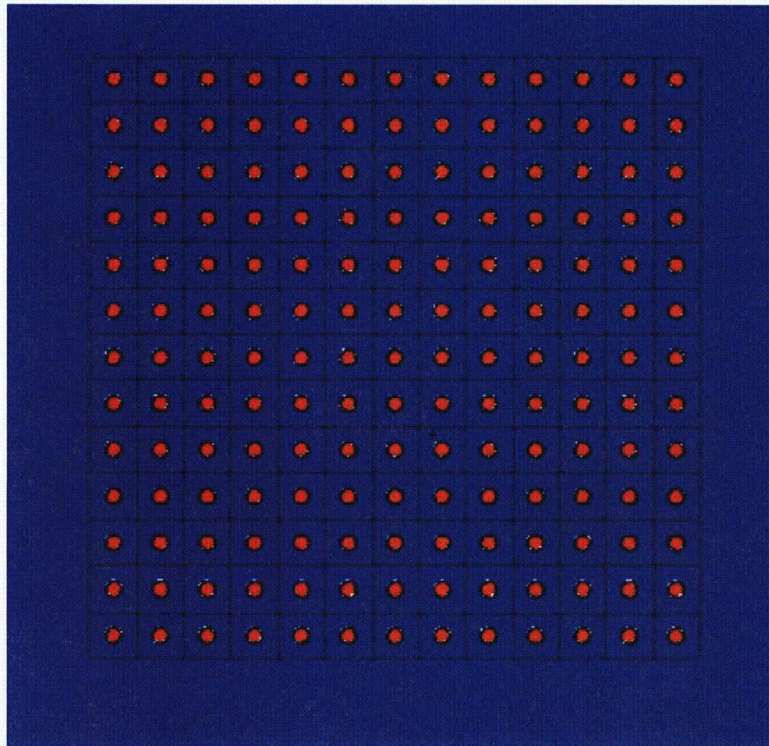


Figure B6.4-1 – AFS-B with 175 MOX Rods



Single array, water reflected, no poison

**Figure B6.4-2 – Optimum Pitch Model**

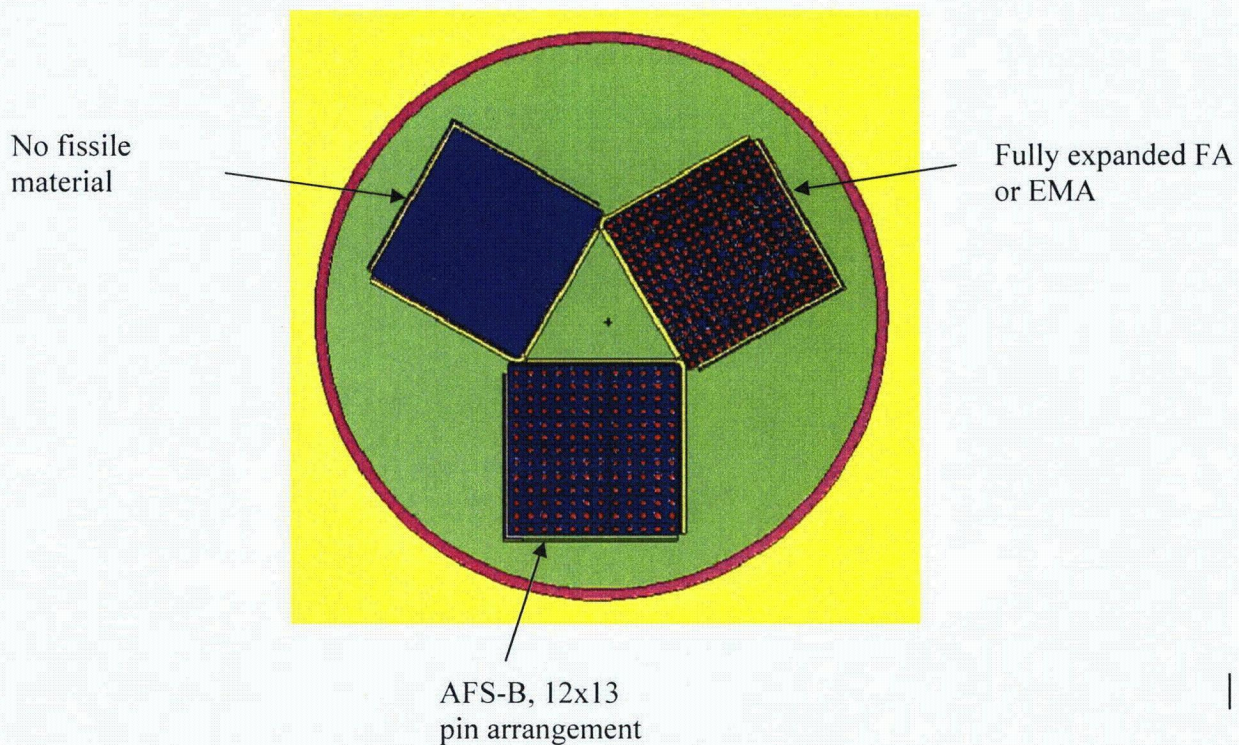


Figure B6.4-3 – AFS-B(12x13)/EMA HAC Single Package Model

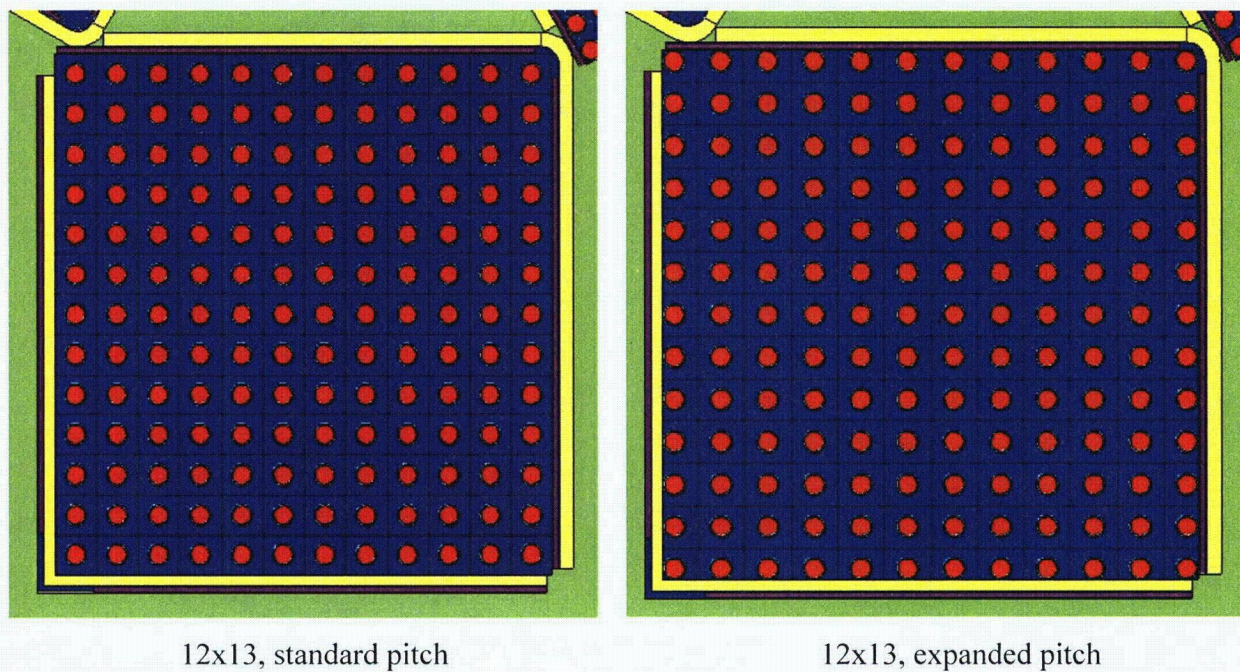
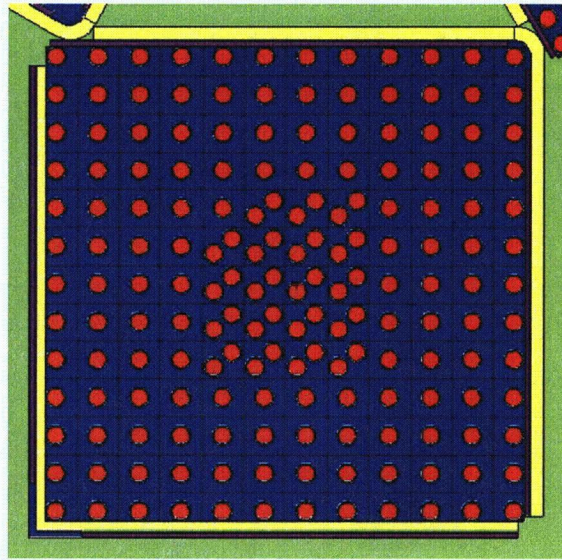
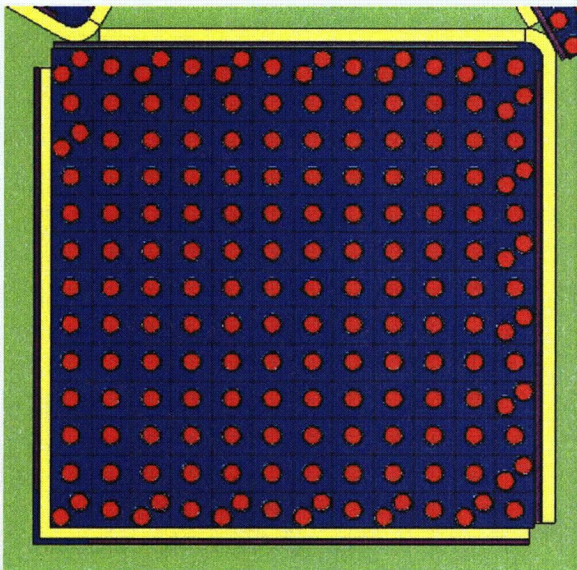


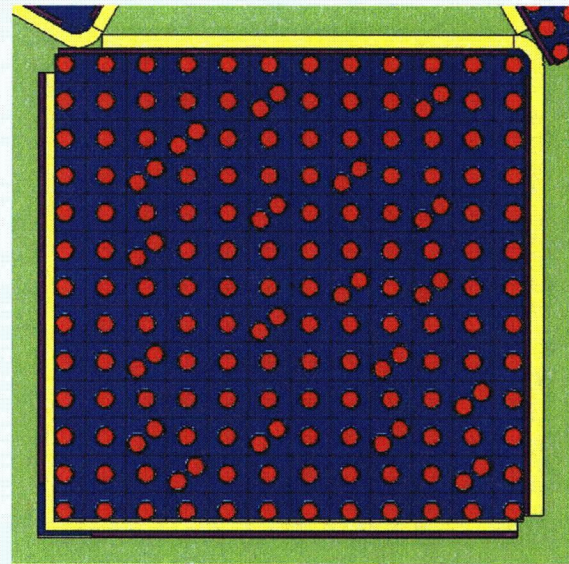
Figure B6.4-4 – Standard and Expanded Pitch Comparison



hs\_12x13max\_ema\_175

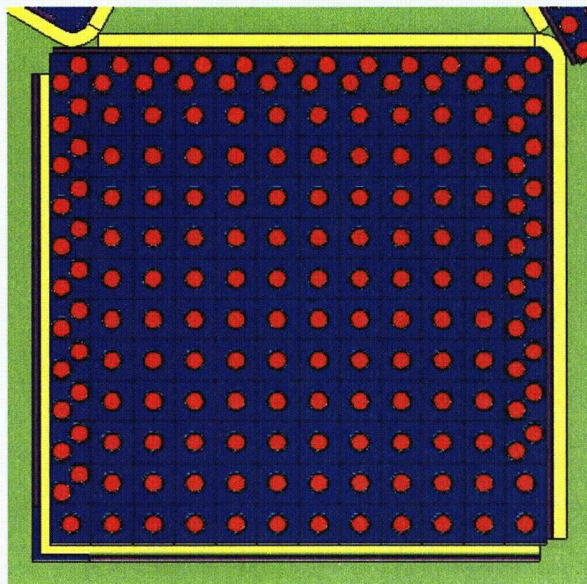


hs\_12x13\_ema\_175

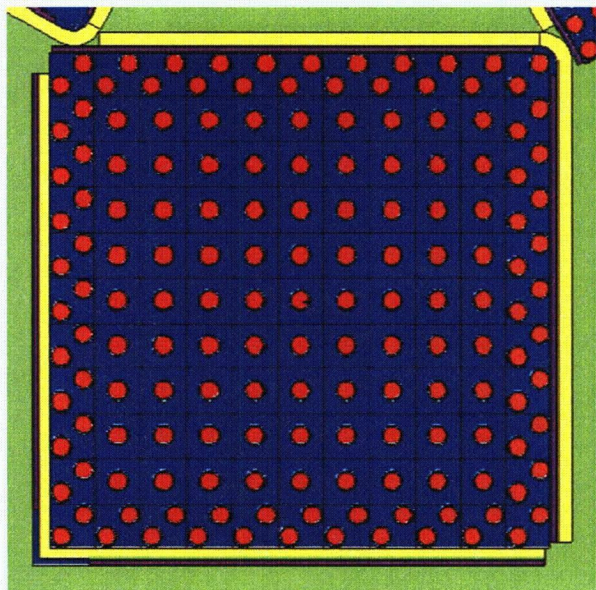


hs\_12x13max\_ema\_175r

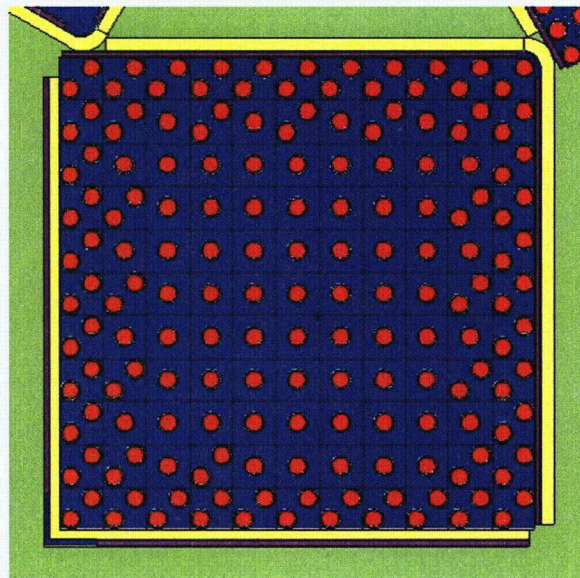
**Figure B6.4-5 – 12x13 Non-Regular Rod Patterns**



hs\_12x12\_ema\_175

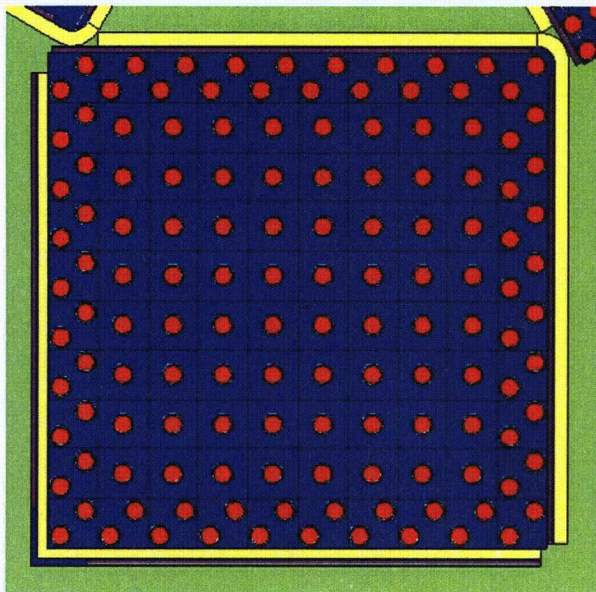


hs\_11x11\_ema\_161

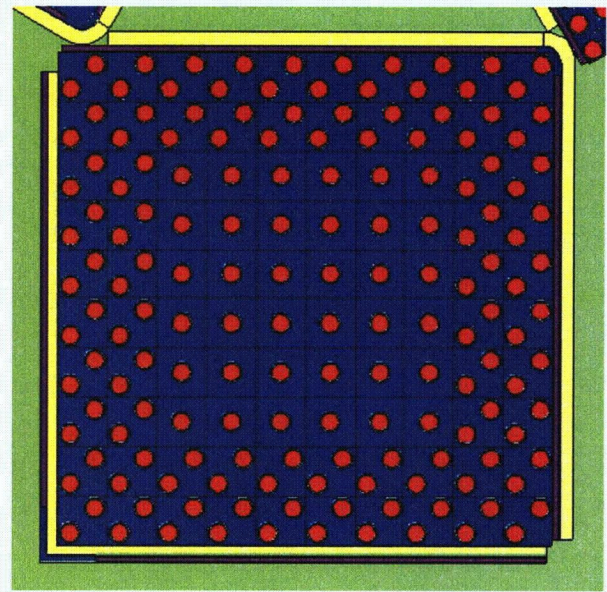


hs\_11x11\_ema\_175

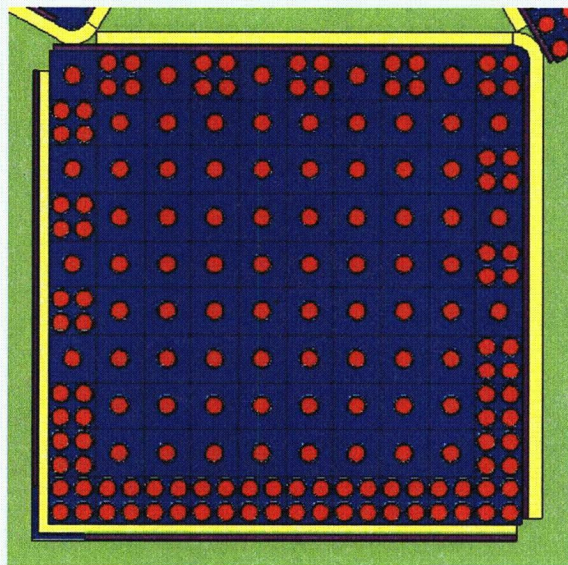
Figure B6.4-6 – 12x12 and 11x11 Non-Regular Rod Patterns



hs\_10x10\_ema\_136



hs\_10x10\_ema\_164



hs\_10x10\_ema\_175

**Figure B6.4-7 – 10x10 Non-Regular Rod Patterns**

## B6.5 Evaluation of Package Arrays Under Normal Conditions of Transport

No MCNP array models are developed for the NCT configuration with a payload of 1 EMA and 1 AFS-B containing 175 rods. Under NCT, in the absence of moderation the reactivity will be bounded by the standard three fuel assembly analysis of Section 6.5, *Evaluation of Package Arrays Under Normal Conditions of Transport*, because the reactivity for the dry condition is governed by the fissile mass in the package. Under the assumed configuration with 1 AFS-B and 1 EMA, the MFFP would contain no more than  $175 + 264 = 439$  fuel rods. The standard three fuel assembly models contain  $264 * 3 = 792$  fuel rods. Therefore, the NCT results for three fuel assemblies bound the AFS-B/EMA configuration. Therefore, no NCT array models for the AFS-B/EMA configuration are required.



This page left intentionally blank.

## B6.6 Package Arrays Under Hypothetical Accident Conditions

### B6.6.1 HAC Array Configuration

Only a limited number of HAC infinite array cases are run for the AFS-B/EMA because it has already been established for this package that the single package and infinite array HAC reactivities are nearly identical (see Table 6.1-1). Neutronic communication between packages is small because the package is large and heavily poisoned. Therefore, the most reactive single package case is run in the infinite array configuration.

For the HAC array, it has been established from the original three fuel assembly analysis (Section 6.6, *Package Arrays Under Hypothetical Accident Conditions*) that the most reactive condition is for full moderation within the packages. For low water density ( $\leq 0.1 \text{ g/cm}^3$ ) between packages, reactivity is maximized and the reactivity fluctuation for different low water densities is statistical in nature. Consequently, void is modeled between the packages. Because the fuel is the same as the standard three fuel assembly analysis, these modeling parameters will also result in the most reactive condition for AFS-B/EMA configuration. Also, axial shifting of rods has been shown in Section B6.4.1.2, *HAC Configuration*, to have little effect on system reactivity other than statistical fluctuation. Therefore, for the HAC array, it is sufficient to infinitely reflect the most reactive single package case from Table B6.4-2.

In this case (ha\_11x11\_ema\_161) it is assumed that the dummy fuel location is modeled as water. In actuality, the dummy fuel assembly is a large steel box with void on the inside that approximates the weight of a fuel assembly. As the neutron transmission is greater through either void or steel compared to water, modeling the dummy fuel assembly could slightly increase the reactivity for the array condition. Therefore, two additional cases are run in which the water in the empty location is replaced with steel or void. The results for these cases are provided in Table B6.6-1. The most reactive case has steel in the empty location, although the three results are statistically equivalent, and the multiplication factor of 0.92400 is less than the USL of 0.9288.

While the maximum  $k_s$  is approaching to the USL, the assumption that the AFS-B provides no constraint to the rods is not realistic, as there is no scenario in which the postulated rod expansion could be realized in actual practice. The AFS-B, even if severely damaged in an accident, would occupy space and preclude the postulated rod expansion

### B6.6.2 HAC Array Results

Results for the HAC single package are provided in Table B6.6-1. The most reactive case is listed in boldface.

**Table B6.6-1 – Criticality Results for an Infinite Array of HAC Packages**

Case	Dummy Assembly	$k_{eff}$	$\sigma$	$k_s (k+2\sigma)$
ha_11x11_ema_161	Water	0.92101	0.00099	0.92299
ha_11x11_ema_161_st	Steel	<b>0.92192</b>	<b>0.00104</b>	<b>0.92400</b>
ha_11x11_ema_161_vd	Void	0.92131	0.00098	0.92327

## **B6.7 Fissile Material Packages for Air Transport**

This section does not apply for the MFFP, because air transport is not claimed.

This page left intentionally blank.

## **B6.8 Benchmark Evaluations**

The benchmark evaluation is provided in Section 6.8, *Benchmark Evaluations*. A USL of 0.9288 is justified.

This page left intentionally blank.

## B6.9 Appendices

Representative MCNP models are included in the following appendices:

- B6.9.1 Single Package Model
- B6.9.2 Infinite Array Model



This page left intentionally blank.

### B6.9.1 Single Package Model

This file is for the worst-case HAC model (hs\_11x11\_ema\_161).

```

175 pin max with 10.85 g/cc Fuel no Nb
c
c *****Fuel Assembly*****
c cells 1 to 3 transform the 3 assemblies to their locations
c 1 4 -1.0 -21 22 -23 24 -25 6 imp:n=1 $ top nozzle, void
c 2 4 -1.0 -21 22 -23 24 -7 26 imp:n=1 $ bottom nozzle, void
c 7 0 -21 22 -23 24 126 -25 fill=20 imp:n=1 $ pins
c
c 201 like 1 but trcl=53 $ assembly 2
c 202 like 2 but trcl=53
c 207 like 7 but fill=21 trcl=53
c 220 like 1 but trcl=54 $ assembly 3
c 221 like 2 but trcl=54
c 222 like 7 but fill=5 trcl=54
c
c -- "box" around fuel
c
c 301 0 (302 -303 300 -304 -906 26):
      (303 -305 300 -301 -906 26) fill=30 imp:n=1 $ "box" cutout
c 302 like 301 but trcl=53
c 303 like 301 but trcl=54
c
c perimeter containing strongback #1 in -y
c 50 0 (26 -906 902 -909 904 -910):
      (26 -906 909 -912 904 -901):
      (26 -906 912 904 -908):
      (26 -906 911 905 -904 -908):
      (26 -906 905 -900 903 -911) fill=7 imp:n=1
c perimeter containing strongback #2
c 51 like 50 but trcl=53
c perimeter containing strongback #3
c 52 like 50 but trcl=54
c
c *****water beyond three units*****
c 131 9 -1.4 -61 -69 64 #7 #50, #51 #52 #301 #302 #303
      #207 #222 imp:n=1
c *****containment*****
c 141 5 -7.94 -62 -66 63 (61:65:-64) imp:n=1 $ outer steel
c 143 5 -7.94 -61 -70 69 imp:n=1 $ upper inner steel
c 145 4 -1.0 -61 -65 70 imp:n=1 $ upper void
c *****beyond containment*****
c 195 0 -881 882 -886 885 -883 884 -66 63 62 imp:n=1 $ w between packages
c 199 0 (881:-882:886:-885:883:-884:66:-63) imp:n=0 $ outside world
c
c Universe 20: Fuel Lattice
c
c 200 4 -1.0 -12 11 -14 13 u=20 lat=1 trcl=30 fill=0:10 0:10 0:0
      6 6 6 6 6 6 6 6 6 6 $ row 11
      6 1 1 1 1 1 1 1 1 1 6 $ row 10
      6 1 1 1 1 1 1 1 1 1 6 $ row 9
      6 1 1 1 1 1 1 1 1 1 6 $ row 8
      6 1 1 1 1 1 1 1 1 1 6 $ row 7
      6 1 1 1 1 1 1 1 1 1 6 $ row 6
      6 1 1 1 1 1 1 1 1 1 6 $ row 5
      6 1 1 1 1 1 1 1 1 1 6 $ row 4
      6 1 1 1 1 1 1 1 1 1 6 $ row 3
      6 1 1 1 1 1 1 1 1 1 6 $ row 2
      6 6 6 6 6 6 6 6 6 6 imp:n=1 $ row 1 (top)
c
c Universe 21: EMA
c
c 201 4 -1.0 -212 211 -214 213 u=21 lat=1 trcl=31 fill=0:16 0:16 0:0
      1 1 1 1 1 1 1 1 1 1 1 1 1 1 1 1 $ row 17
      1 1 1 1 1 1 1 1 1 1 1 1 1 1 1 1 $ row 16
      1 1 1 1 1 4 1 1 4 1 1 4 1 1 1 1 $ row 15
      1 1 1 4 1 1 1 1 1 1 1 1 1 4 1 1 $ row 14
      1 1 1 1 1 1 1 1 1 1 1 1 1 1 1 1 $ row 13
      1 1 4 1 1 4 1 1 4 1 1 4 1 1 4 1 $ row 12
      1 1 1 1 1 1 1 1 1 1 1 1 1 1 1 1 $ row 11
    
```

```

1 1 1 1 1 1 1 1 1 1 1 1 1 1 1 1 $ row 10
1 1 4 1 1 4 1 1 4 1 1 4 1 1 4 1 1 $ row 9
1 1 1 1 1 1 1 1 1 1 1 1 1 1 1 1 $ row 8
1 1 1 1 1 1 1 1 1 1 1 1 1 1 1 1 $ row 7
1 1 4 1 1 4 1 1 4 1 1 4 1 1 4 1 1 $ row 6
1 1 1 1 1 1 1 1 1 1 1 1 1 1 1 1 $ row 5
1 1 1 4 1 1 1 1 1 1 1 1 1 4 1 1 1 $ row 4
1 1 1 1 1 4 1 1 4 1 1 4 1 1 1 1 1 $ row 3
1 1 1 1 1 1 1 1 1 1 1 1 1 1 1 1 $ row 2
1 1 1 1 1 1 1 1 1 1 1 1 1 1 1 1 imp:n=1 $ row 1 (top)
c
c Universe 1: Fuel pin in normal position
c
10 1 -10.85 -1 -4 5 u=1 imp:n=1 $ fuel
11 4 -1.0 -2 1 -4 5 u=1 imp:n=1 $ radial gap
12 7 -6.5 -3 2 -8 5 u=1 imp:n=1 $ clad
13 4 -1.0 3 7 -6 u=1 imp:n=1 $ radially beyond pin
14 4 -1.0 -2 -8 4 u=1 imp:n=1 $ above fuel void
15 7 -6.5 -3 -6 8 u=1 imp:n=1 $ top of fuel cap
16 7 -6.5 -3 -5 7 u=1 imp:n=1 $ bottom of fuel cap
17 4 -1.0 6 u=1 imp:n=1 $ top water to infinity
18 4 -1.0 -7 u=1 imp:n=1 $ bottom water to infinity
c
c Universe 2: Fuel pin shifted up
c
410 1 -10.85 -1 -4 5 trcl=(0 0 23.7109) u=2 imp:n=1 $ fuel
411 4 -1.0 -2 1 -4 5 trcl=(0 0 23.7109) u=2 imp:n=1 $ radial gap
412 7 -6.5 -3 2 -8 5 trcl=(0 0 23.7109) u=2 imp:n=1 $ clad
413 4 -1.0 3 7 -6 trcl=(0 0 23.7109) u=2 imp:n=1 $ radially beyond pin
414 4 -1.0 -2 -8 4 trcl=(0 0 23.7109) u=2 imp:n=1 $ above fuel void
415 7 -6.5 -3 -6 8 trcl=(0 0 23.7109) u=2 imp:n=1 $ top of fuel cap
416 7 -6.5 -3 -5 7 trcl=(0 0 23.7109) u=2 imp:n=1 $ bottom of fuel cap
417 4 -1.0 6 trcl=(0 0 23.7109) u=2 imp:n=1 $ top water to infinity
418 4 -1.0 -7 trcl=(0 0 23.7109) u=2 imp:n=1 $ bottom water to
infinity
c
c Universe 3: Fuel pin shifted down
c
420 1 -10.85 -1 -4 5 trcl=(0 0 -9.4361) u=3 imp:n=1 $ fuel
421 4 -1.0 -2 1 -4 5 trcl=(0 0 -9.4361) u=3 imp:n=1 $ radial gap
422 7 -6.5 -3 2 -8 5 trcl=(0 0 -9.4361) u=3 imp:n=1 $ clad
423 4 -1.0 3 7 -6 trcl=(0 0 -9.4361) u=3 imp:n=1 $ radially beyond pin
424 4 -1.0 -2 -8 4 trcl=(0 0 -9.4361) u=3 imp:n=1 $ above fuel void
425 7 -6.5 -3 -6 8 trcl=(0 0 -9.4361) u=3 imp:n=1 $ top of fuel cap
426 7 -6.5 -3 -5 7 trcl=(0 0 -9.4361) u=3 imp:n=1 $ bottom of fuel cap
427 4 -1.0 6 trcl=(0 0 -9.4361) u=3 imp:n=1 $ top water to infinity
428 4 -1.0 -7 trcl=(0 0 -9.4361) u=3 imp:n=1 $ bottom water to infinity
c
c Universe 4: Instrument/guide tube
c
41 4 -1.0 -18 5 -8 u=4 imp:n=1 $ inside
42 7 -6.5 -19 18 5 -8 u=4 imp:n=1 $ tube
43 4 -1.0 19 5 -8 u=4 imp:n=1 $ beyond tube
44 4 -1.0 8 u=4 imp:n=1
45 4 -1.0 -5 u=4 imp:n=1
c
c Universe 5: Water only
c
46 4 -1.0 -998 u=5 imp:n=1
47 4 -1.0 998 u=5 imp:n=1
c
c Universe 8: Steel only
c
48 6 -7.94 -998 u=8 imp:n=1
49 6 -7.94 998 u=8 imp:n=1
c
c Universe 6: Two fuel pins
c
600 4 -1.0 #601 #602 u=6 imp:n=1
601 0 -600 fill=1(0.5 0.5 0) u=6 imp:n=1
602 0 -603 fill=1(-0.5 -0.5 0) u=6 imp:n=1
c
c Universe 7: Strongback
c
700 6 -7.94 715 -710 u=7 imp:n=1 $ tangential strongback

```

701	6	-7.94	(710 711 718):(-711 713)	u=7	imp:n=1	\$ radial strongback+bend
702	2	-2.713	714 -719 -716	u=7	imp:n=1	\$ tan Al clad
703	21	9.2244E-02	719 -720 -716			
			730 731 732 733 734 735 736 737 738			
			739 740 741 742 743 744 745 746 747			
			750 751 752 753 754 755 756 757 758			
			759 760 761 762 763 764 765 766 767	u=7	imp:n=1	\$ tangential borAl
704	2	-2.713	720 -715 -716	u=7	imp:n=1	\$ tan Al clad
706	2	-2.713	712 -722 -717	u=7	imp:n=1	\$ rad Al clad
707	21	9.2244E-02	722 -723 -717			
			770 771 772 773 774 775 776 777 778			
			779 780 781 782 783 784 785 786 787			
			790 791 792 793 794 795 796 797 798			
			799 800 801 802 803 804 805 806 807	u=7	imp:n=1	\$ radial borAl
708	2	-2.713	723 -713 -717	u=7	imp:n=1	\$ rad Al
710	4	-1.0	(710 711 -718):(716 -710 717 -715):			
			(710 -713 717 -711)	u=7	imp:n=1	
719	6	-7.94	((-717 -712):(-716 -714 717))	-809	u=7	imp:n=1 \$ poison holder
720	4	-1.0	((-717 -712):(-716 -714 717))	809 -810	u=7	imp:n=1
721	6	-7.94	((-717 -712):(-716 -714 717))	810 -811	u=7	imp:n=1
722	4	-1.0	((-717 -712):(-716 -714 717))	811 -812	u=7	imp:n=1
723	6	-7.94	((-717 -712):(-716 -714 717))	812 -813	u=7	imp:n=1
724	4	-1.0	((-717 -712):(-716 -714 717))	813 -814	u=7	imp:n=1
725	6	-7.94	((-717 -712):(-716 -714 717))	814 -815	u=7	imp:n=1
726	4	-1.0	((-717 -712):(-716 -714 717))	815 -816	u=7	imp:n=1
727	6	-7.94	((-717 -712):(-716 -714 717))	816 -817	u=7	imp:n=1
728	4	-1.0	((-717 -712):(-716 -714 717))	817 -818	u=7	imp:n=1
729	6	-7.94	((-717 -712):(-716 -714 717))	818 -819	u=7	imp:n=1
730	4	-1.0	((-717 -712):(-716 -714 717))	819 -820	u=7	imp:n=1
731	6	-7.94	((-717 -712):(-716 -714 717))	820 -821	u=7	imp:n=1
732	4	-1.0	((-717 -712):(-716 -714 717))	821 -822	u=7	imp:n=1
733	6	-7.94	((-717 -712):(-716 -714 717))	822 -823	u=7	imp:n=1
734	4	-1.0	((-717 -712):(-716 -714 717))	823 -824	u=7	imp:n=1
735	6	-7.94	((-717 -712):(-716 -714 717))	824 -825	u=7	imp:n=1
736	4	-1.0	((-717 -712):(-716 -714 717))	825 -826	u=7	imp:n=1
737	6	-7.94	((-717 -712):(-716 -714 717))	826	u=7	imp:n=1
c						
750	6	-7.94	719 -720 -750	u=7	imp:n=1	\$ screws in borAl
751	6	-7.94	719 -720 -751	u=7	imp:n=1	
752	6	-7.94	719 -720 -752	u=7	imp:n=1	
753	6	-7.94	719 -720 -753	u=7	imp:n=1	
754	6	-7.94	719 -720 -754	u=7	imp:n=1	
755	6	-7.94	719 -720 -755	u=7	imp:n=1	
756	6	-7.94	719 -720 -756	u=7	imp:n=1	
757	6	-7.94	719 -720 -757	u=7	imp:n=1	
758	6	-7.94	719 -720 -758	u=7	imp:n=1	
759	6	-7.94	719 -720 -759	u=7	imp:n=1	
760	6	-7.94	719 -720 -760	u=7	imp:n=1	
761	6	-7.94	719 -720 -761	u=7	imp:n=1	
762	6	-7.94	719 -720 -762	u=7	imp:n=1	
763	6	-7.94	719 -720 -763	u=7	imp:n=1	
764	6	-7.94	719 -720 -764	u=7	imp:n=1	
765	6	-7.94	719 -720 -765	u=7	imp:n=1	
766	6	-7.94	719 -720 -766	u=7	imp:n=1	
767	6	-7.94	719 -720 -767	u=7	imp:n=1	
c						
770	6	-7.94	722 -723 -770	u=7	imp:n=1	
771	6	-7.94	722 -723 -771	u=7	imp:n=1	
772	6	-7.94	722 -723 -772	u=7	imp:n=1	
773	6	-7.94	722 -723 -773	u=7	imp:n=1	
774	6	-7.94	722 -723 -774	u=7	imp:n=1	
775	6	-7.94	722 -723 -775	u=7	imp:n=1	
776	6	-7.94	722 -723 -776	u=7	imp:n=1	
777	6	-7.94	722 -723 -777	u=7	imp:n=1	
778	6	-7.94	722 -723 -778	u=7	imp:n=1	
779	6	-7.94	722 -723 -779	u=7	imp:n=1	
780	6	-7.94	722 -723 -780	u=7	imp:n=1	
781	6	-7.94	722 -723 -781	u=7	imp:n=1	
782	6	-7.94	722 -723 -782	u=7	imp:n=1	
783	6	-7.94	722 -723 -783	u=7	imp:n=1	
784	6	-7.94	722 -723 -784	u=7	imp:n=1	
785	6	-7.94	722 -723 -785	u=7	imp:n=1	
786	6	-7.94	722 -723 -786	u=7	imp:n=1	
787	6	-7.94	722 -723 -787	u=7	imp:n=1	
c						

```

790 6 -7.94 722 -723 -790 u=7 imp:n=1
791 6 -7.94 722 -723 -791 u=7 imp:n=1
792 6 -7.94 722 -723 -792 u=7 imp:n=1
793 6 -7.94 722 -723 -793 u=7 imp:n=1
794 6 -7.94 722 -723 -794 u=7 imp:n=1
795 6 -7.94 722 -723 -795 u=7 imp:n=1
796 6 -7.94 722 -723 -796 u=7 imp:n=1
797 6 -7.94 722 -723 -797 u=7 imp:n=1
798 6 -7.94 722 -723 -798 u=7 imp:n=1
799 6 -7.94 722 -723 -799 u=7 imp:n=1
800 6 -7.94 722 -723 -800 u=7 imp:n=1
801 6 -7.94 722 -723 -801 u=7 imp:n=1
802 6 -7.94 722 -723 -802 u=7 imp:n=1
803 6 -7.94 722 -723 -803 u=7 imp:n=1
804 6 -7.94 722 -723 -804 u=7 imp:n=1
805 6 -7.94 722 -723 -805 u=7 imp:n=1
806 6 -7.94 722 -723 -806 u=7 imp:n=1
807 6 -7.94 722 -723 -807 u=7 imp:n=1
c
810 6 -7.94 719 -720 -730 u=7 imp:n=1
811 6 -7.94 719 -720 -731 u=7 imp:n=1
812 6 -7.94 719 -720 -732 u=7 imp:n=1
813 6 -7.94 719 -720 -733 u=7 imp:n=1
814 6 -7.94 719 -720 -734 u=7 imp:n=1
815 6 -7.94 719 -720 -735 u=7 imp:n=1
816 6 -7.94 719 -720 -736 u=7 imp:n=1
817 6 -7.94 719 -720 -737 u=7 imp:n=1
818 6 -7.94 719 -720 -738 u=7 imp:n=1
819 6 -7.94 719 -720 -739 u=7 imp:n=1
820 6 -7.94 719 -720 -740 u=7 imp:n=1
821 6 -7.94 719 -720 -741 u=7 imp:n=1
822 6 -7.94 719 -720 -742 u=7 imp:n=1
823 6 -7.94 719 -720 -743 u=7 imp:n=1
824 6 -7.94 719 -720 -744 u=7 imp:n=1
825 6 -7.94 719 -720 -745 u=7 imp:n=1
826 6 -7.94 719 -720 -746 u=7 imp:n=1
827 6 -7.94 719 -720 -747 u=7 imp:n=1
c
c Universe 30: "box" around fuel
c
c 310 2 -2.713 -313 317 u=30 imp:n=1 $ radial left
c 311 2 -2.713 316 -310 u=30 imp:n=1 $ tangential bot
c 312 2 -2.713 314 -315 317 u=30 imp:n=1 $ radial right
c 315 2 -2.713 311 -312 316 u=30 imp:n=1 $ tangential top
316 6 -7.94 315 312 u=30 imp:n=1
317 4 -1.0 (312 -317 -315):(-316 -312) u=30 imp:n=1
c
320 4 -1.0 -315 317 -320 u=30 imp:n=1 $ radial water gap
321 21 9.2244E-02 313 -314 317 320 -321 u=30 imp:n=1 $ radial boral
322 4 -1.0 -315 317 321 -322 u=30 imp:n=1
323 21 9.2244E-02 313 -314 317 322 -323 u=30 imp:n=1
324 4 -1.0 -315 317 323 -324 u=30 imp:n=1
325 21 9.2244E-02 313 -314 317 324 -325 u=30 imp:n=1
326 4 -1.0 -315 317 325 -326 u=30 imp:n=1
327 21 9.2244E-02 313 -314 317 326 -327 u=30 imp:n=1
328 4 -1.0 -315 317 327 -328 u=30 imp:n=1
329 21 9.2244E-02 313 -314 317 328 -329 u=30 imp:n=1
330 4 -1.0 -315 317 329 -330 u=30 imp:n=1
331 21 9.2244E-02 313 -314 317 330 -331 u=30 imp:n=1
332 4 -1.0 -315 317 331 -332 u=30 imp:n=1
333 21 9.2244E-02 313 -314 317 332 -333 u=30 imp:n=1
334 4 -1.0 -315 317 333 u=30 imp:n=1
c
340 2 -2.713 -313 317 320 -321 u=30 imp:n=1 $ radial Al cladding
341 2 -2.713 -313 317 322 -323 u=30 imp:n=1
342 2 -2.713 -313 317 324 -325 u=30 imp:n=1
343 2 -2.713 -313 317 326 -327 u=30 imp:n=1
344 2 -2.713 -313 317 328 -329 u=30 imp:n=1
345 2 -2.713 -313 317 330 -331 u=30 imp:n=1
346 2 -2.713 -313 317 332 -333 u=30 imp:n=1
c
347 2 -2.713 314 -315 317 320 -321 u=30 imp:n=1 $ radial Al cladding
348 2 -2.713 314 -315 317 322 -323 u=30 imp:n=1
349 2 -2.713 314 -315 317 324 -325 u=30 imp:n=1
350 2 -2.713 314 -315 317 326 -327 u=30 imp:n=1

```

```

351 2 -2.713 314 -315 317 328 -329 u=30 imp:n=1
352 2 -2.713 314 -315 317 330 -331 u=30 imp:n=1
353 2 -2.713 314 -315 317 332 -333 u=30 imp:n=1
c
360 4 -1.0 -312 316 -320 u=30 imp:n=1 $ tangential water gap
361 21 9.2244E-02 310 -311 316 320 -321 u=30 imp:n=1 $ tangential borol
362 4 -1.0 -312 316 321 -322 u=30 imp:n=1
363 21 9.2244E-02 310 -311 316 322 -323 u=30 imp:n=1
364 4 -1.0 -312 316 323 -324 u=30 imp:n=1
365 21 9.2244E-02 310 -311 316 324 -325 u=30 imp:n=1
366 4 -1.0 -312 316 325 -326 u=30 imp:n=1
367 21 9.2244E-02 310 -311 316 326 -327 u=30 imp:n=1
368 4 -1.0 -312 316 327 -328 u=30 imp:n=1
369 21 9.2244E-02 310 -311 316 328 -329 u=30 imp:n=1
370 4 -1.0 -312 316 329 -330 u=30 imp:n=1
371 21 9.2244E-02 310 -311 316 330 -331 u=30 imp:n=1
372 4 -1.0 -312 316 331 -332 u=30 imp:n=1
373 21 9.2244E-02 310 -311 316 332 -333 u=30 imp:n=1
374 4 -1.0 -312 316 333 u=30 imp:n=1
c
380 2 -2.713 316 311 -312 320 -321 u=30 imp:n=1 $ horizontal Al cladding
381 2 -2.713 316 311 -312 322 -323 u=30 imp:n=1
382 2 -2.713 316 311 -312 324 -325 u=30 imp:n=1
383 2 -2.713 316 311 -312 326 -327 u=30 imp:n=1
384 2 -2.713 316 311 -312 328 -329 u=30 imp:n=1
385 2 -2.713 316 311 -312 330 -331 u=30 imp:n=1
386 2 -2.713 316 311 -312 332 -333 u=30 imp:n=1
c
387 2 -2.713 316 -310 320 -321 u=30 imp:n=1 $ horizontal Al cladding
388 2 -2.713 316 -310 322 -323 u=30 imp:n=1
389 2 -2.713 316 -310 324 -325 u=30 imp:n=1
390 2 -2.713 316 -310 326 -327 u=30 imp:n=1
391 2 -2.713 316 -310 328 -329 u=30 imp:n=1
392 2 -2.713 316 -310 330 -331 u=30 imp:n=1
393 2 -2.713 316 -310 332 -333 u=30 imp:n=1
c
c Universe 51: Dummy universe containing fuel
c
c 999 1 -10.31 -999 u=51 imp:n=1 $ for diagnostics only, not used
c 1000 1 -10.31 999 u=51 imp:n=1 $ for diagnostics only, not used
c
c *****Fuel Assembly*****
c fuel pin
1 cz 0.409575 $ fuel radius
2 cz 0.41783 $ radius inside clad
3 cz 0.47498 $ radius outside clad
4 pz 182.88 $ top of fuel
5 pz -182.88 $ bottom of fuel
6 pz 202.7555 $ top of fuel pin
7 pz -184.3405 $ bottom of fuel pin
8 pz 201.4474 $ bottom of top cap
11 px -1.018 $ lattice definition
12 px 1.018
13 py -1.018
14 py 1.018
c
211 px -0.6688 $ EMA lattice definition
212 px 0.6688
213 py -0.6688
214 py 0.6688
c 200 pz -119.38
c guide tube
18 cz 0.57150
19 cz 0.61214
c perimeter of fuel assembly
21 px 10.2391 $ offset from surface 905
22 px -12.1116 $
23 py -6.6593 $ offset from surface 904
24 py -29.0113 $
25 pz 226.466
26 pz -190.95720
126 pz -193.776
c *****containment*****
61 cz 36.1950
62 cz 37.6174

```

```

*63      pz -197.5866 $ 1.5" thick
64      pz -193.7766 $ 1.11" below bottom of fuel (strongback bottom not modeled)
65      pz 235.6866
*66      pz 237.5916
c 67     pz -203.0222
c 68     pz -201.1172
69      pz 226.4664
70      pz 228.0666
c      *****outside of water refl****
72      cz 68.0974
73      pz -228.0666 $ 1' water from 63
76      pz 268.0716 $ 1' water from 66
c
c -- "box"
c
300     py -29.7925 $ defining box in u=0
301     py -29.0114
302     px -12.8928
303     px -12.1117
304     py -7.5675
305     px 9.9672
c
310     25 py 0.04445
311     25 py 0.2604
312     25 py 0.3048
313     25 px 0.04445
314     25 px 0.2604
315     25 px 0.3048
316     25 px 2.54
317     25 py 2.54
c
320     pz -171.049
321     pz -119.532
322     pz -109.758
323     pz -67.412
324     pz -57.638
325     pz -15.316
326     pz -5.542
327     pz 36.855
328     pz 46.629
329     pz 89.002
330     pz 98.776
331     pz 141.097
332     pz 150.871
333     pz 193.548
c
c      extra pins
c
600     c/z 0.5 0.5 0.475
601     c/z -0.5 0.5 0.475
602     c/z 0.5 -0.5 0.475
603     c/z -0.5 -0.5 0.475
c
c      strongback surfaces
c
710     22 px 0
711     22 py 0
712     22 px 0.476
713     22 px 0.7808
714     22 py 0.476
715     22 py 0.7808
716     22 px -0.3114 $ 0.43" less than surface 713
717     22 py -0.54
718     22 cz 0.7808
719     22 py 0.5205
720     22 py 0.7364
722     22 px 0.5205
723     22 px 0.7364
c
730     22 c/y -2.7752 -189.6872 0.47625
731     22 c/y -2.7752 -179.5526 0.47625
732     22 c/y -2.7752 -172.3187 0.47625
733     22 c/y -2.7752 -118.2624 0.47625
734     22 c/y -2.7752 -111.0285 0.47625
735     22 c/y -2.7752 -66.1416 0.47625
    
```

736	22 c/y	-2.7752	-58.9077	0.47625
737	22 c/y	-2.7752	-14.0462	0.47625
738	22 c/y	-2.7752	-6.8123	0.47625
739	22 c/y	-2.7752	38.1254	0.47625
740	22 c/y	-2.7752	45.3593	0.47625
741	22 c/y	-2.7752	90.2716	0.47625
742	22 c/y	-2.7752	97.5055	0.47625
743	22 c/y	-2.7752	142.3670	0.47625
744	22 c/y	-2.7752	149.6009	0.47625
745	22 c/y	-2.7752	194.8180	0.47625
746	22 c/y	-2.7752	202.0519	0.47625
747	22 c/y	-2.7752	213.8172	0.47625
c				
750	22 c/y	-16.7452	-189.6872	0.47625
751	22 c/y	-16.7452	-179.5526	0.47625
752	22 c/y	-16.7452	-172.3187	0.47625
753	22 c/y	-16.7452	-118.2624	0.47625
754	22 c/y	-16.7452	-111.0285	0.47625
755	22 c/y	-16.7452	-66.1416	0.47625
756	22 c/y	-16.7452	-58.9077	0.47625
757	22 c/y	-16.7452	-14.0462	0.47625
758	22 c/y	-16.7452	-6.8123	0.47625
759	22 c/y	-16.7452	38.1254	0.47625
760	22 c/y	-16.7452	45.3593	0.47625
761	22 c/y	-16.7452	90.2716	0.47625
762	22 c/y	-16.7452	97.5055	0.47625
763	22 c/y	-16.7452	142.3670	0.47625
764	22 c/y	-16.7452	149.6009	0.47625
765	22 c/y	-16.7452	194.8180	0.47625
766	22 c/y	-16.7452	202.0519	0.47625
767	22 c/y	-16.7452	213.8172	0.47625
c				
770	22 c/x	-5.9248	-189.6872	0.47625
771	22 c/x	-5.9248	-179.5526	0.47625
772	22 c/x	-5.9248	-172.3187	0.47625
773	22 c/x	-5.9248	-118.2624	0.47625
774	22 c/x	-5.9248	-111.0285	0.47625
775	22 c/x	-5.9248	-66.1416	0.47625
776	22 c/x	-5.9248	-58.9077	0.47625
777	22 c/x	-5.9248	-14.0462	0.47625
778	22 c/x	-5.9248	-6.8123	0.47625
779	22 c/x	-5.9248	38.1254	0.47625
780	22 c/x	-5.9248	45.3593	0.47625
781	22 c/x	-5.9248	90.2716	0.47625
782	22 c/x	-5.9248	97.5055	0.47625
783	22 c/x	-5.9248	142.3670	0.47625
784	22 c/x	-5.9248	149.6009	0.47625
785	22 c/x	-5.9248	194.8180	0.47625
786	22 c/x	-5.9248	202.0519	0.47625
787	22 c/x	-5.9248	213.8172	0.47625
c				
790	22 c/x	-16.9789	-189.6872	0.47625
791	22 c/x	-16.9789	-179.5526	0.47625
792	22 c/x	-16.9789	-172.3187	0.47625
793	22 c/x	-16.9789	-118.2624	0.47625
794	22 c/x	-16.9789	-111.0285	0.47625
795	22 c/x	-16.9789	-66.1416	0.47625
796	22 c/x	-16.9789	-58.9077	0.47625
797	22 c/x	-16.9789	-14.0462	0.47625
798	22 c/x	-16.9789	-6.8123	0.47625
799	22 c/x	-16.9789	38.1254	0.47625
800	22 c/x	-16.9789	45.3593	0.47625
801	22 c/x	-16.9789	90.2716	0.47625
802	22 c/x	-16.9789	97.5055	0.47625
803	22 c/x	-16.9789	142.3670	0.47625
804	22 c/x	-16.9789	149.6009	0.47625
805	22 c/x	-16.9789	194.8180	0.47625
806	22 c/x	-16.9789	202.0519	0.47625
807	22 c/x	-16.9789	213.8172	0.47625
c				
809	pz	-188.417		
810	pz	-181.331	\$ PH 1 (bottom)	
811	pz	-170.541	\$ PH 1	
812	pz	-120.040	\$ PH 2	
813	pz	-109.250		



814 pz -67.920 \$ PH 3  
 815 pz -57.130  
 816 pz -15.824 \$ PH 4  
 817 pz -5.034  
 818 pz 36.347 \$ PH 5  
 819 pz 47.137  
 820 pz 88.494 \$ PH 6  
 821 pz 99.284  
 822 pz 140.589 \$ PH 7  
 823 pz 151.379  
 824 pz 193.040 \$ PH 8  
 825 pz 203.830 \$ PH 8  
 826 pz 212.547

c  
 c hexagonal boundary of one unit lattice cell, close packed

\*881 px 37.6184  
 \*882 px -37.6184  
 \*883 p -0.5000000 0.866025404 0.0000000 37.6184  
 \*884 p -0.5000000 0.866025404 0.0000000 -37.6184  
 \*885 p 0.5000000 0.866025404 0.0000000 -37.6184  
 \*886 p 0.5000000 0.866025404 0.0000000 37.6184

c  
 900 px 11.18006 \$ FIXED for strongbacks touching  
 901 py -5.71956 \$ FIXED for strongbacks touching  
 902 px -11.9593  
 903 py -28.7574 \$ surface 901 minus 9.07"

c  
 c 904 is -7.1354 and 905 is 9.7633 for nominal case (with poison holders).  
 c they are shifted to cut off poison holders to allow for  
 c expansion for damaged cases.

c  
 c To completely "slice off" the poison holders, set  
 c 904 to -6.6593 and 905 to 10.2392.

c  
 904 py -6.6593 \$ tangential strongback lower bound, surface 901 minus total thickness  
 905 px 10.2392 \$ radial strongback left bound, surface 901 minus total thickness  
 906 pz 215.7222  
 908 c/z 9.87856 -7.02106 1.3015  
 909 px -9.9019  
 910 py -6.35448  
 911 py -7.1344 \$ fixed  
 912 px 9.7653 \$ fixed

c  
 998 so 10000  
 999 pz 345.5565

mode n  
 c print  
 kcode 2000 0.9 30 530  
 sdef cell=d1 pos=0 0 0 rad=d3 ext=d4 axs=0 0 1  
 sil 1 7:200:10 207:201:10  
 spl 1 1  
 si3 0.409575  
 si4 182.88  
 cut:n j j 0 0

c  
 c Materials

c  
 m1 92235 -0.249 \$ fuel pellet  
 92238 -82.615  
 94239 -4.972  
 94240 -0.264  
 94241 -0.053  
 8016 -11.847  
 m2 13027 1.0 \$ aluminum cladding for BORAL  
 m4 1001 2 \$ water  
 8016 1  
 mt4 lwtr.01t  
 m5 6000 -0.06 \$ XM-19  
 7014 -0.4  
 14000 -0.75  
 15031 -0.04  
 16032 -0.03  
 23000 -0.3  
 24000 -23.5

```

25055 -6
28000 -13.5
41093 -0.3
42000 -3
26000 -52.12
m6 6000 -0.08 $ SS-304
14000 -1.0
15031 -0.045
24000 -19.0
25055 -2.0
26000 -68.375
28000 -9.5
m7 40000 -1.0 $ Cladding
c 41093 -0.030
m8 82000 1.0 $ lead
m9 6000 -25.1 $ water/steel mix, 5.8% steel by volume
14000 -313.9
15031 -14.1
24000 -5964.9
25055 -627.9
26000 -21465.8
28000 -2982.5
1001 -7240.1
8016 -57462.7
mt9 lwtr.01t
m21 5010 7.3123E-03 $ 35 mg/cm2 B-10, 75% credit
5011 3.9244E-02
6000 1.2248E-02
13027 3.3439E-02
c total 9.2244E-02

```

Translations

```

c tr22 is the intersection of planes 904 and 905
c when the poison holders are present (904 and 905 shift when it is
c desired to "slice off" the poison holders).
c Note that the origin of Universe 7 corresponds to the intersection
c of these planes.
c
*tr22 9.7643 -7.1354 0.0
c
c tr25 is the intersection of planes 300 and 302. The origin of Universe 30
c corresponds to the intersection of these planes.
c
*tr25 -12.8928 -29.7925 0.0
c
c tr30 is computed by taking the coordinates of the intersection of planes
c 22 and 24 and adding half the pitch (note: can't be exact or else planes will
c overlap, causing program termination.)
c
*tr30 -11.0956 -27.9953 0.0
*tr31 -11.6368 -28.5365 0.0
c
c tr53 and tr54 rotate the bottom assembly to create assemblies 2 and 3
c
*tr53 0 0 0 120 30 90 150 120 90 90 90 0 $ +x+y
*tr54 0 0 0 120 150 90 30 120 90 90 90 0 $ -x-y

```

This page left intentionally blank.

## B6.9.2 Infinite Array Model

The infinite array models are geometrically the same as the single package models, although small changes have been made to the outer boundary to simulate the infinite array. Additional cells and surfaces are listed below.

```
195 0 -881 882 -886 885 -883 884 -66 63 62 imp:n=1 $ w between packages
199 0 (881:-882:886:-885:883:-884:66:-63) imp:n=0 $ outside world
```

```
c hexagonal boundary of one unit lattice cell, close packed
*881 px 37.6184
*882 px -37.6184
*883 p -0.5000000 0.866025404 0.0000000 37.6184
*884 p -0.5000000 0.866025404 0.0000000 -37.6184
*885 p 0.5000000 0.866025404 0.0000000 -37.6184
*886 p 0.5000000 0.866025404 0.0000000 37.6184
```

This page left intentionally blank.

## B7.0 PACKAGE OPERATIONS

### B7.1 Package Loading

The AFS-B contents are loaded in the following manner:

1. Remove the 22 bolts that attach the lid of the AFS-B. Remove the AFS-B lid.
2. Load up to 175 standard MOX fuel rods. If less than 175 rods are placed into the box, add steel or aluminum dunnage rods until all space is filled.
3. Place the AFS-B lid on the body. Tighten the 22 bolts to the torque value specified on *Packaging General Arrangement Drawing 99008-60*. For each bolt, bend lock tab against bolt flat.

Once the AFS-B has been loaded, the package loading operations are essentially the same as the operations for fuel assembly loading described in Chapter 7.1, *Package Loading*. The AFS-B and EMA and handled in the same manner as a fuel assembly.

The only difference is the tightening of the swivel clamp pads. Because the AFS-B is constructed of aluminum, a thermal expansion gap is provided. Therefore, modify Step 18 of Section 7.1.2.1, *Loading of Fuel Assemblies into Strongback*, as follows:

- 7.1.2.1, Step 18: Tighten the four (4) 3/4-inch swivel clamp pads on the top plate until the screw pad contacts the AFS-B top. Then loosen each swivel clamp pad 1 – 1½ turns, and lock in place with a hex nut.

### B7.2 Package Unloading

The package unloading operations are the same as the operations for fuel assembly unloading described in Chapter 7.2, *Package Unloading*. The AFS-B and EMA and handled in the same manner as a fuel assembly.

The AFS-B contents are unloaded in the following manner:

1. Remove the 22 bolts that attach the lid of the AFS-B. Remove the AFS-B lid.
2. Unload the fuel and dunnage rods present.
3. Place the AFS-B lid on the body. Tighten the 22 bolts to the torque value specified on *Packaging General Arrangement Drawing 99008-60*. For each bolt, bend lock tab against bolt flat.

### B7.3 Preparation of an Empty Package for Transport

Previously used and empty MFFPs shall be prepared and transported per the requirements of 49 CFR §173.428<sup>1</sup>.

---

<sup>1</sup> Title 49, Code of Federal Regulations, Part 173 (49 CFR 173), *Shippers—General Requirements for Shipments and Packagings*, 10-01-06 Edition.

### **B7.4 Preshipment Leakage Rate Test**

The preshipment leakage rate test is the same as described in Section 7.4, *Preshipment Leakage Rate Test*.

## **B8.0 ACCEPTANCE TESTS AND MAINTENANCE PROGRAM**

### **B8.1 Acceptance Tests**

Per the requirements of 10 CFR §71.85<sup>1</sup>, this section discusses the inspections and tests to be performed prior to first use of the AFS-B rod container.

#### **B8.1.1 Visual Inspections and Measurements**

Each AFS-B rod container shall be examined in accordance with the requirements delineated on the drawings in Appendix B1.4.2, *Packaging General Arrangement Drawings*, prior to use.

#### **B8.1.2 Weld Inspections**

All welds shall be inspected to the requirements delineated on the drawings in Appendix B1.4.2, *Packaging General Arrangement Drawings*.

#### **B8.1.3 Structural and Pressure Tests**

The AFS-B rod container does not require any lifting device load tests or pressure tests.

#### **B8.1.4 Fabrication Leakage Rate Tests**

The AFS-B rod container does not require any leakage rate tests.

#### **B8.1.5 Component and Material Tests**

The AFS-B rod container does not require any component or material tests.

#### **B8.1.6 Shielding Tests**

The AFS-B rod container does not require any shielding tests.

#### **B8.1.7 Thermal Tests**

The AFS-B rod container does not require any thermal tests.

---

<sup>1</sup> Title 10, Code of Federal Regulations, Part 71 (10 CFR 71), *Packaging and Transportation of Radioactive Material*, 01-01-06 Edition.



## **B8.2 Maintenance Program**

The AFS-B rod container does not require a scheduled maintenance program. The parts which are routinely handled during use (the body, the lid, and the lid fasteners) are visually inspected prior to use. Damaged components shall be repaired or replaced prior to use.

## C1.0 GENERAL INFORMATION

Appendix C of the MOX Fresh Fuel Package (MFFP) Safety Analysis Report (SAR) supports the addition of up to three (3) AFS-C rod containers containing Los Alamos Technical Area 18 (TA-18) MOX fuel rods. Two types of TA-18 fuel rods are available, Exxon Nuclear (Exxon) and Pacific Northwest Laboratory (PNL). Because these rods have different outer diameters and lengths, they will be separated within the AFS-C cavity. The AFS-C may transport up to 116 Exxon rods and 69 PNL rods. The maximum number of rods is limited by the cavity size of the AFS-C.

In this SAR Appendix, reference is made to the main SAR for information that has not changed. Referenced tables, figures, and sections that do not contain the letter "C" (e.g., Table 1.2-1, Figure 3.5-1, Section 6.1.1) refer to items in the main SAR. Referenced tables, figures, and sections that contain the letter "C" (e.g., Table C6.4-1, Figure C1.2-1, Section C6.1.1) refer to items in Appendix C.

### C1.1 Introduction

The Mixed Oxide Fresh Fuel Package, Model: **MFFP**, is designed to transport fresh MOX pressurized water reactor (PWR) reactor fuel assemblies. The AFS-C fuel rod container has outer dimensions that are consistent with those of a standard fuel assembly and interfaces with the strongback and clamp arms in the same way.

A full-scale, prototypic certification test unit (CTU) was subjected to a series of hypothetical accident condition (HAC) free and puncture drop tests as part of the original SAR submittal. The results of this testing program are directly applicable to the AFS-C payload because the loaded AFS-C payload weight is bounded by the weight of a fuel assembly (including a BPRA). A detailed discussion of the CTU and certification tests is provided in Appendix 2.12.3, *Certification Test Results*. These tests, coupled with supplementary analytical evaluations, conclusively demonstrated the leaktight<sup>1</sup> containment boundary integrity and criticality control performance of the MFFP.

The thermal analysis for the AFS-C payload is provided in Chapter C3.0, *Thermal Evaluation*. Because an MFFP loaded with three (3) AFS-C containers holding TA-18 rods has the same decay heat as three fuel assemblies, MFFP strongback and shell temperatures are the same as those reported in Chapter 3.0, *Thermal Evaluation*. However, due primarily to the simplistic analytical method employed, both the NCT and HAC maximum fuel rod temperatures for rods within the AFS-C are computed to be higher than the maximum temperature computed for a fuel assembly. These temperatures are well below the respective temperature limits for a fuel rod. The internal pressure under NCT and HAC with the AFS-C payload is bounded by the pressure with three fuel assemblies.

---

<sup>1</sup> Leaktight is defined as  $1 \times 10^{-7}$  standard cubic centimeters per second (scc/s), or less, air leakage per ANSI N14.5-1997, *American National Standard for Radioactive Materials – Leakage Tests on Packages for Shipment*, American National Standards Institute, (ANSI), Inc

Based on the shielding and criticality assessments provided in Chapter C5.0, *Shielding Evaluation*, and Chapter C6.0, *Criticality Evaluation*, the Criticality Safety Index (CSI) for the MFFP is zero (0.0), and the Transport Index (TI) is determined at the time of shipment.

Authorization is sought for shipment of the MFFP containing up to three (3) AFS-C containers with TA-18 MOX rods by all modes of conveyance, except for aircraft, as a Type B(U)F package per the definitions delineated in 10 CFR §71.4.

## C1.2 Package Description

General arrangement drawings of the packaging are provided in Section 1.4.2, *Packaging General Arrangement Drawings*. The addition of the AFS-C does not alter these packaging drawings. A drawing of the AFS-C rod container is given in Section C1.4.2, *Packaging General Arrangement Drawings*.

### C1.2.1 Packaging

The MFFP packaging description is unchanged from the description provided in Section 1.2.1, *Packaging*. The AFS-C rod container is designed to hold up to 116 Exxon fuel rods, up to 69 PNL fuel rods, or both quantities together. The container has outer cross sectional dimensions of 8.4 inches square, a length from bottom to top of 159.9 inches, and an overall length (to the lift ring bolt head) of 161.2 inches. The primary material of construction of the container is ASTM 6061-T651 aluminum alloy. The two side walls, the bottom plate, and the lid are all  $\frac{3}{4}$  inches thick. The side plates are attached to the bottom plate with two longitudinal,  $\frac{3}{8}$ -inch groove welds. The lid is attached with twenty-two (22) zinc-plated, 3/8-16 UNC, SAE J429 Grade 8, hex head cap screws. The two square end pieces are made of solid aluminum alloy, and each are attached to the container with eight (8) zinc-plated SAE J429 3/8-16 UNC hex head cap screws made of Grade 8 alloy steel. The lower square end piece is 2.4 inches thick and the upper square end piece is 3.0 inches thick. Each bolt is secured in place using a thin stainless steel lock tab. Two of the eight bolts on each end go horizontally into the lid, in addition to the 22 cap screws on the top of the lid.

Inside the container is a  $\frac{1}{2}$ -inch thick shelf, made of the same aluminum alloy, which fits into  $\frac{1}{4}$ -inch deep grooves in each side wall. The shelf is supported by  $\frac{1}{4}$ -inch thick aluminum gusset plates on 15.3-inch centers. The gussets and the shelf are located with intermittent  $\frac{1}{8}$ -inch fillet welds, none of which are load bearing. Along the inside of the two side plates are two, 2.1-inch wide grooves, 0.4 inches deep. Each groove holds a 2-inch thick plate of the same aluminum alloy, which serve as bulkheads. The two bulkheads form rod cavities on each end of the container: a 78.3-inch long cavity for Exxon rods at the lower end and a 37.7-inch long cavity for the PNL rods at the top end. The cavity located between the two bulkheads is empty. Both rod cavities are 6.9 inches wide and 3.4 inches deep. The components of the AFS-C feature numerous small holes that ensure flooding or draining of water from its various cavities.

The lid is lifted by means of two,  $\frac{1}{4}$ -20 UNC threaded holes in the lid. The holes are located such that at least half of the hole is blocked by the top of the sidewall, which prevents an overly-long lifting bolt from possibly damaging any fuel rods. The container is lifted from its top end using a swivel hoist ring. All threaded holes may optionally be fitted with helical-coil thread inserts. The label 'AFS-C' is painted prominently on both sides of the container. The AFS-C is finished with a clear anodize treatment.

An external view of the AFS-C rod container is given in Figure C1.2-1. An internal cross sectional view is given in Figure C2.7-1, and views of a typical bulkhead in Figure C2.7-2.

## C1.2.2 Containment System

The containment system description is unchanged from the description provided in Section 1.2.2, *Containment System*.

## C1.2.3 Contents of Packaging

The MFFP may transport up to three (3) AFS-C rod containers, each containing up to 116 Exxon rods, up to 69 PNL rods, or both quantities together. These limits are based upon the number of rods that will fit within the AFS-C inner cavity, although less rods may be necessary in order to meet the decay heat limit for the package. The actual quantity of rods transported will be limited by either the physical space (i.e., the quantities listed above), or by the decay heat limit of 240 Watts total in the MFFP (see Section C1.2.3.3, *Maximum Decay Heat*.) If necessary, for a payload of fewer than the maximum quantities of rods, aluminum or stainless steel dunnage rods are used to take up the remaining space. For shipping less than a total of three (3) AFS-C containers, non-fuel dummy assemblies are utilized in the unoccupied strongback locations. The physical size and weight of the non-fuel dummy assemblies are nominally the same as the MK-BW/MOX1 17 × 17 design.

The physical parameters for the Exxon and PNL fuel rods are provided in Table C1.2-1. The Exxon rods are well characterized. However, known data for the PNL rods are limited to rod OD, rod length, average plutonium mass, and average plutonium isotopics. No records are available for a number of other PNL rod characteristics, such as pellet OD, active fuel height, and maximum plutonium mass. Data listed as "assumed" in Table C1.2-1 represent the most reactive estimated values determined in Chapter C6.0, *Criticality Analysis*, and are considered bounding. In the criticality analysis, the Exxon rods are conservatively limited to 65 g Pu per rod, and the PNL rods are conservatively limited to 42 g Pu per rod.

### C1.2.3.1 Radionuclide Inventory

The average fuel rod isotopics for the Exxon and PNL rods as of 1980 are provided in Table C1.2-2. As these values are averages, these values are not necessarily bounding for criticality purposes. The bounding isotopics used for criticality are discussed in detail in Chapter C6.0, *Criticality Analysis*. Because the values in Table C1.2-2 are 1980 vintage, and Pu-241 has a half life of 14.35 years, the Pu-241 content of the actual rods will be less than the values provided here because most of the Pu-241 will have decayed to Am-241.

### C1.2.3.2 Maximum Payload Weight

The weight of a single loaded AFS-C containing 116 Exxon and 69 PNL rods is approximately 1,230 pounds. This weight is bounded by the 1,580 pound weight of a standard fuel assembly (with BPRA). Three loaded AFS-C containers would weigh approximately 3,690 pounds. Therefore, the maximum payload weight is bounded by the value of 4,740 pounds provided in Section 1.2.3.2, *Maximum Payload Weight*.

**C1.2.3.3 Maximum Decay Heat**

The maximum heat load for the package is unchanged from the value of 240 watts provided in Section 1.2.3.3, *Maximum Decay Heat*. In addition, each AFS-C is limited to a maximum heat load of 80 watts (i.e., combined heat load of the Exxon and PNL rods), the Exxon cavity is limited to a maximum heat load of 80 watts, and the PNL cavity is limited to a maximum heat load of 30 watts.

**C1.2.3.4 Maximum Pressure Buildup**

The maximum normal operating pressure (MNOP) is bounded by the 10 psig value provided in Section 1.2.3.4, *Maximum Pressure Buildup*. The design pressure of 25 psig is also unchanged.

**C1.2.4 Operational Features**

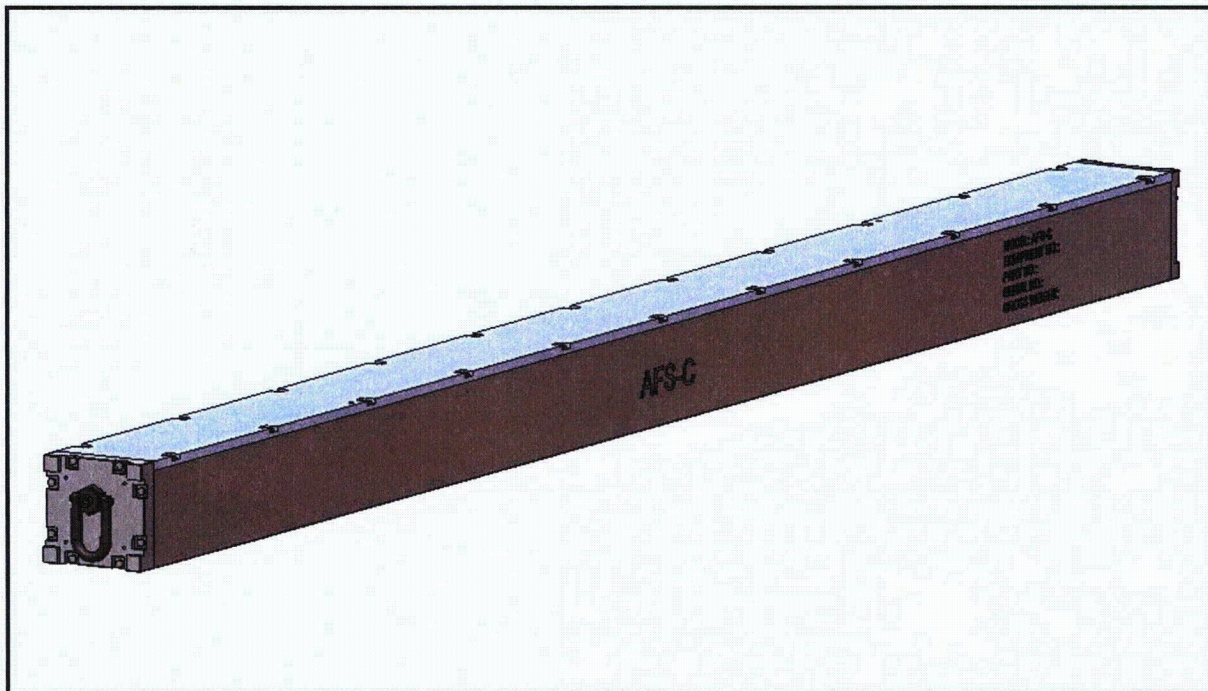
Operating procedures and instructions for loading, unloading, and preparing an empty MFFP for transport with the AFS-C are provided in Chapter C7.0, *Package Operations*.

**Table C1.2-1 – Fuel Rod Data**

Parameter	Exxon		PNL	
	English Value	Metric Value	English Value	Metric Value
Cladding Material	Zircaloy		Zircaloy	
Overall Length	77.26 in	196.24 cm	36.6 in	92.96 cm
Weight per rod	4.0 lb	---	3.3 lb	---
Active Fuel Length	70 in	177.8 cm	28 in (assumed)	71.12 cm (assumed)
Cladding OD	0.451 in	1.1455 cm	0.565 in	1.4351 cm
Cladding ID	0.381 in	0.9677 cm	0.520 in (assumed)	1.3208 cm (assumed)
Pellet OD	0.3716 in	0.9439 cm	0.5135 in (assumed)	1.3043 cm (assumed)
Effective Pellet Density	--	10.85 g/cm <sup>3</sup> (assumed)	--	10.85 g/cm <sup>3</sup> (assumed)
Pu mass (average)	--	58.3 g	--	37.4 g
Pu mass (maximum)	--	65 g (assumed)	--	42 g (assumed)

**Table C1.2-2 – Average Fuel Rod Isotopics**

Isotope	Exxon wt. % (1980 average)	PNL wt. % (1980 average)
U-235	0.71	0.71
U-238	99.29	99.29
Total U	100	100
Pu-238	0.745	0.28
Pu-239	75.13	75.38
Pu-240	17.26	18.10
Pu-241	5.23	5.08
Pu-242	1.55	1.15
Total Pu	100	100

**Figure C1.2-1 – AFS-C Rod Container**

### **C1.3 General Requirements for All Packages**

The AFS-C has no effect on the way in which the MFFP meets the general requirements for packaging.



This page left intentionally blank.

## C1.4 Appendices

### C1.4.1 Nomenclature

The nomenclature list from Section 1.4.1, *Nomenclature*, is applicable. Additional nomenclature listed below.

**AFS-C** – Container used to transport up to 116 Exxon rods and 69 PNL rods. The AFS-C interfaces with the strongback in the same manner as a fuel assembly.

**Exxon Rod** – A type of MOX fuel rod with a length of approximately 77.3-in.

**Pacific Northwest Laboratory (PNL) Rod** – A type of MOX fuel rod with a length of approximately 36.6-in.

**Los Alamos Technical Area 18 (TA-18)** – Building at Los Alamos National Laboratory that currently stores the Exxon and PNL rods.


### C1.4.2 Packaging General Arrangement Drawings

The general arrangement drawings of the body, strongback, and impact limiters are unchanged from those provided in Section 1.4.2, *Packaging General Arrangement Drawings*. The following AFS-C drawing is included in this section:

- 99008-61, Rev. 0, 2 sheets, *AFS-C Assembly*

This page left intentionally blank.

Figure Withheld Under 10 CFR 2.390

	AREVA Federal Services LLC Packaging Projects Tacoma, WA 98402	
	AFS-C ASSEMBLY SAR DRAWING	
	SCALE: 1:5	WT. ~ LBS
	REV: 0	SHEET 1 OF 2
DWG SIZE D	DWG NO. 99008-61	

*Figure Withheld Under 10 CFR 2.390*

## C2.0 STRUCTURAL EVALUATION

This chapter of Appendix C provides a structural evaluation of the MFFP when transporting up to three (3) AFS-C rod containers containing Los Alamos Technical Area 18 (TA-18) MOX fuel rods. Two types of TA-18 fuel rods are available, Exxon Nuclear (Exxon) and Pacific Northwest Laboratory (PNL). Because these rods have different outer diameters and lengths, they will be segregated longitudinally within the AFS-C cavity. The AFS-C may transport up to 116 Exxon rods and 69 PNL rods. The maximum number of rods is limited by the cavity size of the AFS-C. It is demonstrated that all quantities of interest are bounded by the analyses presented in Chapter 2.0, *Structural Evaluation*.

### C2.1 Structural Design

#### C2.1.1 Discussion

A comprehensive discussion of the MFFP design and standard configuration is provided in Section 1.2, *Package Description*. The MFFP drawings show the detailed geometry of the package, as well as the dimension, tolerances, materials, and fabrication requirements, and are provided in Appendix 1.4.2, *Packaging General Arrangement Drawings*. A physical description of the AFS-C is provided in Section B1.2.3, *Contents of Packaging*. The following discussion is limited to the AFS-C.

A physical description of the AFS-C rod container is provided in Section C1.2.3, *Contents of Packaging*, and is shown in the drawings in Appendix C1.4.2, *Packaging General Arrangement Drawings*. The AFS-C container is a robust box designed to provide confinement of the fuel rods under all conditions of transport. The AFS-C container has the same external boundary dimensions as a standard MOX fuel assembly, and thus is loaded, mounted, and unloaded from the strongback in the same manner as a fuel assembly. The structural evaluations and testing performed as part of the original license activities adequately characterize the performance of the MFFP with this payload.

#### C2.1.2 Design Criteria

The MFFP design criteria are unchanged from those provided in Section 2.1.2, *Design Criteria*. The design criteria for the AFS-C rod container are based on the functional requirement that the rod container confine the rods inside the container boundary under all NCT and HAC. Because the AFS-C rod container is transported within the MFFP strongback, it is protected from gross distortion by the fuel control structure (FCS). As shown in Section 2.12.5, *Fuel Control Structure Evaluation*, the FCS provides a limit to any reconfiguration of the fuel assembly which could occur as a result of the worst case HAC event. The MOX fuel assembly consists of a larger number of rods (264) than is contained in the AFS-C rod container (up to 116 Exxon rods and 69 PNL rods). In addition, the rods in the MOX fuel assembly are unconfined by any structure other than the FCS, whereas fuel rods in the AFS-C rod container are confined within a container having significant structure. Therefore, gross distortion of the fuel rods or of the AFS-C container, or escape of the fuel rods or fuel rod fragments from the container, are not of concern.

To enhance criticality safety by preventing the potential for damage to the fuel rods in the HAC free drop impact event, the AFS-C rod container is designed to minimize the relative motion of the rods under impact conditions. To accomplish this, the AFS-C rod container is designed to limit the "rattle space" of the fuel rods (including any dummy rods as necessary) to less than approximately one half rod diameter.

The only components of the AFS-C container which are not supported externally by the strongback or FCS are the internal shelf and rod cavity bulkheads. To ensure that the "rattle space" available to the rods cannot increase as a result of the free drop impact event, these components are designed to have a primary bending stress less than the yield point of their material at NCT maximum temperature.

### C2.1.3 Weights and Center of Gravity

The loaded weight of the AFS-C, conservatively assuming 116 Exxon and 69 PNL rods, is bounded by 1,230 pounds, which is 22% less than the gross weight of 1,580 pounds for a fuel assembly (including a BPRA). Therefore, the weight of the MFFP when transporting one or more AFS-C containers is bounded by the weights given in Section 2.1.3, *Weights and Center of Gravity*, for transport of MOX fuel assemblies.

When transporting both Exxon and PNL fuel rods, the weight is nearly balanced in the AFS-C container, and the center of gravity of the overall MFFP is essentially unchanged from the case of the standard MOX fuel assembly payload, where it is located 103.7 inches from the end of the bottom impact limiter. When transporting AFS-C containers with only Exxon rods, the center of gravity of the MFFP will be shifted approximately 3 inches toward the closed end, compared to the standard MOX fuel payload. When transporting AFS-C containers with only PNL rods, the center of gravity of the MFFP will be shifted approximately 1.5 inches toward the lid end, compared to the standard MOX payload. These shifts of c.g. are small relative to the overall length of the MFFP of approximately 200 inches, and will not have a significant effect on lifting, tiedown, or HAC response of the package.

## C2.2 Materials

The AFS-C is constructed primarily of ASTM B209, 6061-T651 aluminum plate material. The lid and ends are attached with bolts made from SAE J429 Grade 8 material. A stainless steel swivel hoist ring is included for lifting. No non-metallic materials are used in the AFS-C. These materials do not result in any chemical or galvanic reactions, and are not significantly affected by radiation. The material properties for the aluminum material at 200 °F needed for calculations are given in Table C2.2-1, and were taken from the ASME B&PV Code,<sup>1</sup> as noted. Note that although there is limited welding of the 6061 material, welding is not used in regions where the material properties are used in stress analysis.

---

<sup>1</sup> American Society of Mechanical Engineers (ASME) Boiler and Pressure Vessel Code, Section II, Materials, Part D, Properties, 2001 Edition, 2002 and 2003 Addenda.

**Table C2.2-1 - Material Properties of ASTM B209 6061-T651 Aluminum Alloy at 200 °F**

Yield Strength, psi	Coefficient of Thermal Expansion, 10 <sup>-6</sup> in/in/°F
33,700	13.0

Notes:

1. Yield strength from ASME B&PV Code, Section II, Part D, Table Y-1.
2. Coefficient of thermal expansion from ASME B&PV Code, Section II, Part D, Table TE-2.

### C2.3 Fabrication and Examination

The AFS-C rod container is fabricated to the requirements of the drawings shown in Appendix C1.4.2, *Packaging General Arrangement Drawings*. The materials of construction are specified to either ASTM or SAE standards. The rod container is inspected to the dimensional requirements of the drawing. Welds are visually inspected to the AWS D1.2<sup>2</sup> welding code.

### C2.4 Lifting and Tie-down Standards for All Packages

Because the gross weight of the MFFP is lower when transporting an AFS-C rod container, this section is unchanged from Section 2.4, *Lifting and Tie-down Standards for All Packages*.

### C2.5 General Considerations

The AFS-C rod container is evaluated by reasoned argument and by analysis in the following sections. In addition, the results and conclusions of Section 2.5, *General Considerations*, remain unchanged.

### C2.6 Normal Conditions of Transport

#### C2.6.1 Heat

It is demonstrated in Section C3.4, *Thermal Evaluation for Normal Conditions of Transport*, that under NCT the MFFP strongback and shell temperatures associated with the AFS-C payload are bounded by the standard three (3) fuel assembly payload. Therefore, all associated pressure and thermal stresses are bounded by the values presented in Section 2.6.1, *Heat*. For the AFS-C rod container, the bounding temperature of the sidewalls and the internal shelf is 200 °F. Since the AFS-C is vented, it cannot retain pressure.

##### C2.6.1.1 Differential Thermal Expansion

The evaluation of differential thermal expansion given in Section 2.6.1.2, *Differential Thermal Expansion*, is not affected by use of the AFS-C rod container. An additional evaluation of the

<sup>2</sup> ANSI/AWS D1.2, *Structural Welding Code – Aluminum*, American Welding Society (AWS).



differential thermal expansion between the strongback and the AFS-C container will now be made.

From Section 2.6.1.2, *Differential Thermal Expansion*, the design temperature of the strongback is  $T_{SB} = 180$  °F, and the coefficient of thermal expansion for the strongback material is  $\alpha_{SB} = 8.8 \times 10^{-6}$  in/in/°F. As stated above, the bounding temperature for the AFS-C container is  $T_{AFS-C} = 200$  °F, and from Table C2.2-1, the coefficient of thermal expansion is  $\alpha_{AFS-C} = 13.0 \times 10^{-6}$  in/in/°F. The overall length of the container is  $L = 159.9$  inches. The reference temperature is 70 °F. The differential thermal growth of the rod container and the strongback is:

$$\delta = \alpha_{AFS-C}(L)(T_{AFS-C} - 70) - \alpha_{SB}(L)(T_{SB} - 70) = 0.115 \text{ inches}$$

This calculation conservatively assumes that the entire length of the two components is at the respective peak temperatures, and thus overestimates the relative thermal expansion. To prevent axial interference of the AFS-C container with the strongback, the clamp pads will be set with a clearance to the end of the AFS-C container. As stated in Section C7.1, *Package Loading*, the 3/4-10 clamp pad screw will be backed out a minimum of one turn from the position of contact, ensuring a minimum axial clearance between the AFS-C container and the strongback of 0.1 inches at the reference temperature. This is adequate to ensure that the thermal expansion force is negligible or non-existent considering the conservatism of the evaluation above.

### **C2.6.2 Cold**

This section is unchanged from Section 2.6.2, *Cold*.

### **C2.6.3 Reduced External Pressure**

This section is unchanged from Section 2.6.3, *Reduced External Pressure*.

### **C2.6.4 Increased External Pressure**

This section is unchanged from Section 2.6.4, *Increased External Pressure*.

### **C2.6.5 Vibration and Shock**

The vibration normally incident to transportation will have no effect on the AFS-C rod container. The AFS-C container is installed and retained in the same manner as a MOX fuel assembly. The spring loaded clamp arms which hold the container in place will significantly dampen any vibrational loads which could come from the cask body. Furthermore, any fatigue cracks which might occur from vibration, which are too small to be noted during a visual inspection, would have no effect on the ability of the AFS-C to perform its function of confining the rods in a HAC free drop impact. Therefore, vibration and shock are not of concern for the AFS-C rod container.

### **C2.6.6 Water Spray**

This section is unchanged from Section 2.6.6, *Water Spray*.

### **C2.6.7 Free Drop**

Because a loaded AFS-C is lighter than a fuel assembly (including BPRA), the response of the MFFP to a free drop would be essentially the same when compared to the standard payload.

Since the AFS-C rod container is shown to confine the fuel rods in a HAC free drop impact (see Section C2.7.1), its performance will be acceptable for the NCT free drop event.

### **C2.6.8 Corner Drop**

This section is unchanged from Section 2.6.8, *Corner Drop*.

### **C2.6.9 Compression**

This section is unchanged from Section 2.6.9, *Compression*.

### **C2.6.10 Penetration**

This section is unchanged from Section 2.6.10, *Penetration*.

## **C2.7 Hypothetical Accident Conditions**

### **C2.7.1 Free Drop**

The functional criteria of the AFS-C rod container is to confine the Exxon and PNNL fuel rods in the worst-case HAC free drop event. As an additional enhancement to criticality safety, the container should also restrict the relative movement of the rods to minimize the potential for damage to the fuel rods.

The MFFP strongback, including the fuel control structure (FCS), is designed to maintain a complete MOX fuel assembly in a subcritical configuration during the governing free drop event. Using physical test (see Appendix 2.12.3, *Certification Test Results*) and calculations (see Appendix 2.12.5, *Fuel Control Structure Evaluation*), it has been demonstrated that *a*) the fuel rods do not break or fragment, and *b*) the strongback and FCS are capable of confining the rods within a defined geometry. As stated in Section C1.2, *Package Description*, the AFS-C rod container consists of a completely enclosed structure made of 6061-T651 aluminum plates of  $\frac{3}{4}$ -inch nominal thickness. The lid of the container is attached using 22,  $\frac{3}{8}$ -inch diameter bolts. The container has the same boundary dimensions as the MOX fuel assembly, and is mounted in the strongback in the same way. As such, the AFS-C container represents an added level of confinement for the fuel rods, beyond that provided by the strongback and FCS. For this reason, confinement of the fuel rods by the AFS-C container is ensured. Table C2.7-1 presents added detail which supports this conclusion. As stated in Section C2.1.2, *Design Criteria*, the movement of rods in an impact is restricted to a maximum of approximately one-half of a rod diameter.

The rod cavities inside the AFS-C container are formed by the  $\frac{3}{4}$ -inch thick lid plate, the two  $\frac{3}{4}$ -inch thick side plates, the  $\frac{1}{2}$ -inch thick shelf plate, the thick end plates (minimum thickness of 2.4 inches), and the two, 2-inch thick bulkhead plates. The Exxon rod cavity is located at one end of the container and is 78.3 inches long, and the PNL rod cavity is located at the other end, and is 37.7

inches long. The shelf plate is located in longitudinal, ¼-inch deep grooves on the inside face of each ¾-inch thick side plate, and supported against the bottom plate by gussets at 15.3-inch intervals. Figure C2.7-1 shows a cross section of the AFS-C container. The bulkhead plates are located in 0.4-inch deep grooves on the inside face of each side plate. Figure C2.7-2 shows a typical cross section view of a bulkhead plate. The bulkhead plate spans the distance between the two side plates, and closes off one end of each rod cavity. To demonstrate that the rod cavity maintains its internal geometric integrity in the worst-case free drop impact, the following evaluations are performed. The internal geometric integrity assures that the “rattle space” inside the container is minimized to prevent any possible damage to the rods. However, any loss of the rod container contents is precluded by the rod container primary structure, as discussed above.

**Shelf Evaluation.** In the following, it is assumed that the impact occurs with the shelf oriented horizontally with the container lid side up. This orientation governs over all others where some component of the rod load is directed toward the thick sidewalls of the container. Any support from the gusset plates beneath the shelf is conservatively neglected. The shelf is then a plate, simply supported on its two long sides, and free on its two short sides. A governing impact of 180g is taken from Section 2.12.5.2, *Conditions Analyzed*, for the maximum slapdown impact. The loading from the weight of the fuel rods will be taken from the governing case of either the Exxon or PNL rods.

From Table C1.2-1, the Exxon fuel rod weight is 4 lb each, and the length is  $L_{Ex} = 77.3$  inches. From the same table, the PNL fuel rod weight is 3.3 lb each, and the length is  $L_{PNL} = 36.6$  inches. From Figure C2.7-1, the internal width of the cavity is  $b = 6.9$  inches. For 116 Exxon rods, the total weight is  $W_{Ex} = 116 \times 4 = 464$  lb. The total weight of the PNL rods is  $W_{PNL} = 69 \times 3.3 = 228$  lb. Since the rods rest on an area bounded by the rod length and the cavity width, the impact pressure on the shelf is:

$$q = \frac{W_{Ex}g}{L_{Ex}b} = 156.6 \text{ psi for Exxon rods}$$

$$q = \frac{W_{PNL}g}{L_{PNL}b} = 162.5 \text{ psi for PNL rods}$$

Therefore the governing load is  $q = 162.5$  psi, which will conservatively be assumed to apply to the entire shelf, rather than just the area beneath the PNL rods. A formula from Roark,<sup>3</sup> Table 26, Case 1a, is used. Even though this formula assumes simple support on the narrow ends as well as the sides, the maximum stress at the center of the plate, which is more than 10 plate-widths distant from the ends, will not be materially affected. The length of the shelf is  $L_s = 153.5$  inches. The ratio  $a/b$  is  $153.5/6.9 = 22.2$ , from which  $\beta = 0.75$ . The maximum stress at the center of the plate is found from:

$$\sigma = \frac{\beta qb^2}{t^2} = 23,210 \text{ psi}$$

where  $t = 0.5$  inches, and the other quantities are as defined above. From Table C2.2-1, the yield strength of the shelf material at the bounding temperature of 200 °F is 33,700 psi. The margin of safety against yield of the shelf is:

<sup>3</sup> Young, W. C., *Roark's Formulas for Stress and Strain*, Sixth Edition, McGraw-Hill, 1989.

$$MS = \frac{33,700}{23,210} - 1 = +0.45$$

Since the shelf does not yield, the "rattle space" available for the rods does not increase as a result of the slapdown free drop event. Other impact orientations would place lower loadings on the shelf.

**Bulkhead Evaluation.** In this evaluation, stresses associated with the bulkhead are demonstrated to remain below the yield point of the aluminum alloy material in the worst case end drop impact of 120g, taken from Section 2.12.5.2, *Conditions Analyzed*. The governing weight is that of the Exxon fuel rods, having a maximum weight of  $W_{Ex} = 464$  lb. The bulkhead is modeled as a beam, simply supported at each side plate, for a span of  $L = 6.9$  inches, and a width (see Figure C2.7-2) of  $b = 3.3$  inches, assuming a 0.1-in total gap. (Note that the nomenclature has been partially redefined so as to be consistent with common textbook formulas.) The moment of inertia is:

$$I = \frac{bh^3}{12} = 2.2 \text{ in}^4$$

where  $h = 2$  inches. The c-distance is  $h/2 = 1$  inch. The loading per inch of length of the beam is:

$$w = \frac{W_{Ex}g}{L} = 8069.6 \text{ lb/in}$$

where  $g = 120$  for the end drop impact. The bending moment is:

$$M = \frac{wL^2}{8} = 48,024 \text{ in-lb}$$

The bending stress is:

$$\sigma = \frac{Mc}{I} = 21,829 \text{ psi}$$

From Table C2.2-1, the yield strength of the bulkhead material at the bounding temperature of 200 °F is 33,700 psi. The margin of safety against bending yield of the bulkhead is:

$$MS = \frac{33,700}{21,829} - 1 = +0.54$$

The bearing stress on the two grooves in the side plates which support the bulkhead is equal to:

$$\sigma_b = \frac{F}{A} = \frac{W_{Ex}g}{2bt_g} = 27,214 \text{ psi}$$

where a value of  $t_g = 5/16$  (0.31) inches is conservatively used for the 3/8 (0.4) inches deep groove in the side plate. Conservatively, this bearing stress will be compared to the tensile yield strength, even though bearing stress is commonly permitted to reach a much higher value. The margin of safety on bearing yield is:

$$MS = \frac{33,700}{26,953} - 1 = +0.25$$

The groove edge which supports the bulkhead is subject to a shearing load on a plane oriented at 45° to the plane of the bulkhead. The shear area per groove is:

$$A_s = t_g b \sqrt{2} = 1.45 \text{ in}^2$$

The shear stress is:

$$\tau = \frac{W_{\text{Ex}} g}{2A_s} = 19,200 \text{ psi}$$

The shear yield strength is equal to 0.6 times the tensile yield strength. The margin of safety is:

$$MS = \frac{(0.6)33,700}{19,200} - 1 = +0.05$$

Note that in all of these calculations, the yield point of the material is conservatively chosen as a stress criteria, even though the HAC event is classified as a Service Level D loading condition by Regulatory Guide 7.6.<sup>4</sup> Since neither the shelf nor the bulkhead experience yield in the governing slapdown or end drop impacts, the “rattle space” available for the rods does not increase as a result of the worst case free drop event. Thus, the AFS-C rod container supports the geometry assumptions made in the criticality analysis of Chapter 6, *Criticality Evaluation*.

**Table C2.7-1 Comparison of the MOX Fuel Assembly and the AFS-C Rod Container in the MFFP Strongback**

MOX Fuel Assembly	AFS-C Rod Container	Conclusion
Strongback clamps on fuel grids	Strongback clamps on container	AFS-C lid is both bolted in place and clamped in place by the strongback
Max weight of 1,580 lb	Max weight of 1,230 lb	Lighter payload in AFS-C, which applies lower inertia loads to the strongback in free drop impact events
264 rods	116 Exxon plus 69 PNL (185) rods	Fewer rods in AFS-C
Rods self-supporting over span between clamp arms	Rods supported by thick walls and bolted lid of container	AFS-C eliminates rod bending loads
Rods can move axially a limited amount	Rods are confined by thick, bolted end structures	AFS-C confines rods axially
Rod lateral buckling is controlled by strongback and FCS	Rod lateral buckling is controlled by strongback and FCS, plus: <ol style="list-style-type: none"> <li>1. restricted free space inside container</li> <li>2. rods supported by thick walls of container</li> <li>3. rods are shorter than MOX rods</li> </ol>	AFS-C adds a significant layer of rod support to that existing in the basic strongback/FCS

<sup>4</sup> U.S. Nuclear Regulatory Commission, Regulatory Guide 7.6, *Design Criteria for the Structural Analysis of Shipping Cask Containment Vessels*, Revision 1, March 1978.

*Figure Withheld Under 10 CFR 2.390*

**Figure C2.7-1 AFS-C Rod Container Cross Section View**

*Figure Withheld Under 10 CFR 2.390*

**Figure C2.7-2 AFS-C Rod Container Bulkhead Views**

**C2.7.2 Crush**

This section is unchanged from Section 2.7.2, *Crush*.

**C2.7.3 Puncture**

The weight of the MFFP containing up to three AFS-C rod containers is bounded by the weight of the MFFP with a payload of three (3) standard fuel assemblies. Therefore, the system response to a puncture is bounded by the discussion presented in Section 2.7.3, *Puncture*.

## **C2.7.4 Thermal**

### **C2.7.4.1 Summary of Pressures and Temperatures**

Package pressures and temperatures due to the HAC thermal event are presented in Section C3.5.3, *Maximum Temperatures and Pressures*. MFFP strongback and shell temperatures under HAC associated with the AFS-C payload are essentially the same as the standard three (3) fuel assembly payload. From Section C3.5.3.2, *Maximum Pressures*, the maximum internal pressure during the HAC thermal event is 121.4 psig, with the package initially at atmospheric pressure. This pressure is bounded by the 130 psig pressure used in Section 2.7.4, *Thermal*.

### **C2.7.4.2 Differential Thermal Expansion**

This section is unchanged from Section 2.7.4.2, *Differential Thermal Expansion*, as the MFFP strongback and shell temperatures under HAC associated with the AFS-C payload are essentially the same as the standard three (3) fuel assembly payload.

### **C2.7.4.3 Stress Calculations**

As discussed in Section C2.7.4.1, *Summary of Pressures and Temperatures*, a conservative maximum internal pressure of 121.4 psig is calculated for the HAC thermal event. This pressure is lower than the 130 psig pressure used in Section 2.7.4.3, *Stress Calculations*. Therefore, the stresses calculated in Section 2.7.4.3 conservatively bound the stresses resulting from the payload evaluated in this Appendix.

### **C2.7.5 Immersion – Fissile Material**

This section is unchanged from Section 2.7.5, *Immersion – Fissile Material*.

### **C2.7.6 Immersion – All Packages**

This section is unchanged from Section 2.7.6, *Immersion – All Packages*.

### **C2.7.7 Deep Water Immersion Test (for Type B Packages Containing More than $10^5$ A<sub>2</sub>)**

This section is unchanged from Section 2.7.7, *Deep Water Immersion Test*.

### **C2.7.8 Summary of Damage**

The AFS-C rod container maintains its structural integrity and functionality in the worst-case HAC free drop event, which bounds the loadings of all other HAC events on the container. Since the AFS-C rod container is mounted in the same way as a MOX fuel assembly but weighs less, the response of the MFFP to drop and puncture accidents is unchanged when using the AFS-C. Therefore, the AFS-C is acceptable for use as a payload container.



## C2.8 Accident Conditions for Air Transport of Plutonium

This section does not apply for the MFFP, since air transport is not claimed.

## C2.9 Accident Conditions for Fissile Material Packages for Air Transport

This section does not apply for the MFFP, since air transport is not claimed.

## C2.10 Special Form

This section does not apply for the MFFP, since special form is not claimed.

## C2.11 Fuel Rods

This section does not apply for the MFFP, since containment by the fuel rod cladding is not claimed.

## C2.12 Appendices

There are no appendices to Chapter C2.0. The applicability of the appendices to Chapter 2, *Structural Evaluation*, is given in Table C2.12-1.

**Table C2.12-1 – Applicability of Section 2.12 Appendices to the AFS-C Payload**

Appendix	Applicability
2.12.1, Impact Limiter Evaluation	As the weight of the AFS-C is bounded by the weight of a fuel assembly, the impact limiter evaluation from Section 2.12.1 remains bounding.
2.12.2, Certification Test Plan	Unchanged from Section 2.12.2
2.12.3, Certification Test Results	Unchanged from Section 2.12.3
2.12.4, Engineering Test Results	Unchanged from Section 2.12.4
2.12.5, Fuel Control Structural Evaluation	As the weight of the AFS-C is bounded by the weight of a fuel assembly, and because it is more structurally robust than a fuel assembly, the fuel control structural evaluation from Section 2.12.5 remains bounding.
2.12.6, CASKDROP Computer Program	Unchanged from Section 2.12.6
2.12.7, Impact Limiter Weld Joint Test Results	Unchanged from Section 2.12.7
2.12.8, Effect of Bounding Weight on Package Structural Responses	As the weight of the AFS-C is bounded by the weight of a fuel assembly, the package structural responses evaluation from Section 2.12.8 remains bounding.

## C3.0 THERMAL EVALUATION

### C3.1 Description of Thermal Design

This section identifies and describes the principal thermal design aspects of the MOX Fresh Fuel Package (MFFP) for the transportation of the AFS-C rod container loaded with the Los Alamos Technical Area 18 (TA-18) MOX fuel rods. The results presented in this chapter demonstrate the thermal safety of the package and compliance with the thermal requirements of 10 CFR 71<sup>1</sup> and supports the addition of up to three (3) AFS-C rod containers containing TA-18 fuel rods as allowable contents of the MFFP.

The analysis demonstrates that the addition of the AFS-C rod container does not impact the packaging temperatures and that the temperatures reported in Chapter 3.0, *Thermal Evaluation*, remain bounding. However, the peak NCT and HAC fuel cladding temperatures estimated for the fuel rods in an AFS-C rod container are higher than the peak temperature computed for an intact MOX fuel assembly, largely due to the simplified method employed. Nevertheless, the maximum allowable fuel temperature limits are not approached. The internal pressure of the package under HAC is bounded by the pressure resulting from the transportation of three (3) intact MOX fuel assemblies.

#### C3.1.1 Design Features

The principal thermal design features of the MFFP are described in Section 3.1.1, *Design Features*, while the principal features of the AFS-C rod container are described in Section C1.2.3, *Contents of Packaging*.

#### C3.1.2 Content's Decay Heat

The payload for the MFFP under this amendment consists of up to three (3) AFS-C rod containers. Each AFS-C may transport up to 116 Exxon rods and 69 PNL rods. A decay heat loading of 80 watts per AFS-C is assumed for the purposes of this thermal evaluation. A mixed payload of Exxon and PNL TA-18 fuel rods assumes a maximum decay heat of 30 watts within the PNL rods, thus leaving a maximum allowable decay heat load of 50 watts for the Exxon rods. If the PNL fuel rod payload dissipates less than 30 watts, the allowable decay heat load in the Exxon fuel rods can be increased accordingly so long as the maximum decay heat within the AFS-C rod container is 80 watts or less. Transportation of Exxon fuel rods alone assumes a total decay heat load of 80 watts.

The decay heat is assumed to be evenly distributed over the active fuel length of each payload. The Exxon rods have a total length of approximately 77.3 inches and an active fuel length of 70 inches. The PNL rods have a total length of approximately 36.6 inches and an assumed active length of 28 inches.

---

<sup>1</sup> Title 10, Code of Federal Regulations, Part 71 (10 CFR 71), *Packaging and Transportation of Radioactive Material*, 01-01-06 Edition.

### C3.1.3 Summary of Temperatures

The maximum temperatures for the MFFP Packaging under NCT and HAC are summarized in Table C3.1-1. The packaging temperatures are taken from Table 3.4-1 and Table 3.5-1, respectively. While these packaging temperatures are associated with the transportation of three (3) MOX fuel assemblies, they are bounding for the MFFP temperatures arising from the transportation of a payload consisting of up to three (3) AFS-C rod containers loaded with TA-18 fuel rods. Table C3.1-1 also presents the NCT and HAC temperatures for the AFS-C rod container and its payload of fuel rods. The peak temperature within the AFS-C rod container under NCT conditions is 240 °F (see Section C3.4, *Thermal Evaluation for Normal Conditions of Transport*), while the peak temperature achieved under HAC is predicted to be 631 °F (see Section C3.5, *Thermal Evaluation under Hypothetical Accident Conditions*).

### C3.1.4 Summary of Maximum Pressures

The maximum normal operating pressure (MNOP) for the MFFP with the AFS-C rod container loaded with TA-18 fuel rods resulting from the NCT Hot condition and conservative assumptions is 2.8 psig. Further details of the pressure analysis are presented in Section C3.4.2, *Maximum Normal Operating Pressure*.

The maximum peak pressure generated within the package cavity under HAC is conservatively estimated assuming that the entire inventory of organic material within the strongback assembly is totally combusted/pyrolyzed. No organic material is used in the AFS-C rod container.

The maximum pressure under HAC is 121.4 psig (136.1 psia) at the end of the fire when the peak cavity gas temperature is reached. The pressure will then decrease as the package cools. Further details of the analysis are presented in Section C3.5.3, *Maximum Temperatures and Pressures*.

Table C3.1-1 –Summary of Temperatures for NCT and HAC (°F)

Item	Hot NCT	Peak HAC	Maximum Allowable		Minimum Temperature Margin <sup>(1)</sup>
			NCT	HAC	
Peak Exxon Fuel Rod	<b>240</b>	631	<b>392</b>	1,337	152
Peak PNL Fuel Rod	<b>238</b>	627	<b>392</b>	1,337	154
Peak AFS-C Container	191	<b>607</b>	1,100	<b>1,100</b>	493
Avg. AFS-C Container	182	601	-	-	NA
<i>Temperatures for MFFP Package from Table 3.4-1 and Table 3.5-1</i>					
<i>Strongback Structure</i>	<i>178</i>	<i><b>599</b></i>	<i>800</i>	<i><b>800</b></i>	<i>201</i>
<i>Body Shell</i>	<i><b>159</b></i>	<i>1,361</i>	<i><b>800</b></i>	<i>2,500</i>	<i>641</i>
<i>Body Collar</i>	<i>149</i>	<i><b>414</b></i>	<i>800</i>	<i><b>1,000</b></i>	<i>586</i>
<i>Closure Lid</i>	<i><b>147</b></i>	<i>301</i>	<i><b>800</b></i>	<i>1,000</i>	<i>653</i>
<i>Impact Limiter Lugs</i>	<i><b>154</b></i>	<i>1,282</i>	<i><b>800</b></i>	<i>2,500</i>	<i>646</i>
<i>Impact Limiter</i>					
• <i>Max. Foam</i>	<i>149</i>	<i>N/A</i>	<i><b>300</b></i>	<i>N/A</i>	<i>151</i>
• <i>Bulk Avg. Foam</i>	<i>145</i>	<i>N/A</i>	<i><b>300</b></i>	<i>N/A</i>	<i>155</i>
• <i>Skin</i>	<i><b>149</b></i>	<i>1,429</i>	<i><b>800</b></i>	<i>2,500</i>	<i>651</i>
<i>Impact Limiter Bolts</i>					
• <i>Bolt Head</i>	<i><b>154</b></i>	<i>1,283</i>	<i><b>800</b></i>	<i>2,500</i>	<i>646</i>
• <i>Bolt Shaft</i>	<i><b>144</b></i>	<i>1,006</i>	<i><b>800</b></i>	<i>2,500</i>	<i>656</i>
• <i>Bolt Threads</i>	<i><b>144</b></i>	<i>295</i>	<i><b>800</b></i>	<i>2,500</i>	<i>656</i>
<i>O-ring Seals</i>					
• <i>Closure Lid</i>	<i>159</i>	<i><b>339</b></i>	<i>225</i>	<i><b>400</b></i>	<i>61</i>
• <i>Vent/Sampling Port</i>	<i><b>146</b></i>	<i>295</i>	<i>225</i>	<i>400</i>	<i>79</i>

Note: (1) Minimum temperature margin based on **bold** temperatures.

This page left intentionally blank.

## C3.2 Material Properties and Component Specifications

### C3.2.1 Material Properties

The material specifications for the MFFP package are defined in Section 3.2.1, *Material Properties*. The AFS-C rod container is fabricated primarily of clear anodized 6061-T6 aluminum. For the purposes of this calculation the material properties of the aluminum is characterized by a single thermal conductivity point of 96 Btu/hr-ft-°F<sup>1</sup> with an emissivity of 0.76<sup>2</sup>.

The TA-18 MOX fuel rods are assumed to have similar material properties and specifications as those defined for the standard MOX fuel assemblies.

### C3.2.2 Component Specifications

In addition to the materials listed in Section 3.2.2, *Component Specifications*, the only material associated with the AFS-C rod container that is considered temperature sensitive is the aluminum. 6061 aluminum has a melting temperature point of approximately 1,100 °F<sup>1</sup>.

No organic material is used in the AFS-C rod container. The characteristics of the organic material within the MFFP package are defined in Section 3.2.2, *Component Specifications*.

---

<sup>1</sup> American Society of Mechanical Engineers (ASME) Boiler and Pressure Vessel Code, Section II, *Materials, Part D – Properties*, 2001 Edition, with 2002 and 2003 Addenda, New York

<sup>2</sup> Gilmore, D. G., Editor, *Satellite Thermal Control Handbook*, The Aerospace Corporation Press, El Segundo, CA, 1994, pp A-8.

This page left intentionally blank.

## C3.3 General Considerations

### C3.3.1 Evaluations by Analysis

The MFFP with the AFS-C rod container loaded with TA-18 fuel rods is analytically evaluated in accordance with 10 CFR 71 and Regulatory Guide 7.8<sup>1</sup> for the bounding NCT and HAC thermal loads. Section 3.3.1, *Evaluation by Analysis*, summarizes the design basis conditions considered in these evaluations.

#### C3.3.1.1 NCT Analytical Model

The NCT analytical thermal model of the MFFP is based on the Thermal Desktop<sup>®2</sup> and SINDA/FLUINT<sup>3</sup> computer programs. Details of these programs, together with a description of the thermal model for the MFFP, are described in Section 3.3.1.1, *NCT Analytical Model*. That analysis demonstrated that a significant thermal margin exists for all package components.

The AFS-C rod container has outer dimensions similar to a standard fuel assembly and interfaces with the strongback and clamp arms assembly of the MFFP in a similar manner. Further, the maximum heat dissipation is the same as that of a standard MOX fuel assembly. As such, the methodology used to evaluate the thermal performance of the AFS-C rod container loaded with TA-18 fuel rods within the MFFP is conservatively based on use of the maximum strongback temperature achieved for the transportation of the three (3) MOX fuel assemblies as a boundary condition for a 1-dimensional heat transfer analysis within the AFS-C rod container.

Figure C3.3-1 illustrates a cross-section through the portion of the AFS-C rod container loaded with 116 Exxon fuel rods, while Figure C3.3-2 illustrates the cross-section through the portion of the AFS-C loaded with 69 PNL fuel rods. The Exxon fuel rods are expected to be arranged in a consolidated bundle consisting of 8 layers of 14 to 15 rods each and the PNL fuel rods are expected to be arranged in 6 layers of 11 to 12 rods each. The temperature rise between the strongback and the center fuel rod in the consolidated bundle is computed using the 1-dimensional thermal model of the loaded AFS-C rod container illustrated in Figure C3.3-3.

#### Temperature of AFS-C rod container

The heat transfer between the AFS-C rod container and the strongback (i.e., c-to-h and g-to-h in Figure C3.3-3) is computed as a combination of radiation and conduction across an air gap based on the conservative assumption that the AFS-C container is centered within the fuel control structure (FCS) of the strongback assembly. Given the inside dimension for the FCS of 8.7-in, and an outside dimension of 8.4-in for the AFS-C container, the resulting uniform gap is 0.15-in. The heat transfer between the AFS-C container and the FCS is computed as:

<sup>1</sup> Regulatory Guide 7.8, *Load Combinations for the Structural Analysis of Shipping Casks for Radioactive Material*, Revision 1, U. S. Nuclear Regulatory Commission, March 1989.

<sup>2</sup> Thermal Desktop<sup>®</sup>, Version 4.5, Cullimore & Ring Technologies, Inc., Littleton, CO, 2003.

<sup>3</sup> SINDA/FLUINT, *Systems Improved Numerical Differencing Analyzer and Fluid Integrator*, Version 4.5, Cullimore & Ring Technologies, Inc., Littleton, CO, 2001.



$$q' = A \left[ \frac{1}{(\epsilon_c^{-1} - 1) + \frac{1}{F_{c-h}} + (\epsilon_h^{-1} - 1)} \sigma (T_c^4 - T_h^4) + \frac{k}{x} (T_c - T_h) \right] \quad (\text{Eqn. 1})$$

where:

$q'$  = heat transfer rate, Btu/hr

$A$  = heat transfer area, in<sup>2</sup>

$\epsilon_c$  = emissivity of AFS-C rod container = 0.76

$\epsilon_h$  = emissivity of FCS surfaces = 0.20<sup>4</sup>

$F_{c-h}$  = view factor between AFS-C container and FCS surfaces = 1.

$\sigma$  = Stefan-Boltzmann constant =  $1.190278 \times 10^{-11}$  Btu/hr-in<sup>2</sup>-R<sup>4</sup>

$T_c$  = temperature of AFS-C container, °R

$T_h$  = temperature of FCS surfaces, = 178°F or 638°R at the NCT Hot condition<sup>5</sup>

$k$  = thermal conductivity of air, Btu/hr-in<sup>2</sup>-R<sup>6</sup>

$x$  = gap distance between AFS-C and FCS surfaces = 0.15-in

The temperature rise between the center shelf of the AFS-C container and the sidewalls (i.e., e-to-c in Figure C3.3-3) is insignificant due to the combination of the limited heat load and the use of aluminum. Even assuming all 80 watts of decay heat passed between the center shelf and the container sidewalls and that this heat load is limited to the 70-inch active fuel length of the Exxon fuel rods, the  $\Delta T$  required to transfer this heat load is estimated via:

$$\Delta T = \frac{\text{Heat Load}}{\text{Area} \frac{\text{conductivity of aluminum}}{\text{average distance for heat to travel}}}$$

$$\Delta T = \frac{80 \text{ watts} \times 3.412 \text{ Btu/h/watt}}{(0.5 \text{ inches} \times 70 \text{ inches} \times 2 \text{ paths}) \frac{96/12 \text{ Btu/hr - inch - F}}{(8.4 \text{ inches}/4)}}$$

$$\Delta T = 1^\circ \text{F}$$

The  $\Delta T$  required at the joint between the shelf and the container sidewalls (assuming all heat transfers via the intermittent welds) is estimated via:

$$\Delta T = \frac{80 \text{ watts} \times 3.412 \text{ Btu/h/watt}}{(0.125 \text{ inches} \times 7 \text{ inches} \times 70 \text{ inches}/15.3 \text{ inches} \times 2 \text{ paths}) \frac{96/12 \text{ Btu/hr - inch}}{(0.25 \text{ inches})}}$$

$$\Delta T = 1.1^\circ \text{F}$$

<sup>4</sup> Section 3.2.1, *Material Properties*.

<sup>5</sup> Table 3.4-1, *NCT Temperatures*

<sup>6</sup> Table 3.2-6, *Properties of Air*

Finally, the temperature difference to distribute the heat from the joint with the center shelf equally over the sidewalls is estimated via:

$$\Delta T = \frac{80 \text{ watts} \times 3.412 \text{ Btuh/watt}}{(0.75 \text{ inches} \times 70 \text{ inches} \times 4 \text{ paths}) \frac{96/12 \text{ Btu/hr - inch}}{(8.4 \text{ inches}/4)}}$$

$$\Delta T = 0.34^\circ \text{F}$$

Therefore, the center shelf is conservatively predicted to be within 2.5°F of the sidewall temperatures. As such, the estimation of the temperature rise within the consolidated fuel bundle can be computed assuming uniform temperatures on all sides of the AFS-C container.

#### Temperature of outer edges of fuel bundle

The heat transfer between the AFS-C rod container and the consolidated fuel rod bundle (i.e., b-to-c, d-to-e, and f-to-g in Figure C3.3-3) is computed as a combination of radiation and conduction across an air gap based on the conservative assumption that the consolidated fuel bundle is centered within the AFS-C container. The inside dimension of the AFS-C container is 6.9 inches wide and 3.4-inches high and the height and average width of the Exxon fuel rod stack within the rod container (see Figure C3.3-1) is equal to:

$$\begin{aligned} \text{Height} &= \text{fuel rod diameter} \times (1 \text{ row} + 7 \text{ rows} \times \sin 60^\circ) \\ &= 0.451\text{-inches} \times (1 + 6.06) \\ &= 3.18\text{-inches} \end{aligned}$$

$$\begin{aligned} \text{Width} &= \text{fuel rod diameter} \times (14 \text{ rods} + 15 \text{ rods})/2. \\ &= 0.451\text{-inches} \times (14 + 15)/2. \\ &= 6.54\text{-inches} \end{aligned}$$

The height and average width of the PNL fuel rod stack within the rod container (see Figure C3.3-2) is equal to:

$$\begin{aligned} \text{Height} &= \text{fuel rod diameter} \times (1 \text{ row} + 5 \text{ rows} \times \sin 60^\circ) \\ &= 0.565\text{-inches} \times (1 + 4.33) \\ &= 3.01\text{-inches} \end{aligned}$$

$$\begin{aligned} \text{Width} &= \text{fuel rod diameter} \times (11 \text{ rods} + 12 \text{ rods})/2. \\ &= 0.565\text{-inches} \times (11 + 12)/2. \\ &= 6.50\text{-inches} \end{aligned}$$

Therefore, the average gap between the consolidated Exxon fuel rod bundle and the AFS-C rod container is  $(3.4 \text{ inches} - 3.18 \text{ inches})/2 + 1/4$  of the rod diameter, or 0.22-inches on the top and bottom and  $(6.9 \text{ inches} - 6.54 \text{ inches})/2 + 1/4$  of the rod diameter, or 0.29 -inches on the sides.

The average gap on all sides is computed as  $(6.9 \text{ inches} \times 0.22 \text{ inches} + 3.4 \text{ inches} \times 0.29 \text{ inches})/(6.9 \text{ inches} + 3.4 \text{ inches}) = 0.24\text{-inches}$ . In a similar fashion, the average gap on all sides for the PNL consolidated fuel bundle is 0.34-inches.

The heat transfer between the AFS-C container and the outer edges of the consolidated fuel rod bundle is computed as:

$$q' = A \left[ \frac{1}{(\epsilon_b^{-1} - 1) + \frac{1}{F_{b-c}} + (\epsilon_c^{-1} - 1)} \sigma (T_b^4 - T_c^4) + \frac{k}{x} (T_b - T_c) \right] \quad (\text{Eqn. 2})$$

where:

$q'$  = heat transfer rate, Btu/hr

$A$  = heat transfer area, in<sup>2</sup>

$\epsilon_c$  = emissivity of AFS-C rod container = 0.76

$\epsilon_b$  = emissivity of fuel rod surfaces = 0.20

$F_{b-c}$  = view factor between fuel bundle edges and AFS-C container = 1.

$\sigma$  = Stefan-Boltzmann constant =  $1.190278 \times 10^{-11}$  Btu/hr-in<sup>2</sup>-R<sup>4</sup>

$T_c$  = temperature of AFS-C container, °R

$T_b$  = avg. temperature of outer edges of fuel rod surfaces, °R

$k$  = thermal conductivity of air, Btu/hr-in<sup>2</sup>-R

$x$  = avg. gap distance between AFS-C and fuel rod surfaces

#### Temperature of hottest fuel rod

The heat transfer within the consolidated fuel bundle is computed by conservatively assuming the individual rods are separated by a finite distance from each of its neighbors and are not in direct contact. As such, the heat transfer between the rods is computed as radiation and conduction across the air gap separating the individual fuel rods. Since the  $\Delta T$  across the width of the individual fuel rods is insignificant in comparison, it is ignored for the purposes of this calculation. Figure C3.3-4 illustrates the idealized configuration assumed for the fuel bundle for the purposes of estimating the temperature rise within it.

As idealized, the fuel bundle is treated as a series of concentric layers of fuel rods with the temperature in each layer being the same. With the exception of the center rod, the heat transfer via radiation from layer 'n-1' to layer 'n' for  $n \geq 2$  is computed as:

$$q'_{\text{rad}} = \text{Area} \times \left[ \frac{1}{(\epsilon_{n-1}^{-1} - 1) + \frac{1}{F_{n-1 \text{ to } n}} + \frac{\text{Area}_{n-1}}{\text{Area}_n} (\epsilon_n^{-1} - 1)} \sigma (T_{n-1}^4 - T_n^4) \right]$$

$$q'_{\text{rad}} = 2\pi \times r \times L \times 6(n-1) \times \left[ \frac{1}{(0.2^{-1} - 1) + \frac{1}{F_{n-1 \text{ to } n}} + \frac{n-1}{n} (0.2^{-1} - 1)} \sigma (T_{n-1}^4 - T_n^4) \right] \quad (\text{Eqn. 3})$$

where:

$q'_{\text{rad}}$  = radiation heat transfer rate fuel layer 'n-1' to layer 'n', Btu/hr

$r$  = radius of fuel rod, = 0.2255-in for Exxon fuel and 0.2825-in for PNL fuel

$L$  = active length of fuel rod = 70-in for Exxon fuel and 28-in for PNL fuel

$n$  = number of the rod layer, with the center rod at  $n = 0$

$\epsilon_{n-1}$  &  $\epsilon_n$  = emissivity of fuel rod surfaces = 0.20

$$F_{n-1 \text{ to } n} = \text{view factor from fuel layer 'n-1' to layer 'n'} = (2n-1)/(6(n-1))$$

$$\sigma = \text{Stefan-Boltzmann constant} = 1.190278 \times 10^{-11} \text{ Btu/hr-in}^2\text{-R}^4$$

$$T_{n-1} = \text{temperature of fuel rods in layer 'n-1'}, \text{ } ^\circ\text{R}$$

$$T_n = \text{temperature of fuel rods in layer 'n'}, \text{ } ^\circ\text{R}$$

For the radiation heat transfer from the center rod to the next layer (i.e.,  $n=1$ ), the heat transfer is computed as:

$$q_{\text{rad}} = 2\pi \times r \times L \times \left[ \frac{1}{(0.2^{-1} - 1) + \frac{1}{1} + \frac{1}{3}(0.2^{-1} - 1)} \sigma (T_0^4 - T_{n=1}^4) \right] \quad (\text{Eqn. 4})$$

Since no credit is taken for direct contact between the fuel rods, the conduction heat transfer between the rods will be via conduction across the intervening air gap. Each fuel rod will conductively exchange heat with six adjacent rods. Of these conduction points,  $6(2n-1)$  will be between rods in layer 'n-1' to those in rod layer 'n'. The surface area associated with each conduction point is  $2\pi \cdot r \cdot L/6$ , while a conservative separation distance between the surfaces of  $2 \cdot r \cdot (1 - \sin 60^\circ)$  is used. The conduction heat transfer from rod layer 'n-1' to layer 'n' for  $n \geq 1$  is computed as:

$$q_{\text{cond}} = \frac{2\pi \times r \times L/6 \times 6(2n-1) \times k \times (T_{n-1} - T_n)}{2 \times r \times (1 - \sin 60^\circ)}$$

$$q_{\text{cond}} = \frac{\pi \times L \times (2n-1) \times k \times (T_{n-1} - T_n)}{(1 - \sin 60^\circ)} \quad (\text{Eqn. 5})$$

where:

$$q'_{\text{cond}} = \text{conduction heat transfer rate fuel layer 'n-1' to layer 'n'}, \text{ Btu/hr}$$

$$L = \text{active length of fuel rod}$$

$$n = \text{number of the rod layer, with the center rod at } n = 0$$

$$k = \text{thermal conductivity of air, Btu/hr-in}^2\text{-R}$$

$$T_{n-1} = \text{temperature of fuel rods in layer 'n-1'}, \text{ } ^\circ\text{R}$$

$$T_n = \text{temperature of fuel rods in layer 'n'}, \text{ } ^\circ\text{R}$$

### C3.3.1.2 HAC Analytical Model

The analytical thermal model of the MFFP with the AFS-C rod container loaded with TA-18 fuel rods under HAC uses the same methodology used for the NCT evaluation. Since the NCT methodology is based on steady-state conditions and it ignores the effects of thermal mass and transient heating, the predicted HAC temperatures are conservative. The peak strongback temperature presented in Section 3.5, *Thermal Evaluation under Hypothetical Accident Conditions*, is used as a steady-state boundary temperature for the 1-D thermal model of the AFS-C rod container described above.

### C3.3.2 Evaluation by Test

This section is not applicable since evaluation by test was not performed for the MFFP with the AFS-C rod container loaded with TA-18 fuel rods.

### C3.3.3 Margins of Safety

A summary of the maximum temperatures for the MFFP, with their respective temperature margins, for both NCT and HAC are provided in Table 3.3-3.

From Section C3.1.4, *Summary of Maximum Pressures*, the maximum normal operating pressure (MNOP) is 2.8 psig, which is bounded by the calculated MNOP of 2.9 psig for the standard payload of three (3) fuel assemblies. (Note that the reported MNOP for the package is 10 psig, which is obtained by rounding up the 2.9 psig value.) Therefore, the margin of safety (MS) for the 25-psig design pressure is:

$$MS = \frac{25}{2.8} - 1.0 = +7.9$$

From Section C3.1.4, *Summary of Maximum Pressures*, the maximum pressure for HAC is 121.4 psig. This pressure is bounded by the 123.5 psig pressure for the standard three (3) fuel assembly payload. Therefore, the MS of +2.15 reported in Section 3.3.3, *Margins of Safety*, is bounding.

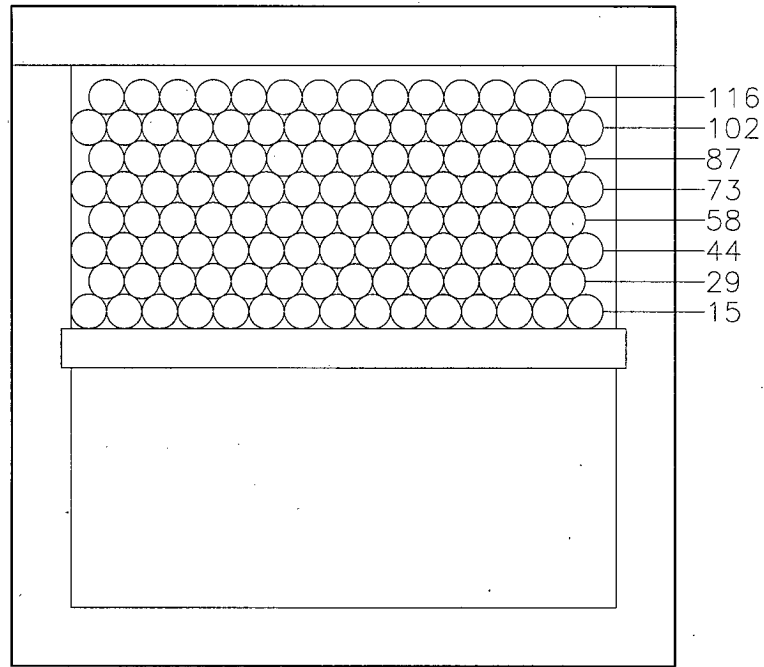


**Figure C3.3-1 - Consolidated Exxon Fuel Rod Bundle within AFS-C Rod Container**

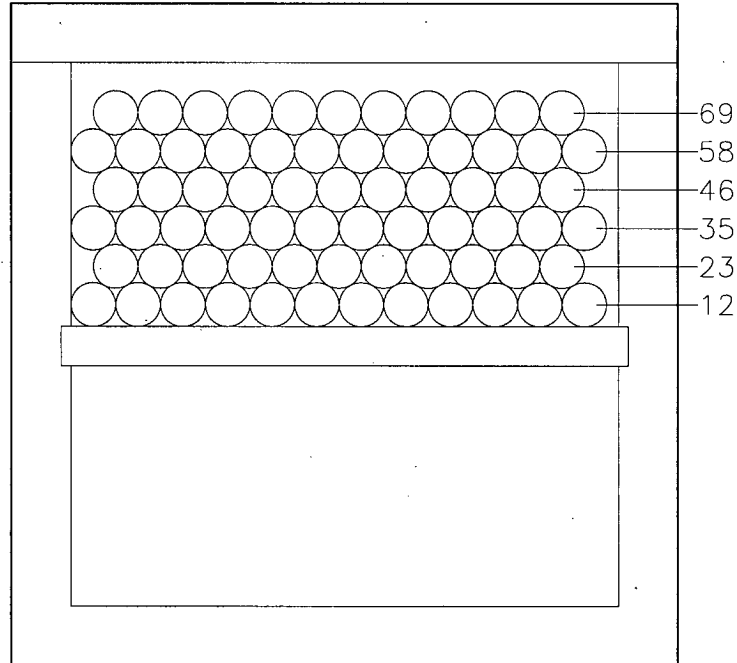
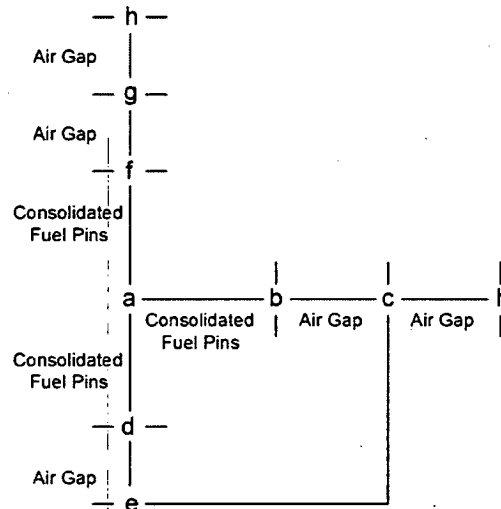


**Figure C3.3-2 - Consolidated PNL Fuel Rod Bundle within AFS-C Rod Container**



- a = center of the consolidated fuel rod bundle
- b = side edge of the consolidated fuel rod bundle
- c = side of AFS-C rod container
- d = bottom side of the consolidate fuel rod bundle
- e = center shelf of AFS-C rod container
- f = top edge of the consolidated fuel rod bundle
- g = top of AFS-C rod container
- h = strongback assembly of MFFP Package

**Figure C3.3-3 - 1-D Thermal Model of AFS-C Rod Box Container**

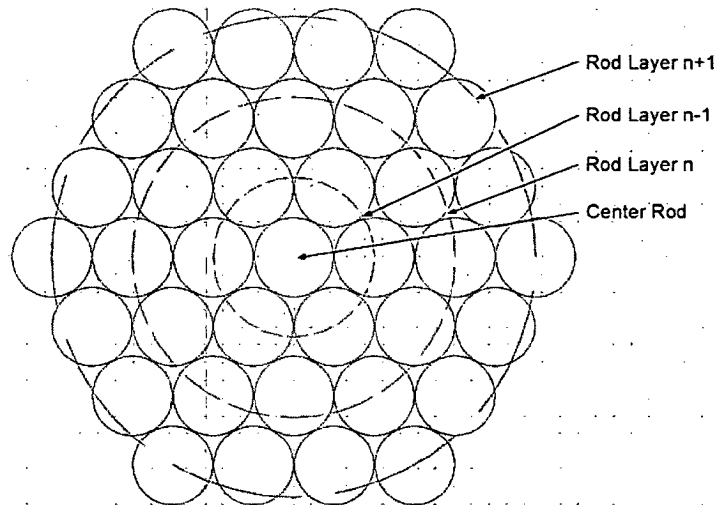


**Figure C3.3-4 - Consolidated Fuel Rod Bundle Modeling**

## C3.4 Thermal Evaluation for Normal Conditions of Transport

### C3.4.1 Heat and Cold

#### C3.4.1.1 Heat

The maximum temperatures for the AFS-C rod container loaded with TA-18 MOX fuel rods are determined assuming the peak temperature of 178 °F for the strongback assembly obtained from Section 3.4.1.1, *Heat*, for the NCT Hot condition. Since this temperature is associated with a decay heat loading of 240 watts, a similar strongback temperature will occur with the transport of up to three (3) AFS-C rod containers with the same total decay heat loading. While the TA-18 fuel rod payload may result in a higher heat flux on a per inch basis, the aluminum sidewalls and center shelf of the AFS-C container and the boron material in the strongback will effectively spread the heat load axially such that the local rise in the peak strongback temperature will be 3 °F or less. This conclusion is based on a sensitivity thermal analysis using the thermal model for the MFFP, described in Section 3.3.1.1, *NCT Analytical Model*. Given this relatively small temperature increase and since the sensitivity modeling does not include the axial spreading of the heat flux within the aluminum sidewalls of the AFS-C rod container, the use of the strongback temperature as a boundary condition for this calculation is an appropriate assumption for the purposes of this safety evaluation.

Based on the 1-dimensional thermal model described above and a decay heat load of 80 watts for the Exxon fuel rods, and an iterative solution of equation #1 from Section C3.3.1.1, *NCT Analytical Model*, the estimated peak sidewall temperature for the AFS-C rod container is 188°F for the section housing the Exxon TA-18 rods, while the average sidewall temperature is 182°F. Adding the 2.5°F  $\Delta T$  determined in Section C3.3.1.1 for the temperature difference between the center shelf and the sidewall, yields a peak AFS-C temperature of 191°F for the NCT Hot condition.

Based on an iterative solution of equation #2 from Section C3.3.1.1, the temperature of the outer surface of the Exxon fuel bundle within the AFS-C rod container is predicted to be 209°F. The associated peak fuel rod temperature is computed by iterative solution of equations #3 to #5. Since the Exxon fuel bundle is 8 rod layers high and 14 to 15 rod layers wide, the peak temperature of the center fuel rod is conservatively predicted by assuming the fuel bundle extends 7 layers in all directions from the center rod. Based on this assumption, the associated peak fuel rod temperature within the AFS-C rod container under NCT Hot conditions is estimated to be 240°F.

Using the same modeling approach used for the Exxon fuel rods, but assuming a decay heat loading of 30 watts and an assumed active fuel length of 28 inches, the peak AFS-C rod container sidewall temperature for the section housing the PNL TA-18 fuel rods is determined to be 187°F, with a peak rod temperature of 238°F. In reality, the aluminum sidewalls of the AFS-C rod container will spread the decay heat in the axial direction, effectively lowering the decay heat loading per inch and resulting in lower temperature rises than those estimated above.

These predicted peak temperatures are bounding whether the other positions in the strongback are occupied by another AFS-C rod container or a dummy fuel assembly. Further, based on the



maximum temperature of 240 °F, none of the organic material within the strongback assembly will experience thermal decomposition and out-gassing under NCT conditions.

The results presented in Section 3.4.1.1, *Heat*, for the MFFP remain valid for the MFFP component temperatures associated with the transport of the AFS-C rod containers loaded with TA-18 fuel rods. Specifically, the closure seals and the impact limiter foam temperatures remain below their associated temperature limits. Additionally, the MFFP analysis demonstrated that the accessible package surfaces remain below 122 °F when transported in an ambient temperature of 100 °F and without insolation, as stipulated by 10 CFR §71.43(g).

#### **C3.4.1.2 Cold**

The minimum temperature distribution for the MFFP with the AFS-C rod containers occurs with a zero decay heat load and an ambient air temperature of -40 °F per 10 CFR §71.71(c)(2). The steady-state analysis of this condition represents a trivial analytical case that requires no thermal calculations be performed. Instead, it is assumed that all package components achieve the -40 °F temperature under steady-state conditions. The -40 °F temperature is within the allowable range of all of the packaging components. The package temperatures for the NCT Cold condition of -20 °F and no insolation are bounded by those presented in Section 3.4.1.2, *Cold*, for the MFFP.

#### **C3.4.2 Maximum Normal Operating Pressure**

The maximum normal operating pressure (MNOP) for NCT is based on an initial package backfill of air at atmospheric pressure at 70 °F (294 K) and an assumed failure rate of 3% of the TA-18 fuel rods. The heat up of the gases in package cavity is assumed to be the same as that determined for the transport of three (3) MOX fuel assemblies for the respective ambient condition. For the purpose of rod pressure determination, the only significant gas contributor is the initial gas backfill within the TA-18 fuel rods as no fission products will exist within the un-irradiated rods.

The bulk average gas temperature from Section 3.4.1.1, *Heat*, for the MFFP under the NCT Hot condition is used as the basis for the MNOP calculation with the AFS-C rod containers. Since the decay heat loading assumed for the MFFP is equal to the heat dissipation associated with the AFS-C rod containers loaded with TA-18 fuel rods, the associated bulk average gas temperature will also be similar. The package cavity has a gross free volume of approximately 105,547 in<sup>3</sup>, based on a package cavity OD of 28.5 inches and a length of 165.45 inches. The displacement volume for the strongback assembly is 11,292 in<sup>3</sup> (see Section 3.4.2, *Maximum Normal Operating Pressure*). The solid volume for an unloaded AFS-C rod container is 4,694 in<sup>3</sup> based on an approximate weight of 460 lbs and a density of 0.098 lbs/in<sup>3</sup>. The volume of 116 Exxon fuel rods is 1,432 in<sup>3</sup> based on a rod diameter of 0.451-in. and a length of 77.26-in. and the volume of 69 PNL fuel rods is 633 in<sup>3</sup> based on a rod diameter of 0.565-in. and a length of 36.6-in.

The solid volume for the dummy fuel assembly is approximately 5,366 in<sup>3</sup>. Since the dummy fuel assembly has a lower solid volume than a loaded AFS-C rod container and since it contains no fuel rods that could fail and release gas, the transport of three (3) AFS-C containers will bound the pressure generated for a payload containing a mix of AFS-C containers and dummy fuel assemblies.

The type and amount of fill gas within each TA-18 fuel rod is unknown. For the purposes of this safety evaluation, the gas quantities associated with the standard MOX fuel rod, as determined in

Section 3.4.2, *Maximum Normal Operating Pressure*, is conservatively used. Based on this assumption, the total gas volume within the maximum payload of 116 Exxon fuel rods and 69 PNL fuel rods is 4.49 g-moles.

The initial gas in the package cavity at the time of sealing is calculated as follows:

$$N_{\text{fill}} = \frac{1 \text{ atm} \times V_{\text{free}}}{R \times T_{\text{fill}}}$$

where:

- $T_{\text{fill}}$  = temperature of air within package cavity at time of package closure
- $R$  = Ideal gas constant (0.08206 atm-liter/gmole-°K)
- $V_{\text{free}}$  = Package cavity free volume  
= Gross cavity volume minus displacement volumes for the AFS-C rod container(s), the dummy fuel assembly(s), and the strongback  
= 73,978 in<sup>3</sup> (1,212 liters)

The MNOP is then calculated as follows:

$$\text{MNOP} = \frac{N_{\text{cask}} RT_{\text{NCT}}}{V_{\text{free}}}$$

$$N_{\text{cask}} = N_{\text{fill}} + \text{Rod Failure Rate} \times N_{\text{MOX fill gas}} + N_{\text{outgassing}}$$

where:

- $N_{\text{cask}}$  = total moles of gas in package cavity
- $N_{\text{fill}}$  = moles air within package cavity at time of package closure
- Rod Failure Rate = assumed percentage of failed rods. A 3% failure rate, which matches the regulatory failure rate for normal conditions of transport of spent fuel assemblies, will bound the expected failure rate for fresh fuel.
- $N_{\text{MOX fill gas}}$  = moles of rod fill gas within package cavity
- $N_{\text{outgassing}}$  = moles gas generated by out-gassing from component material in cask cavity
- $T_{\text{NCT}}$  = Bulk average gas temperature within package (K) at the specific condition  
= 166°F or 347 K<sup>1</sup>

Based on the above relationships and assumptions, the MNOP for the bounding payload combination of three (3) AFS-C rod container loaded with 116 Exxon fuel rods and 69 PNL fuel

<sup>1</sup> Table 3.4-1, *NCT Temperatures*

rods is 17.5 psia (2.8 psig). A significant margin exists between this calculated MNOP and the package's NCT design pressure limit of 39.7 psia (25 psig).

No hydrogen or other combustible gases will be generated as result of the thermal or radiation-induced decomposition of the organic material within the package. This conclusion is based on the low peak temperature achieved under NCT transport conditions and the low radioactivity associated with the un-irradiated MOX fuel rods.

### **C3.4.3 Maximum Thermal Stresses**

The maximum thermal stresses for NCT are bounded by those determined for the MFFP with the MOX fuel assembly payload. See the discussion in Section 2.6.1, *Heat*, and Section 2.6.2, *Cold*.

### **C3.4.4 Evaluation of Package Performance for Normal Conditions of Transport**

The steady-state thermal analysis presented in Section 3.4, *Thermal Evaluation for Normal Conditions of Transport*, demonstrated that the components of the MFFP with the MOX fuel assembly payload are within their respective allowable temperature limits. That evaluation is valid and bounding for the MFFP with the AFS-C rod containers loaded with TA-18 MOX fuel rods. The MNOP resulting from the NCT Hot condition and conservative assumptions is within the maximum design pressure limit of the package.

Therefore, the MFFP with the AFS-C rod container is found to comply with all of the thermal requirements specified in 10 CFR §71.71.

### **C3.5 Thermal Evaluation under Hypothetical Accident Conditions**

This section presents the results of the thermal evaluation of the MFFP with the AFS-C rod container loaded with TA-18 fuel rods under the hypothetical accident conditions (HAC) specified in 10 CFR §71.73(c)(4)<sup>1</sup>.

#### **C3.5.1 Initial Conditions**

The initial conditions assumed for the MFFP are presented in Section 3.5, *Thermal Evaluation under Hypothetical Accident Conditions*. Due to its robust design, no significant damage is assumed to have occurred to the AFS-C rod container(s) and dummy fuel assemblies as a result of the drop events that precede the HAC fire event. Even if damaged, the integrity of these components are not important to the thermal safety of the MFFP package.

#### **C3.5.2 Fire Test Conditions**

No fire tests were performed for the MFFP with the AFS-C rod container loaded with TA-18 fuel rods.

##### **C3.5.2.1 Analytical Model**

The analytical model of the MFFP under HAC is described in Section 3.5.2.1, *Analytical Model*, and Section 3.5.2.2, *Performance of Rigid Polyurethane Foam Under HAC Fire Conditions*. The peak temperature for the AFS-C rod container loaded with TA-18 fuel rods under HAC is estimated using the methodology and 1-dimensional thermal model of the AFS-C rod container described in Section C3.3.1.1, *NCT Analytical Model*.

#### **C3.5.3 Maximum Temperatures and Pressures**

##### **C3.5.3.1 Maximum Temperatures**

The maximum temperatures attained in the MFFP components under HAC with the AFS-C rod container and TA-18 fuel rods are bounded by those presented in Section 3.5.3.1, *Maximum Temperatures*. The peak strongback assembly temperature predicted from the evaluation of the MFFP is 599 °F and the transient analysis demonstrates that the peak temperature condition lasts for less than 15 minutes.

Based on a decay heat load of 80 watts for the maximum payload configuration of 116 Exxon fuel rods and an iterative solution of equation #1 from Section C3.3.1.1, the peak sidewall temperature for the AFS-C rod container under HAC conditions is 604°F, while the peak center shelf temperature is 607°F. In a similar fashion, based on equation #2 from Section C3.3.1.1, the peak temperature on the outer surface of the fuel bundle is predicted to be 613°F.

The associated peak fuel rod temperature is computed by iterative solution of equations #3 to #5 in the same manner as it was under NCT conditions. The peak Exxon fuel rod temperature is

---

<sup>1</sup> Title 10, Code of Federal Regulations, Part 71 (10 CFR 71), *Packaging and Transportation of Radioactive Material*, 01-01-06 Edition.

computed to be 631°F, while the peak PNL fuel rod temperature is 627°F. These temperature levels are within the short-term thermal limits for the fuel rods and all metallic components of the AFS-C rod container.

Although both the peak temperature and the duration of the elevated temperatures within the package are seen as insufficient to cause serious thermal decomposition of the organic material within the strongback, it is conservatively assumed that the organic material on the strongback assembly fully decomposes to the extent that the available oxygen permits.

### C3.5.3.2 Maximum Pressures

With the exception of the consideration for potential out-gassing from organic components within the package cavity and an assumed 100% failure rate for the fuel rods, the maximum pressure attained under HAC is determined in the same manner as described in Section C3.4.2, *Maximum Normal Operating Pressure*. While the MFFP is designed to protect the enclosed fuel rods from catastrophic failure during the pre-fire free and puncture bar drops and the subsequent 30-minute fire event, this analysis conservatively assumes that the cladding on all fuel rods have breached. As stated in Section C3.4.2, *Maximum Normal Operating Pressure*, the maximum amount of fill gas contained within an AFS-C rod container loaded with TA-18 fuel rods is conservatively estimated to be 4.49 g-moles. No significant change in the package cavity free volume is expected as a result of the HAC drop event.

Per Section 3.5.3.2, *Maximum Pressures*, approximately 7 pounds of neoprene rubber ( $C_4H_5Cl$ )<sub>n</sub> and 2.3 pounds of Delrin<sup>®</sup> plastic ( $C_6H_{14}O_2$ )<sub>n</sub> are used in the strongback assembly. The breakdown of these organic materials under HAC is limited by the facts that a limited amount of oxygen exists in the cask cavity and the peak cavity temperature and its duration under HAC are too low to permit complete pyrolysis (i.e., the process of breaking up a substance into other molecules as a result of heating in an inert atmosphere). For this evaluation, it is assumed that 75% of the oxygen is consumed generating carbon monoxide and only 25% is used in the generation of carbon dioxide gas. A larger ratio of carbon dioxide generation will result in a lower cask pressure. Under this conservative assumption, volatilizing the entire mass of neoprene rubber and Delrin<sup>®</sup> plastic would generate approximately 136.6 g-moles of additional gas within the cavity.

The peak pressure generated within the package cavity is estimated to be 136.1 psia (121.4 psig) at the end of the 30 minute fire event when the peak cavity gas temperature is reached. This pressure is bounded by the pressure from a payload of three fuel assemblies (138.2 psia). The pressure will then decrease as the package cools. The predicted peak pressure is considered to have a high degree of conservatism since there is insufficient oxygen within the package cavity to permit the full decomposition of the organic material and because both the relatively low peak temperature and the relatively short duration of the elevated temperatures will prevent any significant decomposition from occurring in the absence of active combustion of the material. It is expected that a majority of the organic material will remain in its original, solid form.

### C3.5.4 Accident Conditions for Fissile Material Packages for Air Transport

This section does not apply for the MFFP since air transport will not be utilized.

### **C3.5.5 Evaluation of Package Performance for Accident Conditions of Transport**

The evaluation of the MFFP with the AFS-C rod container loaded with TA-18 fuel rods under HAC demonstrates that the packaging has sufficient thermal protection remaining after the hypothetical drop and puncture bar damage to protect the thermally sensitive areas of the packaging. All package components are seen as remaining within their associated maximum temperature limits.

This page left intentionally blank.

C3.6 Appendices

C3.6.1 Computer Analysis Results

The safety evaluations are based on hand calculations. The following are reproduction of the spreadsheet pages used to compute the temperatures within the AFS-C rod container.

NCT Conditions - Exxon Fuel

AFS-C box to FCS surfaces		Inches	Btu/hr-in-F	Watts			Watts		Watts		Watts		
Box Width	Rod Length	Avg. Gap	Air k @ 180F	Box emiss	FCS emiss	Decay Heat	Box Temp. F	FCS Temp. F	Grad	Qcond	Qtotal		
8.4	70	0.150	0.00144	0.76	0.2	80	187.7	178	15.99	64.26	80.15		
8.4	159.9	0.150	0.00144	0.76	0.2	80	182.3	178	15.68	65.08	80.96	- Average sidewall temperature	

AFS-C box to fuel rod surfaces		Inches	Btu/hr-in-F	Watts			Watts		Watts		Watts	
Box Width	Box Height	Rod Length	Avg. Gap	Air k @ 200F	Rod emiss	Box emiss	Decay Heat	Rod Temp. F	Box Temp. F	Grad	Qcond	Qtotal
6.9	3.4	70	0.24	0.00148	0.2	0.76	80	209.4	187.7	23.43	56.68	80.11

HAC Conditions - Exxon Fuel

AFS-C box to FCS surfaces		Inches	Btu/hr-in-F	Watts			Watts		Watts		Watts		
Box Width	Rod Length	Avg. Gap	Air k @ 600F	Box emiss	FCS emiss	Decay Heat	Box Temp. F	FCS Temp. F	Grad	Qcond	Qtotal		
8.4	70	0.150	0.00216	0.76	0.2	80	603.7	599	34.66	46.62	81.28		
8.4	159.9	0.150	0.00216	0.76	0.2	80	601.1	599	35.25	47.58	82.83	- Average sidewall temperature	

AFS-C box to fuel rod surfaces		Inches	Btu/hr-in-F	Watts			Watts		Watts		Watts	
Box Width	Box Height	Rod Length	Avg. Gap	Air k @ 600F	Rod emiss	Box emiss	Decay Heat	Rod Temp. F	Box Temp. F	Grad	Qcond	Qtotal
6.9	3.4	70	0.24	0.00216	0.2	0.76	80	613.2	603.7	43.82	36.11	79.93

NCT Conditions - PNL Fuel

AFS-C box to FCS surfaces		Inches	Btu/hr-in-F	Watts			Watts		Watts		Watts	
Box Width	Rod Length	Avg. Gap	Air k @ 180F	Box emiss	FCS emiss	Decay Heat	Box Temp. F	FCS Temp. F	Grad	Qcond	Qtotal	
8.4	28	0.150	0.00144	0.76	0.2	30	187.1	178	5.95	24.12	30.07	

AFS-C box to fuel rod surfaces		Inches	Btu/hr-in-F	Watts			Watts		Watts		Watts	
Box Width	Box Height	Rod Length	Avg. Gap	Air k @ 180F	Rod emiss	Box emiss	Decay Heat	Rod Temp. F	Box Temp. F	Grad	Qcond	Qtotal
6.9	3.4	28	0.34	0.00144	0.2	0.76	30	213.2	187.1	11.36	18.71	30.07

HAC Conditions - PNL Fuel

AFS-C box to FCS surfaces		Inches	Btu/hr-in-F	Watts			Watts		Watts		Watts	
Box Width	Rod Length	Avg. Gap	Air k @ 600F	Box emiss	FCS emiss	Decay Heat	Box Temp. F	FCS Temp. F	Grad	Qcond	Qtotal	
8.4	28	0.150	0.00216	0.76	0.2	30	603.4	599	12.97	17.46	30.43	

AFS-C box to fuel rod surfaces		Inches	Btu/hr-in-F	Watts			Watts		Watts		Watts	
Box Width	Box Height	Rod Length	Avg. Gap	Air k @ 600F	Rod emiss	Box emiss	Decay Heat	Rod Temp. F	Box Temp. F	Grad	Qcond	Qtotal
6.9	3.4	28	0.34	0.00216	0.2	0.76	30	613.7	603.4	19.01	11.05	30.06

**Temperature Legend**  
 - user input temperature  
 - temperature linked to other cells on spreadsheet  
 - temperature obtained from [4] calculation



**PEAK EXXON & PNL ROD TEMPERATURES**

**NCT Conditions - Exxon Fuel**

From Rod Layer	To Rod Layer	Inch Rod Dia.	Inch Rod Length	Btu/hr-in-F Air k @ 220F	Rod emiss	Watt Rod Power	Watt Total Power	F Inner Rod T	F Outer Rod T	Watt Qrad	Watt Qconv	Watt Qtotal
6	7	0.451	70	0.00152	0.2	0.690	87.59	217.4	209.4	11.918	75.882	87.800
5	6	0.451	70	0.00152	0.2	0.690	62.76	224.2	217.4	8.842	54.577	63.419
4	5	0.451	70	0.00152	0.2	0.690	42.07	229.7	224.2	5.994	36.117	42.111
3	4	0.451	70	0.00152	0.2	0.690	25.52	234	229.7	3.701	21.962	25.663
2	3	0.451	70	0.00152	0.2	0.690	13.10	237.1	234	1.908	11.309	13.217
1	2	0.451	70	0.00152	0.2	0.690	4.83	239	237.1	0.670	4.159	4.829
0	1	0.451	70	0.00152	0.2	0.690	0.69	239.9	239	0.064	0.657	0.721

**HAC Conditions - Exxon Fuel**

From Rod Layer	To Rod Layer	Inch Rod Dia.	Inch Rod Length	Btu/hr-in-F Air k @ 600F	Rod emiss	Watt Rod Power	Watt Total Power	F Inner Rod T	F Outer Rod T	Watt Qrad	Watt Qconv	Watt Qtotal
6	7	0.451	70	0.00216	0.2	0.690	87.59	617.7	613.2	27.322	60.742	68.064
5	6	0.451	70	0.00216	0.2	0.690	62.76	621.5	617.7	19.715	43.402	63.117
4	5	0.451	70	0.00216	0.2	0.690	42.07	624.6	621.5	13.246	28.969	42.215
3	4	0.451	70	0.00216	0.2	0.690	25.52	627	624.6	7.989	17.444	25.433
2	3	0.451	70	0.00216	0.2	0.690	13.10	628.8	627	4.241	9.345	13.586
1	2	0.451	70	0.00216	0.2	0.690	4.83	629.9	628.8	1.475	3.426	4.901
0	1	0.451	70	0.00216	0.2	0.690	0.69	630.5	629.9	0.161	0.623	0.784

**NCT Conditions - PNL Fuel**

From Rod Layer	To Rod Layer	Inch Rod Dia.	Inch Rod Length	Btu/hr-in-F Air k @ 200F	Rod emiss	Watt Rod Power	Watt Total Power	F Inner Rod T	F Outer Rod T	Watt Qrad	Watt Qconv	Watt Qtotal
4	5	0.565	28	0.00148	0.2	0.435	26.52	221.8	213.2	4.505	22.093	26.598
3	4	0.565	28	0.00148	0.2	0.435	16.09	228.5	221.8	2.807	13.387	16.194
2	3	0.565	28	0.00148	0.2	0.435	8.26	233.3	228.5	1.451	6.851	8.302
1	2	0.565	28	0.00148	0.2	0.435	3.04	236.3	233.3	0.523	2.569	3.092
0	1	0.565	28	0.00148	0.2	0.435	0.43	237.7	236.3	0.049	0.400	0.449

**HAC Conditions - PNL Fuel**

From Rod Layer	To Rod Layer	Inch Rod Dia.	Inch Rod Length	Btu/hr-in-F Air k @ 600F	Rod emiss	Watt Rod Power	Watt Total Power	F Inner Rod T	F Outer Rod T	Watt Qrad	Watt Qconv	Watt Qtotal
4	5	0.565	28	0.00216	0.2	0.435	26.52	618.3	613.7	9.658	17.195	26.853
3	4	0.565	28	0.00216	0.2	0.435	16.09	621.9	618.3	5.911	10.466	16.377
2	3	0.565	28	0.00216	0.2	0.435	8.26	624.5	621.9	3.030	5.399	8.430
1	2	0.565	28	0.00216	0.2	0.435	3.04	626.1	624.5	1.063	1.994	3.056
0	1	0.565	28	0.00216	0.2	0.435	0.43	626.9	626.1	0.107	0.332	0.439

**Temperature Legend**

- user input temperature
- temperature linked to other cells on spreadsheet
- temperature obtained from AFS-to-FCS worksheet

C3.6.1-2

## C4.0 CONTAINMENT

The AFS-C does not provide containment. Therefore, package containment is unchanged from the description provided in Chapter 4.0, *Containment*.

This page left intentionally blank.

## C5.0 SHIELDING EVALUATION

The compliance of the MFFP with respect to the dose rate limits established by 10 CFR §71.47<sup>1</sup> for normal conditions of transport (NCT) or 10 CFR §71.51(a)(2) for hypothetical accident conditions (HAC) are satisfied when limiting the MFFP package to three (3) AFS-C rod containers, each containing up to 116 Exxon rods and 69 PNL rods having an average radioisotope content listed in Table C1.2-2.

Under these conditions, the maximum surface dose rate will be less than the limit of 200 mrem/hr for NCT and verified by measurement. This dose rate limit is for payload packages prior to addition of any lead, steel or other shielding material for *as-low-as-reasonably-achievable* (ALARA) dose reduction purposes during non-transport handling operations.

Prior to transport, the MFFP package shall be monitored for both gamma and neutron radiation to demonstrate compliance with 10 CFR §71.47. As noted in Section 2.6.7, *Free Drop*, the MFFP package is not significantly deformed under NCT free drop conditions. Therefore, the package will meet the dose rate limits for NCT if the measurements demonstrate compliance with the allowable dose rate levels in 10 CFR §71.47 (200 mrem/hr). The transport index, as defined in 10 CFR §71.4, will be determined by measuring the dose rate a distance of one meter from the package surface per the requirements of 49 CFR §173.403<sup>2</sup>.

Shielding materials are not specifically provided by the MFFP package, and none are permitted within the package to meet the dose rate limits of 10 CFR §71.47 for NCT. Because significant fuel deformation or package deformation does not occur under HAC, the HAC surface dose rates and 1-meter dose rates will not be significantly different from the NCT dose rates. This result ensures that the post-HAC, allowable dose rate of 1 rem/hr a distance of one meter from the package surface per 10 CFR §71.51(a)(2) will be met because the surface dose rate will remain below the 200 mrem/hr limit.

---

<sup>1</sup> Title 10, Code of Federal Regulations, Part 71 (10 CFR 71), *Packaging and Transportation of Radioactive Material*, 01-01-06 Edition.

<sup>2</sup> Title 49, Code of Federal Regulations, Part 173 (49 CFR 173), *Shippers - General Requirements for Shipments and Packagings*, 10-01-06 Edition.

This page left intentionally blank.

## C6.0 CRITICALITY EVALUATION

The following analyses demonstrate that the MFFP complies with the requirements of 10 CFR §71.55<sup>1</sup> and §71.59. The analyses presented herein demonstrate that the criticality requirements are satisfied when three AFS-C rod containers, each containing up to 116 Exxon rods and up to 69 PNL rods, are transported in an MFFP.

### C6.1 Description of Criticality Design

#### C6.1.1 Design Features Important for Criticality

The AFS-C is conservatively ignored in this criticality analysis. However, as noted in Section C2.0, *Structural Evaluation*, the AFS-C sufficiently protects the fuel rods so that rod breach damage to the fuel rods will not occur. Therefore, there are no specific design features of the AFS-C important for criticality. The design features of the MFFP important to criticality are discussed in Section 6.1.1, *Design Features Important for Criticality*.

#### C6.1.2 Summary Table of Criticality Evaluation

The results of the criticality calculations are summarized in Table C6.1-1. The maximum calculated  $k_s$  (i.e.,  $k_{eff} + 2\sigma$ ) for each condition is compared to the upper subcritical limit (USL) of 0.9288. The maximum calculated  $k_s$  values are below the USL.

Note that the results in Table C6.1-1 are artificially high because no credit is taken for the AFS-C, allowing the fuel rods to arrange in the most reactive pitch. In actuality, if the analysis were repeated taking credit for the AFS-C, the reactivity would drop considerably because there is very little space available inside the AFS-C for moderation, as all available void space is filled with dunnage rods.

---

<sup>1</sup> Title 10, Code of Federal Regulations, Part 71 (10 CFR 71), *Packaging and Transportation of Radioactive Material*, 01-01-06 Edition.

**Table C6.1-1 – Summary of Criticality Analysis Results**

<b>Normal Conditions of Transport (NCT)</b>			
<b>Case</b>	<b>k<sub>eff</sub></b>	<b>σ</b>	<b>k<sub>s</sub></b>
Single Unit Maximum k <sub>s</sub>	0.2383	0.0006	0.2396
Infinite Array Maximum k <sub>s</sub>	0.4899	0.0005	0.4910
<b>Hypothetical Accident Conditions (HAC)</b>			
<b>Case</b>	<b>k<sub>eff</sub></b>	<b>σ</b>	<b>k<sub>s</sub></b>
Single Unit Maximum k <sub>s</sub>	0.8929	0.0010	0.8948
Infinite Array Maximum k <sub>s</sub>	0.8972	0.0010	0.8991
USL	0.9288		

**C6.1.3 Criticality Safety Index**

An infinite number of MFFPs are evaluated in a close-packed hexagonal array. Therefore, “N” is infinite, and in accordance with 10 CFR §71.59 the criticality safety index (CSI) is  $50/N = 0$ .

## C6.2 Fissile Material Contents

The contents are three AFS-C rod containers, each containing up to 116 Exxon rods and up to 69 PNL rods. Physical data for the two rod types are summarized in Table C6.2-1. Because MCNP utilizes metric inputs but the drawings are in English units, both English and metric values for dimensional information are provided in this table.

The Exxon rods are well characterized. However, known data for the PNL rods are limited to rod OD, rod length, average plutonium mass, and average plutonium isotopics. No records are available for a number of other PNL rod characteristics, such as pellet OD, active fuel height, and maximum plutonium mass. When a PNL rod characterization value is not known, parametric criticality runs are performed for a range of reasonable values (the parametric analysis is discussed in Section C6.4.1.2.2, *HAC Single Package: PNL Rods Only*). The "assumed" PNL values reported in Table C6.2-1 are consistent with the most reactive case of this parametric analysis and are considered bounding.

The payload cavity of an MFFP can accommodate one triangular strongback assembly containing up to three AFS-C rod containers. The number of rods that may fit within each AFS-C has been determined based on the AFS-C cavity cross sectional area of 3.4-in x 6.9-in and the outer diameter of the fuel rods (provided in Table C6.2-1). The AFS-C may fit 116 Exxon rods (4 layers of 15 rods and 4 layers of 14 rods) and 69 PNL rods (3 layers of 12 rods and 3 layers of 11 rods) in a tightly-packed arrangement. The AFS-C contains separate compartments for Exxon and PNL rods. If less than the maximum number of rods is placed in an AFS-C, the excess planar volume is filled with stainless steel or aluminum dunnage rods. Note that neither the AFS-C nor dunnage rods are required for criticality control, although the presence of these items protects the rods from cladding breach in an accident.

The average isotopic composition of each rod type as of 1980 is reported in Table C6.2-2. However, the isotopic composition varies within the rods of each type. The isotopic composition and plutonium mass is known for each of the Exxon rods, although similar information for the PNL rods is not available. The isotopics selected for analysis bound the known isotopics of the Exxon rods by maximizing Pu-241 wt. %, minimizing Pu-240 wt. %, and setting the balance wt. % to be Pu-239. This assumption is highly conservative because no credit is taken for the decay of Pu-241, which has undergone nearly two half-lives of decay since 1980. The average PNL isotopics are similar to the average Exxon isotopics, so it may be inferred that this isotopic set is also bounding for the PNL rods.

Cladding for both rod types is modeled as pure zirconium, and both rod types utilize natural uranium in the fuel matrix. To be consistent with the MOX fuel assembly analysis in Chapter 6.0, *Criticality Evaluation*, it is assumed that the effective pellet density for each rod type is 10.85 g/cm<sup>3</sup>. The 10.85 g/cm<sup>3</sup> density is very high and represents 100% theoretically dense MOX pellet material smeared over the pellet gaps and dish/chamfers.

The mass of Pu per rod drives the system reactivity and is modeled precisely, while the mass of natural uranium modeled in each fuel rod has a negligible effect on the reactivity and is selected to maintain an effective pellet density of 10.85 g/cm<sup>3</sup>. In most of the MCNP models, 60 g of Pu is modeled in the Exxon rods, and 40 g of Pu is modeled in the PNL rods. The maximum measured Pu mass in any Exxon rod is 60 g, while the 40 g Pu assumed for the PNL rods is chosen to



reasonably bound the average PNL value of 37.4 g Pu. After the criticality analysis was complete, it was decided to add additional conservatism by increasing the mass of Pu in each fuel rod. Rather than repeat the entire analysis, only the most reactive cases are run with 65 g Pu for the Exxon rods (a 5 g increase in Pu) and 42 g Pu in the PNL rods (a 2 g increase in Pu). For this reason, the data in Table C6.2-3 is presented for all the Pu masses utilized, and the columns marked "bounding" resulted in the highest reactivity.

Fuel pellet composition is input to MCNP as a weight percent for each isotope of interest. The Pu mass and effective pellet density ( $10.85 \text{ g/cm}^3$ ) are set as fixed quantities and uranium oxide is added as needed to obtain the desired density. Therefore, the mass of uranium is not conserved when comparing Exxon1 to Exxon2, or comparing PNL1, PNL2, PNL3, and PNL4, because conserving the mass of uranium would result in non-physical pellet densities. However, the bounding rod descriptions utilize maximum fissile masses, as shown in Table C6.2-3.

As the Exxon rods are well defined, only one set of dimensional inputs is required for this rod type. However, parametric studies are performed on the PNL rod active fuel length and pellet diameter because these quantities are not well defined, which causes the material specifications to vary in order to maintain the target Pu mass. All of the various PNL rod permutations are included in Table C6.2-3.

Note that the Pu/(Pu+U) values given in Table C6.2-3 are artificially selected to give the target density of  $10.85 \text{ g/cm}^3$  and will not correspond precisely to the true values. Therefore, these values should not be considered limits. This approach is different than the MOX fuel assembly analysis in Chapter 6.0, *Criticality Evaluation*, for which a maximum Pu/(Pu+U) = 6.0% is stipulated, but a maximum plutonium mass per assembly is not explicitly treated as a limit.

Two values are selected for the PNL rod active fuel length, 36" and 28". The 36" value represents almost no plenum, while the 28" value represents a plenum length comparable in size to the Exxon rod plenum length. Two different PNL pellet diameters are also investigated, 0.4856" and 0.5135". The smaller pellet diameter is computed assuming that the Exxon and PNL rods have the same cladding and gap thickness:  $0.4856" = 0.565" - (0.451" - 0.3716")$ . The larger pellet diameter is computed assuming that the MFFP and PNL rods have the same cladding and gap thickness:  $0.5135" = 0.565" - (0.374" - 0.3225")$ . The MOX fuel rod data (rod OD = 0.374" and pellet OD = 0.3225") are obtained from Table 6.2-2 and Table 6.2-3, respectively.

Table C6.2-1 – Fuel Rod Data

Parameter	Exxon		PNL	
	English Value	Metric Value	English Value	Metric Value
Cladding Material	Zircaloy-2		Zircaloy-2	
Overall Length	77.26 in	196.24 cm	36.6 in	92.96 cm
Active Fuel Length	70 in	177.8 cm	28 in (assumed)	71.12 cm (assumed)
Cladding OD	0.451 in	1.1455 cm	0.565 in	1.4351 cm
Cladding ID	0.381 in	0.9677 cm	0.520 in (assumed)	1.3208 cm (assumed)
Pellet OD	0.3716 in	0.9439 cm	0.5135 in (assumed)	1.3043 cm (assumed)
Effective Pellet Density	--	10.85 g/cm <sup>3</sup> (assumed)	--	10.85 g/cm <sup>3</sup> (assumed)
Pu mass (average)	--	58.3 g	--	37.4 g
Pu mass (maximum)	--	65 g (assumed)	--	42 g (assumed)

Table C6.2-2 – Fuel Rod Isotopics

Isotope	Exxon wt. % (1980 average)	PNL wt. % (1980 average)	MCNP wt. %
U-235	0.71	0.71	0.71
U-238	99.29	99.29	99.29
Total U	100	100	100
Pu-238	0.745	0.28	0
Pu-239	75.13	75.38	79.5
Pu-240	17.26	18.10	14
Pu-241	5.23	5.08	6.5
Pu-242	1.55	1.15	0
Total Pu	100	100	100

**Table C6.2-3 – MCNP Fuel Rod Compositions Utilized**

Isotope	Exxon1	Exxon2 (bounding)	PNL1	PNL2	PNL3	PNL4 (bounding)
Density (g/cm <sup>3</sup> )	10.85	10.85	10.85	10.85	10.85	10.85
Active Fuel Height (in)	70	70	36	28	28	28
Pellet OD (in)	0.3716	0.3716	0.4856	0.4856	0.5135	0.5135
Pu mass (g)	60	65	40	40	40	42
Pu/(Pu+U)	5.041%	5.462%	3.829%	4.920%	4.400%	4.620%
U-235	0.594%	0.592%	0.602%	0.595%	0.598%	0.597%
U-238	83.115%	82.746%	84.175%	83.220%	83.675%	83.483%
Pu-239	3.533%	3.828%	2.683%	3.448%	3.084%	3.238%
Pu-240	0.622%	0.674%	0.473%	0.607%	0.543%	0.570%
Pu-241	0.289%	0.313%	0.219%	0.282%	0.252%	0.265%
O	11.847%	11.847%	11.848%	11.847%	11.848%	11.848%
Total	100%	100%	100%	100%	100%	100%
U-235 (g)	8.0	8.0	7.1	5.5	6.2	6.2
U-238 (g)	1121.9	1116.9	997.8	767.3	862.7	860.7
Pu-239 (g)	47.7	51.7	31.8	31.8	31.8	33.4
Pu-240 (g)	8.4	9.1	5.6	5.6	5.6	5.9
Pu-241 (g)	3.9	4.2	2.6	2.6	2.6	2.7
O (g)	159.9	159.9	140.5	109.2	122.2	122.1
Fissile (U235+Pu239+ Pu241) (g)	59.6	63.9	41.5	39.9	40.6	42.3

Note: The Pu/(Pu+U) values are not limiting values.

## C6.3 General Considerations

Criticality calculations for the MFFP are performed using the three-dimensional Monte Carlo computer code MCNP5<sup>1</sup>.

### C6.3.1 Model Configuration

#### C6.3.1.1 Contents Model

The AFS-C and dunnage rods are not modeled in the criticality evaluation. Because the AFS-C is not modeled, the fuel rods are assumed to arrange themselves in the most reactive configuration within the cavity formed between the strongback and FCS. Models are developed for three scenarios: (1) only Exxon rods, (2) only PNL rods, and (3) with both rod types combined. To maintain model symmetry, a variety of regular square arrangements are modeled for the Exxon rods, including 11x11, 10x10, 9x9, and 8x8. For the PNL rods, 9x9, 8x8, and 7x7 arrangements are considered. (Note that the Exxon 11x11 arrangement (121 rods) is not physically possible due to the 116 rod limit of the AFS-C cavity, and the PNL 9x9 arrangement (81 rods) is not possible due to the 69 rod limit of the AFS-C cavity.) A limited number of non-regular pitch cases are also developed.

Stainless steel or aluminum dunnage rods are used in the AFS-C to prevent lateral movement of the fuel rods. These dunnage rods are ignored in the criticality models.

The rod arrangements of the contents represents an extremely conservative and incredible arrangement, as the AFS-C, even if damaged in an accident, would displace a large volume and would not allow the rod arrangements assumed in this analysis.

#### C6.3.1.2 Packaging Model

The packaging model is unchanged from the description provided in Section 6.3.1.2, *Packaging Model*.

### C6.3.2 Material Properties

The material properties are unchanged from the descriptions provided in Section 6.3.2, *Material Properties*.

### C6.3.3 Computer Codes and Cross-Section Libraries

The computer codes and cross section libraries are unchanged from the descriptions provided in Section 6.3.3, *Computer Codes and Cross-Section Libraries*.

---

<sup>1</sup> MCNP5, "MCNP – A General Monte Carlo N-Particle Transport Code, Version 5; Volume II: User's Guide," LA-CP-03-0245, Los Alamos National Laboratory, April, 2003.

### C6.3.4 Demonstration of Maximum Reactivity

Reactivity of the NCT cases is negligible. The most reactive single package model is for the HAC Case G13 (see Table C6.4-7). The parameters of the most reactive single package model are:

- 11x11 array of Exxon rods (lower layer) and 9x9 array of PNL rods (upper layer) in each AFS-C.
- 65 g Pu per Exxon rod, and 42 g Pu per PNL rod.
- Fully moderated with water, including the pellet to cladding gap.
- Steel reflection, which bounds reflection by water.
- Miscellaneous minor steel components in the package are homogenized into the water region inside the package.

The most reactive HAC array model (Case J12, see Table C6.6-1) uses the most reactive HAC single package model as a base case. Properties of the most reactive HAC array model are:

- Infinite hexagonal reflection.
- Low density ( $0.1 \text{ g/cm}^3$ ) water between packages (note that this result is statistically equivalent to modeling void between packages).

## C6.4 Single Package Evaluation

Compliance with the requirements of 10 CFR §71.55 is demonstrated by analyzing an optimally moderated single-unit MFFP. The figures and descriptions provided in Section 6.3.1, *Model Configuration*, describe the basic geometry of the single-unit models, although the contents are different.

### C6.4.1 Single Package Configuration

#### C6.4.1.1 NCT Configuration

Under NCT conditions, the internals of the package are assumed to be dry. In the absence of internal moderation, reactivity will be a maximum for the maximum fuel mass. It has been established that the AFS-C will not contain more than 116 Exxon rods and 69 PNL rods. The total number of rods is conservatively bounded by assuming an 11x11 array of Exxon rods and a 9x9 array of PNL rods within each AFS-C.

In conjunction with the HAC single package models, parametric runs are performed on the PNL rods to determine the optimum values for the active fuel height, pellet OD, and cladding ID. The results of this analysis are used in the NCT models. For a discussion of the method used to determine the geometry of the PNL rod, see Section C6.4.1.2.2, *HAC Single Package: PNL Rods Only*.

For Cases A1 through A3, the fuel rods are modeled with the Exxon rods in a lower region and the PNL rods stacked on top of the Exxon rods in an upper region. (The internal geometry arrangement is the same as the HAC single package Case G1.) This configuration is run with three different reflector materials: water, steel, and lead. The results in Table C6.4-1 indicate that lead is the most reactive reflector for a dry system. In Case A4, the lead reflected case is further modified to place all of the fuel rods in a single 13x13 array, which is an axially tighter configuration. (The internal geometry arrangement is the same as the HAC single package Case G5.) Because internal moderation is not an issue for the NCT cases, this more axially compact arrangement is more reactive.

In Cases A1 through A4, the Exxon rods are modeled with 60 g Pu, and the PNL rods are modeled with 40 g Pu. To add conservatism, the most reactive case from above (Case A4) is rerun with 65 g Pu in the Exxon rods and 42 g Pu in the PNL rods (Case A5). Case A5 is the most reactive case, with  $k_s = 0.23958$ . This value is far below the USL of 0.9288.

#### C6.4.1.2 HAC Configuration

For the HAC single package analysis, water is present inside the package and the fuel rods are assumed to be arranged in the most reactive configuration. Consistent with the most reactive models from Section 6.4, *Single Package Evaluation*, all base cases are modeled with a steel reflector and steel hardware is homogenized into the water surrounding the FCS cavities (note that moderating water within the FCS cavities does not contain homogenized steel). The most reactive case is also run with a water reflector to confirm that the steel reflector is bounding.

The analysis is performed in three steps. First, only Exxon rods are present in the package. Second, only PNL rods are present in the package. Third, both types of rods are present in the package simultaneously.

#### C6.4.1.2.1 HAC Single Package: Exxon Rods Only

Each AFS-C is assumed to contain up to 121 Exxon rods but no PNL rods. As the AFS-C cannot contain more than 116 Exxon rods, this scenario represents an excess of 5 rods. 121 rods have been selected both to bound the total mass of Pu and to simplify model preparation, as 121 rods may be arranged in an 11x11 square lattice to fill the cavity formed by the strongback and FCS. No credit is taken for geometric control provided by the AFS-C for criticality purposes, although the geometric constraint provided by the AFS-C limits the maximum number of Exxon rods to 116.

The most reactive Exxon rod pitch is first determined by simply modeling an arbitrary number of Exxon rods (11x11) in a square array reflected by water. Only one cluster of rods is modeled, and the packaging is not modeled, as shown in Figure C6.4-1. In the absence of neutron poison, the reactivity is high. The pitch is varied and the array is free to expand until the maximum reactivity is obtained. The results in Table C6.4-2 indicate that the most reactive rod pitch is 2.6 cm (Case B4). As the inner dimension of the strongback/FCS cavity is 8.8", the number of rods that will fit at the optimum pitch is approximately  $[(8.8)(2.54)/2.6]^2 \sim 74$ .

Because the optimum pitch results in a reduced number of rods that may fit in the cavity, there is a reactivity tradeoff between the pitch and the fissile mass, because these quantities cannot be optimized simultaneously. If all rods are modeled at the optimum pitch, only ~74 rods will fit rather than the maximum of 121. Conversely, if 121 rods are modeled, the pitch will be below the optimum value and the system will be undermoderated. If a non-regular pitch is assumed, the optimum pitch may be maintained throughout a portion of the cavity while rods are allowed to cluster along the edges of the cavity. The criticality analysis considers all of these scenarios.

Because the AFS-C is not modeled, sufficient axial clearance is present in the model to allow double stacking of the Exxon rods. This fact is advantageous for modeling purposes because it is not necessary to omit any rods from the model as the pitch is expanded. A double stacking arrangement is assumed where a lower group rests on the bottom of the MFFP, and an upper group is stacked above the lower group. Therefore, as the pitch expands, the rods that no longer fit in the lower group are shifted to the upper group.

Initially, all 121 rods (11x11) are modeled in the lower group and the upper group is filled with water. When 100 rods are modeled in the lower group (10x10), the excess 21 rods are moved to the upper group. This pattern is continued until there are 64 rods in the bottom group and 57 rods in the upper group. The top group is always modeled at the optimum pitch of 2.6 cm. The axial stacking arrangement is shown in Figure C6.4-2 for Case C2. The planar views for this case are shown in Figure C6.4-3 for both the lower and upper groups.

Results are provided in Table C6.4-3 for a number of rod arrangements. Among the cases with a regular pitch for all rods (Cases C1 through C9), Case C1 (121 lower rods and no upper rods) is the most reactive. Although the rod arrangement is undermoderated, this arrangement is more reactive than cases where rods are split between the lower and upper groups.

The relative worth of the shifted rods is also investigated. Comparing Cases C3 and C4 (9x9 lower), the reactivity is statistically unchanged when the 40 upper rods are replaced with water, indicating that the reactivity contribution of the 40 rods in the upper group is negligible. A similar conclusion may be obtained when comparing Cases C5 and C6 (8x8 lower).

The optimum pitch of 2.6 cm may be confirmed by comparing Cases C5 and C7. In Case C7, the lower 8x8 array is fully expanded to the maximum extent (3.0294 cm), while in Case C5 the pitch of the lower array is fixed at 2.6 cm, leaving a gap of water around the 8x8 array, see Figure C6.4-4. The reactivity for the optimum pitch case is significantly higher than the reactivity for the overmoderated case. It is also interesting to note that when Case C7 is run with no lower rods (Case C8) and no upper rods (Case C9), it becomes apparent that the reactivity for Case C7 is dominated by the upper and not the lower rods. Therefore, for all cases examined, reactivity is dominated by either the lower or upper group of rods, and it does not appear that neutronic interaction between these groups plays a significant role in the reactivity.

In Cases C1 through C9, the lattice is assumed to be regular, and the most reactive case has 121 rods in the lower group. In cases C20 through C29, non-regular lattices are investigated. For Cases C20 through C23 (shown in Figure C6.4-5), the pitch is maintained at near optimum (9x9 lattice from Case C3) while extra rods are placed into the regions around the edges. For Cases C24 through C27 (shown in Figure C6.4-6), a tighter 10x10 lattice is used, which is more reactive. All cases are bounded by the regular lattice Case C1, although Cases C1 and C27 are statistically equivalent. The maximum  $k_s = 0.88627$  is achieved for Case C1, which is below the USL of 0.9288.

#### **C6.4.1.2.2 HAC Single Package: PNL Rods Only**

The basic analysis methodology utilized on the Exxon rods is repeated for the PNL rods. However, initial parametric runs are needed because, unlike the Exxon rods, the PNL rods are not as well characterized. Three key pieces of information that are not known are the active fuel height, the cladding ID, and the pellet OD. The approach is to vary each of these parameters within a range of reasonable values to determine the most reactive condition. This fuel rod description is then used in the remainder of the models.

The overall length of a PNL fuel rod is 36". Therefore, it is assumed that the active fuel length may vary between the ranges of 36" to 28". For the parametric models in which the active fuel height is investigated (Cases D1 and D2), the cladding thickness (0.035") and pellet-to-cladding gap (0.0047") are assumed to be the same as the Exxon rods. These dimensions may be used to compute the pellet OD and cladding ID based upon the known rod OD. The rods are modeled in a 9x9 array reflected by water (similar to the Exxon array shown in Figure C6.4-1) with a fixed pitch of 3.2 cm. Because the internal rod geometry is not well characterized, minor details such as end caps are neglected and the rods are simply modeled as pellets and cladding.

Results are provided in Table C6.4-4. In Case D1, the active fuel height is 36", while for Case D2, the active fuel height is 28". The fuel pellet composition changes with active fuel height to maintain a constant pellet density of 10.85 g/cm<sup>3</sup> and Pu mass of 40 g, as discussed in Section C6.2. Because Case D2 is more reactive than Case D1, it is concluded that a shorter active fuel height is more reactive. Therefore, the remaining parametric cases are performed with an active fuel height of 28".



In Case D3, the pellet OD is the same as Case D2, while the cladding thickness is consistent with the standard MOX fuel assembly. The MOX fuel assembly cladding thickness is 0.0225", which results in a large pellet-to-cladding gap for this case. In Case D4, both the cladding thickness and pellet-to-cladding gap are consistent with the standard MOX fuel assembly. As the MFFP pellet-to-cladding gap is 0.00325", the PNL pellet OD must expand accordingly. Case D4 is the most reactive, although the effects of cladding thickness, pellet-to-cladding gap, and pellet OD do not have a strong influence on the reactivity. Consistent with Case D4, subsequent PNL rod models have an active fuel height of 28", a pellet OD of 0.5135", and a cladding ID of 0.5200".

An optimum PNL rod pitch study is performed similar to the optimum rod pitch study performed for the Exxon rods, although a 9x9 array is assumed because a lesser number of PNL rods may fit in the AFS-C. The array geometry is similar to the Exxon model shown in Figure C6.4-1. The results provided in Table C6.4-5 indicate that maximum reactivity is reached at a pitch of 3.2 cm. Note that the optimum PNL rod pitch is larger than the optimum Exxon rod pitch of 2.6 cm.

The same technique utilized in the Exxon-only models is utilized in the PNL-only models. However, because the AFS-C cannot fit more than 69 PNL rods, a bounding 9x9 square array of rods is assumed, which represents an additional 12 rods. The rods are divided between lower and upper groups. As the pitch in the lower group increases, reducing the number of rods in the lower group, an equivalent number of rods is added to the upper group. The pitch for the upper group of rods is always set at the optimum value of 3.2 cm. For convenience, the z-position of the interface between the lower and upper groups is assumed to be at the same location as the Exxon rod models. This assumption will facilitate model preparation when the PNL and Exxon rods are combined (see Section C6.4.1.2.3, *HAC Single Package: Combined Exxon and PNL Rods*).

Results are provided in Table C6.4-6. The trends in the PNL results are the same as the Exxon results, although the system reactivity is lower. The most reactive condition (Case F1) occurs when all 81 rods are in the lower group. Rods that have been shifted to the upper group contribute little to the reactivity. The optimum moderation is reached when the bottom array is modeled with a 7x7 square lattice, which results in a pitch of 3.2 cm. However, in this scenario 32 rods have been shifted upward and the reactivity is significantly less than the case in which all 81 rods are in the lower group.

Because the most reactive configuration occurs when all the rods are in the lower group, in Cases F20 through F26 the lower rods are arranged in a non-regular pitch. In this manner, many of the rods may be moderated at or near the optimum value, although other rods must necessarily be undermoderated when these rods are clustered together. Various non-regular pitch models are developed, as shown in Figure C6.4-8 and Figure C6.4-9. As shown in Table C6.4-6, none of the non-regular pitch models are more reactive than the regular 9x9 pitch model. The maximum  $k_s = 0.85551$  is achieved for Case F1, which is below the USL of 0.9288.

#### **C6.4.1.2.3 HAC Single Package: Combined Exxon and PNL Rods**

In Sections C6.4.1.2.1 and C6.4.1.2.2, the Exxon and PNL rods are addressed separately. In actuality, the rods may be stacked in a basket that is placed in the AFS-C cavity. In the current section, the two rod types are combined within the AFS-C.

The most reactive Exxon-only model (Case C1) and the most reactive PNL-only model (Case F1) are combined into an AFS-C. It is assumed that the Exxon rods comprise the lower group and the

PNL rods comprise the upper group, as shown in Figure C6.4-10. Note that in the actual loaded arrangement, the rods are loaded into separate compartments that are separated by approximately 37-in, although this separation is not credited in the analysis. The results shown in Table C6.4-7 indicate that the reactivity does not increase appreciably when the rods are combined within an AFS-C because the most reactive group (the Exxon rods in this case) dominates. This result is consistent with the results of the previous sections, as the reactivity of the Exxon-only and PNL-only models do not change appreciably when the upper rods are replaced with water.

No credit is taken for axial separation provided by the AFS-C, so additional cases are developed in which the Exxon and PNL rods are mixed within the lower group. Because the PNL rods are short and could conceivably double-stack upon each other, the active fuel length of the PNL rods that slide into the lower region is doubled (56") to more closely match the active fuel length of the Exxon rods. The PNL rods in the upper region are modeled with the standard active fuel length of 28" and most reactive PNL pitch of 3.2 cm.

Both 12x12 and 13x13 array cases are run with most or all of the rods in the lower group. Three configurations are developed for the 12x12 models (Cases G2 through G4), as shown in Figure C6.4-11. For a 12x12 array, there are  $144 - 121 = 23$  locations available for PNL rods. As each location contains two PNL rods,  $81 - 2*23 = 35$  PNL rods remain in the upper region. The upper rods are modeled at the optimum PNL pitch of 3.2 cm.

Four configurations are developed for the 13x13 models (Cases G5 through G8), as shown in Figure C6.4-12. For a 13x13 array, there are  $169 - 121 = 48$  locations available for PNL rods, which exceeds the number of PNL rods available ( $48*2 = 96 > 81$ ). Therefore, 41 double-length PNL rods are modeled in the lower region, as well as 7 water holes. In Cases G5 through G7, 121 Exxon rods and 82 PNL rods are modeled, while in Case G8, 114 Exxon rods and 68 PNL rods are modeled, which are similar to the number of rods that could actually be transported within the AFS-C (i.e., 116 Exxon rods and 69 PNL rods). All cases are less reactive than Case G1, in which the two rod types are axially separated.

In Cases G9 through G12, the limiting case (G1) is modified to confirm some of the initial base assumptions taken from the standard fuel assembly analysis in Section 6.4, *Single Package Evaluation*. In Case G9, the steel reflector is replaced with a water reflector. The reactivity drops slightly, as expected. It is assumed that a lead reflector would be statistically equivalent to the steel reflector, consistent with Section 6.4. In Case G10, the internal water, which has been homogenized with steel components, is modeled as ordinary water. The reactivity drops slightly, consistent with the behavior in Section 6.4. In Cases G11 and G12, the internal water density is modeled at reduced values of  $0.95 \text{ g/cm}^3$  and  $0.90 \text{ g/cm}^3$ , respectively. Reactivity drops as the internal water density drops, as expected. Note that Cases G11 and G12 should be compared against Case G10, because the homogenized steel has been omitted from these cases for convenience.

When comparing the Exxon-only cases (Case C1 through C29), the PNL-only cases (Cases F1 through F26), and the combined cases (Cases G1 through G12), the maximum reactivity is achieved for Case G1. In this case, 121 Exxon rods are modeled in the lower group, and 81 PNL rods are modeled in the upper group. Note that the reactivity is statistically equivalent to Case C1, in which no PNL rods are present. Therefore, it may be concluded that the PNL rods have a minor impact on the reactivity.

In all of the previous HAC single package cases, the Exxon rods are modeled with 60 g Pu, and the PNL rods are modeled with 40 g Pu. To add conservatism, the most reactive case from above (Case G1) is rerun with 65 g Pu in the Exxon rods and 42 g Pu in the PNL rods (Case G13). Case G13 is the most reactive case, with  $k_s = 0.89475$ . This value is below the USL of 0.9288.

### C6.4.2 Single Package Results

The optimum pitch search results are provided in Table C6.4-2 and Table C6.4-5 for Exxon and PNL rods, respectively. (The multiplication factors are high because no poison plates are modeled.) The PNL rod parametric study results are provided in Table C6.4-4. The remaining tables present the single package results. The most reactive case in each table is listed in boldface.

**Table C6.4-1 – Criticality Results for NCT Single Package**

Case No.	Filename	Reflector	$k_{eff}$	$\sigma$	$k_s$ ( $k_{eff}+2\sigma$ )
A1	nsc_pb	Lead	0.16738	0.00050	0.16838
A2	nsc_st	Steel	0.16521	0.00047	0.16615
A3	nsc_h2o	Water	0.13931	0.00044	0.14019
A4	nsc_pb2	Lead	0.23030	0.00059	0.23148
<b>Case A5 is Case A4 with increased Pu mass in the fuel rods</b>					
A5	nsc_pb2h	Lead	<b>0.23834</b>	<b>0.00062</b>	<b>0.23958</b>

**Table C6.4-2 – Exxon Rod Optimum Pitch Study Results**

Case No.	Filename	Pitch (cm)	$k_{eff}$	$\sigma$	$k_s$ ( $k_{eff}+2\sigma$ )
B1	11x11_p1	2.0	0.94625	0.00099	0.94823
B2	11x11_p11	2.2	0.98556	0.00100	0.98756
B3	11x11_p12	2.4	1.00537	0.00099	1.00735
<b>B4</b>	<b>11x11_p13</b>	<b>2.6</b>	<b>1.01493</b>	<b>0.00104</b>	<b>1.01701</b>
B5	11x11_p14	2.8	1.00856	0.00100	1.01056
B6	11x11_p15	3.0	0.99715	0.00096	0.99907

Note: Scoping study; no poison plates.

**Table C6.4-3 – HAC Single Package, Exxon Rods Only**

Case No.	Filename	Bottom Pitch (cm)	Number in Lower Group	Number in Upper Group	$k_{eff}$	$\sigma$	$k_s$ ( $k_{eff}+2\sigma$ )
<b>Regular Lattice Cases</b>							
C1	hse_b11x11_t0	2.1208	121	0	0.88443	0.00092	0.88627
C2	hse_b10x10_t21	2.3562	100	21	0.86949	0.00097	0.87143
C3	hse_b9x9_t40	2.6508	81	40	0.83604	0.00095	0.83794
C4	hse_b9x9_t0	2.6508	81	0	0.83645	0.00096	0.83837
C5	hse_b8x8_t57	2.6	64	57	0.80936	0.00100	0.81136
C6	hse_b8x8_t0	2.6	64	0	0.80948	0.00102	0.81152
C7	hse_b8x8e_t57	3.0294	64	57	0.78095	0.00097	0.78289
C8	hse_b0_t57	NA	0	57	0.78316	0.00092	0.78500
C9	hse_b8x8e_t0	3.0294	64	0	0.77597	0.00094	0.77785
<b>Non-Regular Lattice Cases</b>							
C20	hse_b9x9_105_t16	2.6508	105	16	0.86236	0.00099	0.86434
C21	hse_b9x9_109_t12	2.6508	109	12	0.86090	0.00096	0.86282
C22	hse_b9x9_113_t8	2.4836	113	8	0.87403	0.00098	0.87599
C23	hse_b9x9_121	2.6508	121	0	0.86975	0.00095	0.87165
C24	hse_b9x9_121c2	2.6508	121	0	0.84431	0.00095	0.84621
C25	hse_b10x10_121	2.3562	121	0	0.87573	0.00101	0.87775
C26	hse_b10x10_121c2	2.3562	121	0	0.87247	0.00097	0.87441
C27	hse_b10x10_121c3	2.3562	121	0	0.88399	0.00099	0.88597
C28	hse_b10x10_121c4	2.3562	121	0	0.87952	0.00094	0.88140
C29	hse_b10x10_121c5	2.2354	121	0	0.88203	0.00095	0.88393

**Table C6.4-4 – PNL Rod Parametric Study Results**

Case No.	Filename	Active Fuel Height (in)	Pellet OD (in)	Cladding ID (in)	$k_{eff}$	$\sigma$	$k_s$ ( $k_{eff}+2\sigma$ )
D1	hsp_para1	36	0.4856	0.4950	0.95016	0.00092	0.95200
D2	hsp_para2	28	0.4856	0.4950	0.96743	0.00096	0.96935
D3	hsp_para3	28	0.4856	0.5200	0.96552	0.00100	0.96752
D4	hsp_para4	28	0.5135	0.5200	0.97171	0.00094	0.97359

**Table C6.4-5 – PNL Rod Optimum Pitch Study Results**

Case No.	Filename	Pitch (cm)	$k_{eff}$	$\sigma$	$k_s$ ( $k_{eff}+2\sigma$ )
E1	9x9_p14	2.8	0.95817	0.00102	0.96021
E2	9x9_p15	3.0	0.97067	0.00097	0.97261
<b>D4</b>	<b>hsp_para4</b>	<b>3.2</b>	<b>0.97171</b>	<b>0.00094</b>	<b>0.97359</b>
E3	9x9_p17	3.4	0.96626	0.00096	0.96818
E4	9x9_p18	3.6	0.95506	0.00102	0.95710

Note: Scoping study, no poison plates.

**Table C6.4-6 – HAC Single Package, PNL Rods Only**

Case No.	Filename	Bottom Pitch (cm)	Number in Lower Group	Number in Upper Group	$k_{eff}$	$\sigma$	$k_s$ ( $k_{eff}+2\sigma$ )
<b>Regular Lattice Cases</b>							
F1	hsp_b9x9_t0	2.6148	81	0	0.85357	0.00097	0.85551
F2	hsp_b8x8_t17	2.9880	64	17	0.83339	0.00098	0.83535
F3	hsp_b7x7e_t32	3.4862	49	32	0.78205	0.00099	0.78403
F4	hsp_b7x7_t32	3.2	49	32	0.80302	0.00096	0.80494
F5	hsp_b7x7_t0	3.2	49	0	0.79669	0.00099	0.79867
<b>Non-Regular Lattice Cases</b>							
F20	hsp_8x8_81	2.9880	81	0	0.84687	0.00096	0.84879
F21	hsp_8x8_81c2	2.9880	81	0	0.83939	0.00099	0.84137
F22	hsp_8x8_81c3	2.7960	81	0	0.84475	0.00095	0.84665
F23	hsp_8x8_81c4	2.7960	81	0	0.83525	0.00097	0.83719
F24	hsp_7x7_81	3.2	73	8	0.83204	0.00091	0.83386
F25	hsp_7x7_82	3.2	82	0	0.81319	0.00094	0.81507
F26	hsp_7x7_82c2	3.2	82	0	0.80830	0.00099	0.81028

Table C6.4-7 – HAC Single Package, Combined Exxon and PNL Rods

Case No.	Filename	Bottom Pitch (cm)	Number in Lower Group	Number in Upper Group	$k_{eff}$	$\sigma$	$k_s$ ( $k_{eff}+2\sigma$ )
G1	hsc_b11x11_t9x9	2.1208	121 Exxon	81 PNL	0.88605	0.00092	0.88789
G2	hsc_b12x12_t35	1.8632	121 Exxon 46 PNL	35 PNL	0.86705	0.00101	0.86907
G3	hsc_b12x12_t35c2	1.8632	121 Exxon 46 PNL	35 PNL	0.87047	0.00097	0.87241
G4	hsc_b12x12_t35c3	1.9278	121 Exxon 46 PNL	35 PNL	0.86880	0.00097	0.87074
G5	hsc_b13x13_t0	1.7198	121 Exxon 82 PNL	0	0.84800	0.00102	0.85004
G6	hsc_b13x13_t0c2	1.7198	121 Exxon 82 PNL	0	0.85788	0.00096	0.85980
G7	hsc_b13x13_t0c3	1.7672	121 Exxon 82 PNL	0	0.84519	0.00097	0.84713
G8	hsc_e114_p68	1.7672	114 Exxon 68 PNL	0	0.85344	0.00098	0.85540
G9	hsc_b11x11_t9x9_h2o	2.1208	121 Exxon	81 PNL	0.88261	0.00095	0.88451
G10	hsc_b11x11_t9x9_ih2o	2.1208	121 Exxon	81 PNL	0.88220	0.00097	0.88414
G11	hsc_b11x11_t9x9_w95	2.1208	121 Exxon	81 PNL	0.86114	0.00098	0.86310
G12	hsc_b11x11_t9x9_w90	2.1208	121 Exxon	81 PNL	0.83769	0.00094	0.83957
<b>Case G13 is Case G1 with increased Pu mass in the fuel rods</b>							
G13	hsc_b11x11_t9x9h	2.1208	121 Exxon	81 PNL	0.89285	0.00095	0.89475

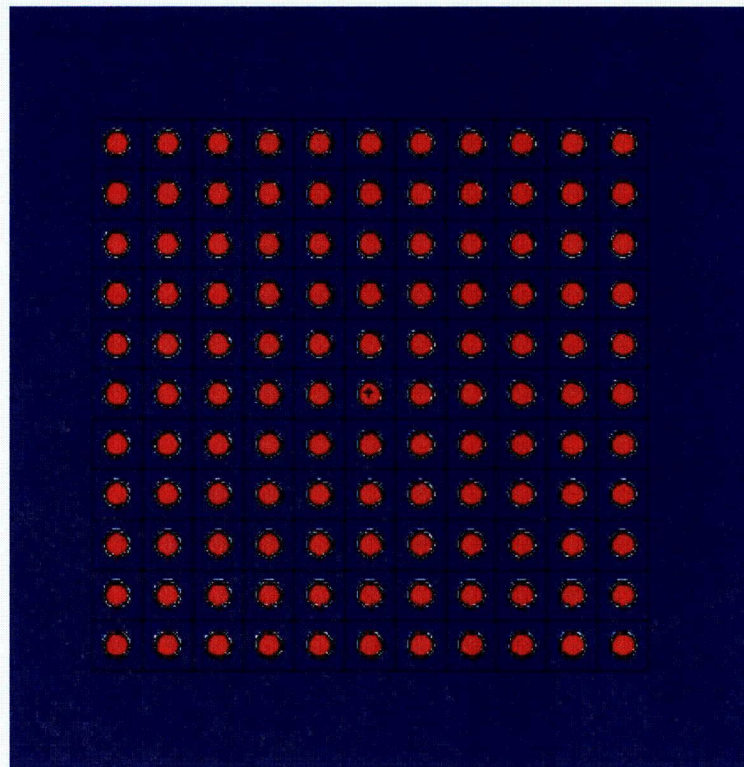


**Figure C6.4-1** – Exxon Rod Optimum Pitch Study (Cases B1 through B6)

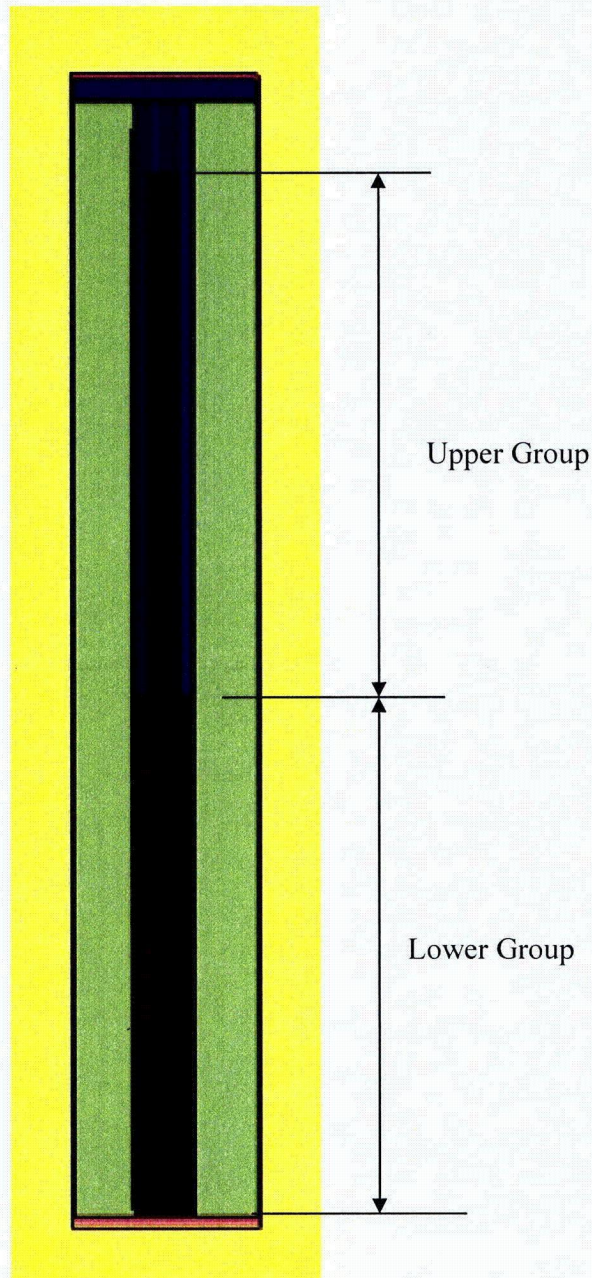


Figure C6.4-2 – Exxon Case C2 (side view)



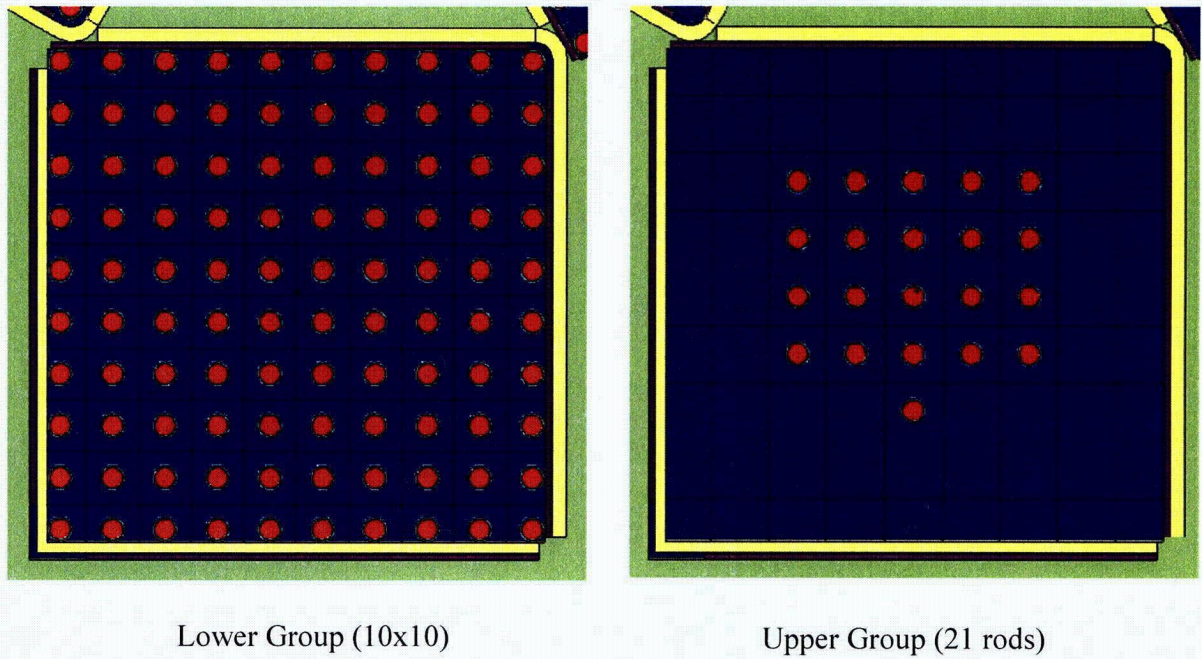


Figure C6.4-3 – Exxon Case C2 (planar view)

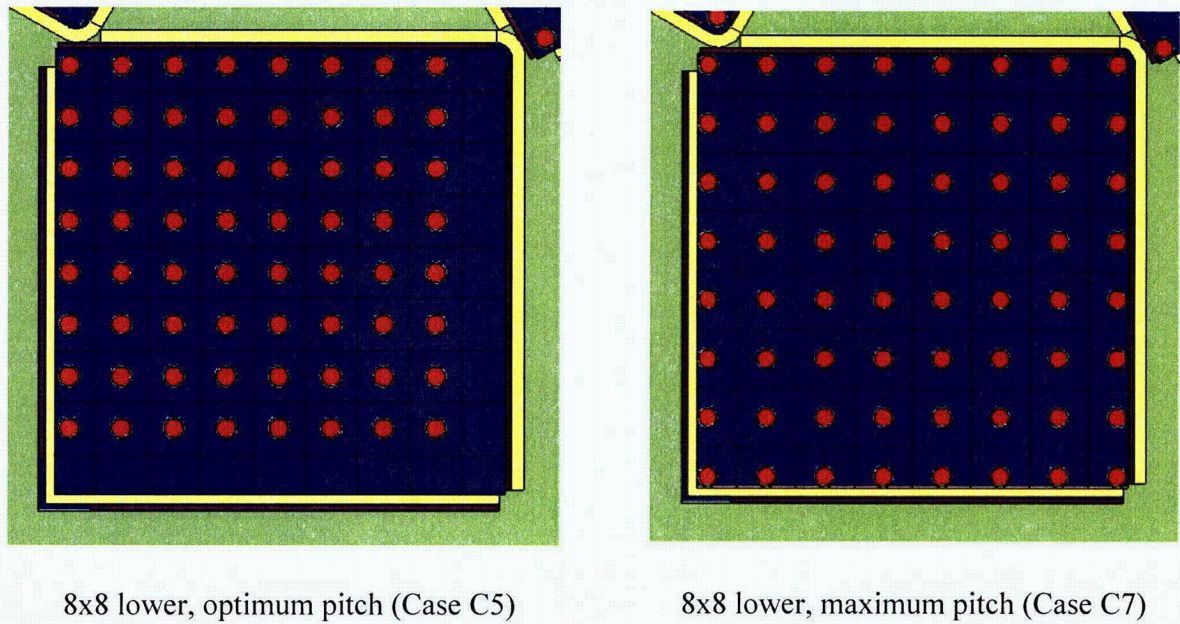
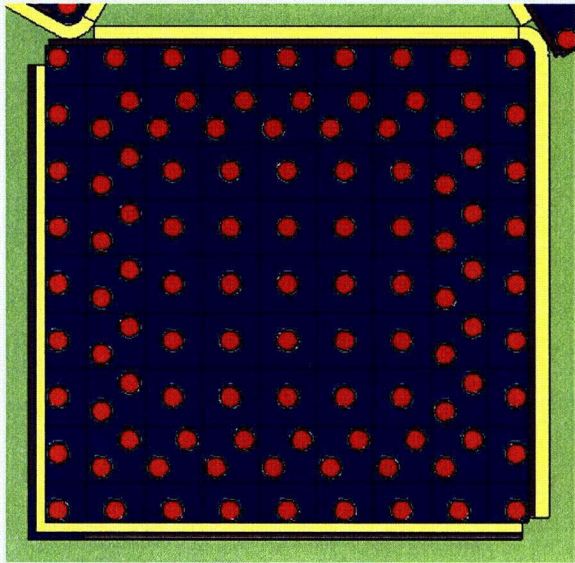
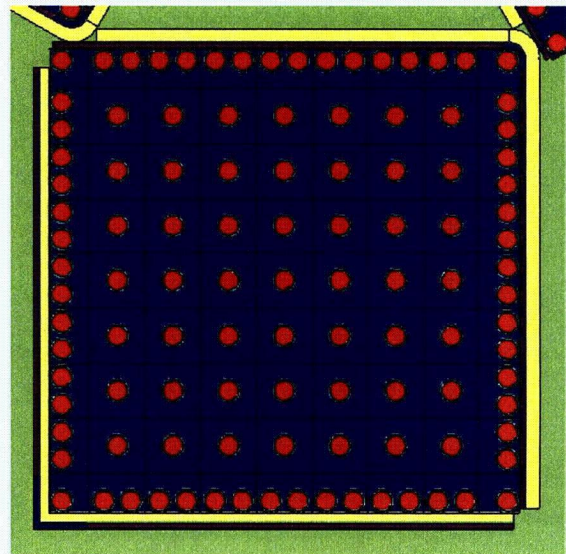


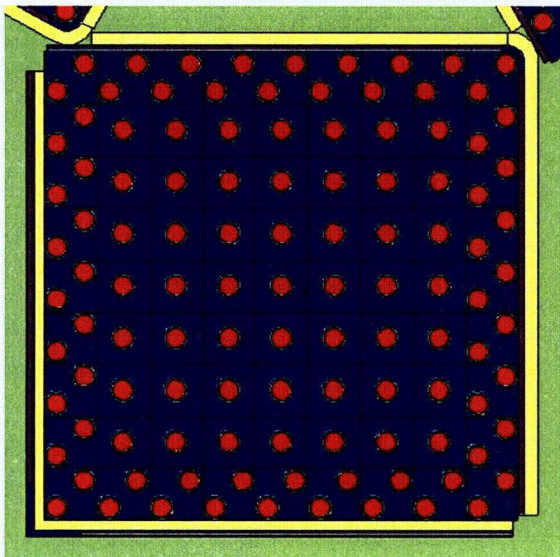
Figure C6.4-4 – Configurations for Exxon Cases C5 and C7



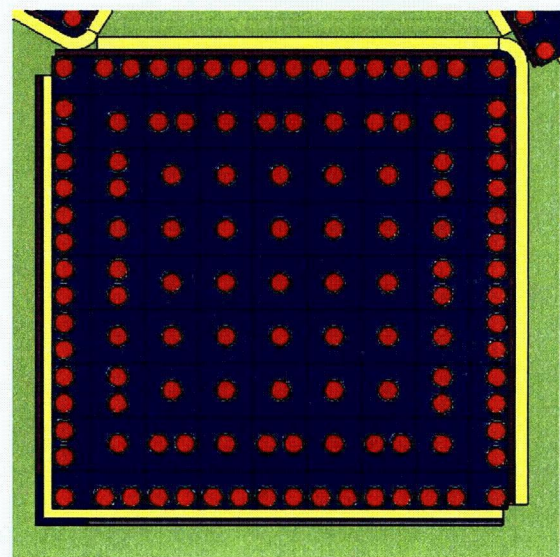
Case C20 (9x9, 105 lower, 16 upper)



Case C21 (9x9, 109 lower, 12 upper)

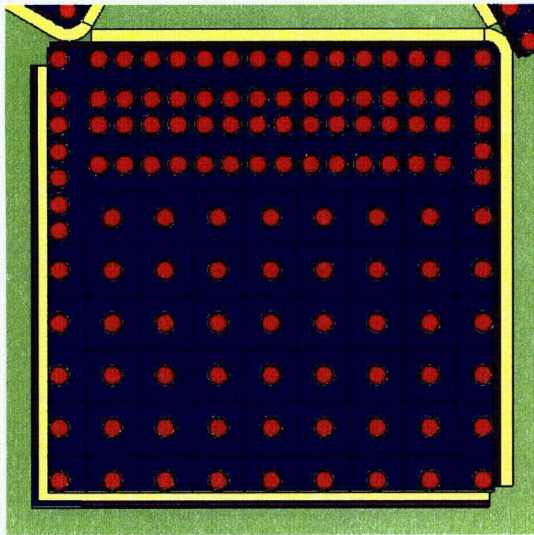


Case C22 (9x9, 113 lower, 8 upper)

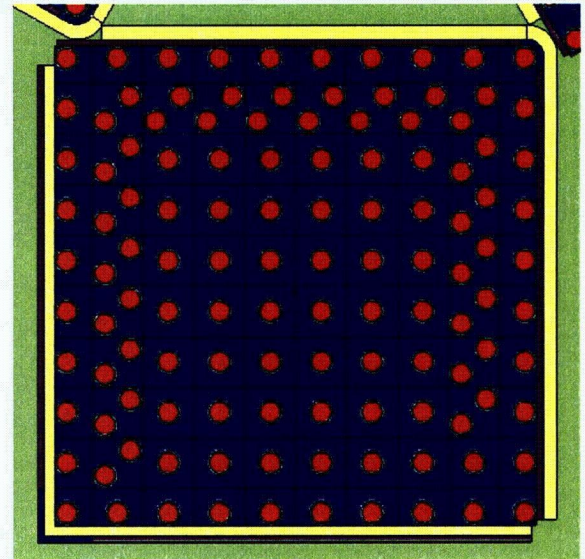


Case C23 (9x9, 121 lower, 0 upper)

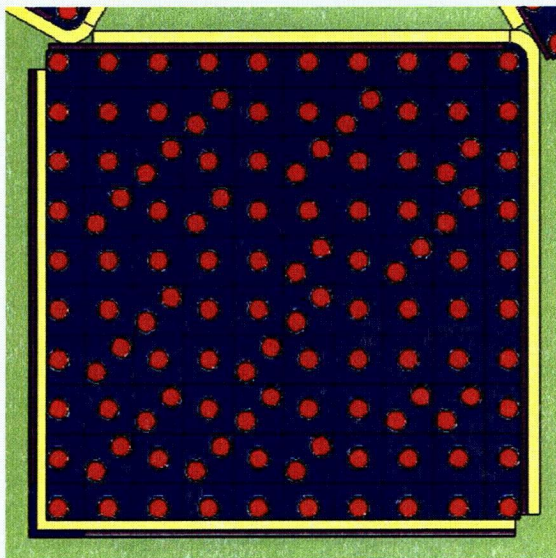
**Figure C6.4-5** – Non-Regular Configurations for Cases C20 through C23



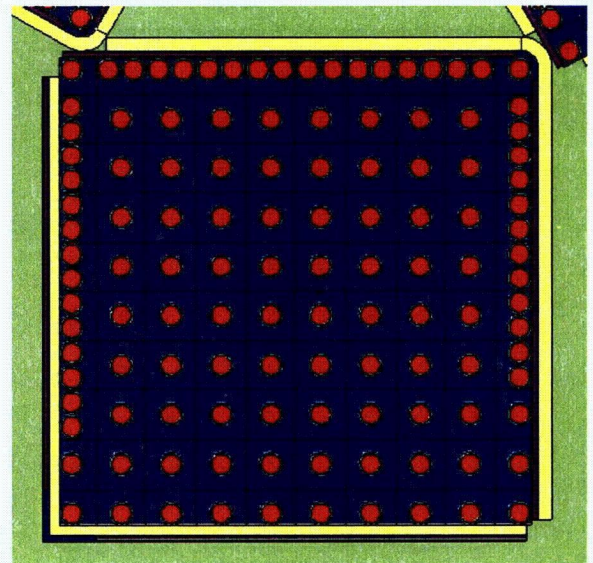
Case C24 (9x9, 121 lower, 0 upper)



Case C25 (10x10, 121 lower, 0 upper)

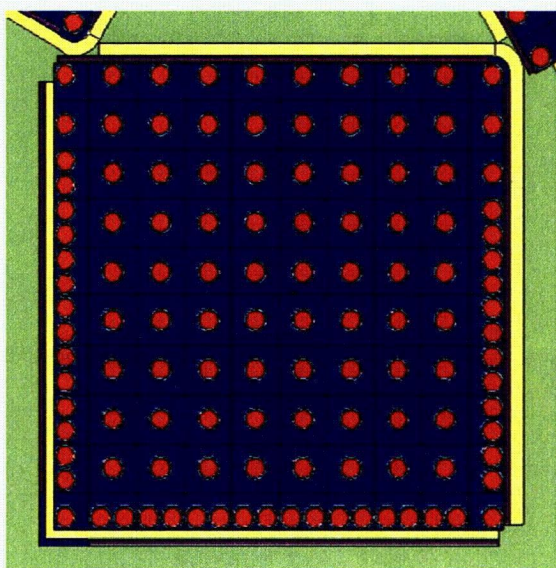


Case C26 (10x10, 121 lower, 0 upper)

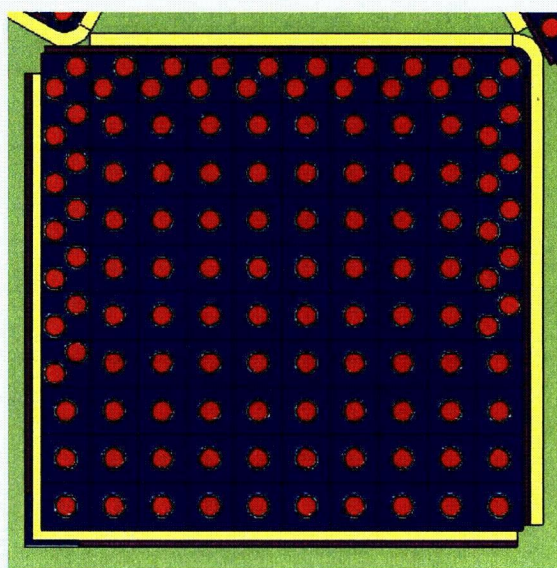


Case C27 (10x10, 121 lower, 0 upper)

**Figure C6.4-6** – Non-Regular Configurations for Cases C24 through C27

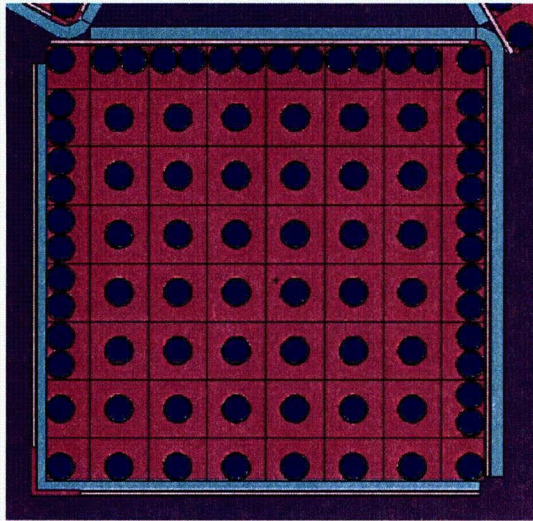


Case C28 (10x10, 121 lower, 0 upper)

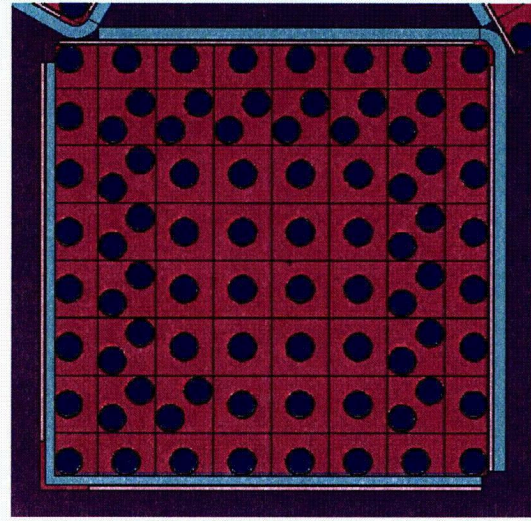


Case C29 (10x10, 121 lower, 0 upper)

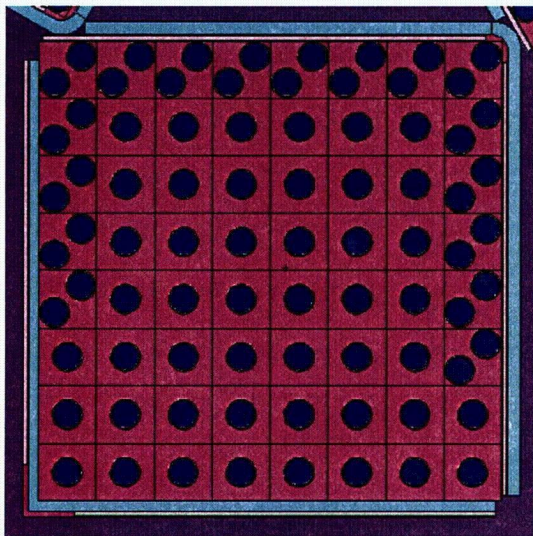
**Figure C6.4-7 – Non-Regular Configurations for Cases C28 and C29**



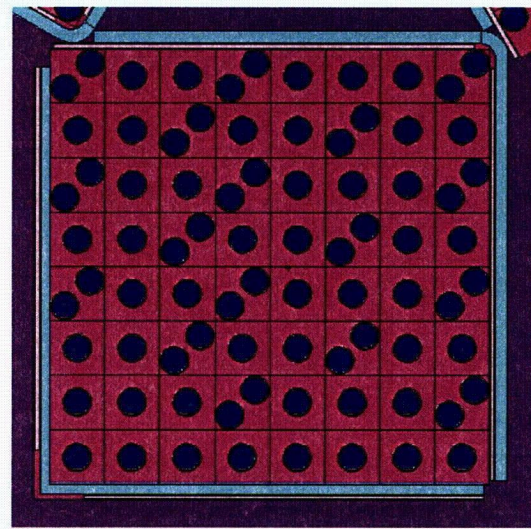
Case F20 (8x8, 81 lower, 0 upper)



Case F21 (8x8, 81 lower, 0 upper)

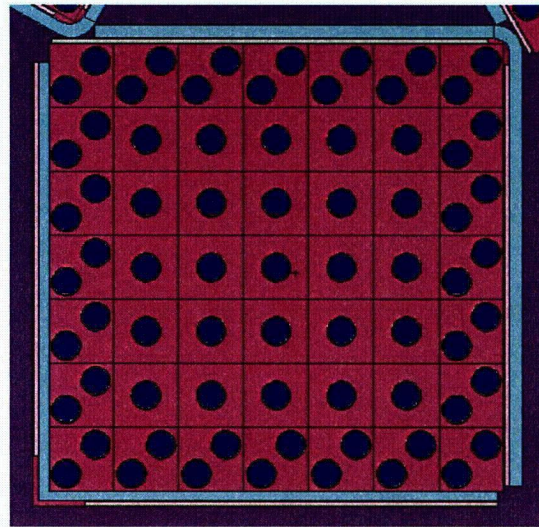


Case F22 (8x8, 81 lower, 0 upper)

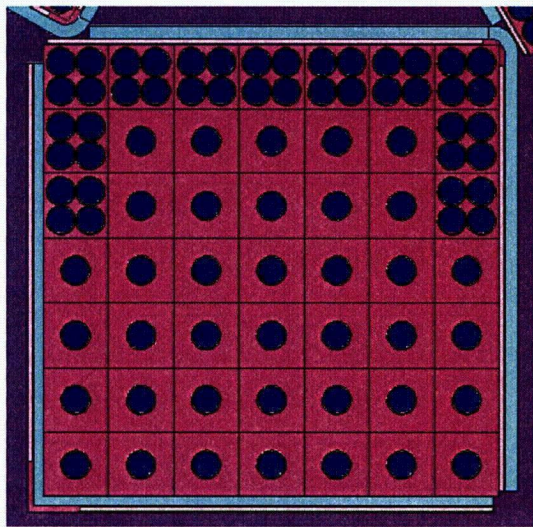


Case F23 (8x8, 81 lower, 0 upper)

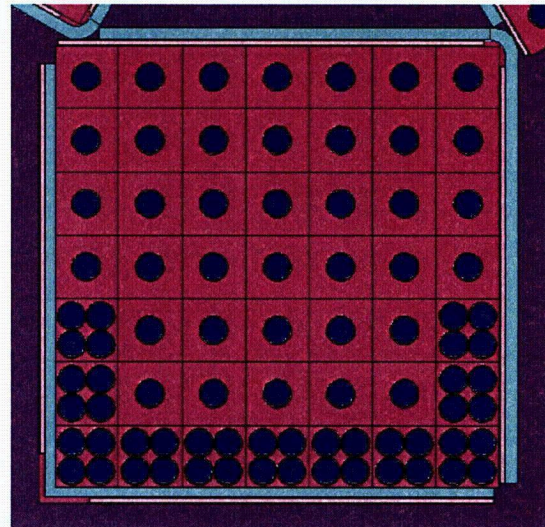
**Figure C6.4-8** – Non-Regular Configurations for Cases F20 through F23



Case F24 (7x7, 73 lower, 8 upper)



Case F25 (7x7, 82 lower, 0 upper)



Case F26 (7x7, 82 lower, 0 upper)

Figure C6.4-9 – Non-Regular Configurations for Cases F24 through F26

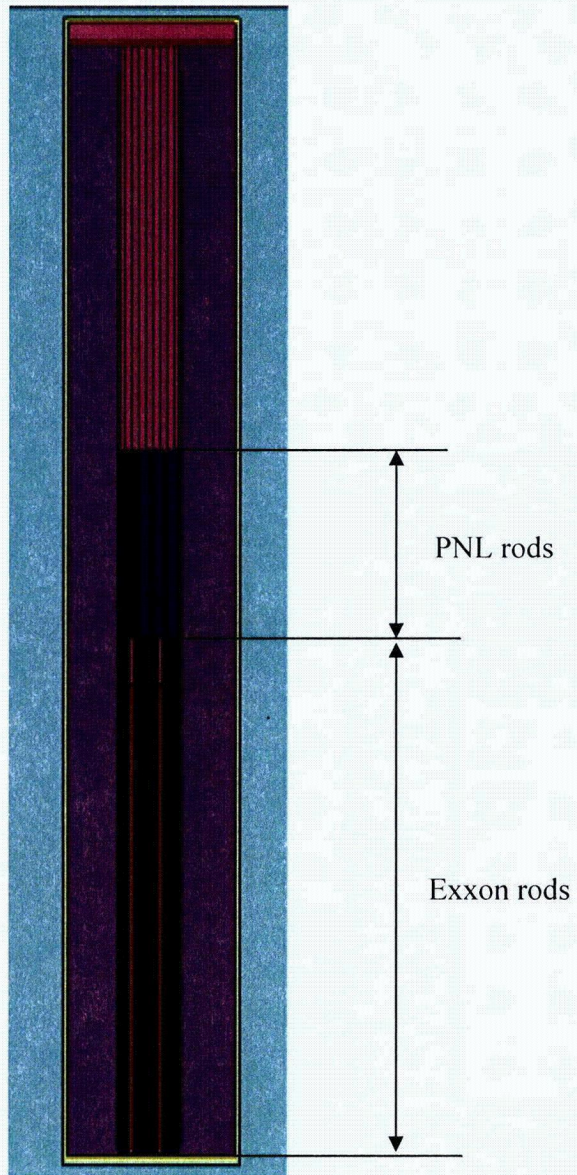
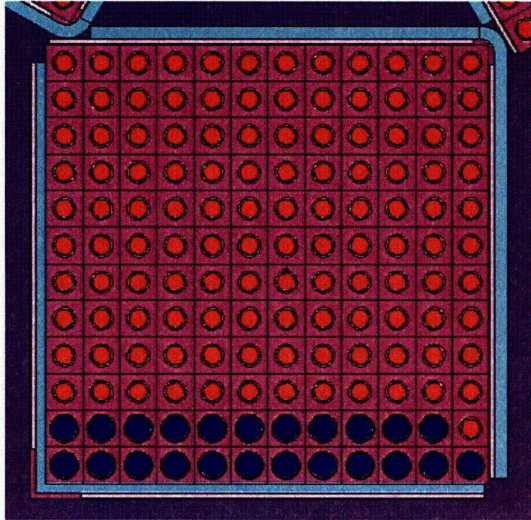
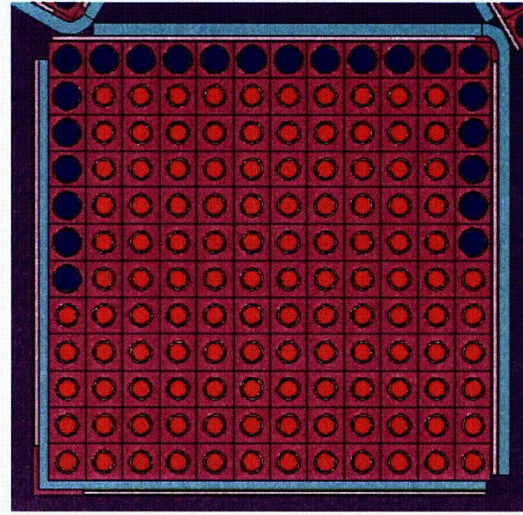


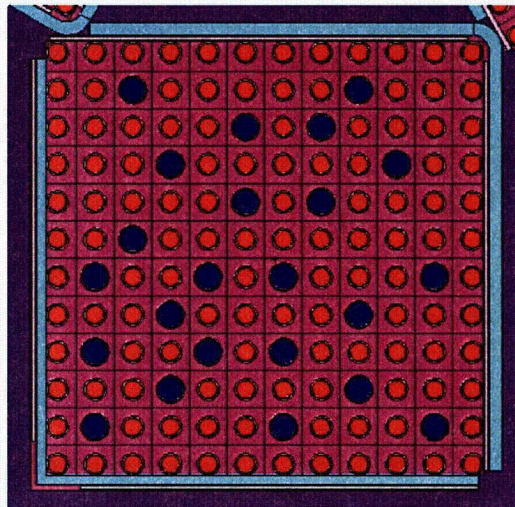
**Figure C6.4-10** – Combined Exxon and PNL Rod Cases



Case G2 (12x12, Configuration 1)



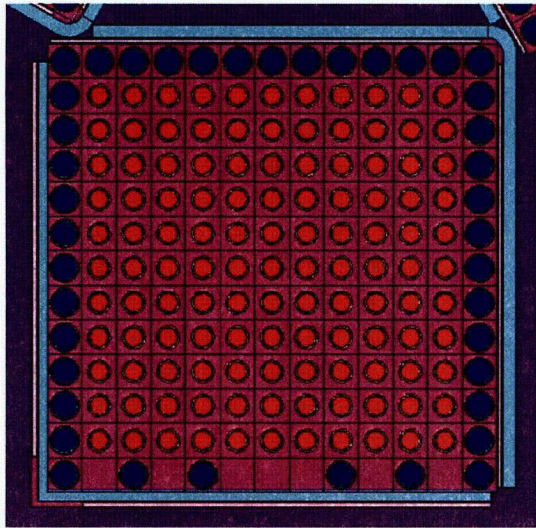
Case G3 (12x12, Configuration 2)



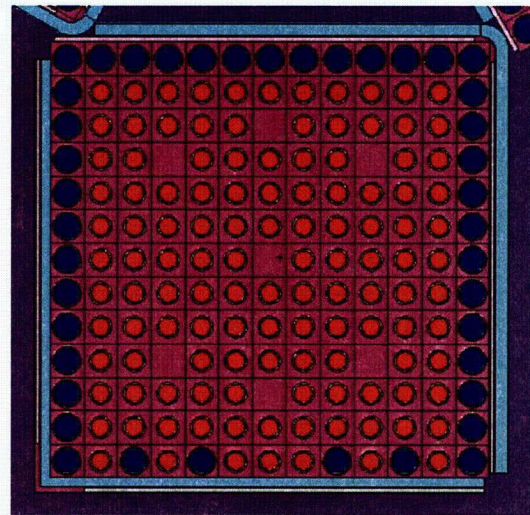
Case G4 (12x12, Configuration 3)

**Figure C6.4-11** – Configurations for Combined Rod Cases G2 through G4

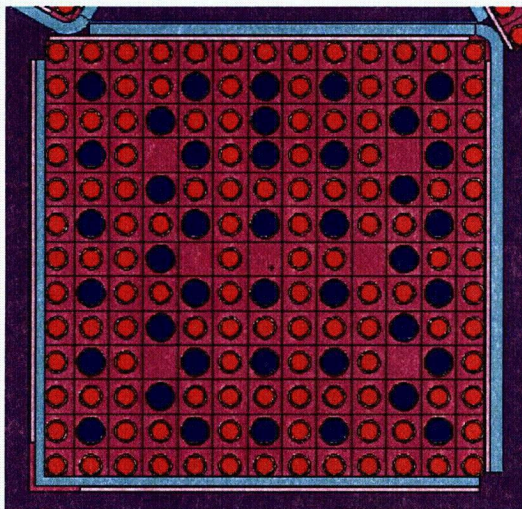




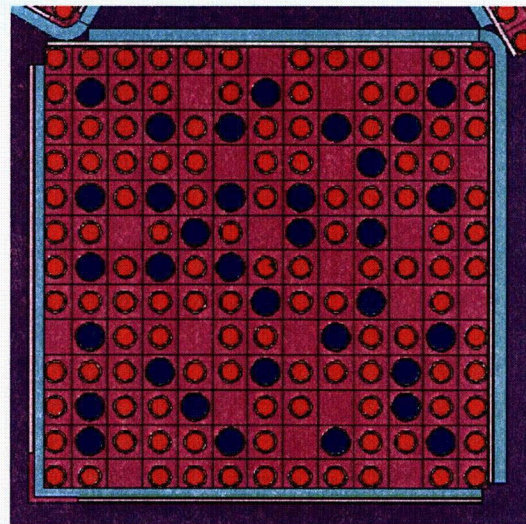
Case G5 (13x13, Configuration 1)



Case G6 (13x13, Configuration 2)



Case G7 (13x13, Configuration 3)



Case G8 (13x13, Configuration 4)

**Figure C6.4-12** – Configurations for Combined Rod Cases G5 through G8

## C6.5 Evaluation of Package Arrays Under Normal Conditions of Transport

### C6.5.1 NCT Array Configuration

An infinite close-packed hexagonal array is modeled for NCT conditions. No water is modeled inside of the package, although the water density is allowed to vary between packages. Based upon the analysis in Section 6.5, *Evaluation of Package Arrays Under Normal Conditions of Transport*, it is anticipated that the most reactive condition will be with no water between the packages.

Because the axial orientation of the Exxon and PNL rods will have an effect on the reactivity, cases are run in which the two rod types are both separate and combined. In both of these cases, void is modeled between packages. In Case H1, the rods are modeled in separate groups (like Case G1), while in Case H2, the rods are modeled in the same group (like Case G5). The results in Table C6.5-1 indicate that Case H2 is more reactive than Case H1.

Several additional cases are run with the internal configuration of Case H2 and variable water density between the packages. Only a limited number of cases are executed to confirm that reactivity is optimized with no water between the packages. As expected, the results in Table C6.5-1 confirm that adding water between the packages decreases reactivity.

In cases H1 through H5, the Exxon rods are modeled with 60 g Pu, and the PNL rods are modeled with 40 g Pu. To add conservatism, the most reactive case from above (Case H2) is rerun with 65 g Pu in the Exxon rods and 42 g Pu in the PNL rods (Case H6). Case H6 is the most reactive case, with  $k_s = 0.49095$ . This value is far below the USL of 0.9288.

### C6.5.2 NCT Array Results

The results for the NCT array cases are provided in Table C6.5-1. The most reactive configuration is listed in boldface.

**Table C6.5-1 – NCT Array Results**

Case No.	Filename	Water Density Between Packages (g/cm <sup>3</sup> )	$k_{eff}$	$\sigma$	$k_s$ ( $k_{eff}+2\sigma$ )
H1	nac_o0_long	0	0.41430	0.00048	0.41526
H2	nac_o0	0	0.47132	0.00051	0.47234
H3	nac_o05	0.05	0.46488	0.00061	0.46610
H4	nac_o10	0.1	0.44628	0.00058	0.44744
H5	nac_o100	1.0	0.29218	0.00054	0.29326
<b>Case H6 is Case H2 with increased Pu mass in the fuel rods</b>					
<b>H6</b>	<b>nac_o0h</b>	<b>0</b>	<b>0.48991</b>	<b>0.00052</b>	<b>0.49095</b>

This page left intentionally blank.

## C6.6 Package Arrays Under Hypothetical Accident Conditions

### C6.6.1 HAC Array Configuration

The HAC array configuration is similar to the NCT array configuration. Reflective surfaces are placed around the package to simulate a close-packed hexagonal array, see Figure C6.6-1. The top and bottom package surfaces are also set as reflective boundaries.

Cases are run for various combinations of internal and external moderator density. Case J1 is simply the most reactive single package model (Case G1) with reflective boundary conditions. Because there could be axial interaction effects between the package arrays, in Case J2 the PNL rods are shifted all the way to the top of the package, while the Exxon rods remain at the bottom of the package. The reactivity is statistically equivalent to Case J1 and the internal configuration of Case J1 is used for the remainder of the cases.

It is apparent from the analysis in Section 6.6, *Package Arrays Under Hypothetical Accident Conditions*, that the reactivity is somewhat insensitive to the water density between the packages under HAC. Because the package is very large and the contents are poisoned on all sides, the packages are largely isolated from one another and the infinite array results are very close to the single package results. This observation is confirmed in Cases J3 through J6, in which the external moderator density is varied between  $0.05 \text{ g/cm}^3$  and  $1.0 \text{ g/cm}^3$ . The reactivity of these cases are statistically equivalent, although the maximum reactivity occurs for case J4.

In Cases J7 through J11, the internal moderator density is reduced while the external moderator is modeled as void. For simplicity, the homogenized steel/water mixture internal to the package is modeled as water for these cases. Comparison of Cases J1 and J7 indicates that removing the homogenized steel has a negligible effect on the reactivity. As expected, reactivity drops quickly as the internal moderation is reduced, indicating that full water moderation is the most reactive condition.

In cases J1 through J11, the Exxon rods are modeled with 60 g Pu, and the PNL rods are modeled with 40 g Pu. To add conservatism, the most reactive case from above (Case J4) is rerun with 65 g Pu in the Exxon rods and 42 g Pu in the PNL rods (Case J12). Case J12 is the most reactive case, with  $k_s = 0.89913$ . This value is below the USL of 0.9288.

In Cases J13 through J15, the effect on the reactivity of replacing an AFS-C with a dummy fuel assembly is investigated. A dummy fuel assembly is a hollow stainless steel box that mimics the weight of a standard fuel assembly. As a dummy fuel assembly filled with air could increase transmission between packages, cases are run in which an AFS-C is replaced by water (Case J13), void (Case J14), and steel (Case J15). Of course, replacing an AFS-C with a dummy fuel assembly will greatly reduce the fissile mass in a package, and the reactivity is expected to reduce. Case J4, with an external water density of  $0.1 \text{ g/cm}^3$ , is used as the base model. As expected, the reactivity drops in all cases compared to the base model. Replacing two AFS-C containers with dummy assemblies would further reduce the reactivity.

**C6.6.2 HAC Array Results**

Results for the HAC single package are provided in Table C6.6-1. The most reactive case is listed in boldface.

**Table C6.6-1 – Criticality Results for an Infinite Array of HAC Packages**

Case No.	Filename	Water Density (g/cm <sup>3</sup> )		k <sub>eff</sub>	σ	k <sub>s</sub> (k <sub>eff</sub> +2σ)
		Internal	External			
J1	ha_i100_o0	1	0	0.88784	0.00098	0.88980
J2	ha_i100_o0c2	1	0	0.88767	0.00098	0.88963
J3	ha_i100_o05	1	0.05	0.88858	0.00102	0.89062
J4	ha_i100_o10	1	0.1	0.88883	0.00099	0.89081
J5	ha_i100_o50	1	0.5	0.88725	0.00099	0.88923
J6	ha_i100_o100	1	1	0.88639	0.00098	0.88835
J7	ha_i100b_o0	1	0	0.88636	0.00097	0.88830
J8	ha_i95_o0	0.95	0	0.86787	0.00093	0.86973
J9	ha_i90_o0	0.9	0	0.84513	0.00095	0.84703
J10	ha_i75_o0	0.75	0	0.77254	0.00097	0.77448
J11	ha_i50_o0	0.5	0	0.62899	0.00088	0.63075
<b>Case J12 is Case J4 with increased Pu mass in the fuel rods</b>						
<b>J12</b>	<b>ha_i100_o10h</b>	<b>1</b>	<b>0.1</b>	<b>0.89717</b>	<b>0.00098</b>	<b>0.89913</b>
<b>Dummy Fuel Assembly Cases</b>						
J13	ha_i100_o10_dw	1	0.1	0.86969	0.00097	0.87163
J14	ha_i100_o10_dv	1	0.1	0.87115	0.00098	0.87311
J15	ha_i100_o10_ds	1	0.1	0.87246	0.00097	0.87440

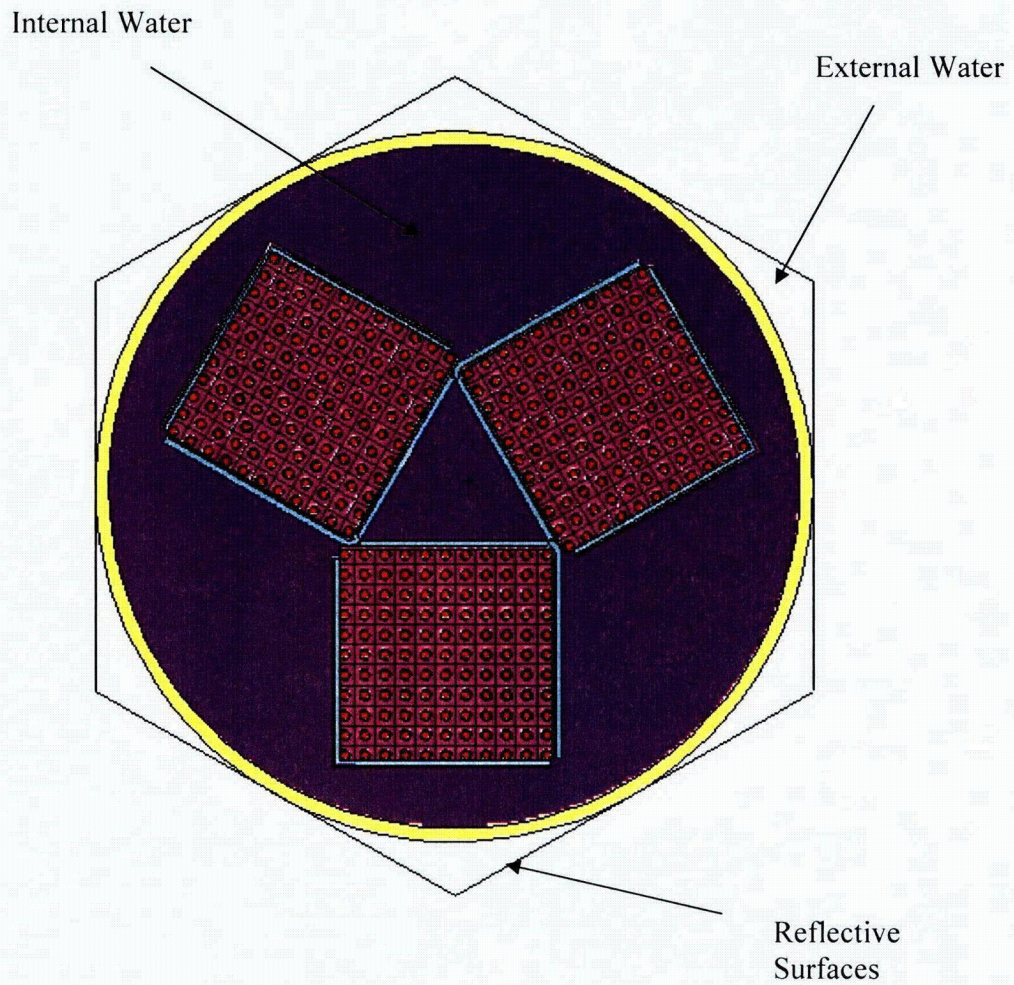


Figure C6.6-1 – HAC Array Geometry

This page left intentionally blank.

## **C6.7 Fissile Material Packages for Air Transport**

This section does not apply for the MFFP, because air transport is not claimed.



This page left intentionally blank.

## C6.8 Benchmark Evaluations

The benchmark evaluation is provided in Section 6.8, *Benchmark Evaluations*. A USL of 0.9288 is justified.

This page left intentionally blank.

## C6.9 Appendices

Representative MCNP models are included in the following appendices:

- C6.9.1 Single Package Model
- C6.9.2 Infinite Array Model

This page left intentionally blank.

### C6.9.1 Single Package Model

This file is for the worst-case HAC single package model (hsc\_b11x11\_t9x9h).

```

TA18
c
c *****Fuel Assembly*****
c cells 1 to 3 transform the 3 assemblies to their locations
c 1 4 -1.0 -21 22 -23 24 -25 6 imp:n=1 $ top nozzle, void
c 2 4 -1.0 -21 22 -23 24 -7 26 imp:n=1 $ bottom nozzle, void
c 7 0 -21 22 -23 24 126 -410 fill=20 imp:n=1 $ Exxon pins
c 8 0 -21 22 -23 24 410 -25 fill=21 imp:n=1 $ PNL pins
c
c 201 like 1 but trcl=53 $ assembly 2
c 202 like 2 but trcl=53
c 207 like 7 but trcl=53
c 208 like 8 but trcl=53
c 220 like 1 but trcl=54 $ assembly 3
c 221 like 2 but trcl=54
c 222 like 7 but trcl=54
c 223 like 8 but trcl=54
c
c -- "box" around fuel
c
c 301 0 (302 -303 300 -304 -906 26):
      (303 -305 300 -301 -906 26) fill=30 imp:n=1 $ "box" cutout
c 302 like 301 but trcl=53
c 303 like 301 but trcl=54
c
c perimeter containing strongback #1 in -y
c 50 0 (26 -906 902 -909 904 -910):
      (26 -906 909 -912 904 -901):
      (26 -906 912 904 -908):
      (26 -906 911 905 -904 -908):
      (26 -906 905 -900 903 -911) fill=7 imp:n=1
c perimeter containing strongback #2
c 51 like 50 but trcl=53
c perimeter containing strongback #3
c 52 like 50 but trcl=54
c
c *****water beyond three units*****
c 131 9 -1.4 -61 -69 64 #7 #8 #50 #51 #52 #301 #302 #303
      #207 #208 #222 #223 imp:n=1
c
c *****containment*****
c 141 5 -7.94 -62 -66 63 (61:65:-64) imp:n=1 $ outer steel
c 143 5 -7.94 -61 -70 69 imp:n=1 $ upper inner steel
c 145 4 -1.0 -61 -65 70 imp:n=1 $ upper void
c
c *****beyond containment*****
c 195 6 -7.94 -72 -76 73 (62:66:-63) imp:n=0.25 $ one foot refl
c 199 0 (72:76:-73) imp:n=0 $ outside world
c
c
c Universe 20: Exxon Fuel Lattice (lower)
c
c 200 4 -1.0 -12 11 -14 13 u=20 lat=1 trcl=30 fill=0:10 0:10 0:0
      1 1 1 1 1 1 1 1 1 1 $ row 11
      1 1 1 1 1 1 1 1 1 1 $ row 10
      1 1 1 1 1 1 1 1 1 1 $ row 9
      1 1 1 1 1 1 1 1 1 1 $ row 8
      1 1 1 1 1 1 1 1 1 1 $ row 7
      1 1 1 1 1 1 1 1 1 1 $ row 6
      1 1 1 1 1 1 1 1 1 1 $ row 5
      1 1 1 1 1 1 1 1 1 1 $ row 4
      1 1 1 1 1 1 1 1 1 1 $ row 3
      1 1 1 1 1 1 1 1 1 1 $ row 2
      1 1 1 1 1 1 1 1 1 1 imp:n=1 $ row 1 (top)
c
c
c Universe 21: PNL Fuel Lattice (upper)
c
c 201 4 -1.0 -412 411 -414 413 u=21 lat=1 trcl=31 fill=0:8 0:8 0:0
      2 2 2 2 2 2 2 2 2 $ row 9
      2 2 2 2 2 2 2 2 2 $ row 8
      2 2 2 2 2 2 2 2 2 $ row 7
      2 2 2 2 2 2 2 2 2 $ row 6

```

```

2 2 2 2 2 2 2 2 2 2 $ row 5
2 2 2 2 2 2 2 2 2 2 $ row 4
2 2 2 2 2 2 2 2 2 2 $ row 3
2 2 2 2 2 2 2 2 2 2 $ row 2
2 2 2 2 2 2 2 2 2 2 imp:n=1 $ row 1 (top)
c
c Universe 1: Exxon Fuel pin in normal position
c
c 10 1 -10.85 -401 -404 405 u=1 imp:n=1 $ fuel
c 11 4 -1.0 -402 401 -404 405 u=1 imp:n=1 $ radial gap
c 12 7 -6.5 -403 402 -408 405 u=1 imp:n=1 $ clad
c 13 4 -1.0 403 407 -406 u=1 imp:n=1 $ radially beyond pin
c 14 4 -1.0 -402 -408 404 u=1 imp:n=1 $ above fuel void
c 15 7 -6.5 -403 -406 408 u=1 imp:n=1 $ top of fuel cap
c 16 7 -6.5 -403 -405 407 u=1 imp:n=1 $ bottom of fuel cap
c 17 4 -1.0 406 u=1 imp:n=1 $ top water to infinity
c 18 4 -1.0 -407 u=1 imp:n=1 $ bottom water to infinity
c
c Universe 2: PNL Fuel pin in normal position
c
c 430 3 -10.85 -421 -424 425 u=2 imp:n=1 $ fuel
c 431 4 -1.0 -422 421 -424 425 u=2 imp:n=1 $ radial gap
c 432 7 -6.5 -423 422 -424 425 u=2 imp:n=1 $ clad
c 433 4 -1.0 (423:424:-425) u=2 imp:n=1 $ radially beyond pin
c
c Universe 2: Fuel pin shifted up
c
c 410 1 -10.85 -1 -4 5 trcl=(0 0 23.7109) u=2 imp:n=1 $ fuel
c 411 4 -1.0 -2 1 -4 5 trcl=(0 0 23.7109) u=2 imp:n=1 $ radial gap
c 412 7 -6.5 -3 2 -8 5 trcl=(0 0 23.7109) u=2 imp:n=1 $ clad
c 413 4 -1.0 3 7 -6 trcl=(0 0 23.7109) u=2 imp:n=1 $ radially beyond pin
c 414 4 -1.0 -2 -8 4 trcl=(0 0 23.7109) u=2 imp:n=1 $ above fuel void
c 415 7 -6.5 -3 -6 8 trcl=(0 0 23.7109) u=2 imp:n=1 $ top of fuel cap
c 416 7 -6.5 -3 -5 7 trcl=(0 0 23.7109) u=2 imp:n=1 $ bottom of fuel cap
c 417 4 -1.0 6 trcl=(0 0 23.7109) u=2 imp:n=1 $ top water to
infinity
c 418 4 -1.0 -7 trcl=(0 0 23.7109) u=2 imp:n=1 $ bottom water to
infinity
c
c Universe 3: Fuel pin shifted down
c
c 420 1 -10.85 -1 -4 5 trcl=(0 0 -9.4361) u=3 imp:n=1 $ fuel
c 421 4 -1.0 -2 1 -4 5 trcl=(0 0 -9.4361) u=3 imp:n=1 $ radial gap
c 422 7 -6.5 -3 2 -8 5 trcl=(0 0 -9.4361) u=3 imp:n=1 $ clad
c 423 4 -1.0 3 7 -6 trcl=(0 0 -9.4361) u=3 imp:n=1 $ radially beyond pin
c 424 4 -1.0 -2 -8 4 trcl=(0 0 -9.4361) u=3 imp:n=1 $ above fuel void
c 425 7 -6.5 -3 -6 8 trcl=(0 0 -9.4361) u=3 imp:n=1 $ top of fuel cap
c 426 7 -6.5 -3 -5 7 trcl=(0 0 -9.4361) u=3 imp:n=1 $ bottom of fuel cap
c 427 4 -1.0 6 trcl=(0 0 -9.4361) u=3 imp:n=1 $ top water to infinity
c 428 4 -1.0 -7 trcl=(0 0 -9.4361) u=3 imp:n=1 $ bottom water to
infinity
c
c Universe 4: Instrument/guide tube
c
c 41 4 -1.0 -18 5 -8 u=4 imp:n=1 $ inside
c 42 7 -6.5 -19 18 5 -8 u=4 imp:n=1 $ tube
c 43 4 -1.0 19 5 -8 u=4 imp:n=1 $ beyond tube
c 44 4 -1.0 8 u=4 imp:n=1
c 45 4 -1.0 -5 u=4 imp:n=1
c
c Universe 5: Water only
c
c 46 4 -1.0 -998 u=5 imp:n=1
c 47 4 -1.0 998 u=5 imp:n=1
c
c Universe 7: Strongback
c
c 700 6 -7.94 715 -710 u=7 imp:n=1 $ tangential strongback
c 701 6 -7.94 (710 711 718):(-711 713) u=7 imp:n=1 $ radial strongback+bend
c 702 2 -2.713 714 -719 -716 u=7 imp:n=1 $ tan Al clad
c 703 21 9.2244E-02 719 -720 -716
730 731 732 733 734 735 736 737 738
739 740 741 742 743 744 745 746 747
750 751 752 753 754 755 756 757 758
759 760 761 762 763 764 765 766 767 u=7 imp:n=1 $ tangential boron

```

704	2	-2.713	720 -715 -716	u=7	imp:n=1	\$ tan Al clad
706	2	-2.713	712 -722 -717	u=7	imp:n=1	\$ rad Al clad
707	21	9.2244E-02	722 -723 -717			
			770 771 772 773 774 775 776 777 778			
			779 780 781 782 783 784 785 786 787			
			790 791 792 793 794 795 796 797 798			
			799 800 801 802 803 804 805 806 807	u=7	imp:n=1	\$ radial boral
708	2	-2.713	723 -713 -717	u=7	imp:n=1	\$ rad Al
710	4	-1.0	(710 711 -718):(716 -710 717 -715):			
			(710 -713 717 -711)	u=7	imp:n=1	
719	6	-7.94	((-717 -712):(-716 -714 717))	-809	u=7	imp:n=1 \$ poison holder
720	4	-1.0	((-717 -712):(-716 -714 717))	809 -810	u=7	imp:n=1
721	6	-7.94	((-717 -712):(-716 -714 717))	810 -811	u=7	imp:n=1
722	4	-1.0	((-717 -712):(-716 -714 717))	811 -812	u=7	imp:n=1
723	6	-7.94	((-717 -712):(-716 -714 717))	812 -813	u=7	imp:n=1
724	4	-1.0	((-717 -712):(-716 -714 717))	813 -814	u=7	imp:n=1
725	6	-7.94	((-717 -712):(-716 -714 717))	814 -815	u=7	imp:n=1
726	4	-1.0	((-717 -712):(-716 -714 717))	815 -816	u=7	imp:n=1
727	6	-7.94	((-717 -712):(-716 -714 717))	816 -817	u=7	imp:n=1
728	4	-1.0	((-717 -712):(-716 -714 717))	817 -818	u=7	imp:n=1
729	6	-7.94	((-717 -712):(-716 -714 717))	818 -819	u=7	imp:n=1
730	4	-1.0	((-717 -712):(-716 -714 717))	819 -820	u=7	imp:n=1
731	6	-7.94	((-717 -712):(-716 -714 717))	820 -821	u=7	imp:n=1
732	4	-1.0	((-717 -712):(-716 -714 717))	821 -822	u=7	imp:n=1
733	6	-7.94	((-717 -712):(-716 -714 717))	822 -823	u=7	imp:n=1
734	4	-1.0	((-717 -712):(-716 -714 717))	823 -824	u=7	imp:n=1
735	6	-7.94	((-717 -712):(-716 -714 717))	824 -825	u=7	imp:n=1
736	4	-1.0	((-717 -712):(-716 -714 717))	825 -826	u=7	imp:n=1
737	6	-7.94	((-717 -712):(-716 -714 717))	826	u=7	imp:n=1
c						
750	6	-7.94	719 -720 -750	u=7	imp:n=1	\$ screws in boral
751	6	-7.94	719 -720 -751	u=7	imp:n=1	
752	6	-7.94	719 -720 -752	u=7	imp:n=1	
753	6	-7.94	719 -720 -753	u=7	imp:n=1	
754	6	-7.94	719 -720 -754	u=7	imp:n=1	
755	6	-7.94	719 -720 -755	u=7	imp:n=1	
756	6	-7.94	719 -720 -756	u=7	imp:n=1	
757	6	-7.94	719 -720 -757	u=7	imp:n=1	
758	6	-7.94	719 -720 -758	u=7	imp:n=1	
759	6	-7.94	719 -720 -759	u=7	imp:n=1	
760	6	-7.94	719 -720 -760	u=7	imp:n=1	
761	6	-7.94	719 -720 -761	u=7	imp:n=1	
762	6	-7.94	719 -720 -762	u=7	imp:n=1	
763	6	-7.94	719 -720 -763	u=7	imp:n=1	
764	6	-7.94	719 -720 -764	u=7	imp:n=1	
765	6	-7.94	719 -720 -765	u=7	imp:n=1	
766	6	-7.94	719 -720 -766	u=7	imp:n=1	
767	6	-7.94	719 -720 -767	u=7	imp:n=1	
c						
770	6	-7.94	722 -723 -770	u=7	imp:n=1	
771	6	-7.94	722 -723 -771	u=7	imp:n=1	
772	6	-7.94	722 -723 -772	u=7	imp:n=1	
773	6	-7.94	722 -723 -773	u=7	imp:n=1	
774	6	-7.94	722 -723 -774	u=7	imp:n=1	
775	6	-7.94	722 -723 -775	u=7	imp:n=1	
776	6	-7.94	722 -723 -776	u=7	imp:n=1	
777	6	-7.94	722 -723 -777	u=7	imp:n=1	
778	6	-7.94	722 -723 -778	u=7	imp:n=1	
779	6	-7.94	722 -723 -779	u=7	imp:n=1	
780	6	-7.94	722 -723 -780	u=7	imp:n=1	
781	6	-7.94	722 -723 -781	u=7	imp:n=1	
782	6	-7.94	722 -723 -782	u=7	imp:n=1	
783	6	-7.94	722 -723 -783	u=7	imp:n=1	
784	6	-7.94	722 -723 -784	u=7	imp:n=1	
785	6	-7.94	722 -723 -785	u=7	imp:n=1	
786	6	-7.94	722 -723 -786	u=7	imp:n=1	
787	6	-7.94	722 -723 -787	u=7	imp:n=1	
c						
790	6	-7.94	722 -723 -790	u=7	imp:n=1	
791	6	-7.94	722 -723 -791	u=7	imp:n=1	
792	6	-7.94	722 -723 -792	u=7	imp:n=1	
793	6	-7.94	722 -723 -793	u=7	imp:n=1	
794	6	-7.94	722 -723 -794	u=7	imp:n=1	
795	6	-7.94	722 -723 -795	u=7	imp:n=1	
796	6	-7.94	722 -723 -796	u=7	imp:n=1	



```

797 6 -7.94 722 -723 -797 u=7 imp:n=1
798 6 -7.94 722 -723 -798 u=7 imp:n=1
799 6 -7.94 722 -723 -799 u=7 imp:n=1
800 6 -7.94 722 -723 -800 u=7 imp:n=1
801 6 -7.94 722 -723 -801 u=7 imp:n=1
802 6 -7.94 722 -723 -802 u=7 imp:n=1
803 6 -7.94 722 -723 -803 u=7 imp:n=1
804 6 -7.94 722 -723 -804 u=7 imp:n=1
805 6 -7.94 722 -723 -805 u=7 imp:n=1
806 6 -7.94 722 -723 -806 u=7 imp:n=1
807 6 -7.94 722 -723 -807 u=7 imp:n=1
c
810 6 -7.94 719 -720 -730 u=7 imp:n=1
811 6 -7.94 719 -720 -731 u=7 imp:n=1
812 6 -7.94 719 -720 -732 u=7 imp:n=1
813 6 -7.94 719 -720 -733 u=7 imp:n=1
814 6 -7.94 719 -720 -734 u=7 imp:n=1
815 6 -7.94 719 -720 -735 u=7 imp:n=1
816 6 -7.94 719 -720 -736 u=7 imp:n=1
817 6 -7.94 719 -720 -737 u=7 imp:n=1
818 6 -7.94 719 -720 -738 u=7 imp:n=1
819 6 -7.94 719 -720 -739 u=7 imp:n=1
820 6 -7.94 719 -720 -740 u=7 imp:n=1
821 6 -7.94 719 -720 -741 u=7 imp:n=1
822 6 -7.94 719 -720 -742 u=7 imp:n=1
823 6 -7.94 719 -720 -743 u=7 imp:n=1
824 6 -7.94 719 -720 -744 u=7 imp:n=1
825 6 -7.94 719 -720 -745 u=7 imp:n=1
826 6 -7.94 719 -720 -746 u=7 imp:n=1
827 6 -7.94 719 -720 -747 u=7 imp:n=1
c
c Universe 30: "box" around fuel
c
c 310 2 -2.713 -313 317 u=30 imp:n=1 $ radial left
c 311 2 -2.713 316 -310 u=30 imp:n=1 $ tangential bot
c 312 2 -2.713 314 -315 317 u=30 imp:n=1 $ radial right
c 315 2 -2.713 311 -312 316 u=30 imp:n=1 $ tangential top
316 6 -7.94 315 312 u=30 imp:n=1
317 4 -1.0 (312 -317 -315):(-316 -312) u=30 imp:n=1
c
320 4 -1.0 -315 317 -320 u=30 imp:n=1 $ radial water gap
321 21 9.2244E-02 313 -314 317 320 -321 u=30 imp:n=1 $ radial boral
322 4 -1.0 -315 317 321 -322 u=30 imp:n=1
323 21 9.2244E-02 313 -314 317 322 -323 u=30 imp:n=1
324 4 -1.0 -315 317 323 -324 u=30 imp:n=1
325 21 9.2244E-02 313 -314 317 324 -325 u=30 imp:n=1
326 4 -1.0 -315 317 325 -326 u=30 imp:n=1
327 21 9.2244E-02 313 -314 317 326 -327 u=30 imp:n=1
328 4 -1.0 -315 317 327 -328 u=30 imp:n=1
329 21 9.2244E-02 313 -314 317 328 -329 u=30 imp:n=1
330 4 -1.0 -315 317 329 -330 u=30 imp:n=1
331 21 9.2244E-02 313 -314 317 330 -331 u=30 imp:n=1
332 4 -1.0 -315 317 331 -332 u=30 imp:n=1
333 21 9.2244E-02 313 -314 317 332 -333 u=30 imp:n=1
334 4 -1.0 -315 317 333 u=30 imp:n=1
c
340 2 -2.713 -313 317 320 -321 u=30 imp:n=1 $ radial Al cladding
341 2 -2.713 -313 317 322 -323 u=30 imp:n=1
342 2 -2.713 -313 317 324 -325 u=30 imp:n=1
343 2 -2.713 -313 317 326 -327 u=30 imp:n=1
344 2 -2.713 -313 317 328 -329 u=30 imp:n=1
345 2 -2.713 -313 317 330 -331 u=30 imp:n=1
346 2 -2.713 -313 317 332 -333 u=30 imp:n=1
c
347 2 -2.713 314 -315 317 320 -321 u=30 imp:n=1 $ radial Al cladding
348 2 -2.713 314 -315 317 322 -323 u=30 imp:n=1
349 2 -2.713 314 -315 317 324 -325 u=30 imp:n=1
350 2 -2.713 314 -315 317 326 -327 u=30 imp:n=1
351 2 -2.713 314 -315 317 328 -329 u=30 imp:n=1
352 2 -2.713 314 -315 317 330 -331 u=30 imp:n=1
353 2 -2.713 314 -315 317 332 -333 u=30 imp:n=1
c
360 4 -1.0 -312 316 -320 u=30 imp:n=1 $ tangential water gap
361 21 9.2244E-02 310 -311 316 320 -321 u=30 imp:n=1 $ tangential boral
362 4 -1.0 -312 316 321 -322 u=30 imp:n=1

```

```

363 21 9.2244E-02 310 -311 316 322 -323 u=30 imp:n=1
364 4 -1.0 -312 316 323 -324 u=30 imp:n=1
365 21 9.2244E-02 310 -311 316 324 -325 u=30 imp:n=1
366 4 -1.0 -312 316 325 -326 u=30 imp:n=1
367 21 9.2244E-02 310 -311 316 326 -327 u=30 imp:n=1
368 4 -1.0 -312 316 327 -328 u=30 imp:n=1
369 21 9.2244E-02 310 -311 316 328 -329 u=30 imp:n=1
370 4 -1.0 -312 316 329 -330 u=30 imp:n=1
371 21 9.2244E-02 310 -311 316 330 -331 u=30 imp:n=1
372 4 -1.0 -312 316 331 -332 u=30 imp:n=1
373 21 9.2244E-02 310 -311 316 332 -333 u=30 imp:n=1
374 4 -1.0 -312 316 333 u=30 imp:n=1
c
380 2 -2.713 316 311 -312 320 -321 u=30 imp:n=1 $ horizontal Al cladding
381 2 -2.713 316 311 -312 322 -323 u=30 imp:n=1
382 2 -2.713 316 311 -312 324 -325 u=30 imp:n=1
383 2 -2.713 316 311 -312 326 -327 u=30 imp:n=1
384 2 -2.713 316 311 -312 328 -329 u=30 imp:n=1
385 2 -2.713 316 311 -312 330 -331 u=30 imp:n=1
386 2 -2.713 316 311 -312 332 -333 u=30 imp:n=1
c
387 2 -2.713 316 -310 320 -321 u=30 imp:n=1 $ horizontal Al cladding
388 2 -2.713 316 -310 322 -323 u=30 imp:n=1
389 2 -2.713 316 -310 324 -325 u=30 imp:n=1
390 2 -2.713 316 -310 326 -327 u=30 imp:n=1
391 2 -2.713 316 -310 328 -329 u=30 imp:n=1
392 2 -2.713 316 -310 330 -331 u=30 imp:n=1
393 2 -2.713 316 -310 332 -333 u=30 imp:n=1
c
c Universe 51: Dummy universe containing fuel
c
c 999 1 -10.31 -999 u=51 imp:n=1 $ for diagnostics only, not used
c 1000 1 -10.31 999 u=51 imp:n=1 $ for diagnostics only, not used
c
c *****Fuel Assembly*****
c Exxon fuel pin
401 cz 0.471932 $ fuel radius
402 cz 0.48387 $ radius inside clad
403 cz 0.57277 $ radius outside clad
404 pz 88.9 $ top of fuel
405 pz -88.9 $ bottom of fuel
406 pz 106.8404 $ top of fuel pin
407 pz -89.4 $ bottom of fuel pin
408 pz 106.3404 $ bottom of top cap
c
410 pz 2.46 $ divide between different pins
411 px -1.3074 $ PNL lattice definition (upper)
412 px 1.3074
413 py -1.3074
414 py 1.3074
c
421 cz 0.652145 $ fuel radius
422 cz 0.6604 $ radius inside clad
423 cz 0.71755 $ radius outside clad
424 pz 35.56 $ top of fuel
425 pz -35.56 $ bottom of fuel
c
11 px -1.0604 $ Exxon lattice definition (lower)
12 px 1.0604
13 py -1.0604
14 py 1.0604
c
200 pz -119.38
c guide tube
18 cz 0.57150
19 cz 0.61214
c perimeter of fuel assembly
21 px 10.2391 $ offset from surface 905
22 px -12.1116 $
23 py -6.6593 $ offset from surface 904
24 py -29.0113 $
25 pz 226.466
26 pz -190.95720
126 pz -193.776
c *****containment*****
61 cz 36.1950

```

```

62      cz      37.6174
63      pz     -197.5866 $ 1.5" thick
64      pz     -193.7766 $ 1.11" below bottom of fuel (strongback bottom not modeled)
65      pz      235.6866
66      pz      237.5916
c      67      pz     -203.0222
c      68      pz     -201.1172
69      pz      226.4664
70      pz      228.0666
c      *****outside of water refl****
72      cz      68.0974
73      pz     -228.0666 $ 1' water from 63
76      pz      268.0716 $ 1' water from 66
c
c  -- "box"
c
300     py     -29.7925 $ defining box in u=0
301     py     -29.0114
302     px     -12.8928
303     px     -12.1117
304     py     -7.5675
305     px      9.9672
c
310     25 py   0.04445
311     25 py   0.2604
312     25 py   0.3048
313     25 px   0.04445
314     25 px   0.2604
315     25 px   0.3048
316     25 px   2.54
317     25 py   2.54
c
320     pz     -171.049
321     pz     -119.532
322     pz     -109.758
323     pz     -67.412
324     pz     -57.638
325     pz     -15.316
326     pz     -5.542
327     pz      36.855
328     pz      46.629
329     pz      89.002
330     pz      98.776
331     pz     141.097
332     pz     150.871
333     pz     193.548
c
c      strongback surfaces
c
710     22 px   0
711     22 py   0
712     22 px   0.476
713     22 px   0.7808
714     22 py   0.476
715     22 py   0.7808
716     22 px  -0.3114 $ 0.43" less than surface 713
717     22 py  -0.54
718     22 cz   0.7808
719     22 py   0.5205
720     22 py   0.7364
722     22 px   0.5205
723     22 px   0.7364
c
730     22 c/y  -2.7752 -189.6872 0.47625
731     22 c/y  -2.7752 -179.5526 0.47625
732     22 c/y  -2.7752 -172.3187 0.47625
733     22 c/y  -2.7752 -118.2624 0.47625
734     22 c/y  -2.7752 -111.0285 0.47625
735     22 c/y  -2.7752 -66.1416 0.47625
736     22 c/y  -2.7752 -58.9077 0.47625
737     22 c/y  -2.7752 -14.0462 0.47625
738     22 c/y  -2.7752 -6.8123 0.47625
739     22 c/y  -2.7752 38.1254 0.47625
740     22 c/y  -2.7752 45.3593 0.47625
741     22 c/y  -2.7752 90.2716 0.47625
    
```

742	22	c/y	-2.7752	97.5055	0.47625
743	22	c/y	-2.7752	142.3670	0.47625
744	22	c/y	-2.7752	149.6009	0.47625
745	22	c/y	-2.7752	194.8180	0.47625
746	22	c/y	-2.7752	202.0519	0.47625
747	22	c/y	-2.7752	213.8172	0.47625
c					
750	22	c/y	-16.7452	-189.6872	0.47625
751	22	c/y	-16.7452	-179.5526	0.47625
752	22	c/y	-16.7452	-172.3187	0.47625
753	22	c/y	-16.7452	-118.2624	0.47625
754	22	c/y	-16.7452	-111.0285	0.47625
755	22	c/y	-16.7452	-66.1416	0.47625
756	22	c/y	-16.7452	-58.9077	0.47625
757	22	c/y	-16.7452	-14.0462	0.47625
758	22	c/y	-16.7452	-6.8123	0.47625
759	22	c/y	-16.7452	38.1254	0.47625
760	22	c/y	-16.7452	45.3593	0.47625
761	22	c/y	-16.7452	90.2716	0.47625
762	22	c/y	-16.7452	97.5055	0.47625
763	22	c/y	-16.7452	142.3670	0.47625
764	22	c/y	-16.7452	149.6009	0.47625
765	22	c/y	-16.7452	194.8180	0.47625
766	22	c/y	-16.7452	202.0519	0.47625
767	22	c/y	-16.7452	213.8172	0.47625
c					
770	22	c/x	-5.9248	-189.6872	0.47625
771	22	c/x	-5.9248	-179.5526	0.47625
772	22	c/x	-5.9248	-172.3187	0.47625
773	22	c/x	-5.9248	-118.2624	0.47625
774	22	c/x	-5.9248	-111.0285	0.47625
775	22	c/x	-5.9248	-66.1416	0.47625
776	22	c/x	-5.9248	-58.9077	0.47625
777	22	c/x	-5.9248	-14.0462	0.47625
778	22	c/x	-5.9248	-6.8123	0.47625
779	22	c/x	-5.9248	38.1254	0.47625
780	22	c/x	-5.9248	45.3593	0.47625
781	22	c/x	-5.9248	90.2716	0.47625
782	22	c/x	-5.9248	97.5055	0.47625
783	22	c/x	-5.9248	142.3670	0.47625
784	22	c/x	-5.9248	149.6009	0.47625
785	22	c/x	-5.9248	194.8180	0.47625
786	22	c/x	-5.9248	202.0519	0.47625
787	22	c/x	-5.9248	213.8172	0.47625
c					
790	22	c/x	-16.9789	-189.6872	0.47625
791	22	c/x	-16.9789	-179.5526	0.47625
792	22	c/x	-16.9789	-172.3187	0.47625
793	22	c/x	-16.9789	-118.2624	0.47625
794	22	c/x	-16.9789	-111.0285	0.47625
795	22	c/x	-16.9789	-66.1416	0.47625
796	22	c/x	-16.9789	-58.9077	0.47625
797	22	c/x	-16.9789	-14.0462	0.47625
798	22	c/x	-16.9789	-6.8123	0.47625
799	22	c/x	-16.9789	38.1254	0.47625
800	22	c/x	-16.9789	45.3593	0.47625
801	22	c/x	-16.9789	90.2716	0.47625
802	22	c/x	-16.9789	97.5055	0.47625
803	22	c/x	-16.9789	142.3670	0.47625
804	22	c/x	-16.9789	149.6009	0.47625
805	22	c/x	-16.9789	194.8180	0.47625
806	22	c/x	-16.9789	202.0519	0.47625
807	22	c/x	-16.9789	213.8172	0.47625
c					
809		pz	-188.417		
810		pz	-181.331	\$ PH 1 (bottom)	
811		pz	-170.541	\$ PH 1	
812		pz	-120.040	\$ PH 2	
813		pz	-109.250		
814		pz	-67.920	\$ PH 3	
815		pz	-57.130		
816		pz	-15.824	\$ PH 4	
817		pz	-5.034		
818		pz	36.347	\$ PH 5	
819		pz	47.137		

```

820 pz 88.494 $ PH 6
821 pz 99.284
822 pz 140.589 $ PH 7
823 pz 151.379
824 pz 193.040 $ PH 8
825 pz 203.830 $ PH 8
826 pz 212.547
c
900 px 11.18006 $ FIXED for strongbacks touching
901 py -5.71956 $ FIXED for strongbacks touching
902 px -11.9593
903 py -28.7574 $ surface 901 minus 9.07"
c
c 904 is -7.1354 and 905 is 9.7633 for nominal case (with poison holders).
c they are shifted to cut off poison holders to allow for
c expansion for damaged cases.
c
c To completely "slice off" the poison holders, set
c 904 to -6.6593 and 905 to 10.2392.
c
904 py -6.6593 $ tangential strongback lower bound, surface 901 minus total thickness
905 px 10.2392 $ radial strongback left bound, surface 901 minus total thickness
906 pz 215.7222
908 c/z 9.87856 -7.02106 1.3015
909 px -9.9019
910 py -6.35448
911 py -7.1344 $ fixed
912 px 9.7653 $ fixed
c
998 so 10000
999 pz 345.5565

mode n
c print
kcode 2000 0.9 30 530
sdef cell=d1 pos=0 0 0 rad=d3 ext=d4 axs=0 0 1
si1 1 7:200:10 207:200:10 222:200:10 8:201:430 208:201:430 223:201:430
sp1 121 121 121 81 81 81
si3 0.652145
si4 88.9
cut:n j j 0 0
c
c Materials
c
m1 92235 -0.592 $ Exxon fuel pellet
92238 -82.746
94239 -3.828
94240 -0.674
94241 -0.313
8016 -11.847
m2 13027 1.0 $ aluminum cladding for BORAL
m3 92235 -0.597 $ PNL fuel pellet
92238 -83.483
94239 -3.238
94240 -0.570
94241 -0.265
8016 -11.848
m4 1001 2 $ water
8016 1
mt4 lwtr.01t
m5 6000 -0.06 $ XM-19
7014 -0.4
14000 -0.75
15031 -0.04
16032 -0.03
23000 -0.3
24000 -23.5
25055 -6
28000 -13.5
41093 -0.3
42000 -3
26000 -52.12
m6 6000 -0.08 $ SS-304
14000 -1.0
15031 -0.045

```

```

24000      -19.0
25055      -2.0
26000     -68.375
28000      -9.5
m7. 40000     -1.0  $ Cladding
c   41093     -0.030
m8  82000      1.0  $ lead
m9   6000     -25.1  $ water/steel mix, 5.8% steel by volume
    14000     -313.9
    15031     -14.1
    24000    -5964.9
    25055    -627.9
    26000   -21465.8
    28000   -2982.5
    1001    -7240.1
    8016   -57462.7
mt9 lwtr.01t
m21 5010    7.3123E-03 $ 35 mg/cm2 B-10, 75% credit
    5011    3.9244E-02
    6000    1.2248E-02
    13027   3.3439E-02
c   total 9.2244E-02
c
c   Translations
c
c   tr22 is the intersection of planes 904 and 905
c   when the poison holders are present (904 and 905 shift when it is
c   desired to "slice off" the poison holders).
c   Note that the origin of Universe 7 corresponds to the intersection
c   of these planes.
c
c *tr22    9.7643 -7.1354 0.0
c
c   tr25 is the intersection of planes 300 and 302. The origin of Universe 30
c   corresponds to the intersection of these planes.
c
c *tr25   -12.8928 -29.7925 0.0
c
c   tr30 is computed by taking the coordinates of the intersection of planes
c   22 and 24 and adding half the pitch (note: can't be exact or else planes will
c   overlap, causing program termination.)
c
c *tr30   -11.5389 -28.4386 -104.38 $ lower fuel (Exxon lower)
c *tr31   -11.3941 -28.2938 38.03  $ upper fuel (PNL upper)
c
c   tr53 and tr54 rotate the bottom assembly to create assemblies 2 and 3
c
c *tr53    0 0 0          120 30 90   150 120 90   90 90 0 0 $ +x+y
c *tr54    0 0 0          120 150 90   30 120 90   90 90 0 0 $ -x-y

```

This page left intentionally blank.

## C6.9.2 Infinite Array Model

The infinite array models are geometrically the same as the single package models, although small changes have been made to the outer boundary to simulate the infinite array. Additional cells and surfaces are listed below.

```
195 0          -881 882 -886 885 -883 884 -66 63 62 imp:n=1 $ w between packages
199 0          (881:-882:886:-885:883:-884:66:-63) imp:n=0 $ outside world
```

```
c          hexagonal boundary of one unit lattice cell, close packed
*881      px   37.6184
*882      px  -37.6184
*883      p   -0.5000000      0.866025404      0.0000000      37.6184
*884      p   -0.5000000      0.866025404      0.0000000     -37.6184
*885      p    0.5000000      0.866025404      0.0000000     -37.6184
*886      p    0.5000000      0.866025404      0.0000000      37.6184
```



This page left intentionally blank.

## C7.0 PACKAGE OPERATIONS

### C7.1 Package Loading

The AFS-C contents are loaded in the following manner:

1. Remove the 22 bolts that attach the lid of the AFS-C. Remove the AFS-C lid.
2. Load up to 116 Exxon rods and up to 69 PNL rods into the AFS-C. Place the Exxon rods into the Exxon cavity (long), and place the PNL rods into the PNL cavity (short). Within each cavity, add steel or aluminum dunnage rods until all space is filled. Alternately, the Exxon rods may be shipped with an empty PNL cavity, or the PNL rods may be shipped with an empty Exxon cavity. Ensure that the loaded AFS-C meets the applicable heat load limits.
3. Place the AFS-C lid on the body. Tighten the 22 bolts to the torque value specified on *Packaging General Arrangement Drawing 99008-61*. For each bolt, bend lock tab against bolt flat.

Once the AFS-C has been loaded, the package loading operations are essentially the same as the operations for fuel assembly loading described in Chapter 7.1, *Package Loading*. The AFS-C is handled in the same manner as a fuel assembly.

The only difference is the tightening of the swivel clamp pads. Because the AFS-C is constructed of aluminum, a thermal expansion gap is provided. Therefore, modify Step 18 of Section 7.1.2.1, *Loading of Fuel Assemblies into Strongback*, as follows:

- 7.1.2.1, Step 18: Tighten the four (4) 3/4-inch swivel clamp pads on the top plate until the screw pad contacts the AFS-C top. Then loosen each swivel clamp pad 1 – 1½ turns, and lock in place with a hex nut.

### C7.2 Package Unloading

The package unloading operations are the same as the operations for fuel assembly unloading described in Chapter 7.2, *Package Unloading*. The AFS-C is handled in the same manner as a fuel assembly.

The AFS-C contents are unloaded in the following manner:

1. Remove the 22 bolts that attach the lid of the AFS-C. Remove the AFS-C lid.
2. Unload the fuel and dunnage rods present.
3. Place the AFS-C lid on the body. Tighten the 22 bolts to the torque value specified on *Packaging General Arrangement Drawing 99008-61*. For each bolt, bend lock tab against bolt flat.

### **C7.3 Preparation of an Empty Package for Transport**

Previously used and empty MFFPs shall be prepared and transported per the requirements of 49 CFR §173.428<sup>1</sup>.

### **C7.4 Preshipment Leakage Rate Test**

The preshipment leakage rate test is the same as described in Section 7.4, *Preshipment Leakage Rate Test*.

---

<sup>1</sup> Title 49, Code of Federal Regulations, Part 173 (49 CFR 173), *Shippers-General Requirements for Shipments and Packagings*, 10-01-06 Edition.

## **C8.0 ACCEPTANCE TESTS AND MAINTENANCE PROGRAM**

### **C8.1 Acceptance Tests**

Per the requirements of 10 CFR §71.85<sup>1</sup>, this section discusses the inspections and tests to be performed prior to first use of the AFS-C rod container.

#### **C8.1.1 Visual Inspections and Measurements**

Each AFS-C rod container shall be examined in accordance with the requirements delineated on the drawings in Appendix C1.4.2, *Packaging General Arrangement Drawings*, prior to use.

#### **C8.1.2 Weld Inspections**

All welds shall be inspected to the requirements delineated on the drawings in Appendix C1.4.2, *Packaging General Arrangement Drawings*.

#### **C8.1.3 Structural and Pressure Tests**

The AFS-C rod container does not require any lifting device load tests or pressure tests.

#### **C8.1.4 Fabrication Leakage Rate Tests**

The AFS-C rod container does not require any leakage rate tests.

#### **C8.1.5 Component and Material Tests**

The AFS-C rod container does not require any component or material tests.

#### **C8.1.6 Shielding Tests**

The AFS-C rod container does not require any shielding tests.

#### **C8.1.7 Thermal Tests**

The AFS-C rod container does not require any thermal tests.

---

<sup>1</sup> Title 10, Code of Federal Regulations, Part 71 (10 CFR 71), *Packaging and Transportation of Radioactive Material*, 01-01-06 Edition.

## **C8.2 Maintenance Program**

The AFS-C rod container does not require a scheduled maintenance program. The parts which are routinely handled during use (the body, the lid, and the lid fasteners) are visually inspected prior to use. Damaged components shall be repaired or replaced prior to use.